UNIVERSITY OF GHANA

COLLEGE OF BASIC AND APPLIED SCIENCES

INVESTIGATING FACTORS INFLUENCING VARIATION IN *P. FALCIPARUM* INVASION PHENOTYPING ASSAYS

A Dissertation Submitted to the board of graduate studies, University of Ghana, Legon, in partial fulfilment of the requirements for the award of Doctor of Philosophy in Molecular Cell Biology of Infectious Diseases

BY

LATY GAYE THIAM

(10556633)

WEST AFRICAN CENTRE FOR CELL BIOLOGY OF INFECTIOUS PATHOGENS

JULY 2019

DECLARATION

The experimental work presented in this thesis was done by me, Laty Gaye THIAM, at the Department of Biochemistry of Cell and Molecular Biology, University of Ghana, under the supervision of Prof. Gordon A. Awandare (West African Centre for Cell Biology of Infectious Pathogens and Department of Biochemistry, Cell and Molecular Biology, University of Ghana, Legon), Dr Makhtar Niang (Immunology Unit, Pasteur Institute, Dakar, Senegal), Dr Kwadwo A. Kusi (Department of Immunology, Noguchi Memorial Institute for Medical Research, University of Ghana, Legon) and Dr Theresa M. Gwira (West African Centre for Cell Biology of Infectious Pathogens and Department of Biochemistry, Cell and Molecular Biology, University of Ghana, Legon).

All references have been duly cited.

……..

Laty Gaye THIAM (Student)

……..

Prof. Gordon A. Awandare (Supervisor)

……

Dr Makhtar Niang (Co-Supervisor)

……

Dr Kwadwo A. Kusi (Co-Supervisor)

……

Dr Theresa M. Gwira (Co-Supervisor)

ABSTRACT

Malaria caused by *P. falciparum*, is the most life-threatening human parasitic disease, claiming over 400,000 deaths from about 200 million cases in 2017. Despite the yet unsuccessful efforts in the quest for an effective malaria vaccine, antigens expressed in the erythrocytic stage of *P. falciparum* represent highly promising vaccine candidates given their natural exposure to the immune system. Understanding the mechanism of erythrocyte invasion by *P. falciparum* mainly during active clinical infection is an important step towards developing an effective vaccine to counter the deleterious outcomes of this parasitic infection. However, comparison of pioneering studies assessing the invasion phenotypic diversity of *P. falciparum* is precluded by the lack of consensus in the protocols used in individual studies. As such, efforts towards the development of standard protocols necessitate the assessment of the impact of potential sources of variation in the measured outcome. Here, the effect of short-term culture adaptation on the invasion phenotypes of *P. falciparum* clinical isolates was assessed using freshly isolated parasites from children presenting an acute malaria illness. We also assessed the effect of short-term cryopreservation on the parasites' invasion phenotype relative to the *ex vivo* invasion phenotype of the isogenic parasites. The effect of blood donor variability and some erythrocyte phenotypic features in the parasites' invasion phenotype were also assessed here. Furthermore, we assessed the invasion phenotypic diversity of *P. falciparum* clinical isolates from four areas of varying transmission intensity in Ghana and compared the expression levels of the major parasites' invasion-related ligands across isolates. Finally, we tested the invasion inhibitory activity of antibodies against two novel *P. falciparum* antigens and assessed the naturally-derived antibody responses against both antigens in children presenting at the hospital with symptomatic malaria. We showed that short-term cryopreservation has a minimal effect on the parasites' invasion phenotype while short-term

culture adaptation was found to affect the genotypic diversity and, to a lesser extent, the phenotypic diversity of *P. falciparum* clinical isolates. Blood donor variability was also found to affect *P. falciparum* invasion efficiency. However, this variation was associated with none of the erythrocyte phenotypic features tested here (e.g. blood group, hemoglobin genotype, receptor density). The erythrocyte invasion phenotyping experiments showed the predominance of sialic acid independent invasion pathway in Ghanaian clinical isolates and a high dependency on the CR1/PfRh4 mediated invasion pathway across all isolates. Moreover, invasion into trypsin-treated erythrocytes was found to be strongly correlated with the invasion into chymotrypsin-treated erythrocytes. The assessment of the transcript levels of invasion-related genes showed significantly higher expression levels of PfEBA family genes relative to the PfRh family genes, while the pattern of expression was similar across sites. Further analysis revealed a strong negative correlation between PfEBA175 and all other genes except for PfEBA140. Furthermore, the growth inhibition assays showed different ranges of dose-dependent inhibitory activities of individual antibodies against the target antigens used in his study. However, the combination of antibodies against different antigens showed no synergistic invasion inhibitory activities across all isolates. Finally, the level of antibody responses against the different antigens were strongly associated with transmission intensity. Taken together, our findings showed that differences in protocols may account for most of the variations in previously reported invasion phenotyping data across different countries. Therefore, this work has provided preliminary data upon which more rigorous experimental design should be based on for the optimization and establishment of standardized invasion phenotyping assays, which is critical for large-scale studies.

ACKNOWLEDGEMENTS

Being engaged on a PhD journey has been for me both a painful and enjoyable experience. Today, while there is no word to describe my feelings, I realized that I couldn't have come this far without the help, the support, the trust of great people that made me enjoy this though journey. A simple THANK YOU will not be enough to show my appreciation to all these wonderful people that have paved the way to this point, but I will leave a BIG THANK YOU here while I am looking for a better word to express my feelings to you all.

On a prime note, I am grateful to my honorific supervisory team, for their patience, help, support and mentorship throughout this journey. My special thanks to Professor Gordon Awandare, for accepting me as a PhD student, with no reservation, for his support, his trust and consideration to my little person. I have learnt a lot from him, without his help, I could not have finished my dissertation successfully.

To Dr Makhtar Niang, who is more than a supervisor, but a mentor, I owe a dept of gratitude. He has inspired my interest in research and has always been of great help. To Dr K.A. Kusi and T.M. Gwira, I am more than grateful for your support, your care and your sense of responsibilities.

My special Thanks to Dr Yaw Aniweh, who has been instrumental in all aspect of this work. He has been a mentor, a friend, a brother and a confident throughout this journey. I can't thank you much for all the support you have been to me, but God knows better.

To the members of the Immunology and Cell Biology Lab, you are just WONDERFUL. Through each of you, I have learnt a lot from the essence of team work to the smallest social consideration of individuals irrespective of their position. Most interestingly, you have helped me sharpen my emotional intelligence.

I would like to acknowledge all faculty and staff of the BCMB department and WACCIP as well, their support has been tremendous. Big thanks to WACCBIP that fully funded my PhD work through the World Bank ACE Project.

I am thankful to my family for their support, care and encouragement throughout this journey. Special thanks to my Dad and Mom for putting in place the necessary means and care for me to come this far.

I am grateful for the patience, understanding and support I received from my lovely wife, Sane.

Last but not least, a special thanks to my colleagues of the second cohort of WACCIP PhD program, you have been wonderful from day zero, God bless you all.

TABLE OF CONTENTS

LIST OF FIGURES

LIST OF TABLES

LIST OF ABREVIATIONS

AMA1:	apical membrane protein 1
ACT:	artemisinin-based combination therapy
ANOVA:	analysis of variance
APC:	allophycocyanin
BF:	bright field
BSA:	bovine serum albumin
BSG :	basigin
CFDA-SE :	carboxyfluorescein diacetate succinimidyl ester
CPM:	complete parasite medium
CR1:	complement receptor 1
CTFR;	Cell Trace Far-Red
CT:	chymotrypsin treated
CyRPA:	cysteine-rich protective antigen
DAF:	decay accelerating
DDAO-SE:	dichloro dimethyl acridin one succinimidyl ester
DMSO:	dimethyl sulphoxide
DNA:	deoxyribonucleic acid

EBA:	erythrocytes binding antigen
ELISA:	enzyme-linked immunosorbent assays
FITC:	fluorescein isothiocyanate
FSC-A:	forward scatter area
FSC-H:	forward scatter high
GIA:	growth inhibition assay
GLURP:	glutamate-rich protein
GMS:	greater Mekong sub-region
GPI:	glycosylphosphatidylinositol
GYPA:	glycophorin A
GYPC:	glycophorin B
G6PD:	glucose-6-phos
Hb:	hemoglobin
HCT:	haematocrit
IgG:	immunoglobulin G
IPA:	invasion phenotyping assay
IPT:	intermittent preventive treatment
IRB:	institutional review board

KDa:	kilo Dalton
LEKMA:	Ledzokuu-Krowor Municipal Assembly
MCH:	mean corpuscular hemoglobin concentration
MCHC:	mean corpuscular hemoglobin concentration
MCV:	mass cell volume
MDG:	millennium development goal
MFI:	mean fluorescence intensity
mM:	millimolar
MSP:	merozoite surface protein
MSRP:	merozoite surface related-protein
MTRAP:	merozoite thrombospondin-related anonymous protein
NCP:	national control programs
NHS:	normal human serum
nm:	nano meter
NT:	neuraminidase treated
PBS:	phosphate buffer saline
PCR:	polymerase chain reaction
PE:	phycoerythrin

PLT: platelet

PfAARP: asparagine-rich protein

PTRAMP: thrombospondin related apical merozoite protein

RAMA: rhoptry associated membrane antigen

RAP: rhoptry associated protein

RESA: ring infected erythrocyte surface antigen

RIMA: ring infected membrane antigen

RH: reticulocyte binding-like homologue

PfRipr: *P. falciparum* RH5 interacting protein

RNA: ribonucleic acid:

PfROM: *P. falciparum* rhomboid protease

RON: rhoptry neck protein

RPM: ribonucleic acid

RPMI: Roswell park memorial institute

RT: room temperature

RT qPCR: real-time quantitative polymerase chain reaction

SA sialic acid

SD : standard deviation

SDG: sustainable development goal

SERA: serine repeat antigen

SEM: standard error of the mean

SG I: SYBR green I

SI: stain index

SP: signal peptide

SPATR: secreted protein with altered thrombospondin repeat domain

SUB: subtilisin-like protein

SSC-A: forward scatter area

TJ: tight junction

TMD: transmembrane domain

TMB: tetramethyl benzidine

TT: trypsin treated

UT: untreated

µL: microliter

µM: micromolar

WBC: white blood count

WHO: World Health Organisation

CHAPTER ONE: INTRODUCTION

1.1. BACKGROUND

Despite tremendous efforts towards the effective control of malaria, the disease continues to be a major public health issue worldwide and constitutes a huge burden on the economies of endemic countries. In 2017 alone, over two hundred million malaria cases were reported globally, resulting in about half a million case fatalities (WHO, 2018b). There is currently no vaccine that fully protects against malaria and therefore treatment for the disease relies on chemotherapeutics, with artemisinin-based combination therapies (ACTs) being the most effective drug regimens. However, the emergence of artemisinin resistance in the Greater Mekong Sub-region (GMS) of Asia and its possible spread towards other regions, especially Africa, is a great threat for national malaria control programs (NCPs). Therefore, to achieve the goal of elimination and possibly eradication, there is the need to develop affordable and permanent strategies. Of utmost importance in defining strategies to counter the everlasting malaria threat is the development of an effective vaccine against *P. falciparum*, the causative agent of the most severe forms of the disease. This goal, however, continues to be thwarted by the persistent lack of clear understanding of the bulk of biological mechanisms that govern the outcomes of malaria infection. For instance, the exact mechanisms driving red blood cell invasion by the malaria parasite are still unclear, and so are the specific host and/or parasites factors associated with the high mortality rates in some at-risk groups, hence the need for a better understanding of the host-parasite interactions during malaria infection.

1.2. SPECIFIC AIMS

Despite notable advances in the control of malaria, recent data suggest that currently available control strategies need to be reinforced to achieve the goal of elimination in high transmission areas (WHO, 2018a). With the growing threats of insecticide and drug resistance developed by the vector and the parasites, respectively, developing an efficient vaccine remains the most effective strategy in preventing the disease. Efforts towards malaria vaccine development have been multidirectional, targeting both pre-erythrocytic and blood stages, though their efficacy has been modest in clinical trials so far (Draper et al., 2015; Rts, 2015). Given the parasite's exposure to the immune system arms during its erythrocytic development, *P. falciparum* blood-stage antigens represent good potential targets for vaccine development (Wright & Rayner, 2014). Besides, given the association of parasite's blood stage with the disease occurrence, a malaria vaccine targeting this specific stage would be of utmost importance in the battle against the disease burden. Erythrocyte invasion is a complex process involving a large repertoire of parasite antigens and is essential for parasite survival (Beeson et al., 2016). The feasibility of targeting blood-stage antigens has previously been supported by both *in vitro* and *in vivo* studies (Aniweh, Gao, Gunalan, & Preiser, 2016; Arama & Troye-Blomberg, 2014; Badiane et al., 2013; Chiu et al., 2016; Foquet et al., 2018; Kisalu et al., 2018; Srinivasan et al., 2017). However, several blood-stage vaccine candidates that underwent early clinical trials (e.g. AMA1, MSP1) have been challenged by their extensive genetic complexity or their lack of immunogenicity (Arama & Troye-Blomberg, 2014). There is, therefore, an imperative need to down select for relatively conserved antigens that trigger high titers of strain transcending invasion inhibitory antibodies and cell-mediated immune responses to provide long-lasting protection. One way to achieve such a goal is through investigation of the phenotypic and genotypic invasion diversity of *P. falciparum* clinical isolates (WAMIN, 2016). There are multiple approaches

for phenotyping *P. falciparum* invasion profiles, however, a majority of the studies in this field have been conducted in laboratory-adapted strains, which are not as clinically relevant as *P. falciparum* field isolates. To date, there is only a handful of studies that have focused on investigating the invasion diversity of *P. falciparum* clinical isolates, with the majority of them from sub-Saharan Africa (WAMIN, 2016), where the highest malaria-related mortality occurs. However, the comparison of results from these pioneering studies is hampered by their use of different protocols (Table 2.1), therefore challenging the use of these results as a baseline for the screening of large-scale vaccine targets. Thus, there is an obvious need for new approaches to more rapidly and rationally prioritize and down-select potential vaccine candidates. In this study, we postulate that differences in protocols in a large-scale investigation of *P. falciparum* phenotypic diversity preclude the identification of the real biological differences between clinical isolates. In addition, given the suggested relationship between *P. falciparum* invasion phenotype and transmission intensity (Bowyer et al., 2015; H. E. Mensah-Brown et al., 2015), we postulate that the use of standard protocols would be important in assessing the phenotypic diversity of clinical isolates from areas of various transmission intensity. Furthermore, since *P. falciparum* invasion of erythrocytes is a multistep process with multiple parasite ligands simultaneously engaged, it would be necessary to test multiple vaccine targets in combinatory assays to determine optimal combination of antigens.

1.2.1. SPECIFIC AIM 1

To investigate the effects of potential sources of variation in protocols for *ex vivo* phenotyping of *P. falciparum* clinical isolates.

Hypothesis 1: Differences in cryopreservation and thawing protocols affect the true biological differences in parasite phenotypes and would further affect the comparison of large-scale data from areas of different endemicity.

Freshly collected *P. falciparum* clinical isolates were used to investigate the effect of cryopreservation and thawing protocols on parasite *ex vivo* invasion phenotypes and *in vitro* culture-adaptation. Parasites were either introduced into *in vitro* culture straight from the field or cryopreserved for a minimum duration of three months before *in vitro* culture. For parasites that grew well, *ex vivo* invasion phenotyping experiments were conducted during the first cycle. Moreover, in all cases, parasites multiplication rates were monitored by flow cytometry during the first three *in vitro* replication cycles at least. Two distinct thawing protocols were used to revive cryopreserved parasites and the same assays were conducted to monitor the parasites *in vitro* adaptation and invasion phenotypes following cryopreservation. Kruskal Wallis was used to test for statistical differences in invasion efficiency prior to and after cryopreservation and where significant, Dunn's multiple comparison test was used as post hoc analysis. The same statistics were used to test for statistical differences in parasites multiplication rates following thawing with different protocols as compared to freshly culture-adapted isolates.

Additional investigations were conducted to test the following hypothesis.

Hypothesis 2: Blood donor variability affects P. *falciparum* invasion phenotype

To test this hypothesis, we collected blood samples from twenty asymptomatic adults to investigate the effect of blood donor variability on *P. falciparum* invasion profiles using both laboratory and clinical isolates. A complete haematological screening was conducted for all samples, including sickling, haemoglobin (Hb) and G6PD genotyping. The expression levels of specific erythrocyte surface receptors were also quantified using monoclonal antibodies and expressed as mean fluorescent intensity (MFI). Henceforth, for each given receptor, donors were classified as low, medium or high expresser. A standard flow cytometry-based invasion assay was used to assess the parasite invasion rates in enzyme-treated erythrocytes from different donors. The Friedman test was used to test for differences in invasion efficiency between donors following enzyme treatment, while the Spearman rank test was used to assess the relationship between different variables such as the surface expression of erythrocyte receptors and invasion efficiency in enzyme-treated erythrocytes.

Further investigations in this aim involved the optimization of a newly developed cytoplasmic dye for the staining of target erythrocytes. In recent years, flow cytometry has become a cornerstone in investigating *P. falciparum* phenotypic diversity. Consequently, current flow cytometry-based *P. falciparum* invasion phenotyping assays necessitate the use of cytoplasmic dyes for proper discrimination between donor and acceptor erythrocytes. Therefore, to broaden the applicability of such an assay in a wider range of flow cytometry instruments, we first optimized the staining conditions of a newly developed cytoplasmic dye, Cell Trace Far Red and assessed its suitability for use in *P. falciparum* invasion phenotyping assays.

1.2.2. SPECIFIC AIM 2

To establish the breadth of parasite phenotypic and genotypic invasion diversity across areas of varying transmission intensity in Ghana

Hypothesis 1: The use of standardized approaches provides more relevant data with regards to the parasite phenotypic and genotypic invasion diversity and will help in designing strain transcendent invasion blocking vaccines.

A better understanding of the major invasion pathways used by *P. falciparum* clinical isolates is of utmost importance to anticipate possible drawbacks in the down selection of potential blood-stage vaccine candidates. *P. falciparum* clinical isolates, collected from areas of different endemicity in Ghana were *ex vivo* cultured in O+ erythrocytes. Invasion phenotyping assays were conducted for all parasites that successfully grew using enzyme-treated erythrocytes as previously described (H. E. Mensah-Brown et al., 2015). The Kruskal Wallis test was used to compare the parasite invasion rates across various transmission areas while the Spearman rank correlation was used to assess the relationship between variables. Patient demographics and clinical data were also used to assess their relationship with the observed parasites invasion profiles. Additionally, the expression levels of *P. falciparum* invasion-related genes were assessed by real-time quantitative polymerase chain reaction (RT-qPCR) and their relationship with invasion efficiency was also assessed.

1.2.3. SPECIFIC AIM 3

To assess the invasion inhibitory effect of antibodies targeting novel *P. falciparum* blood-stage antigens

Hypothesis 1: Antibodies against functionally conserved blood-stage antigens will provide strain transcendent invasion blocking activity, if any, and constitute a great value in both efficacy and cost effectiveness as potential vaccine candidates.

Given the high polymorphism rates that precluded a bulk of the malaria vaccine candidates, including the licensed RTS, S, we opted for a reverse vaccinology approach whereby vaccine candidates are first tested for their ability to neutralize invasion in both *P. falciparum* laboratory and clinical isolates. Candidate genes were selected based on some specific features common to invasion-related genes, such as the presence of a glycosylphosphatidylinositol (GPI) anchor, transmembrane domains (TMD) and/or a signal peptide (SP), the peak of expression in the late stage of the parasites' asexual replication and so on. Antibodies against synthetic predicted B-cell epitopes were used in standard growth inhibitory assays to determine their neutralizing potential. We also tested the synergistic effect of the combination of antibody pairs against the same or different candidates to determine their compatibility as potential components of a multi-antigen vaccine. In addition, candidate-specific antibodies that generated inhibition activity of at least 50% at the highest concentration were used in ELISAs to test for the level of the naturally-induced immune response in both symptomatic children and exposed adults from malaria-endemic areas.

CHAPTER TWO: LITERATURE REVIEW

2.1. GLOBAL TRENDS OF MALARIA TRANSMISSION

Malaria still remains the most lethal human parasitic disease, killing nearly half a million people annually, with over 216 million cases reported in 91 countries in 2016 (WHO, 2017). Sub-Saharan Africa, which accounts for the bulk of all malaria-related deaths, continues to be the most afflicted by the disease burden, in most cases attributed to *P. falciparum*, the deadliest among the human malaria parasites. This situation mainly emerged as a result of lack of appropriate preventive measures, but also the lack of prompt diagnosis and treatment (WHO, 2015). In 2014, about one third of people at risk in this region lived in households without insecticide-treated mosquito nets (ITN), and the bulk of the most vulnerable people (infant and pregnant women) did not receive a single dose of intermittent preventive treatment (IPT) (WHO, 2015). Although there is still a lot to do for sustainable malaria intervention coverage, the global malaria agenda has considerably reduced the malaria burden worldwide, over the last decade. Malaria incidence rate was reduced by 37%, whilst the malaria-specific mortality rates have been reduced by 60% in all age groups worldwide, leading to the meeting of the Millennium Development Goal (MDG) target 6c, which was *"to have halted and began to reverse the incidence of malaria"* (WHO, 2015). This remarkable progress, achieved through both preventive and therapeutic approaches, has encouraged the international community's idea of malaria elimination/eradication. There is now a proposed framework for transition from disease control to elimination by shifting from the MDGs to Sustainable Development Goals (SDGs) for the next fifteen years (WHO, 2015). However, in addition to the socio-economic factors that could jeopardize the ability of countries to stay on track (WHO, 2018a), the sustainability of these achievements is

threatened by the lack of sufficient knowledge of the parasites biology, the emergence of multidrug-resistant parasites and the lack of an efficient malaria vaccine.

2.2. PROGRESS AND CHALLENGES IN MALARIA VACCINE DEVELOPMENT

In the early 1980s, the combination of focus monitoring with ring vaccination campaigns led to the eradication of Smallpox, which so far is the only human infectious disease to have been eradicated. Smallpox eradication raised hopes for accomplishing such progress for other infectious diseases, including malaria whose associated mortality has significantly decreased from a peak of 1,817,000 in 2004 to 238,000 in 2010 (Murray et al., 2012). In spite of these promising steps, to date, there is no effective malaria vaccine, though multiple approaches have been tried for developing one (Long & Zavala, 2016). So far, more than 30 malaria vaccine candidates have been tested (Crompton, Pierce, & Miller, 2010) and for which only one (RTS,S) has reached the phase III clinical trial with only 30-50% efficacy (Neafsey et al., 2015). Challenges for developing an efficient malaria vaccine include the lack of appropriate animal model, the lack of adequate research funding, and the size of the parasite's genome (e.g. *P. falciparum* has >5400 genes), which is organized in a way that less than 1% of the parasite's antigens are accessible to the immune system (A. V. Hill, 2011). Besides, progress towards an efficient vaccine has for long been thwarted by the development of strain-specific immunity resulting from the high level of polymorphism in the parasite populations (Arama & Troye-Blomberg, 2014). Thus, considering both phenotypic and genetic variations displayed by *P. falciparum* clinical isolates would be crucial for the screening and validation of new vaccine targets (WAMIN, 2016). Another challenge in developing vaccines against malaria is the complexity of the parasite life cycle, involving distinct stages targeted by different immune system arms so that antibodies against

the sporozoite stage are completely different from those against the merozoite. This is because of the expression of stage-specific antigens (Hoffman, Vekemans, Richie, & Duffy, 2015a), therefore, focusing on developing stage-specific vaccines, preferably prior to the development of transmissible stages, would be a great step toward malaria elimination.

2.3. *PLASMODIUM FALCIPARUM* BLOOD STAGE: A CAPTIVATING VACCINE TARGET

Human infection by *P. falciparum* is initiated by the invasion of hepatocytes, which leads to the release of asexual blood-stage parasites (merozoites), responsible for the malaria clinical manifestations. Sexual stages, which are crucial for maintaining the disease transmission are generated during the blood stage. Blood stage vaccines, which could neutralize merozoites before the invasion, would likely prevent the disease progression and block transmission as well (WAMIN, 2016). Thus, focusing on parasite proteins required for erythrocyte invasion as primary vaccine targets would be a good strategy to tackle the malaria burden (Crompton, Pierce, et al., 2010). However, this approach is challenged by the ever-evolving nature of the host immune response in adaptation to the highly redundant ligand-mediated pathways used for erythrocyte invasion (Cowman & Crabb, 2006; Gaur, Mayer, & Miller, 2004). As a result, vaccines for blocking erythrocyte invasion would likely need to target multiple parasite ligands and be able to block different *P. falciparum* clones, hence, the need for a better understanding of the biology of erythrocyte invasion.

2.4. BIOLOGY OF MALARIA PARASITES

Malaria is a vector-borne disease transmitted by the female *Anopheles* mosquito and caused by apicomplexan parasites of the genus (Snow, Guerra, Noor, Myint, & Hay, 2005). In over 30 *Anopheles* species susceptible to transmitting the parasites, *A. gambiae, A. funestus* and *A. arabiensis* remain the major vectors in sub-Saharan Africa (Sinka et al., 2010). Four species specifically infect humans, namely, *P. falciparum, P. malariae, P. ovale* and *P. vivax*. *P. knowlesi*, until recently known to be restricted to non-human primates, can occasionally cause symptomatic malaria in humans (Antinori, Galimberti, Milazzo, & Corbellino, 2013). parasites are obligate intracellular pathogens presenting a complex life cycle, completed through infection of two alternate hosts, the female *Anopheles* vector and the human vertebrate host. life cycle is typically completed through a sexual reproduction (sporogony) in the mosquito vector followed by an asexual multiplication (schizogony) in the vertebrate host. In humans, the infection starts with an asymptomatic stage following hepatocytes' invasion by the parasite's sporozoite form (Prudencio, Mota, & Mendes, 2011). Sporozoites, inoculated through the mosquito bite, primarily infect the host hepatocytes following their migration to the liver through the bloodstream. Except for *P. vivax* and *P. ovale*, which sometimes enter into dormant stages (hypnozoites) that can cause relapses, the parasite liver stage is monocyclic. Upon hepatocyte invasion, the parasites develop and mature into pre-erythrocytic schizonts, from which the erythrocytic forms of the parasite, merozoites, are released in the bloodstream 9-15 days post-infection (Antinori, Galimberti, Milazzo, & Corbellino, 2012). To maintain a persistent infection and develop transmission stages, *P. falciparum* must invade and multiply in the host erythrocytes. The clinical manifestations result from the cyclical invasion of the host erythrocytes, which triggers the host immune system. During this active phase of asexual multiplication, a small proportion of parasites develop into sexual stages, male and female gametocytes, which are taken up by

an *Anopheles* mosquito during a blood meal (Figure 2.1). Once in the mosquito gut, both gametocytes are activated to respectively become male and female gametes, which, upon fertilization, form a zygote to start the sporogonic cycle. Henceforth, the zygote develops into elongated and motile forms, the ookinetes, which invade the mosquito midgut where they mature into oocytes containing large numbers of sporozoites. Following oocyst rupture, the sporozoites migrate to the mosquito salivary glands, ready to infect a new host and perpetuate the life cycle.

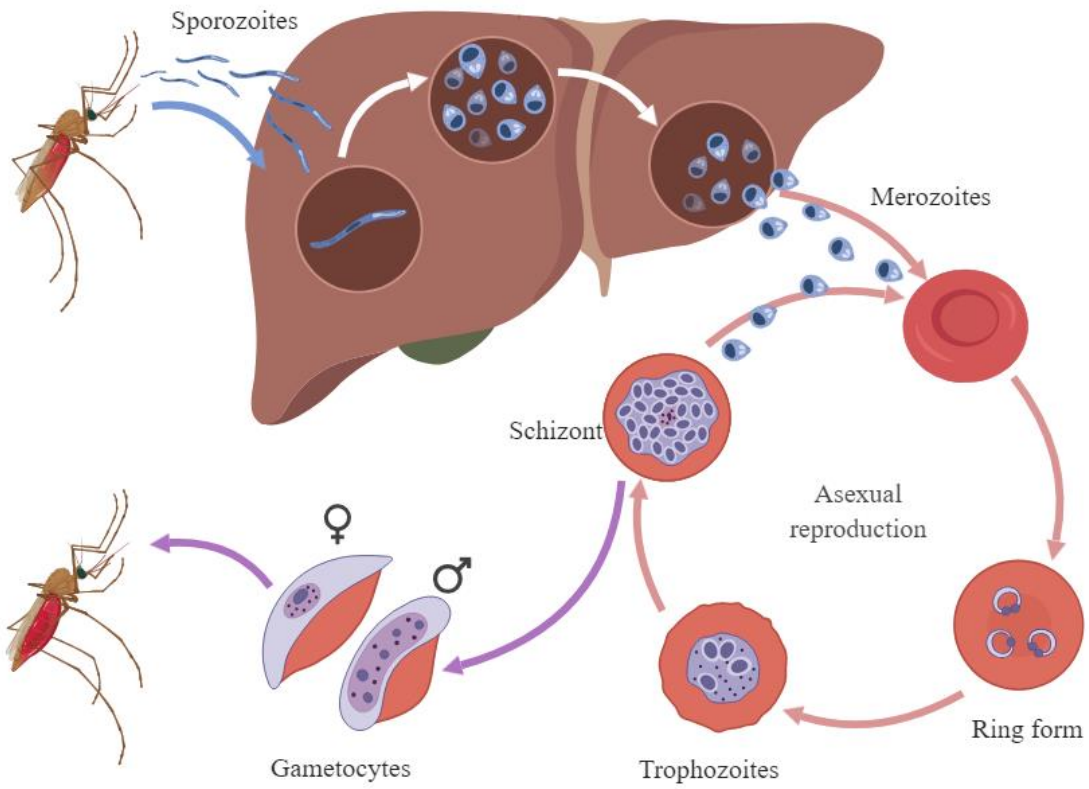

Figure 2.1: *Plasmodium falciparum* life cycle. The infection begins with the inoculation of sporozoites, the infective form of the liver cells, during the blood meal of an infected mosquito. The infective sporozoites then migrate from the injection site to the neighbouring blood vessels where they find their way to the host liver. In the liver, the sporozoite passes through the Kupffer cells and manage to infect the hepatocytes where they develop into pre-erythrocytic schizonts, which, upon maturation release the erythrocyte infective parasite forms, the infective merozoites. Once released in the bloodstream, the merozoites specifically infect the host erythrocytes, where they develop into rings, trophozoites and finally schizont parasites through an asexual replication process termed schizogony. Daughter merozoites (16 to 32) are periodically released (~ every 48 hours) into the bloodstream to infect new erythrocytes and the cycle goes on. During this period, some parasites develop and mature into sexual stage parasites, gametocytes, which are then taken up by the mosquito vector during another blood meal. In the mosquito gut, the gametocytes are activated and the mosquito cycle follows as described above upon fertilization of the female macrogamete by a male microgamete. Figure was generated from www.biorender.com

2.5. *PLASMODIUM FALCIPARUM* ASEXUAL REPLICATION

The clinical manifestations as well as the burden of mortality associated with malaria result from the asexual reproduction of the merozoite. This stage, crucial for the parasite's survival, is characterized by series of invasion and re-invasion of the human erythrocytes, a stage during which, the merozoite is periodically exposed to the immune system arms (Wright & Rayner, 2014). To successfully invade erythrocytes and to escape the immune pressure, *P. falciparum*'s merozoites deploy an array of ligands, derived from specific secretory organelles such as micronemes, rhoptries and so forth.

2.5.1. MEROZOITE INTERNAL ORGANIZATION

Merozoites, the blood-stage invasive forms of , are pear-shaped single cells, covered in a fibrillary coat of surface proteins and responsible for the parasite's intraerythrocytic replication (Figure 2.2). Besides the usual eukaryotic organelles, essential for protein synthesis and trafficking, the merozoite contains specialized secretory organelles typical to Apicomplexan parasites. These organelles gradually release their contents to drive processes leading to erythrocyte invasion and the parasite's intracellular development (Gaur & Chitnis, 2011). The major organelles comprise: (i) the micronemes, which are bottle-shaped organelles, with distinguishable bulb and neck (Bannister et al., 2003; Lal et al., 2009). (ii) The rhoptries, which are elongated club-shaped glands (Bannister, Hopkins, Fowler, Krishna, & Mitchell, 2000; Counihan, Kalanon, Coppel, & de Koning-Ward, 2013), consisting of two distinct regions, an apical (rhoptry neck) and a distal lipid-rich end, the rhoptry bulb (Bannister et al., 2003; Counihan et al., 2013; Duraisingh, Triglia, et al., 2003). (iii) The dense granules, named after their apparent density under electron microscopy, contain proteins seemingly involved in the host cell remodeling (Counihan et al., 2013;

Mercier, Adjogble, Daubener, & Delauw, 2005), (iv) and the exonemes and mononeme, the most recently discovered *P. falciparum* secretory organelles (Janse & Waters, 2007; Singh, Plassmeyer, Gaur, & Miller, 2007b; Yeoh et al., 2007). While mononeme is a single fibre-like organelle, lying under the merozoite inner membrane complex (Singh et al., 2007b), the exonemes, however, share a similar shape with dense granule (Yeoh et al., 2007).

2.5.2. *P. FALCIPARUM* ERYTHROCYTE INVASION-RELATED PROTEINS

2.5.2. a. Merozoite surface proteins

The bulk of the merozoite surface proteins (MSPs) are glycophosphatidylinositol (GPI) anchored proteins associated with other partner proteins, integral membrane proteins or peripherally-associated proteins (Gilson et al., 2006). Highly expressed on the merozoite surface, the majority of the MSPs present structures (e.g. Cysteine-rich EGF domains) predicted to be involved in early invasion steps (Cowman, Tonkin, Tham, & Duraisingh, 2017). MSPs are categorized into three different classes, GPI anchored, transmembrane (TM) domain-containing and the surface proteins that have neither GPI-anchored nor TM-domain (Gilson et al., 2006). Majority of the GPI-anchored MSPs undergo extensive processing events to facilitate their functional interaction with other invasion related proteins (Beeson et al., 2016). For instance, MSP1 processing facilitates merozoite egress through Spectrin binding (Das et al., 2015), but also, the formation of an invasion complex in association with other binding partners (Paul et al., 2018). However, MSP1 is predicted to play a role in the food vacuole biogenesis (Dluzewski et al., 2008) through its smallest processed fragment ($MSP1_{19}$). Unlike MSP1, the function of MSP2 is yet to be defined (Boyle et al., 2014). Other GPI-anchored MSPs include; MSP4, 5 and 10, but also Pf12, 38

and 92. Besides, although MSP4 and 10 share the same structural conformation with MSP1 (Black, Wang, Hibbs, Werner, & Coppel, 1999; Black, Wang, Wu, & Coppel, 2003), only MSP10 is shown to undergo processing, whist MSP4 is internalized in the infected erythrocyte (Black et al., 2003; Boyle et al., 2014). Consequently, MSP10 is involved in merozoite invasion through binding to neuraminidase, trypsin and chymotrypsin sensitive erythrocyte receptor, whilst MSP4 is predicted to play a post-invasion role (Garcia et al., 2007; Puentes et al., 2005). MSP5 shares related attributes with MSP4 (Wu, Black, Wang, Hibbs, & Coppel, 1999), however, its function is yet to be well defined (Beeson et al., 2016). Other GPI-anchored MSPs, such as Pf12, Pf38 and Pf92, are characterized by the presence of a 6-Cys motif, which has been shown to modulate the host immune response (Healer et al., 1997; Molina-Cruz et al., 2013). So far, only Pf92 has been shown to play a role during the invasion process, through active recruitment of Factor H causing downregulation of the complement-mediated pathway (Kennedy et al., 2016). Along with GPI-anchored MSPs, a large surface of the merozoite is coated by peripherally-associated proteins such as MSP3/MSP6, MSP7, the glutamate-rich protein (GLURP), the serine-repeat antigen (SERA) family protein. MSP6, also known as MSP3.2, shares common features with MSP3 which constitutes one of the largest multigene families expressed on the merozoite surface, with eight members (MSP3.1-MSP3.8) (Singh et al., 2009). Both MSP3 and 6 have been reported to interact with the MSP1-derived complex during the initial step of erythrocyte invasion (Kauth et al., 2006; Koussis et al., 2009a). MSP7, another membrane-associated protein expressed by a multigene family with five other MSP7-related proteins (MSRPs) (Gardner, Hall, et al., 2002; Mello et al., 2002), is characterized by the presence of an unstructured and acidic internal domain (Kadekoppala & Holder, 2010). MSP7 is translated as a 42 kDa precursor, which undergoes two successive processing events (Pachebat et al., 2007), yielding a 20 and 33 kDa fragments ($MSP7_{20}$ and $MSP7_{33}$). $MSP7_{33}$ is further processed into

a 22 and a 19 kDa fragments ($MSP7_{22}$ and $MSP7_{19}$) (Pachebat et al., 2007; Pachebat et al., 2001), which have been shown to be associated to the MSP1 multiprotein complex (Kadekoppala & Holder, 2010). Functionally, MSP7 has recently been shown to interact with the erythrocyte P-selectin receptor during the invasion (Perrin, Bartholdson, & Wright, 2015). Another *P. falciparum* multigene MSP family is the SERA family proteins which comprise 9 members (SERA1-9) (Gardner, Shallom, et al., 2002; Gardner et al., 1998), characterized by the presence of serine or cysteine catalytic domains (Hodder et al., 2003). Of all SERAs, SERA5 (P126), is the only member that undergoes proteolytic processing from a 120 kDa precursor to 47, 56 and 18 kDa, named as P47, P56 and P18, respectively (Aoki et al., 2002; Fairlie et al., 2008). From there, P56 is further processed into 50 and 6 kDa, prior to merozoite release (Debrabant & Delplace, 1989; Li, Matsuoka, Mitamura, & Horii, 2002; Li, Mitamura, Fox, Bzik, & Horii, 2002). SERA3 processing has also been reported in the liver stage of *P. berghei* (Schmidt-Christensen, Sturm, Horstmann, & Heussler, 2008), however, a clear function of SERA family proteins is yet to be defined. GLURP is a mainstay gene for molecular genotyping of *P. falciparum* isolates (Kumar et al., 2014; Mwingira et al., 2011), and considered as an excellent vaccine candidate though its real function is yet to be elucidated (Beeson et al., 2016; Theisen et al., 1998).

2.5.2. b. Microneme-derived proteins

With an estimated size of about 75 x 150 nm (Carruthers & Tomley, 2008), *P. falciparum* micronemes are located at the apical end of the merozoite. Along with the rhoptries, the micronemes are part of the merozoite major secretory organelles, discharging their contents in a timely manner during the invasion. Micronemal proteins play crucial functions throughout the invasion process, notably with the establishment of the tight junction through the apical membrane protein 1 (AMA1) (Lamarque et al., 2011). AMA1, initially translated

as an 88 kDa protein, is processed into smaller fragment of 66 kDa prior to its relocation to the merozoite surface (Narum & Thomas, 1994), where it interacts with the rhoptry neck protein (RON) complex to form the tight junction (Srinivasan et al., 2011). Housed among other invasion-related proteins in the micronemes are, members of the erythrocyte binding like antigens (EBAs/EBLs), including, PfEBA140, PfEBA165, PfEBL175 and PfEBA181 and PfEBL1 (Figure 2.2) (reviewed in (Tham, Healer, & Cowman, 2012)), as well as proteins containing specific domains such as the thrombospondin-related anonymous protein (MTRAP), thrombospondin related apical merozoite protein (PTRAMP), and surface protein containing an altered thrombospondin repeat domain, SPATR (Baum et al., 2006; Cowman, Berry, & Baum, 2012). Additionally, two of the major proteins currently under consideration as potential components of a multiplex malaria vaccine (Healer et al., 2019), namely the *P. falciparum* PfRh5 interacting protein (PfRipr) and the cysteine-rich protective antigen (PfCyRPA) are also shown to be located in the micronemes (L. Chen et al., 2011; Reddy et al., 2015).

2.5.2. c. Rhoptry-derived proteins

The *P. falciparum* rhoptry organelles play a crucial role in erythrocyte invasion and release their contents throughout the invasion process (Counihan et al., 2013). Rhoptry compartments contain specific sets of protein classes (reviewed in (Counihan et al., 2013)). rhoptry–neck proteins are generally conserved within the genus as well as in other apicomplexan parasites (Alexander, Arastu-Kapur, Dubremetz, & Boothroyd, 2006; Alexander, Mital, Ward, Bradley, & Boothroyd, 2005; Besteiro, Michelin, Poncet, Dubremetz, & Lebrun, 2009; Cao et al., 2009; Lebrun et al., 2005; Morahan, Sallmann, Huestis, Dubljevic, & Waller, 2009; Proellocks et al., 2009; Straub, Cheng, Sohn, & Bradley, 2009). These proteins are mainly involved in early steps of erythrocyte invasion such as the

random merozoite attachment and tight junction formation (TJ) (Counihan et al., 2013). Rhoptry-neck proteins that have been shown to be involved in merozoites invasion include the reticulocyte binding like homologues (Rhs) family proteins, namely, PfRh1, PfRh2a, PfRh2b, PfRh4 and PfRh5. Antibodies to members of this family have been shown to block merozoite invasion (Aniweh et al., 2016; Chiu et al., 2014; Tham et al., 2009). Important for the process of merozoite invasion is the formation of protein complexes. PfRh5 has been shown to be involved in interactions with PfCyRPA, PfRipr and PfP113 (Baum et al., 2009; L. Chen et al., 2011; Crosnier et al., 2011; Hayton et al., 2008; Reddy et al., 2015; L. E. Rodriguez et al., 2008; Rodriguez, Lustigman, Montero, Oksov, & Lobo, 2008), and, with PfRhopH3, a member of the *P. falciparum* high molecular weight protein complex (PfRhopH) localized in the rhoptry-bulb (Prakash et al., 2017). Among other rhoptry-neck proteins are the so-called rhoptry neck proteins (PfRON-1, -2, -3, -4, -6 and -12), and the *P. falciparum* asparagine rich protein (PfAARP), the *P. falciparum* rhoptry associated membrane antigen (PfRAMA) and Pf34. A complex involving PfRON-2, -4, -5 and AMA1 has been shown to be crucial at the TJ (Alexander et al., 2005; Besteiro et al., 2009; Gilson & Crabb, 2009; Richard et al., 2010), with a peptide that interrupted this complex shown to impair merozoite invasion. So far, Pf34 is the only rhoptry-neck protein known to harbour a GPI anchor (Gilson et al., 2006; Proellocks et al., 2007), however, its functional role or processing events is poorly understood. PfAARP has also been shown to be expressed at late schizont stage and is localized at the rhoptry-neck and transported on the merozoite surface where it interacts with an unknown receptor (Wickramarachchi, Devi, Mohmmed, & Chauhan, 2008). Unlike rhoptry-neck proteins, rhoptry-bulb proteins, play wider functional roles from initial attachment to the parasitophorous vacuole formation (Counihan et al., 2013; Kats, Black, Proellocks, & Coppel, 2006). The most widely characterized rhoptry-bulb proteins include the high molecular weight rhoptry protein complex (RhopH), the

rhoptry associated proteins (RAP1, 2 and 3), and RAMA (Anand et al., 2016; Counihan et al., 2017; Howard, Narum, Blackman, & Thurman, 1998; Ito, Schureck, & Desai, 2017; Lopez et al., 2004; Pinzon et al., 2008; Reyes, Patarroyo, Vargas, Rodriguez, & Patarroyo, 2007; Richard et al., 2009; Sam-Yellowe & Perkins, 1991; Sam-Yellowe, Shio, & Perkins, 1988; Sherling et al., 2017; Wickramarachchi et al., 2008). The *P. falciparum* high molecular weight protein complex, formed by RhopH1, 2 and 3, is discharged from the invading merozoite following initial contact with the erythrocyte surface (Sam-Yellowe & Perkins, 1991; Sam-Yellowe et al., 1988). RhopH2 and 3 are both encoded by single genes, while RhopH1 is encoded by a multigene family, namely, *clag2, clag3.1, clag3.2, clag8 and clag9* (Kaneko et al., 2001). So far, of all RhopH proteins, only RhopH3 has been shown to play a functional role in invasion through interaction with the human cyclophilin B (Prakash et al., 2017). RAMA is so far the only rhoptry-bulb protein harbouring a GPI tail (Topolska, Lidgett, Truman, Fujioka, & Coppel, 2004). Prior to schizont rupture, RAMA is proteolytically processed from a 170 kDa precursor to 60 kDa (p60), which, upon egress, binds to an unknown glycosylated erythrocyte receptor (Pinzon et al., 2008; Topolska et al., 2004). Furthermore, the processed form of RAMA has been shown to be part of an invasion-related multimolecular lipid raft protein complex including RhopHs (Pinzon et al., 2008). Rhoptry associated proteins (RAP1-3) are also involved in an invasion-related complex, known as the low molecular weight protein complex involving RAP1 and 2, which has been implicated in severe malarial anaemia (Sterkers et al., 2007). However, unlike RAP1 and 3, RAP2 erythrocyte binding partner has been identified as CD147 (Basigin) (Zhang et al., 2018). In addition to sharing the same erythrocyte receptor, both RAP2 and Rh5 are refractory to genetic disruption (Baum et al., 2009; Zhang et al., 2018), which make them excellent targets for inclusion in a potential malaria vaccine.

2.5.2. d. Dense-granule-derived proteins

First reported in *P. knowlesi*, the dense granules are approximately 80 nm in diameter and have been named as such because of their appearance under electron microscopy (Bannister, Butcher, Dennis, & Mitchell, 1975). These electron-dense organelles are uniformly distributed within the merozoite's cytoplasm and are believed to discharge their contents during the early intra-erythrocytic development, with the establishment of pores into the parasitophorous vacuole membrane, just after the invasion (Bannister et al., 1975; Culvenor, Day, & Anders, 1991). Among other proteins secreted in the parasitophorous vacuole are the ring infected erythrocyte surface antigen (RESA) (Culvenor et al., 1991), and the ring infected membrane antigen (RIMA), a small protein of 14 kDa transported into the erythrocyte along with the invading merozoite (Gardner, Hall, et al.; Trager, Rozario, Shio, Williams, & Perkins, 1992).

2.5.2. e. Exonemes-derived proteins

P. falciparum exonemes, first reported by Yeoh and colleagues, are electron-dense organelles harbouring protease-like proteins involved in merozoite egress from the infected erythrocyte (Yeoh et al., 2007). *P. falciparum* subtilisin-like proteins 1, 2 and 3 (PfSUB1-3) have been identified to be hosted in these organelles and to be involved in a wide range of events during the invasion. Of all three PfSUB proteins, only PfSUB1 is reported to be essential for the parasite's survival and is involved in egress through proteolytic processing of PfSERA5 (Yeoh et al., 2007). PfSUB1 inhibition has been associated with a dose-dependent antibody inhibition of egress and reduced invasiveness of the released merozoites (Yeoh et al., 2007). PfSUB2 has been shown to shed merozoite surface antigens during invasion (Olivieri et al., 2011);(Green, Hinds, Grainger, Knuepfer, & Holder, 2006), while PfSUB3, reported being non-essential in *P. falciparum*, is expressed in both sexual and

asexual stages as well as the sporozoites. Altogether, PfSUB proteins are involved in the maturation of other PfSERA proteins also necessary for egress (Arastu-Kapur et al., 2008; Harris et al., 2005; Koussis et al., 2009b).

2.5.2. f. Mononeme-derived proteins

Erythrocyte invasion by *P. falciparum* merozoites is facilitated by the proteolytic processing of invasion related genes. One of the protease families involved in this process is the *P. falciparum* rhomboid protease (PfROM) family. In *P. falciparum*, the ROM proteases have been shown to be housed in a single merozoite organelle, the mononeme (Singh, Plassmeyer, Gaur, & Miller, 2007a). Unlike PfSUB proteins, which act before merozoite egress, PfROM proteins have been shown to act following egress through the cleavage of microneme and rhoptry-derived proteins, henceforth, facilitating the invasion process (Singh et al., 2007a).

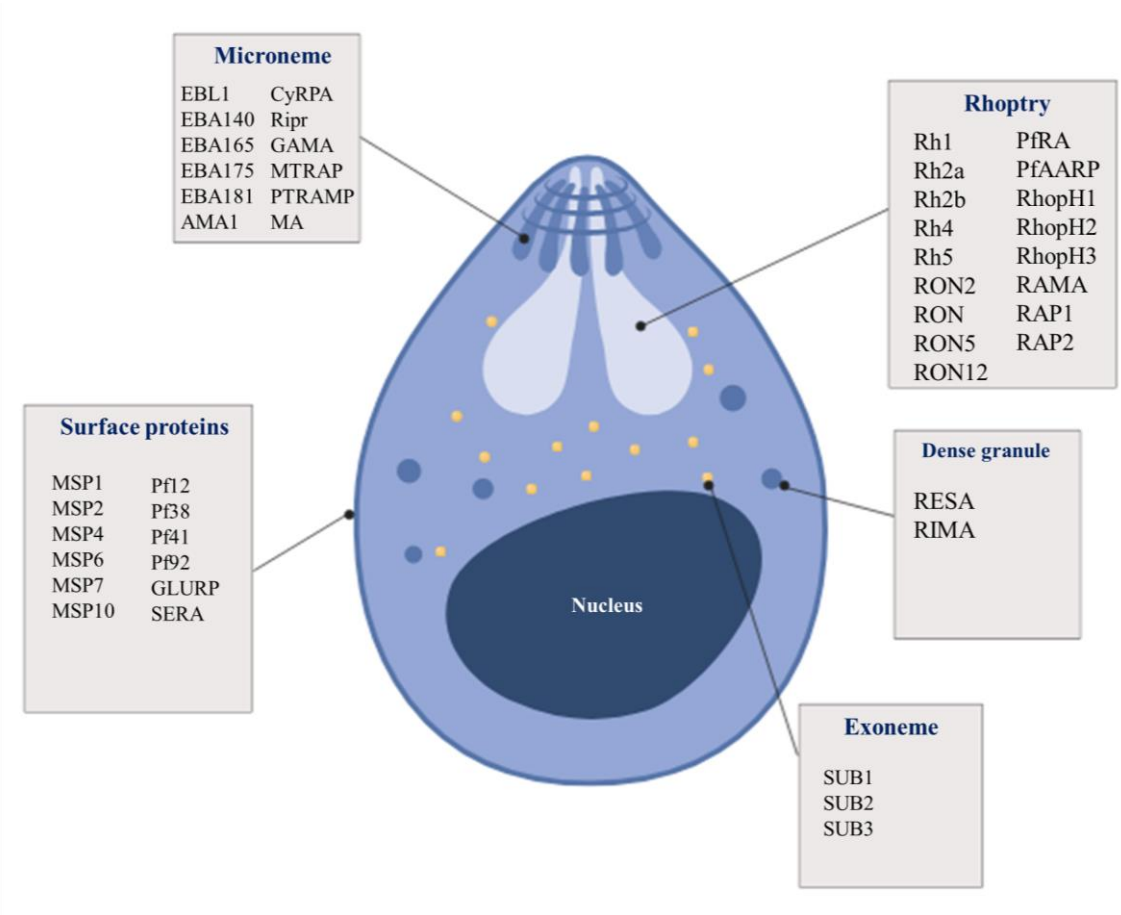

Figure 2.2: *Plasmodium falciparum* merozoite internal organization showing the rhoptries, micronemes, dense granules, exonemes and other invasion-related proteins. Figure was generated from www.biorender.com.

2.5.3. NATURAL ANTIBODY RESPONSES TO *P. FALCIPARUM* INVASION-RELATED ANTIGENS

As a result of their abundance on the merozoite surface, MSPs represent the prime targets of the host immune response during the blood stage of the parasite's life cycle. Consequently, as an immune evasion mechanism, *P. falciparum* employs different diversity-generating strategies to circumvent the action of host-mediated antibody responses (Wright & Rayner, 2014). The most commonly used strategies deployed by the parasites include i) the surface-expression of distinct variants of the same antigen, hence the multi-allelic signature harboured by most of the MSP genes or ii) the expression of different members of a multigene family protein such as the 6-cysteine proteins (Wright & Rayner, 2014). Even though there is a lack of sterile immunity against the blood stage of *P. falciparum*, MSPs are known to trigger strong antibody responses in long-term malaria-exposed individuals. Antibodies against MSPs have been shown to mediate phagocytosis events and to enhance anti-disease protection through merozoite opsonization (Chiu et al., 2015; D. L. Hill et al., 2013; Osier et al., 2014). Dent and colleagues showed that protective antibodies against *P. falciparum* MSPs are gradually acquired in children living in endemic areas as compared to the full antibody repertoire recognized by adults (Dent et al., 2015). Another study, by Osier and colleagues, reported an inverse correlation between anti-MSP IgGs seroprevalence and the occurrence of malaria-related clinical manifestations in Kenyan children, where protection was more pronounced in children presenting high antibody titers against different MSP antigens (Osier et al., 2008). However, the immunogenicity of most MSPs seems to be restricted in a much narrowed window of epitopes as seen in the case of SERA5, the predominantly expressed member of its family, where only antibodies against the N-terminal fragment were able to trigger adequate protection to the disease occurrence (Aoki et al., 2002). However, as earlier reported in a clinical trial conducted in Gabon (Mordmuller et

al., 2010), the already existing or developing antibody responses to most MSP antigens constitutes a major hindrance in assessing the efficacy of vaccine candidates derived from these antigens, hence the need for well-designed clinical trials approaches to circumvent these challenges. Unlike MSPs, organelles-derived *P. falciparum* antigens, mainly members of the EBA and Rh families, are known to be actively involved in erythrocyte invasion with already established erythrocyte interacting receptors for most of them (Tham et al., 2012). Because of their crucial roles in the invasion, these proteins represent key invasion inhibitory vaccine targets which, could provide a strong immunity to the recipient. Intriguingly, this, once again is compromised by another immune evasion mechanism developed by the parasite, namely the so-called alternative invasion pathways, defined by the parasite's ability to commutate the usage of these ligands in a highly coordinated manner (Lopaticki et al., 2011). However, in spite of their functional redundancy, members of these family proteins are naturally targeted by the host humoral response. PfEBA antigens, namely, PfEBA175, PfEBA140 and PfEBA181, have been shown to trigger high titers of protective antibodies in a cohort of children in Papua New Guinea (Richards et al., 2010). The same study reported an antigen-dependent production of immunoglobulin (Ig) subclasses and this was strongly correlated to age and parasite density (Richards et al., 2010). However, though these high antibody titers provided both protection against symptomatic malaria and reduction of the parasite density, this did not prevent parasite reinvasion of erythrocytes (Richards et al., 2010), therefore, confirming earlier work that reported these genes as non-essential for erythrocyte invasion, following genetic disruption experiments (Gilberger et al., 2003; Maier, Baum, Smith, Conway, & Cowman, 2009; Reed et al., 2000; Thompson, Triglia, Reed, & Cowman, 2001). On the other hand, of all PfRh proteins, only PfRh4 and 5 have been shown to interact with known erythrocytes receptors, namely the human complement receptor 1 (CR1) and basigin, respectively (Crosnier et al., 2011; Tham et al., 2010).

However, whilst only PfRh5 has been shown to play an essential invasion-related function (Baum et al., 2009; Crosnier et al., 2011; Hayton et al., 2008), both antigens have been shown to trigger levels of antibody responses enough to limit the occurrence of malaria symptoms as well as high density parasitemia in Papua New Guinean children (Reiling et al., 2012; Tran et al., 2014). Additionally, despite the report of poor immunogenicity associated to PfRh5 (Douglas et al., 2011), studies from Mali and Papua New Guinea have respectively shown this immunogenicity to be gradually acquired in naturally exposed children, but also to be associated to a delay in the occurrence of symptomatic malaria in children presenting anti-PfRh5 IgGs as compared to non-responders (Chiu et al., 2014; Tran et al., 2014). However, because of the ever-evolving immune evasion strategies developed by the malaria parasite, developing an effective blood-stage vaccine for this life-threatening disease necessitates considering both the phenotypic and genotypic diversity of the parasite. Therefore, the best vaccine approach that will likely provide a sterile immunity, if possible, in addition to including targets able to trigger cross-strain immunity, should also be able to block different invasion pathways used by the parasite. So far, of all micronemes and rhoptries proteins reported to play roles in the invasion, only PfAMA1 and PfRh5 have been shown to be transiently used in this process and to be refractory to genetic disruption as well. Interestingly, while the former is highly polymorphic within the parasite's population, there is a report showing a positive correlation between the amplitude of the anti-Rh5 response and the presence of high titers of AMA1-specific IgG levels (Tran et al., 2014). This calls for more adequate techniques for the screening of invasion blocking vaccine candidates but also the need for well-designed human clinical trials for assessing vaccine efficacy in endemic areas.

2.5.4. RED BLOOD CELL INVASION AND INVASION PATHWAYS

Erythrocyte invasion is a crucial step for parasite survival. The invasion process occurs in four distinct steps involving ligands mainly derived from the secretory organelles (Figure 2.3). This four-step process is thought to be initiated by the weak reversible interactions by the parasite glycophosphatidyl inositol (GPI)-anchored proteins such as merozoite surface proteins (MSPs) (Beeson et al., 2016). The discharge of micronemal and rhoptry ligands have been shown to herald interactions necessary for the formation of the tight junction (TJ) (Singh, Alam, Pal-Bhowmick, Brzostowski, & Chitnis, 2010). The TJ, which is a commitment to invasion, is established when the merozoite opposes its apical end in contact with the erythrocyte. The initiation of the TJ formation involves both microneme and rhoptry-derived proteins (Harvey, Gilson, & Crabb, 2012; Tham et al., 2012), mainly EBA and the Rh proteins (Cowman & Crabb, 2006; Gaur et al., 2004). Members of these two protein families interact in a synergistic manner during erythrocyte invasion (Lopaticki et al., 2011) and depending on the ligand-receptor interaction involved, merozoites can invade erythrocytes using various pathways (Koch & Baum, 2016). Ligands mediating these invasion pathways, each bind to a specific receptor on the erythrocyte surface and are differentially expressed in clinical isolates from different endemic areas (Baum, Pinder, & Conway, 2003b; Bowyer et al., 2015; Lantos et al., 2009; Lobo et al., 2004; H. E. Mensah-Brown et al., 2015). In malaria research, erythrocyte invasion by *P. falciparum* is categorized as occurring via two major pathways: the sialic acid (SA)-dependent and the SA-independent, based on the parasite's reliance on SA residues present on the erythrocytes' glycophorin proteins (Hadley et al., 1987). Accordingly, *P. falciparum* phenotypic diversity has for long been characterized based on these invasion pathways.

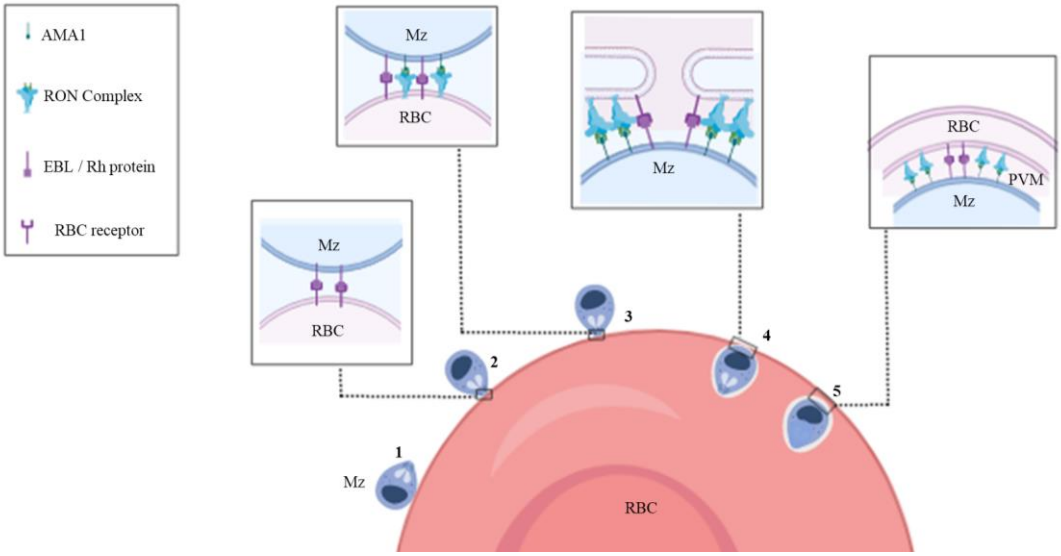

Figure 2. 3: The process of erythrocyte invasion by *P. falciparum* merozoite. Erythrocyte invasion by *P. falciparum* merozoite (Mz) occurs in four distinct steps. (1) Mz released from bursting schizont first interacts with surrounding uninfected erythrocytes through a reversible process termed attachment. This attachment is thought to particularly involve MSPs and to trigger downstream signals that initiate the release of invasion-related ligands from the apical organelles. (2) Following the initial contact with an uninfected erythrocyte, the Mz reorientates itself so that its apical end is adjacent to the erythrocyte membrane. This step is believed to facilitate the establishment of ligand-receptor interactions between the parasite involving members of the PfEBL and PfRh family proteins, but also to cause the deformation of the host cell membrane to further the parasite's commitment to invasion. (3) Upon parasite reorientation, the next step of invasion is the establishment of the tight junction involving parasites complexes such as the AMA1-RON complex. This step is immediately followed by the parasite's ingress (4) during which the Mz actively invades the erythrocyte using its actinomyosin motor. Upon completion of the invasion process, the Mz is enveloped in a newly formed compartment, termed the parasitophorous vacuole, which results from partly from the erythrocyte membrane associated with parasite proteins thought to be mainly derived from the rhoptries figure was generated from www.biorender.com.

2.5.5. *PLASMODIUM FALCIPARUM* PHENOTYPIC DIVERSITY

The most widely used approach for characterizing merozoite phenotypic diversity involves the use of enzymes to restrict the repertoire of erythrocyte surface receptors. These enzymes include neuraminidase, which cleaves SA residues (Hadley et al., 1987) and the proteases trypsin and chymotrypsin which cleave particular sites on peptide backbones (WAMIN, 2016). SA-dependent invasion is mainly mediated by neuraminidase sensitive binding of PfEBA175, PfEBL1, PfEBA140, PfEBA181, PfRh1, PfRh2a and PfRh2b ligands while the SA-independent pathway relies on the binding of PfRh4 or PfRh5 to neuraminidase resistant receptors present on the surface of the erythrocyte (Baum et al., 2003b; Tham et al., 2012). The combinatory usage of these enzymes' enabled the characterization of some ligand interacting receptors, including glycophorin (GYP) A, GYPB, GYPC, complement receptor (CR) 1 and the basigin receptor, which respectively bind to the PfEBA175, PfEBL1, PfEBA140, PfRh4 and PfRh5 merozoite ligands (Awandare et al., 2011; Spadafora et al., 2010; Tham et al., 2012). With the exception of PfRh5, the only known essential ligand involved in invasion (Crosnier et al., 2011; Douglas et al., 2011; H. E. Mensah-Brown et al., 2015), there is a degree of redundancy in ligand-receptor interactions during merozoite invasion (Beeson et al., 2016). Unlike enzymes that are more likely to cleave multiple receptors at the same time, the use of specific antibodies against the PfEBA and PfRh proteins has been shown to produce more reliable data with regards to the role of merozoite ligands involved in invasion (Anand et al., 2016; Aniweh et al., 2016; Badiane et al., 2013; Crosnier et al., 2011; Douglas et al., 2011; Patel et al., 2013; Reddy et al., 2014). However, this approach is challenged by the lack of standardized reagents for large-scale studies (WAMIN, 2016). Alongside the above-mentioned approaches, genetically engineered erythrocytes (Crosnier et al., 2016; Niang et al., 2014; Patel et al., 2013) as well as transgenic parasites with target disrupted genes (Crosnier et al., 2016; Wang et al., 2016) have been

used to study the reliance of merozoites on a particular ligand-receptor interactions during invasion. Altogether, these pioneering studies suggest that an efficient malaria vaccine should be able to address challenges associated with *P. falciparum* clinical isolates, which constitute the populations of interest in malaria research. However, unlike laboratory-adapted strains, only a few studies have focused on clinical isolates phenotypic characterization of clinical isolates, and though there are only a few studies characterizing *P. falciparum* clinical isolates phenotypic diversity, cross-study comparison of the data from these pioneering studies is impaired by their use of different protocols (Table 2.1) (WAMIN, 2016). Thus, combining large-scale phenotypic studies using standard protocols with transcriptomic and whole-genome analyses could facilitate the comparison of data from large-scale phenotype-genotype investigations (WAMIN, 2016).

Tableau 1Table 2. 1: Cross study comparison of pioneering using enzyme treatment to assess invasion phenotype of P. falciparum clinical isolates

Sample information					**Target erythrocytes**			**Assay set up**		
Author, year	Origin (s)	Numb of isolates	Cryopreservation	Culture adaptation	Blood group	Treatment	Labelling	Assay length	Parasite labelling	Analysis
(Okoyeh *et al.*, 1999)	India	15	Yes	Yes, Five cycles	A^+	N (50 U/mL) T (1 mg/mL)	No	24 hrs for 7 days	Giemsa stain	Light microscopy
(Baum *et al.*, 2003)	Gambia	38	No	No	O^+	N (20mU/mL) T (1 mg/mL)	Yes, FITC 4 ug/mL	48-65 hrs	Ethidium bromide	Fluorescent microscopy analysis
(Lobo *et al.*, 2004)	Brazil	14	Yes	Yes, Five cycles	A^+	N (100 mU/mL) T (19.4 mg/mL) C (1 mg/mL)	No	28 hrs for 7 days	Giemsa stain	Light microscopy
(Nery *et al.*, 2006)	Kenya	42	Yes	No	O^+	N (50 mU/mL) T (1 mg/mL) C (1 mg/mL)	No	24 hrs	Giemsa stain	Light microscopy
(Jennings *et al.*, 2007)	Senegal	17	No	No	O^+	N (66 mU/mL) T (1 mg/mL) C (1 mg/mL)	No	48-72 hrs	Giemsa stain	Light microscopy with a Miller graticule

Table 2. 1 continued: Cross study comparison of pioneering using enzyme treatment to assess invasion phenotype of *P. falciparum* clinical isolates

Sample information						**Target erythrocytes**		**Assay set up**		
Author, year	Origin (s)	Numb of isolates	Cryopreservation	Culture adaptation	Blood group	Treatment	Labelling	Assay length	Parasite labelling	Analysis
(Bei *et al.*, 2007)	Tanzania	11	Yes	No	O^+	N (66.7 mU/mL) T (1 mg/mL) C (1 mg/mL)	No	One cycle	Not indicated	Not indicated
(Deans *et al.*, 2007)	Kenyan	31	No	No	O^+	N (50 mU/mL) T (1 mg/mL) C (1 mg/mL)	No	24 hrs for 7 days	Giemsa stain	Light microscopy
(Lantos *et al.*, 2009)	Senegal	34	No	No	O^+	N (66 mU/mL) T (0.04 or 1 mg/mL) C (1 mg/mL) T (0.4 mg/mL) + N (66 mU/mL) T (0.4 mg/mL) + C (1 mg/mL)	No	Not precised	Giemsa stain	Light microscopy with a Miller graticule
(Gomez-Escobar *et al.*, 2010)	Gambia	263	No	No	O^+	N (20mU/mL) T (1 mg/mL) C (1 mg/mL)	Yes, FITC (15 ug/mL)	48-64 hrs	Ethidium bromide	Flow cytometry

Table 2. 3 continued: Cross study comparison of pioneering using enzyme treatment to assess invasion phenotype of *P. falciparum* clinical isolates

Sample information						**Target erythrocytes**		**Assay set up**		
Author, year	Origin (s)	Numb of isolates	Cryopreservation	Culture adaptation	Blood group	Treatment	Labelling	Assay length	Parasite labelling	Analysis
(Lopez-Perez *et al.*, 2012)	Brazil, Colombia and Peru	6 16 8	Yes	Yes, ~two weeks	A^+	N (100 mU/mL) T (10 mg/mL) C (2 mg/mL)	No	20 hrs	Giemsa stain	Light microscopy
(Badiane *et al.*, 2013)	Senegal	66	Yes	No	O^+	N (66.7 mU/mL) T (1 mg/mL) C (1 mg/mL) T (66.7 mg/mL) + C (1 mg/mL)	No	48 hrs	Giemsa stain and SYBR Green I	Light microscopy and Flow cytometry
(Mensah-Brown *et al.*, 2015)	Ghana	52	Yes	No	O^+	N (25 mU/mL) T (1 mg/mL) C (1 mg/mL)	Yes, DDAO-SE (20 µM)	48 hrs	SYBR Green I	Flow cytometry
(Bowyer *et al.*, 2015)	Ghana Guinea Senegal	34 12 21	Yes	No	O^+	N (25 mU/mL) T (1 mg/mL) C (1 mg/mL)	Yes DDAO-SE (20 µM)	48 hrs	SYBR Green I	Flow cytometry

This table summarizes the results from pioneering studies focusing on investigating the invasion phenotypes of *P. falciparum* clinical isolates from across various countries. In total 13 different studies involving 628 isolates collected from 10 different countries across the world. The table highlights the major variations in the protocols used in these studies including, the enzyme concentrations, the nature of isolates (Fresh or cryopreserved), the blood group of target erythrocytes, the length of assays and so on so forth. Keys: N: neuraminidase, T: trypsin, C: chymotrypsin, DDAO-SE: dichloro dimethyl acridin one succinimidyl ester, FITC: fluorescein isothiocyanate

CHAPTER THREE: SPECIFIC AIM ONE

3.1. SHORT TERM CRYOPRESERVATION AND THAWING PROTOCOLS HAVE MINIMAL EFFECTS ON *PLASMODIUM FALCIPARUM EX VIVO* INVASION PROFILE

Hypothesis 1: *Differences in cryopreservation and thawing protocols affect the true reflection of biological differences in parasite phenotypes and would further affect the comparison of large-scale data from areas of different endemicity.*

To address this hypothesis, invasion phenotyping assays were performed in *P. falciparum* clinical isolates of the same isogenic backgrounds at different time intervals. Cryopreserved isolates were thawed at different time points using distinct protocols and, for each batch of isolates, both the parasite multiplication rate and the invasion phenotype were compared to the freshly uncultured or short-term culture adapted isogenic isolates. Furthermore, the effect of short-term culture adaptation on the parasite genotypes and subsequent invasion phenotype was also assessed here. Results from these investigations are presented.

3.1.1. Abstract

Ex vivo phenotyping of *P. falciparum* erythrocyte invasion diversity could play a crucial role in the identification and down selection of potential malaria vaccine targets but is also a key indicator of the biological relationship of the host-parasite interface. However, direct processing of *P. falciparum* clinical isolates is challenged by the lack of appropriate laboratory settings in remote areas. As a result, cryopreservation has been used as a means of biopreservation of collected isolates for further analysis, although relevant information about its real effect on the parasites invasion phenotype is lacking. Here, we investigated the combined effect of short-term cryopreservation and thawing protocols on *P. falciparum ex vivo* invasion profile. *P. falciparum* clinical isolates of the same isogenic backgrounds were assessed for their invasion phenotypes prior to, and following cryopreservation at different time points for a maximum period of 12 months. In addition, we also assessed the effect of different thawing protocols on the parasites' early *in vitro* adaptation and subsequent invasion phenotype. Our findings indicate that natural *P. falciparum* infections mostly occur as polyclonal infections, as demonstrated here using the *msp-1* and *2* genes as molecular markers for parasite clonality. We also show that short-term culture adaptation selects for parasite clonality and could be a driving force for variation in invasion phenotypes as compared to *ex vivo* data where almost all parasite clones of a given isolate are present. Furthermore, our data suggest that cryopreserved isolates experience a delayed asexual replication during the early *in vitro* replicative cycle. However, there was no significant variation in invasion phenotype following short-term cryopreservation. Altogether, our data suggest that short-term cryopreservation of uncultured *P. falciparum* clinical isolates has a minimal effect on the parasites' invasion phenotypes as compared to their *ex vivo* phenotypes.

3.1.2. Introduction

P. falciparum clinical isolates are of great importance in understanding the molecular mechanisms governing the malaria pathogenesis. Thus, unravelling their biological features is essential for both therapeutic and preventive approaches. Despite the remarkable achievements in the control efforts for malaria elimination, progress towards disease eradication are thwarted by the lack of relevant data about the parasite's complex biology. Recently published data emphasized the importance of freshly collected isolates, being more clinically relevant for deciphering the nature of host-parasite interactions involved in malaria pathogenesis (WAMIN, 2016; Yap et al., 2019). *P. falciparum*, responsible for the most life-threatening forms of malaria, has a very sophisticated strategy for efficiently invading human erythrocytes and evading the host immune response (Cowman et al., 2017; Wright & Rayner, 2014).

Understanding the molecular mechanisms that interplay at the host-parasites interface would be a crucial move towards the identification as well as the down-selection of potential vaccine and drug targets against the parasite. *P. falciparum* invasion phenotyping assays represent a key step in the process of vaccine development and therefore necessitate the use of isolates clinically representative of the parasites *in vivo* form. This, emphasizes the relevance of conducting such assays during the first *in vitro* if not *ex vivo* replicative cycles of the parasites. Direct processing of clinical isolates requires advanced laboratory equipment, which is not always available in the field in remote areas, hence the need for cryopreserving the collected samples for further processing (WAMIN, 2016).

In the last decade, many laboratories reported data with regards to the invasion phenotypes of *P. falciparum* clinical isolates. However, cross-study comparison of these data is challenged by the use of different approaches to characterize such phenotypes (WAMIN,

2016). Bulk of these phenotypic data was collected from cryopreserved parasites (Lobo et al., 2004; Lopez-Perez et al., 2012; Nery et al., 2006; Okoyeh et al., 1999) while only a few were from uncultured *P. falciparum* clinical isolates (Baum et al., 2003b; Jennings et al., 2007; Lantos et al., 2009). Moreover, in some cases parasites were allowed to grow for at least five cycles *in vitro* prior to assay set up (Lobo et al., 2004; Lopez-Perez et al., 2012; Okoyeh et al., 1999), therefore providing room for clonal selection, if any.

Unlike laboratory strains, *P. falciparum* clinical isolates are most of the time representative of a population of different clones, presenting each intrinsic characteristic that could dictate their *in vitro* adaptability. Given that different clones of the same isolate express distinct versions of surface antigens (Cortés, 2008), it could be that different clones use different invasion pathways and only the major pathways used by individual clones of a given isolate will be reflected during invasion phenotyping experiments. For instance, PfEBA-175 expression level was shown to be positively correlated to invasion efficiency in neuraminidase-treated cells while the PfRh2b level was correlated with parasite multiplication rate (Nery et al., 2006). Moreover, differential expression of invasion-related genes in *P. falciparum* clinical isolates involving upregulation of PfRh1 expression was observed in cryopreserved parasites as compared to freshly isolated parasites from Kenya (Nery et al., 2006).

Alongside the cryopreservation, different laboratories may use different thawing protocols prior to the parasite *in vitro* culturing. There remains, therefore, an unaddressed question of whether cryopreservation and subsequent thawing protocols affect *P. falciparum* invasion phenotype, and if yes, to which extent. Furthermore, the consequences of variations in cryopreservation and thawing protocols in *P. falciparum in vitro* culture is an

underrepresented area in malaria research, especially with respect to parasite adaptation and subsequent invasiveness during *ex vivo* phenotyping assays.

Previous literature has reported similar *ex vivo* adaptation rates in pre-cryopreserved isolates (Bowyer et al., 2015) as compared to fresh clinical isolates (Gomez-Escobar et al., 2010). However, these conclusions were drawn from studies using isolates of different isogenic backgrounds, which are phenotypically and functionally distinct. Using parasites from the same isogenic backgrounds, this study aimed to investigate the effect of freeze-thaw protocols in *P. falciparum ex vivo* phenotyping and early *in vitro* adaptation. In so doing, we hoped to shed light on the influence of short-term culture adaptation or cryopreservation on the phenotype of *P. falciparum* clinical isolates as compared to their *ex vivo* data.

3.1.3. Materials and methods

3.1.3.1. Samples collection and processing

P. falciparum clinical isolates were collected from symptomatic children, aged between 2 to 14 years, visiting the LEKMA Hospital, in Accra between February 2017 and January 2018. The study was approved by the Noguchi Memorial Institute for Medical Research (IRB00001276) and the Ghana National Health Service Ethical Review Boards (GHC-ERC: 005/12/2017). For all children, consent forms were endorsed by the parents or guardians. Samples were collected in ACD vacutainers (BD Biosciences) and processed within two hours following collection. Upon arrival to the laboratory, the infected erythrocytes were separated from the leucocytes through centrifugation at 2000 rpm and washed twice with RPMI1640 medium (Sigma). About 200 µL of packed erythrocytes were put straight in culture, while the remaining of the sample was frozen in glycerolyte following the standard protocol (EVIMalaR, 2013) and stored in liquid nitrogen. Frozen vials, ~500 µL each, were

revived at different time intervals using two distinct sodium chloride-based protocols. Vials were thawed using either a two-step protocol (12% NaCl and 1.6% NaCl) or a three-step protocol (12% NaCl, 1.8% NaCl and 0.9% NaCl supplemented with 0.2 % Glucose) as per standard procedure (EVIMalaR, 2013). To minimize the effect of possible confounders, all reagents used in this study were prepared from single batches and stored as in single-use aliquots.

3.1.3.2. *Plasmodium falciparum in vitro* culture

P. falciparum clinical isolates were cultured as per standard protocols (EVIMalaR, 2013). In brief, isolates were maintained at 37º C in RPMI1640 (Sigma), supplemented with 5% Albumax (Gibco), 2 mg/mL sodium bicarbonate, 50 µg/ml gentamycin (Sigma) and 2% AB^+ heat-inactivated normal human serum (PAN Biotech, UK). All cultures were adjusted at 4% hematocrit using O^+ erythrocytes from a single donor and incubated in an atmosphere of 2% O_2, 5% CO_2 and balanced with Nitrogen. For isolates cultured upon arrival to the lab, the parasites multiplication rate (PMR), defined as the ratio of the parasitemia before and after invasion, was monitored for the first two *in vitro* cycles and fresh erythrocytes were only added after 96 hours in culture, while fresh erythrocytes were immediately added upon thawing of cryopreserved isolates. Following the addition of fresh erythrocytes, growth tests were performed to assess the PMR every 48 hours for the first three *in vitro* replicative cycles for the cryopreserved isolates and for up to 12 cycles for freshly culture adapted isolates. Sample aliquots, taken following each replicative cycle were stained with 1 µM of Hoechst 33342 (Sigma Aldrich, UK) and the resulting parasitemia was assessed using flow cytometry. After each cycle, flasks were diluted to 0.5% parasitemia and the growth test was considered successful only when the resulting PMR, measured after 48 hours, was greater than one (>1). The median PMR of successful growth tests after twelve successive

replicative cycles following the addition of fresh erythrocytes were considered as PMR of culture-adapted isolates.

3.1.3.3. *Plasmodium falciparum* genotyping

P. falciparum genomic DNA (gDNA) was extracted from filter paper spots using the QIAamp DNA Blood Mini Kit (Qiagen, Hilden, Germany) and eluted in 30 µL elution buffer following the manufacturer's instructions. The concentration and purity of the eluted gDNA were estimated using a NanoDrop One (Thermo Fisher Scientific, Madison, WI, USA). For each isolate, the presence of single or multiple parasite clones was assessed using a nested PCR approach as described earlier (Snounou et al., 1999). The assays were performed using primers targeting the highly polymorphic regions of *msp1* (block 2) and *msp2* (block 3) (Supplementary Table 3. A1). All isolates that grew successfully during culture adaptation were genotyped after 28 days in culture and the number of clones was compared to that of the fresh isogenic isolate.

3.1.3.4. Enzyme treatment and erythrocyte invasion phenotyping assays

Invasion phenotyping assays were performed using enzyme-treated erythrocytes (targets) from a single donor. Target erythrocytes were treated with either 250 mU/mL of neuraminidase, 1 mg/mL of trypsin or chymotrypsin for 1 hour at 37º C with gentle shaking and washed thrice with RPMI1640. Treated erythrocytes were then labelled with 20 µM of carboxyfluorescein diacetate, succinimidyl ester (CFDA-SE) (Thermo Fisher Scientific) for two hours at 37º C with gentle shaking and protected from light exposure. For each isolate, schizont-infected erythrocytes were adjusted at 2% parasitemia and coincubated in 96 well plates with an equal volume of target erythrocytes. All assays were performed in triplicates in a total volume of 100 µL at 2% haematocrit and incubated at 37º C for 24 hours. Assays

were removed from the incubator and spin at 2,000 rpm for 3 minutes, after which the supernatant was discarded, replaced with a solution of 1 mM Hoechst 33342 to label the parasites' DNA and incubated for an hour at 37º C. Flow cytometry analyses were performed on a BD LSR Fortessa X-20 cytometer (BD Biosciences, Belgium) equipped with UV, Red and Blue lasers. Invasion into target erythrocytes was determined by analysis of the proportion of Hoechst positive erythrocytes in a total of 50,000 counted CFDA-SE positive cells. Per cent invasion into enzyme-treated erythrocytes was expressed relative to the invasion efficiency into labelled untreated erythrocytes.

3.1.4. Results

3.1.4.1. *In vitro* culture adaptation of *P. falciparum* clinical isolates

Samples used in this study were collected from 25 symptomatic Ghanaian children, aged between 2 to 14 years, and introduced into standard culture conditions. To monitor the *in vitro* growth patterns of freshly collected *P. falciparum* clinical isolates, parasites were initially allowed to grow in the patient-derived erythrocytes for a minimum period of 96 hours (two asexual replicative cycles) after which freshly washed O^+ erythrocytes were added and growth tests were performed for isolates that successfully grew. As measured by flow cytometry, *P. falciparum* clinical isolates showed specific growth patterns during the first 96 hours of *in vitro* adaptation with a peak parasitemia observed in almost all isolates between 48- and 72-hours post-inoculation (Figure 3.1A). Monitoring of the PMR during these first two *in vitro* cycles revealed that most of the isolates had less than two-fold increase in parasitemia from one cycle to another. Furthermore, of the 25 isolates tested in this study, 12 successfully (48%) grew following culture dilution with fresh erythrocytes. We used parasitemia to assess the parasite multiplication rate through successive growth tests for a maximum period of about twelve successive replication cycles. As a result, all isolates

showed a minimum of 8 successful growth tests (66.67% success rate, Figure 3.1B, Table 3.A2) with a median PMR of 1.77 (range 1.13 – 2.43).

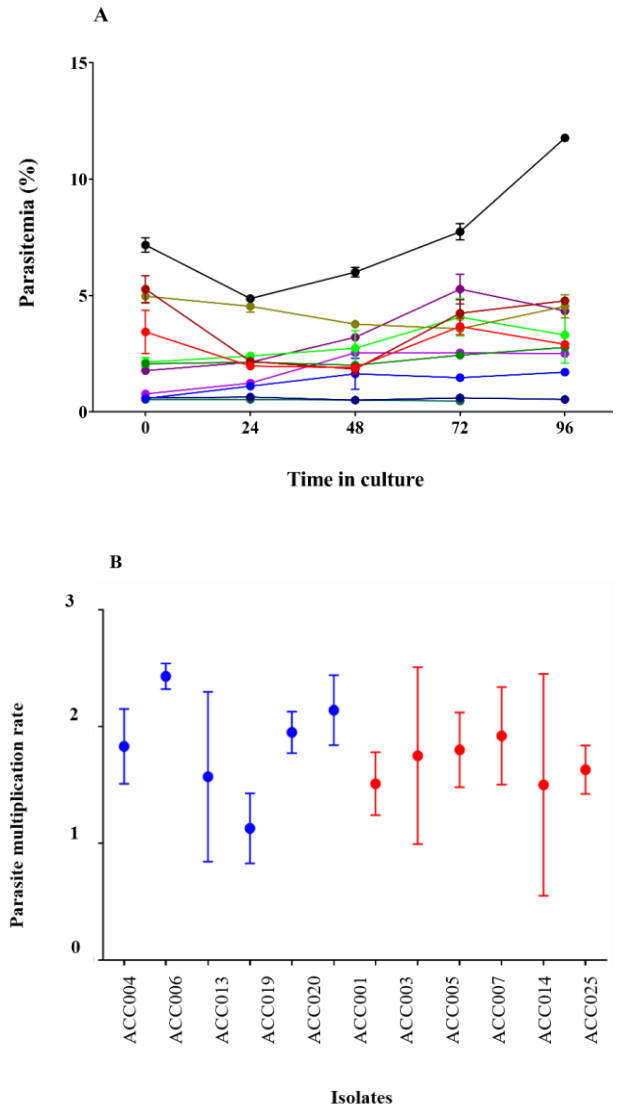

Figure 3. 1: Early in vitro adaptation of *P. falciparum* clinical isolates. (A) The initial parasitemia (at H0) of each sample was recorded upon arrival from the field and the parasitemia of *ex vivo* cultured isolates were monitored for 96 hours. The medium in the culture flasks was changed daily and supplemented with fresh erythrocytes only after 96 hours in vitro. (B) Parasite multiplication rates of successfully culture-adapted parasites following culture dilution with fresh erythrocytes. Here, are presented the mean and standard errors of the PMRs of parasites with 8 to 9 (red-coloured dots) and parasites with 10-12 (blue-coloured dots) successful growth tests over a period of 28 days *in vitro*.

3.1.4.2. Genotypic diversity of *P. falciparum* clinical isolates

Unlike laboratory strains, *P. falciparum* clinical isolates frequently harbour multiple parasite clones which could modulate the parasite's *in vitro* adaptability. Here, we assessed the presence of multiple parasites clones in each of the tested isolates using the highly polymorphic regions of *msp1* and *msp2* genes (Figure 3.A1-2). All 25 isolates were shown to be polyclonal, harbouring at least three distinct clones of *msp1* and *msp2*. The total number of alleles detected was 74 and 44 for *msp1* and *msp2*, respectively (Table 3.1). For *msp1*, the allele frequencies were 36.47% (27/74), 32.43% (24/74) and 31.10% (23/74) for K1, MAD20 and RO33, respectively, while those for the *msp2* allelic families were 54.54% (24/44) and 45.46% (20/44) for 3D7 and FC27, respectively. The prevalence of multiple infections was respectively 16 and 14 for *msp1* and *msp2*, while the multiplicity of infections was 2.6 and 1.76, respectively for the two genes (Table 3.1).

Table 3. 1: *Plasmodium falciparum* genetic diversity and msp-1 and msp-2 allelic diversities

Allelic type	N (%)	Allelic type	N (%)
msp-1		msp-2	
K1	22 (15.83)	3D7	22 (40.74)
MAD20	21 (15.11)	FC27	18 (33.33)
RO33	23 (16.57)	3D7/FC27	14 (24.93)
K1/MAD20	18 (12.95)		
K1/RO33	20 (14.39)		
MAD20/RO33	19 (13.67)		
K1/MAD20/RO33	16 (11.51)		
Total combination	139 (100)		54 (100)
Total k1	27 (36.47)	Total 3D7	24 (54.54)
Total MAD20	24 (32.43)	Total FC27	20 (45.46)
Total RO33	23 (31.10)		
Total Alleles	74		44
MI	16 (64)		14 (76)
MOI	2.64		1.76

MI: Prevalence of multiple-infections, MOI: Multiplicity of infection

The expected heterozygosity (H_E), is defined as the probability of being infected by at least two distinct alleles at a given locus was calculated as follow: $H_E = [n / (n-1)] [(1-\sum pi^2)]$, with n being the number of isolates and pi the allele frequency at a given locus (Diouf et al., 2019). Here, the H_E was found to 0.35 and 0.52 for *msp1* and *msp2*, respectively. However, there was no relationship between the number of genotypes per isolates and the PMR (data not shown).

3.1.4.3. Short-term culture adapted isolates harbour lower number of parasite clones

To measure the effect of short-term culture adaptation on the parasites' genotypes, ten of the culture adapted isolates were genotyped at day 28 post-inoculation using the *msp1* and *2* allelic families. Our analysis showed a reduction in the number of clones per isolate at day 28 as compared to day 0. The maximum number of clones per isolate was reduced from 4 to 2 for the *msp1* gene, while that of *msp2* was reduced from 2 to 1 (Table 3.2). Of all *msp1* allelic families, K1 was the most predominant at both day 0 and day 28, with a percentage of 41.9% and 58.3%, respectively (Table 3.2). MAD20 and RO33 which were present at the same proportion at day 0 (29.0%, each), represented respectively 16.6% and 25.0% of the total number of alleles (Table 3.2). For *msp2*, there were little changes in the proportions of the respective allelic families, with 3D7 being the most predominant allele representing 63.1% and 61.5% at day 0 and 28, respectively (Table 3.2). Out of the eight isolates harbouring the MAD20 allelic family at day 0, only two were detected with a copy of the allele at day 28, while the RO33 allele, initially present in nine isolates at day 0, was detected in only three isolates at day 28. K1, initially detected in all ten isolates, was still present in seven of them at day 28. Of all three, *msp1* allelic families, only K1 and RO33 were simultaneously detected in the same isolates at day 28, while MAD20 was only detected as single infections (Table 3.2). For the *msp2* gene, out of the seven isolates harbouring the FC27 allelic family at day 0, only four persisted at day 28, while the 3D7 allelic family, initially present in all ten isolates at day 0; was detected in eight of them at day 28. As for *msp1*, both allelic families of *msp2* were present in some isolates (three) as coinfections, while two and four isolates presented single infections of FC27 and 3D7, respectively at day 28. However, there was no specific dominant combination of *msp1* and *2* detected in our isolates at day 28. Moreover, aside those detected at day 0, there were no newly detected

alleles in our isolates at day 28, therefore suggesting the absence of detectable cross-contamination during culture adaptation.

Table 3. 2: Comparative analysis of *P. falciparum* genetic diversity prior and following short-term culture adaptation

		MSP-1			MSP-2		MSP-1			MSP-2	
		Day 0					Day 28				
	Isolates	K1	MAD20	RO33	3D7	FC27	K1	MAD20	RO33	3D7	FC27
Number of clones per isolate	ACC01	2	1	1	1	1	1	0	0	0	1
	ACC03	2	1	1	2	1	1	0	1	1	0
	ACC04	1	2	1	1	1	0	1	0	0	1
	ACC05	1	1	1	1	1	0	1	0	1	0
	ACC06	2	1	0	2	1	1	0	0	1	1
	ACC13	1	1	1	1	1	1	0	1	1	1
	ACC14	1	1	1	1	1	1	0	0	1	1
	ACC15	1	1	1	1	0	1	0	0	1	0
	ACC18	1	0	1	1	0	0	0	1	1	0
	ACC19	1	0	1	1	0	1	0	0	1	0
Total		13	9	9	12	7	7	2	3	8	5
Percentage		41.94	29.03	29.03	63.16	36.84	58.33	16.67	25.00	61.54	38.46

3.1.4.4. Early *in vitro* adaptation of *P. falciparum* clinical isolates following short-term cryopreservation

Culture-adaptation of *P. falciparum* clinical isolates has been reported as more labor-intensive than immediate *ex vivo* processing. Moreover, there are earlier reports of *P. falciparum* clonal selection during *in vitro* adaptation (K. Chen et al., 2014). To ascertain the effect of cryopreservation on *P. falciparum* early *in vitro* adaptation, we compared the PMR of short-term cryopreserved clinical isolates to that of their freshly cultured isogenic counterparts. Two vials of the same isolate were simultaneously revived using two distinct NaCl-based thawing protocols. Parasitemias were adjusted to 0.5-1% using a single erythrocyte donor and the PRM was monitored during the first three asexual replicative cycles. Successful monitoring of the PMR of isolates prior to and following cryopreservation (one-year interval) revealed differences in PMR between cryopreserved isolates and the matched freshly culture-adapted counterparts (Figure 3.2A). The median PMR was 1.62 for fresh isolates while that of cryopreserved isolates was 1.12 and 1.27 following two-step and three-step thawing, respectively. However, the difference in PMR was only significant when comparing fresh isolates and cryopreserved parasites thawed using a two-step protocol (Figure 3.2A), while no significant difference was observed between isogenic isolates thawed using distinct protocols (Figure 3.2A-B). Flow cytometry analysis of the DNA content of revived cryopreserved parasites revealed different peaks following Hoechst 33342 staining suggesting the presence of different parasite stages after 48-, 96- and 144-hours post-incubation (Figure 3.A3). This was further confirmed by Giemsa staining and light microscopy imaging revealing the persistence of some late parasite stages after the first *in vitro* replicative cycle (Figure 3.A3). Given, the high number of clones per isolate, as

confirmed by the genotyping experiments, it is possible that some clones may have higher fitness, therefore, providing an advantage to outgrow clones with lesser fitness.

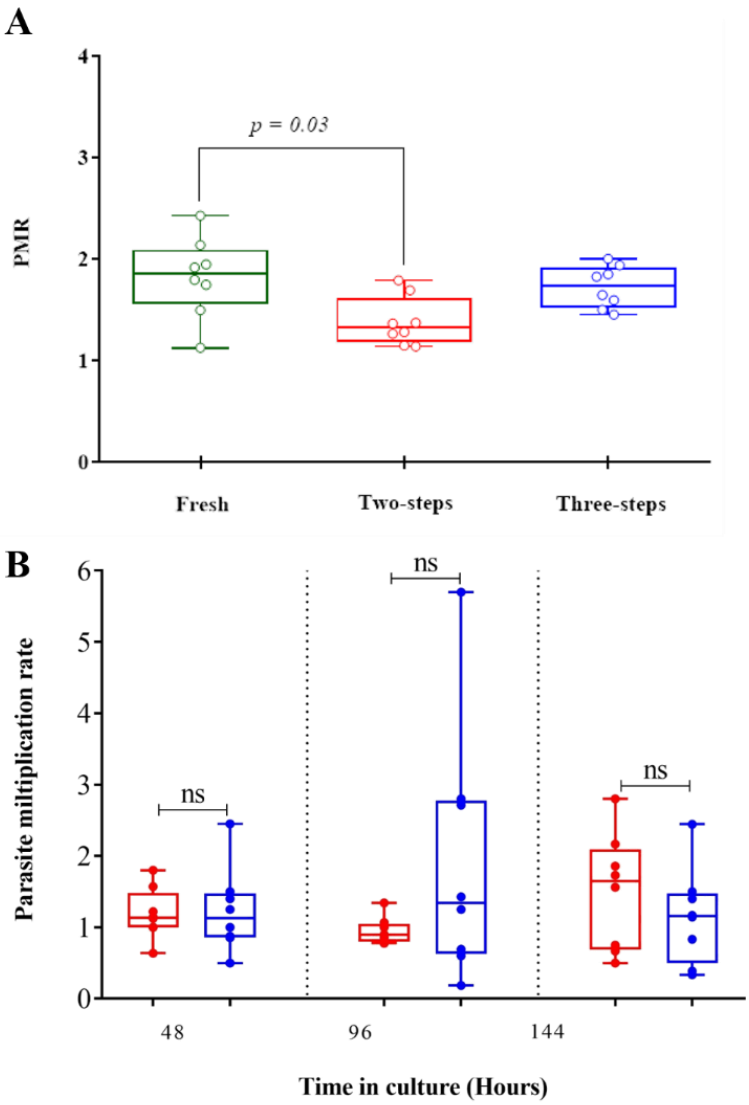

Figure 3. 2: Multiplication rates of P. *falciparum* clinical isolates before and after cryopreservation. A-B**:** Box and whiskers plots showing the PMR of fresh cultured *P. falciparum* clinical isolates (green) or thawed with a two-step (red) or three-step (blue) protocol following cryopreservation. Kruskal Wallis test was conducted to compare the PMR of fresh versus cryopreserved isolates after three *in vitro* replicative cycles (A) or to compare the PMR of isolates thawed with different protocols after each replicative cycle (B).

3.1.4.5. Short-term culture adaptation has minimal effect on *P. falciparum* invasion phenotype

In most cases, *P. falciparum* clinical isolates present multiple parasite clones with different levels of fitness during *in vitro* adaptation. As a result, *P. falciparum ex vivo* assays are usually challenged by the low parasite multiplication rate during the first *in vitro* replicative cycles of the parasites. Consequently, in most cases, invasion phenotyping of *P. falciparum* clinical isolates has been conducted following short-term culture-adaptation (Lobo et al., 2004; Lopez-Perez et al., 2012; Nery et al., 2006; Okoyeh et al., 1999). Here, to assess the effect of short-term culture adaptation on *P. falciparum* invasion phenotype, we compared the *ex vivo* invasion phenotype of four isolates to that obtained after 28 days in culture. Of the four isolates tested, only one (ACC014) had a different invasion phenotype with regards to its dependency on sialic acid as compared to the *ex vivo* phenotype (Figure 3.3). Changes in invasion profile, defined as the combination of sensitivity to the three enzymes, was observed in two isolates (ACC014 and ACC015). These variations could be a result of technical variations during the assay set up or culture-related effect, such as the introduction of fresh erythrocytes different from the patient-derived erythrocytes during early *in vitro* culture-adaptation. Further information is therefore needed to better assess the mechanism of such variation.

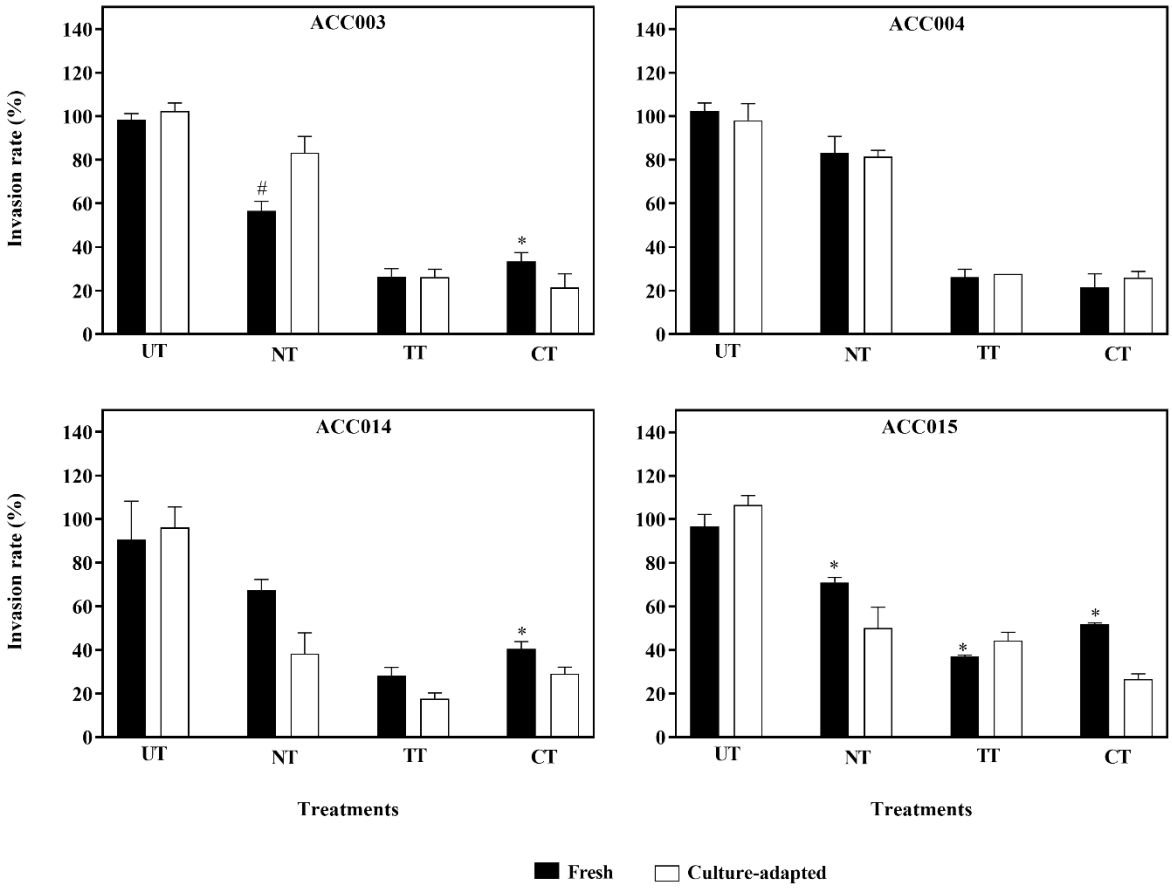

Figure 3. 3: Invasion phenotypes of *P. falciparum* clinical isolates before and after short-term culture adaptation. The *ex vivo* phenotype of freshly collected isolates (black bars) obtained during the first the asexual replicative cycle upon arrival in the laboratory was compared to that obtained after a short-term *in vitro* adaptation of about 28 days (white bars). The Mann Whitney U test was used to assess the differences in invasion efficiency between the different time points, (#: $p = 0.009$ and *: $p = 0.002$).

3.1.4.6. Cryopreservation has minimal effect on *P. falciparum* invasion phenotype

Cryopreserved isolates were thawed at different time intervals (from 3 to 12 months) and assayed for their ability to invade enzyme-treated erythrocytes as compared to their fresh uncultured counterparts. Given the challenges associated to the parasites' *in vitro* adaptability during the first rounds of asexual replication, and also to avoid clonal selection

following long term culture adaptation, all assays were set during the first two replicative cycles. Parasitemias were adjusted to 1% for all isolates and invasion assays were considered successful only when invasion efficiency into control erythrocytes (untreated) was at least one-fold greater than the starting parasitemia. Of the 25 isolates collected in this study, seven had sufficient number of cryopreserved vials (six vials) to be thawed at all the time-points and successfully phenotyped over the course of one-year post cryopreservation. All isolates showed a sialic acid independent pathway with the invasion of neuraminidase treated erythrocytes greater than 50% relative to that of untreated control erythrocytes (Figure 3.4, Figure 3.A4). Overall, there was no variation in the parasites' invasion pathway (defined as the combination of sensitivity to the three enzyme) with regards to their dependency on the sialic acid residues of the glycoproteins following cryopreservation as compared to fresh uncultured isolates and this was consistent with both thawing protocols used in this study (Figure 3.4). The most common invasion profile was neuraminidase resistant, trypsin sensitive and chymotrypsin sensitive (NrTsCs). However, three out of the seven isolates showed changes in invasion profiles in trypsin and chymotrypsin treated erythrocytes following cryopreservation with the apparition of three novel phenotypes (NrTrCs, NrTsCr and NrTrCr) after six-month post cryopreservation (Figure 3.4). Nevertheless, none of the novel phenotypes persisted after twelve-month post cryopreservation, suggesting a technical or random effect associated with these changes.

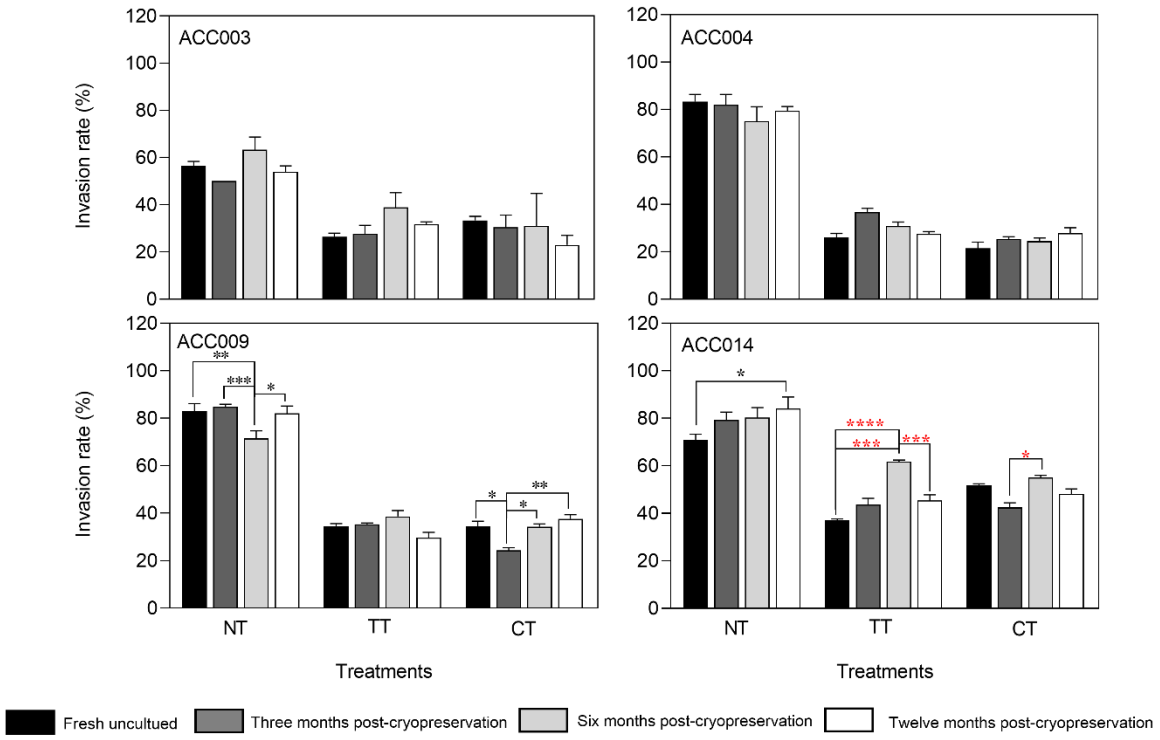

Figure 3. 4: Invasion phenotypes of *P. falciparum* clinical isolates before and after short-term cryopreservation. The assays were set up between 24- and 36-hours following sample processing and the parasites were incubated for another 18 to 24 hours prior to flow cytometry analysis. For each isolate, the invasion phenotype of freshly culture adapted parasites (black bars) was compared to that obtained after three months (dark grey bars), six months (light grey bars) and twelve months (white bars) post cryopreservation. Kruskal Wallis was conducted to test for statistical differences in invasion efficiency of fresh versus cryopreserved isolates. Red stars denote significant differences associated with changes in invasion profile of a given treatment and black stars depict significant differences with no changes in the invasion profile.

3.1.5. Discussion

The phenotypic diversity of *P. falciparum* clinical isolates has widely been reported in the last two decades (WAMIN, 2016). However, conducting such assays in uncultured clinical isolates has been precluded by the lack of appropriate laboratory settings in remote areas where the highest malaria burden occurs. Consequently, majority of the pioneering works was conducted in cryopreserved *P. falciparum* clinical isolates and in some cases after short-term culture adaptation following parasite thawing (Lobo et al., 2004; Lopez-Perez et al., 2012; Nery et al., 2006; Okoyeh et al., 1999). However, the effect of such procedures in the parasite's invasion phenotype has never been reported.

In this study, we investigated the effect of cryopreservation and different thawing protocols on *P. falciparum in vitro* adaptation and invasion phenotyping assays. We showed that *P. falciparum* clinical isolates show specific growth patterns during the early *in vitro* culture adaptation. Nevertheless, almost all isolates showed a peak parasitemia between 48 and 72 hours, while the majority of the isolates did not recover following culture dilution with fresh erythrocytes. Likewise, earlier studies have reported such findings, mainly attributed to the failure of many patients in reporting prior antimalarial treatment (Baum et al., 2003b).

Given that *P. falciparum in vitro* adaptation could also be influenced by the number of parasites clones present in a given isolate, our genotyping analysis revealed that all *P. falciparum* clinical isolates used in this study presented distinct parasite clones with an MOI of 2.64 and 1.76 for *msp1* and *msp2*, respectively. With regards to *msp1*, the MOI value reported here was in agreement with recently published data from asymptomatic Senegalese children (2.5), while that of *msp2* from the same cohort was much higher (4.7) (Diouf et al., 2019). The predominance of K1 and 3D7 allelic families reported here is in agreement with previous reports from Ghana, Ethiopia and Senegal (Diouf et al., 2019; Kobbe et al., 2006;

Mohammed et al., 2015), while studies from Uganda and Sudan reported the predominance of RO33 and FC27, respectively for the two genes (Hamid, Mohammed, & El Hassan, 2013; Peyerl-Hoffmann et al., 2001).

In this study, the median PMR of short-term culture adapted isolates was 1.77, consistent with previous reports (Lantos et al., 2009), however, there was no relationship between the observed PMR and the number of parasite clones per isolate. Furthermore, of the 12 culture adapted isolates tested in this study, 10 were successfully genotyped at day 28 post culture inoculation and our data show an apparent clonal selection following short-term culture adaptation. This is in agreement with previous data that also reported culture adaptation of *P. falciparum* clinical isolates as a modulator of the parasite's susceptibility to a wide range of drugs as compared to their fresh uncultured counterparts (Chaorattanakawee et al., 2015).

Our data also show the persistence of K1 at day 28 in almost all isolates harbouring this allelic family on day 0, while MAD20 prevalence significantly decreased at day 28. Furthermore, MAD20 was outgrown by K1 in all isolates harbouring mixed infections with more than one allele of K1. Likewise, MAD20 has been reported to be outcompeted by K1 in natural malaria infections (Sondo et al., 2019).

Here, we show that for some isolates, the invasion phenotype following culture adaptation varies as compared to the parasites' *ex vivo* phenotype. This, therefore, suggests a possible effect of short-term culture adaption and/or clonal selection in the parasite invasion phenotype. However, this could also be as a result of technical variations during invasion assay set up (e.g. efficiency of enzyme treatment) and given the small number of isolates tested for this experiment (only four isolates), there is a need for further confirmation with a larger number of isolates and possibly a longer culture adaptation time.

The present study also investigated the effect of cryopreservation and thawing protocols in the parasites' early *in vitro* adaptation and invasion phenotype as compared to their freshly cultured isogenic counterparts. Our data show that cryopreserved *P. falciparum* clinical isolates used in this study have a lower multiplication rate during the first *in vitro* cycles as compared to their fresh isogenic counterparts, however, this difference in PMR was only significant when freshly cultured isolates were compared to those revived using a two-step NaCl protocol. This could be as a result of a simple artefact during culture adaptation or possibly due to the fitness of the different parasite clones in a given isolate. It is therefore possible that the parasite-induced stress during the thawing process may accentuate the low fitness of certain clones, this effect could be further enhanced when parasites are thawed using a three-step protocol.

Another potential factor that could affect the early *in vitro* adaptation of revived cryopreservation in the addition of fresh erythrocyte following parasites revival. Given the difference between the freshly added erythrocytes and the patient-derived erythrocytes, initially present in the freshly cultured parasites, there is a possibility that the lower multiplication rate observed post-cryopreservation is solely due to the parasite adaptation to the new erythrocytes. However, given the observed differences in the PMR post cryopreservation and to minimize the effect of clonal selection, invasion phenotyping assays were only performed in isolates that yielded appropriate parasitemia during the first *in vitro* replicative cycles.

As a result, our data show that most of the isolates assayed following cryopreservation maintained a relatively stable invasion phenotype regardless of the length of cryopreservation or the thawing protocol used for the revival of the parasites. To our knowledge, this is the first study to investigate the effect of short-term culture adaptation

and cryopreservation on *P. falciparum* invasion phenotype using clinical isolates from the same isogenic backgrounds. Altogether, these results suggest that short-term culture adaptation could influence the invasion phenotype of *P. falciparum* clinical isolates due to clonal selection during *in vitro* culturing, but this needs further confirmatory studies with a larger number of isolates. However, the parasites *ex vivo* phenotype following cryopreservation, without any prior culture adaptation, seems not to affect the parasites invasion phenotype relative to the *ex vivo* data.

3.2. BLOOD DONOR VARIABILITY IS A MODULATORY FACTOR FOR *P. FALCIPARUM* INVASION PHENOTYPING ASSAYS

Hypothesis 2: *Blood donor variability affects P. falciparum invasion phenotype*

In this study, blood samples from twenty healthy adults were collected to investigate the effect of blood donor variability in *P. falciparum* invasion phenotyping assays. Erythrocytes (red blood cells) from individual donors were classified based on commonly phenotypic features such as the blood group, sickling and G6PD status or the expression levels of specific surface receptors. Invasion efficiency of both *P. falciparum* laboratory and clinical isolates was then assessed following enzyme treatment of target erythrocyte and the data gathered from these investigations are presented in the following manuscript.

3.2.1. Abstract

Human red blood cells represent the cornerstone of *P. falciparum in vitro* experiments and play a crucial role in investigating the natural phenotypic diversity of *P. falciparum* clinical isolates. term *P. falciparum in vitro* experiments. Consequently, invasion phenotyping experiments rely on erythrocyte of different backgrounds. However, the actual contribution of the host erythrocyte in invasion remains unknown and therefore challenging the idea of conducting large scale comparative studies. Here, we used erythrocyte of different blood groups harbouring different hemoglobin genotypes to assess the relative contribution of blood donor variability in *P. falciparum* invasion phenotyping assays. For each donor, we investigated the relationship between parasite invasion phenotypes and erythrocyte phenotypic characteristics including expression levels of surface receptors (GYPA, GYPC, CR1 and DAF), blood group (O^+, O^-, A^+ and B^+), and hemoglobin genotypes (AA, AS and AC). We found that, following enzyme treatment of erythrocyte from different donors, invasion efficiency varies in both *P. falciparum* clinical and laboratory strains. Across all isolates, differences in invasion profile were only observed following treatment with either trypsin or chymotrypsin. The availability of erythrocyte phenotypic characteristics e.g. blood group, hemoglobin genotype, expression levels of receptor surface, for each donor enabled us to investigate the relationship between the parasite's invasion phenotype and each of these characteristics. Primarily, we showed that the surface expression of key erythrocyte surface receptors and their sensitivity to enzyme treatment significantly differed across donors. Invasion efficiency correlated neither with susceptibility to enzyme treatment nor with expression levels of the selected erythrocyte surface receptors. Upon further analysis, we find no relationship between *P. falciparum* invasion phenotype and blood group or hemoglobin genotype. Put together, the findings suggest that, instead of commonly

shared erythrocyte features, *P. falciparum* invasion phenotype could rather be driven by more intrinsic properties, such as the erythrocytes specific biophysical features (tension, bending modulus…).

3.2.2. Introduction

Malaria-associated pathologies only manifest during the blood stage of the parasite's life cycle. This stage is initiated through alternating rounds of asexual replications within the host red blood cell (erythrocyte), following the parasite's initial replication in hepatocytes. *P. falciparum* merozoites, the parasite's invasive blood forms, have the sole purpose to invade erythrocytes and perpetuate the asexual replicative cycle. Given their importance in the parasite's successful invasion and further multiplication within the host cell, merozoite antigens, and particularly invasion-related antigens represent attractive blood-stage vaccine targets. Thus, unravelling the nature of ligand-receptor interactions involved in erythrocyte invasion is crucial in malaria vaccine development.

Although recent studies have enabled considerable progress to be made in our understanding of the molecular basis of erythrocyte invasion by parasites (Cowman et al., 2017; Scully, Kanjee, & Duraisingh, 2017), little is known about the actual contribution of the host cell. Also, though there is clarity on the redundancy of ligand-receptor interactions involved in invasion, the functional relevance of a number of these interactions are uncertain, hence the postulation of their possible involvement in signal transduction on either side between the parasite and the host erythrocyte (Prinz et al., 2016; Tham et al., 2015).

Pioneering studies have individually reported major invasion profiles of *P. falciparum* clinical isolates across various endemic countries and have led to the hypothesis that *P. falciparum*

invasion profile is driven by the intensity of ongoing transmission in a given area (Baum et al., 2003b; Bei et al., 2007; Bowyer et al., 2015; Deans et al., 2007; Gomez-Escobar et al., 2010; Jennings et al., 2007; Lantos et al., 2009; Lobo et al., 2004; Lopez-Perez et al., 2012). However, this has been contradicted by more recent findings which have shown no relationship between endemicity and invasion profile when parasites from countries of varying endemicity were subjected to similar protocols to assess their respective invasion profiles (Bowyer et al., 2015). Therefore, this emphasizes that conducting large-scale *P. falciparum* phenotyping studies may inevitably require more rigorous protocols to anticipate potential challenges. One of the major drawbacks that may preclude the design of such assays is the consistency in the usage of donor erythrocytes (WAMIN, 2016). Human erythrocytes polymorphisms have been shown to be associated to the distribution of *P. falciparum* globally (Sironi, Forni, Clerici, & Cagliani, 2018; Williams, 2006) and this heterogeneity may account for differences in the reported invasion profiles using erythrocytes from various origins.

Unlike the bulk of eukaryotic cells, mature erythrocytes which are readily available in the peripheral blood and mostly used for *P. falciparum in vitro* culturing are enucleated and despite the progress made in generating immortalized erythroid cell-lines retaining a mature phenotype, upscaling the production of these cells for universal usage is challenging (Dias et al., 2011; Hirose et al., 2013; Huang et al., 2014; Kanjee et al., 2017; Kurita et al., 2013). It is therefore of utmost importance to investigate the contribution of donor erythrocytes in characterizing *P. falciparum* phenotypic diversity. In this study, we present results from preliminary investigations aimed at assessing the relative contribution of blood donor variability in *P. falciparum* invasion phenotyping assays (IPAs).

Blood samples from twenty asymptomatic adults of different blood groups and hemoglobin genotypes were used in a standard two-color flow cytometry-based invasion assay to test the invasion profiles of six parasite strains; three laboratory lines 3D7, Dd2 and W2mef and three freshly culture-adapted clinical isolates MISA010, MISA011 and MISA018. Given that each erythrocyte donor may present a specific genetic background, we tested for each donor, the sensitivity to enzyme treatment and the surface expression of key erythrocyte receptors that mediates *P. falciparum* invasion. Altogether, the data generated here were used to assess the potential relationship between donor erythrocyte characteristics and *P. falciparum* invasion phenotypes.

3.2.3. Materials and Methods

3.2.3.1. Blood collection and processing

The use of human erythrocytes for this study was approved by the Institutional Review Board (IRB) of the Noguchi Memorial Institute of Medical Research Ethics Committee and written informed consent was sought from all participants. Venous blood samples from adult donors, representing different erythrocyte phenotypes (AA, AS or AC) and/or different blood groups (O^+, O^-, A^+ or B^+), were collected in ACD Vacutainers (BD Biosciences, USA) and washed three times with RPMI 1640 (Sigma Aldrich, UK) to separate the erythrocytes from the other blood components. For each sample, part of the resulting erythrocyte pellet was used for IPAs while the remaining was cryopreserved for further experiments. Full blood screening, including blood group typing and hemoglobin genotyping, was performed as per standard protocols at the Korle-Bu Teaching Hospital, Accra, Ghana.

3.2.3.2. *P. falciparum* isolates and culture conditions

Both *P. falciparum* clinical isolates (MISA010, MISA011 and MISA018) and laboratory lines (3D7, Dd2 and W2mef) were maintained in culture at 4% haematocrit in complete parasite medium (RMPI 1640 containing 25 mM HEPES, 5 % Albumax II, 2 mg/mL sodium bicarbonate and 50 ug/mL Gentamicin) and incubated at 37 ° C in an atmosphere of 5.5 % CO2, 2 % O2 and balance N2 gas mixture. Parasites were maintained in culture using a single donor O^+ erythrocytes and routinely synchronized using 5 % D-Sorbitol (Sigma Aldrich, UK).

3.2.3.3. Invasion assay set up

For each donor, erythrocytes were treated with different enzymes, neuraminidase (250 mU), trypsin (1 mg/mL) or chymotrypsin (1mg/mL) or left untreated and labelled with 20 µM carboxyfluorescein diacetate succinimidyl ester (CFDA-SE) as described earlier (Theron, Hesketh, Subramanian, & Rayner, 2010). For each isolate, schizont stage parasites were inoculated in a 1:1 ratio into fresh enzyme-treated and labelled erythrocytes from a given donor. Experiments were conducted in triplicates in a 96 well plate and repeated at least two times. Parasites were incubated for about 24 hours, after which the cells were stained with 5 µM Hoechst 33342 to label the parasite's genomic material and the invasion efficiency was assessed by flow cytometry. The percentage of erythrocytes positive for both dyes was recorded as the invasion efficiency and the parasite's invasion phenotype was determined by comparing invasion rates in enzyme-treated erythrocytes to that of untreated cells. To minimize the effect of any possible confounders that may arise during the sample processing or assay set up, erythrocytes from a single donor, used for routine parasite culturing, were included in all assays and used to finally normalize the resulting parasitemia.

3.2.3.4. Characterization of erythrocyte surface receptors

The surface expression of selected erythrocyte receptors known or predicted to be involved in invasion was quantified by flow cytometry using specific monoclonal antibodies. Freshly washed erythrocytes were coincubated for an hour at 1% haematocrit in 1% BSA in 1X PBS with either mouse anti-human IgGs: Glycophorin AB (GYPAB) (1:400, Sigma Aldrich UK), GYPA (Clone E4, 1:100, Santa Cruz Biotech, US), GYPC (Clone E3, 1:100, Santa Cruz Biotechnology, US), Complement receptor 1 (CR1) (Clone J3D3, 1:50, Santa Cruz Biotechnology, US) or Decay-accelerating factor (DAF) (Clone NaM16-4D3, 1:50, Santa Cruz Biotechnology, US). The erythrocyte pellets were collected by centrifugation at 2000 rpm, washed twice with PBS and subsequently coincubated with either Alexa Fluor 700, APC or PE-labelled anti-mouse IgGs (Santa Cruz Biotechnology, US). All incubations were done at 37°C for one hour and protected from light exposure. The data were acquired using a BD LSR Fortessa X-20 (BD Biosciences, Belgium) flow cytometer and analyzed using FlowJo v10.5.0 (FlowJo, LLC, Ashland OR) and GraphPad Prism v.7.01 (GraphPad Software, Inc.).

3.2.3.5. Antibody-dependent invasion inhibition assays

To ascertain the relative contribution of receptor density in the invasion efficiency, CFDA-labelled erythrocytes from different donors were pre-incubated with different concentrations of antibodies at 37°C for an hour. The erythrocytes were pelleted by centrifugation at 2000 rpm for 3 minutes, gently washed with PBS and the excess washed out prior to the addition of schizont-infected cells. The antibody-bound erythrocytes were then coincubated at 2% haematocrit with equal volumes of parasitized erythrocytes from two different parasite lines

(3D7 and MISA011) at 37°C for 24 hours. Parasites were monitored for reinvasion and parasitemia was finally quantified by flow cytometry.

3.2.3.6. Statistical analyses

All statistics were performed using GraphPad Prism v.7.01 (GraphPad Software, Inc.). The data were analyzed as the mean and standard error of pooled data from at least two independent experiments conducted each in triplicates. Statistical significance between invasion efficiency into enzyme-treated erythrocytes from different donors was ascertained using two-way ANOVA coupled with the Tukey's multiple comparison tests for pairwise analysis. Spearman correlation or the Kruskal Wallis tests were used for ascertaining the relationship between variables or to compare different groups, respectively.

3.2.4. Results

3.2.4.1. Demographic and haematological characteristics of the study participants

Blood samples used in this study were collected from twenty non-related asymptomatic adults, comprising fifteen males and five females, all resident in Accra (Ghana). Donors were questioned about their most recent clinically diagnosed malaria symptoms and to eliminate possible confounders, only individuals with no recent history of clinical malaria (at least two years) were considered. Additionally, erythrocytes from a single donor, used for routine parasite culturing, were included in all assays to normalize the resulting parasitemia. All but one sample were subjected to clinical diagnosis to screen for possible hemoglobin disorders while all samples were subjected to ABO blood group typing as presented in Table 3.3. In brief, the

majority of the donors (14/20) presented a normal hemoglobin genotype (AA), while four donors were diagnosed with sickle cell trait (AS) in addition to two other donors harbouring an AC genotype. Blood group O^+ was the commonest in all donors (10/20), followed by the A^+ and B^+ (5 and 4, respectively), while O^- was the least common blood group in the study participants. Of all donors, only one presented a severe deficiency of the G6PD expression. Full blood count was also carried out to assess other hematological indices (Table 3.3).

Table 3. 3: Clinical and hematological indices of study participants

ID	Gender	Blood group	Sickling	Hb genotype	G6PD	WBC (10^9/L)	RBC (10^12/L)	HGB (g/dL)	HCT (%)	MCV (fL)	MCH (pg)	MCHC (g/dL)	PLT (10^9/L)
GH000**	M	O+	-	AA	Normal	4.34	5.16	13.0	42.8	83.0	25.2	30.4	153
GH001	F	O+	-	AA	Normal	7.98	3.93	11.5	38.9	98.9	29.3	29.6	342
GH002	M	B+	-	AA	Normal	5.91	6.04	15.0	51.5	85.2	24.8	29.1	231
GH003	M	B+	+	AS	Normal	3.16	5.34	15.1	46.7	87.4	28.3	32.3	220
GH004	M	O+	+	AS	Normal	4.38	6.26	13.7	44.8	71.5	21.9	30.6	218
GH005	M	O+	-	AA	Normal	6.82	5.31	14.3	47.1	88.7	26.9	30.4	202
GH006	F	A+	-	AA	Normal	6.88	3.83	12.3	39.4	102.8	32.1	31.2	273
GH007	M	O-	-	AA	Normal	5,07	4,77	14,5	43,6	91,4	30,4	33,3	228
GH008	M	A+	-	AA	NA	NA	NA	NA	NA	NA	NA	NA	NA
GH009	M	O+	-	AA	Normal	5,59	3,76	13,3	39,9	106,2	35,4	33,3	317
GH010	M	A+	+	AS	Normal	5.57	6.30	16.3	51.7	82.0	25.9	31.5	258
GH011	M	O+	-	AA	Normal	3.86	5.21	15.4	48.3	92.7	29.6	31.9	169
GH012	M	O+	-	AA	Normal	4.74	5.94	15.2	49.5	83.4	25.6	30.7	197
GH013	F	B+	-	AA	Normal	5.53	4.57	13.5	43.0	94.0	29.5	31.4	244
GH014	F	B+	+	AS	Normal	5.73	4.61	12.9	40.2	87.1	28.0	32.1	251
GH015	M	O+	-	AA	Normal	7.90	4.95	14.6	46.8	94.6	29.5	31.2	253
GH016	M	A+	-	AC	Normal	5.49	4.74	13.2	39.6	83.5	27.8	33.3	244
GH017	M	A+	-	AA	Full Defect	3,02	3,85	9,9	31,5	81,8	25,7	31,4	209
GH018	F	O+	NA	NA	NA	NA	NA	NA	NA	NA	NA	NA	NA
GH019	M	O+	-	AC	Normal	7.70	5.48	14.6	45.2	82.5	26.6	32.3	260
GH020	M	O+	-	AA	Normal	5.94	5.35	15.7	49.1	91.8	29.3	32.0	187

** Erythrocytes from this donor were used for routine parasite culturing and for data normalization

3.2.4.2. Invasion phenotypes of *P. falciparum* into erythrocytes from different donors

To explore whether blood donor variability mediates *P. falciparum* invasion phenotype, we investigated the invasion efficiency of *P. falciparum* isolates of diverse background into enzyme-treated erythrocytes from different donors. Enzyme treatment of erythrocytes restricts the repertoire of receptors available for invasion and therefore would affect the invasion efficiency of parasites relying on enzyme-sensitive receptors. Using monoclonal antibodies against the human GYPAB (specific to sialic acid residues), GYPA and CR1, we first validated the efficacy of enzyme treatments in removing specific receptors on the erythrocyte surface. Neuraminidase removes sialic acid (SA) residues on the erythrocyte glycoproteins, while trypsin and chymotrypsin cleave peptide backbones of other receptors such as GYPA, GYPB, GYPC and CR1 (Bei & Duraisingh, 2012; Tham et al., 2012). Surface staining of enzyme-treated erythrocytes from different donors reveals various levels of sensitivity to enzyme treatment between donors (Figure 3.5). We next co-incubated enzyme-treated and labelled erythrocytes from different donors with schizont-infect erythrocytes of different *P. falciparum* isolates in a standard invasion assay for 24 hours prior to flow cytometry analysis. Mean invasion rates between donors in each treatment group were compared using two-way ANOVA, with Tukey's multiple comparison tests. As shown in figure 3.6, invasion efficiency significantly differs from donor to donor, with the clinical isolates showing little to moderate sensitivity to neuraminidase treatment (Table 3.3, Table 3.A2-3), while *P. falciparum* laboratory strains invaded neuraminidase treated erythrocytes with respect to their reliance on sialic acid residues (Table

3.A5-7). With trypsin and chymotrypsin treatments, both laboratory and clinical isolates showed moderate to marked sensitivity to treatment as compared to untreated control erythrocytes.

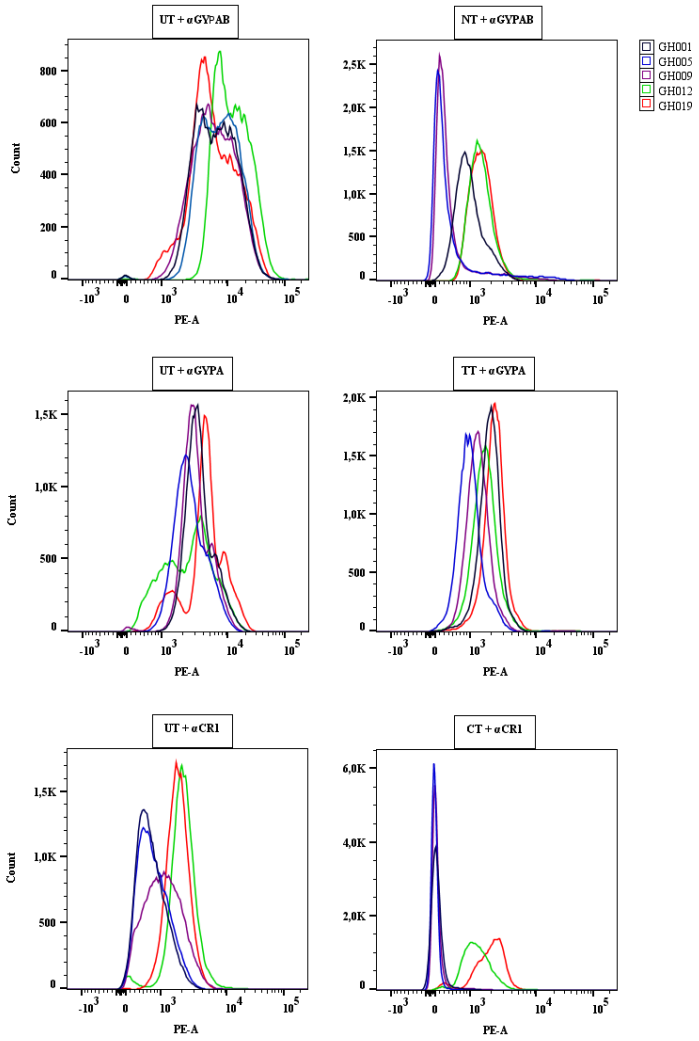

Figure 3. 5: Efficacy of enzyme treatment of erythrocytes from different donors. Histogram plots showing the fluorescent intensity associated with antibodies against specific erythrocyte receptor prior to, and after treatment with different enzymes (NT: neuraminidase treatment, TT: trypsin treatment, CT: chymotrypsin treatment). Target erythrocytes from five different donors were coincubated for an hour with mouse anti-human GYPAB (top panel), GYPA (middle panel) or CR1 (bottom panel), then washed twice and incubated with goat anti-mouse-PE conjugated antibodies. The data was collected with a BD LSR Fortessa II cytometer and graphs plotted using FlowJo v.10.01.

Overall, variations in invasion profiles (defined as the combination of sensitivity to the three enzymes) were mainly driven by sensitivity to trypsin and chymotrypsin treatments, while that of neuraminidase remained unchanged for all isolates (Table 3.A3-7). Four different profiles were observed in the SA-independent isolates (3D7, MISA010, MISA011 and MISA018), with the clinical isolates showing the highest level of variation as compared to 3D7. Of the two SA-dependent *P. falciparum* isolates used in the study, W2mef and Dd2, the former presented the highest level of variation in invasion profile (Figure 3.A5). Given that trypsin and chymotrypsin treatments affect the peptide backbones of the target erythrocyte receptors, we hypothesize that the observed variations in invasion profile after trypsin and chymotrypsin treatments might be driven by the differential expression of receptors on the surface of donor erythrocytes.

Table 3. 4: Invasion profiles of a freshly adapted *P. falciparum* clinical isolate, MISA011, following invasion assays with erythrocytes from twenty different donors.

			% invasion relative to untreated control		
Donor erythrocytes	Gender	Invasion profile	Neuraminidase (250 mU/ml)	Trypsin (1mg/ml)	Chymotrypsin (1mg/ml)
O+/AA	F	NrTsCr	115.89 ± 2.33	42.39 ± 10.26	56.75 ± 26.27
B+/AA	M	NrTsCr	103.03 ± 8.11	25.06 ± 9.42	50.35 ± 6.36
B+AS	M	NrTsCs	110.71 ± 24.1	35.71 ± 19.19	46.43 ± 17.56
O+AS	M	NrTsCs	105.14 ± 8.52	30.28 ± 8.39	40 ± 14.97
O+AA	M	NrTsCs	101.96 ± 18.13	33.44 ± 5.92	35.89 ± 9.95
A+/AA	F	NrTrCs	99.06 ± 14.35	55.14 ± 15.69	46.48 ±7.23
O-/AA	M	NrTsCs	83.89 ± 14.81	30.09 ± 11.83	32.2 ± 13.89
A+/AA	M	NrTsCs	72.55 ± 11.24	32.84 ± 8.9	42.53 ± 6.85
O+/AA	M	NrTsCs	105.60 ± 9.64	37.58 ± 9.36	37.36 ± 9.78
A+/AS	M	NrTsCs	88.04 ± 10.32	36.14 ±21.78	31.26 ± 11.93
O+/AA	M	NrTsCs	59.76 ± 6.28	23.15 ± 6.24	29.67 ± 5.31
O+/AA	M	NrTsCs	71.73 ± 9.29	33.30 ± 11.85	43.01 ± 16.62
B+/AA	M	NrTrCs	81.81 ± 3.84	50.65 ± 9.00	79.11 ± 7.65
B+/AS	F	NrTsCs	60.53 ± 3.84	26.29 ± 9.55	36.45 ± 13.45
O+/AA	M	NrTrCs	91.38 ± 16.01	29.79 ± 14.67	37.70 ± 11.05
A+/AC	M	NrTsCs	72.56 ± 3.98	20.76 ± 2.02	28.31 ± 1.70
A+/AA	M	NrTsCs	82.31 ± 7.00	19.72 ± 3.85	32.60 ± 4.98
O+/AA	F	NrTrCs	83.20 ± 13.44	72.56 ± 7.87	26.05 ± 2.31
O+/AC	M	NrTsCs	113.26 ±12.97	32.33 ± 19.87	27.45 ± 12.71
O+/AA	M	NrTsCs	66.80 ± 3.25	23.33 ± 7.43	34.31 ± 11.03

Key: N: neuraminidase, T: trypsin, C: chymotrypsin, s: sensitive, r: resistantData represent mean values ± the standard deviation from two independent experiments conducted in triplicates. A cut-off of 50% was taken as a threshold to classify the observed profile as sensitive (≤50%) or resistance (>50%) for each given treatment.

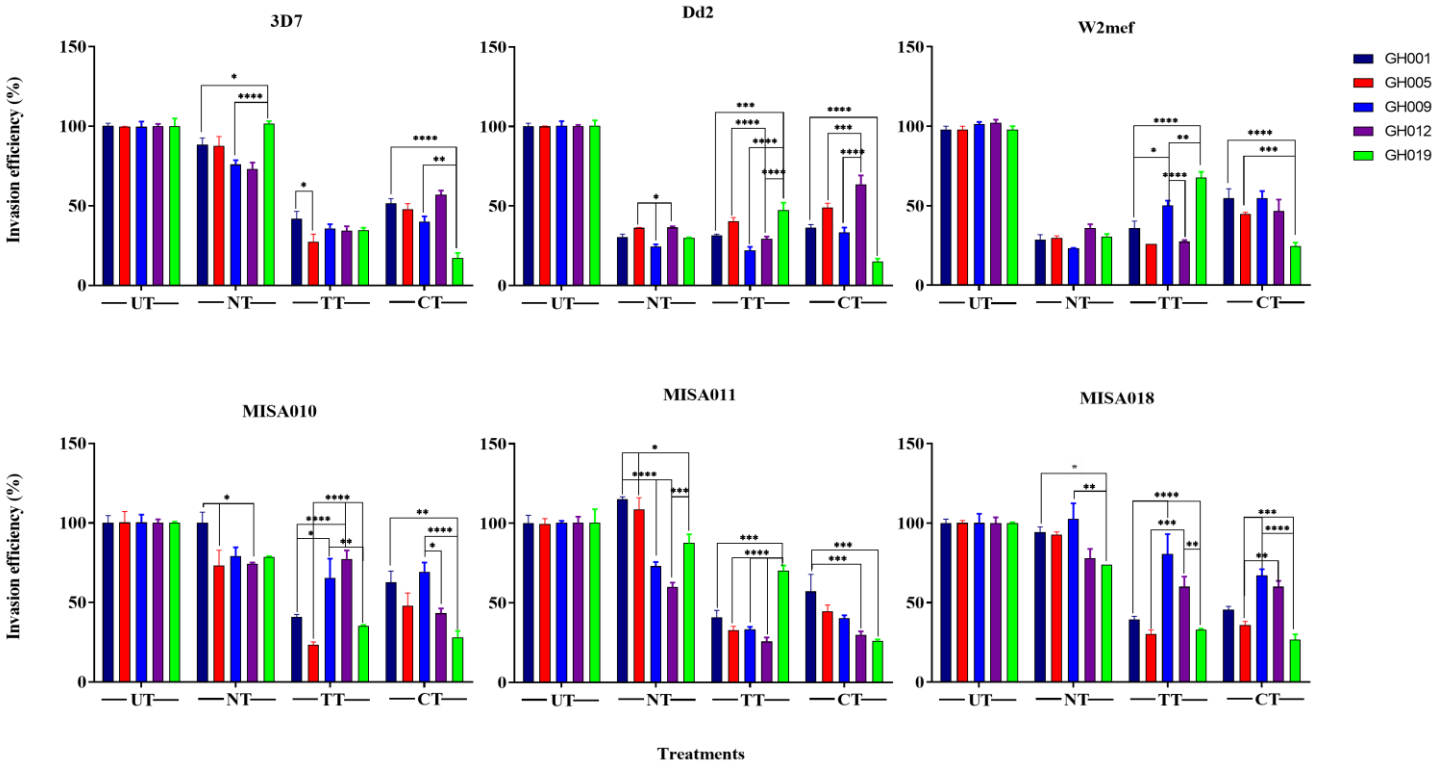

Figure 3. 6: *P. falciparum* invasion phenotypes into erythrocytes from five different donors. The assay was set up along with a single donor erythrocyte used as a control for normalizing the resulting parasitemia. Statistical tests were performed using the Friedman test ($p = 0.03$ (*), $p = 0.002$ (**), $p = 0.0002$ (***), $p < 0.0001$ (****)).

Keys: UT = untreated, NT = neuraminidase treated, TT = trypsin treated and CT = chymotrypsin treated

3.2.4.3. Relationship between receptor density and sensitivity to enzyme treatment

Having shown that the sensitivity to enzyme treatment varies from donor to donor, we sought to investigate the cause of the observed differences and under the hypothesis of a possible interplay between the expression levels of erythrocyte surface antigens and their sensitivity to enzyme treatment. Using a panel of murine monoclonal antibodies, the surface expression of key erythrocyte antigens (receptors), including GYPA, GYPC, CR1 and DAF, was quantified by flow cytometry. Given the major role played by sialic acid moieties during the invasion, we also included antibodies specific to these residues (GYPAB) to ascertain their expression level. As expected, the expression levels of key erythrocyte surface receptors significantly varied between donors (Figure 3.7). The data were stratified following normalization and donors were classified as high (Mean+2SD), medium (between Mean±1SD) and low expressers (Mean-2SD). To investigate the relationship between receptor density and sensitivity to enzyme treatment, the median fluorescence intensity (MFI) of labelled antibodies on enzyme-treated erythrocytes was measured and expressed as the percentage of the MFI of the corresponding untreated donor erythrocytes. The efficiency of enzyme treatment was then expressed as follows: 100 – (MFI $_{\text{Treated}}$ Erythrocyte / MFI $_{\text{Control}}$ Erythrocyte x 100). We carried out a Spearman correlation test and observed no correlation between receptor density and the efficiency of enzyme treatment (Figure 3.8). Moreover, no relationship was also observed between receptor density and invasion efficiency into enzyme-treated erythrocytes (Figure 3.A6).

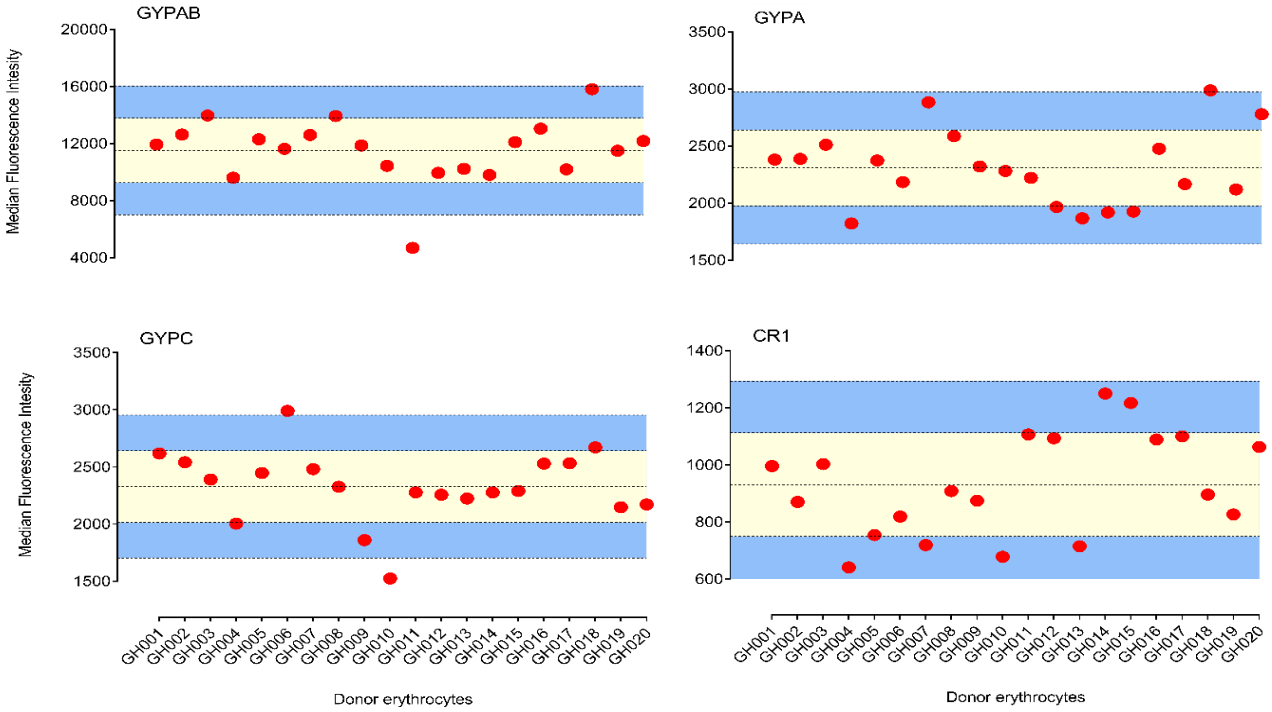

Figure 3. 7: Variation of surface expression of erythrocyte receptors between donors. Dot plots of relative MFI (Y-axis) associated with fluorescently labelled antibodies against specific erythrocyte receptors (GYPAB, GYPA, GYPC, CR1 and DAF) from 20 blood donors (X-axis). Data were acquired by a flow cytometer and processed with FlowJo v.10.01. Graphs were plotted using GraphPad Prism.

3.2.4.4. Relationship between receptor density and *P. falciparum invasion* efficiency

Given that the expression level of specific erythrocyte surface receptors has been shown to significantly contribute to *P. falciparum* invasion efficiency (Bei, Brugnara, & Duraisingh, 2010; Crosnier et al., 2011; Dankwa et al., 2017; Egan et al., 2015; Ye et al., 2018), we sought to rule out any effect of enzyme treatment that could mask a possible correlation between these variables. We selected five different donors (Donors 6-10, refer to Figure 3.7), with different levels of expression of individual receptors and conducted antibody-mediated invasion inhibitory assays using different concentrations of specific anti-human monoclonal antibodies. Dilutions were optimized to prevent the formation of cell aggregates. As expected, both parasite lines showed a concentration-dependent antibody invasion inhibition with an almost similar invasion pattern with regard to the different donors (Figure 3.9A-B). However, no linear relationship was observed between the invasion efficiency and the relative abundance of target surface receptors (Figure 3.9). This, therefore, emphasizes that invasion efficiency could be driven by other erythrocyte specific properties different from the surface expression of the selected receptors.

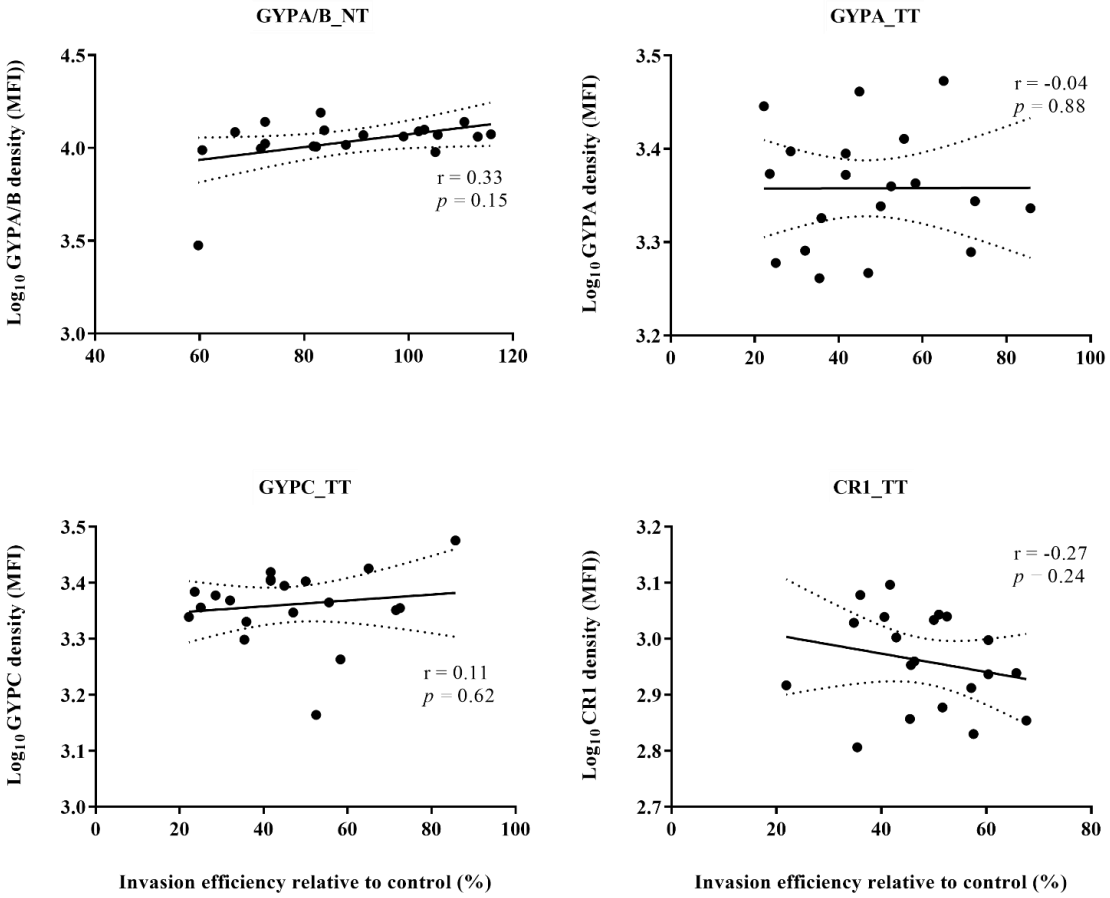

Figure 3.8: Correlation of antigen density of erythrocyte surface molecules with the efficiency of enzyme treatment. The density of erythrocyte surface receptors, labelled with specific monoclonal antibodies prior to, and following enzyme treatment was quantified by flow cytometry using fluorescently labelled secondary antibodies. The resulting data were analysed with FlowJo v.10.01 and the Spearman R correlation were performed using GraphPad Prism v.7.01.

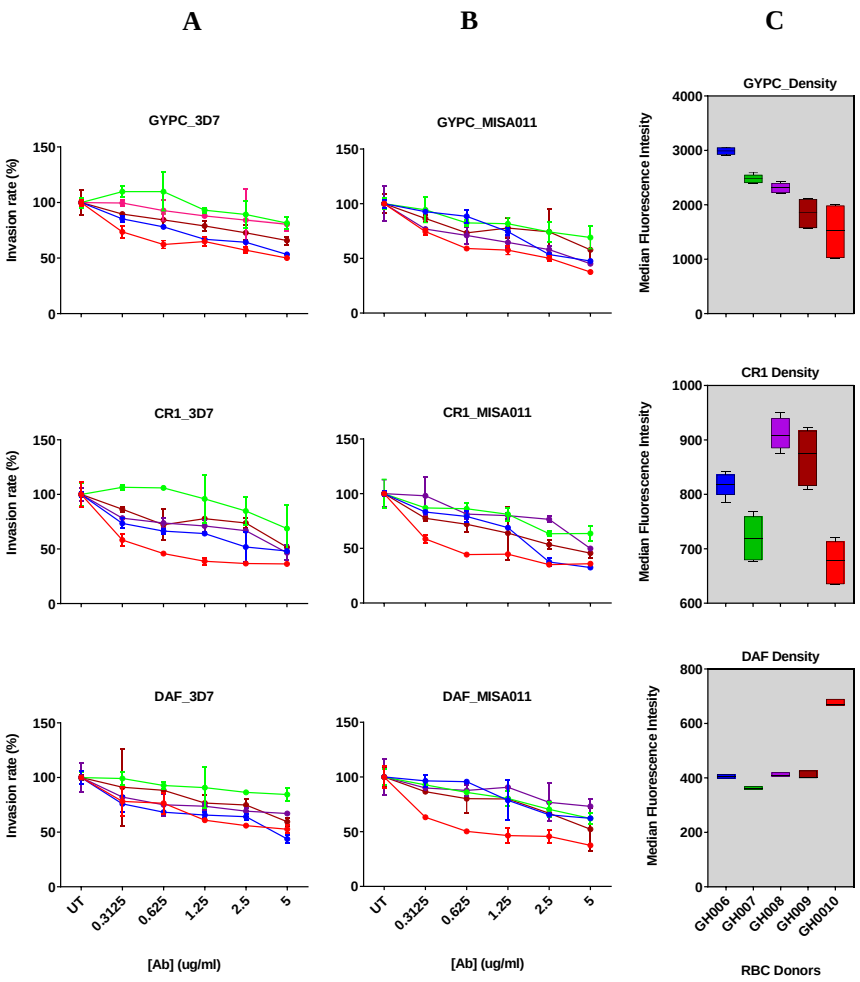

Figure 3. 9: Antibody-dependent invasion inhibition assays in donor erythrocytes with different levels of surface antigens. Schizont-infected erythrocytes were co-incubated with antibody-sensitized uninfected erythrocytes from donors expressing different levels of erythrocyte receptors. The parasites' DNA was labelled with Hoechst 33342 18-24 hours' post-incubation and the resulting parasitemia was quantified by flow cytometry. For each donor, the parasitemia in the corresponding mock-treated erythrocytes was used to ascertain the antibody-dependent invasion inhibitory, following normalization using a single erythrocyte donor (also used for the parasites *in vitro* culturing). A and B represent the antibody-dependent invasion inhibition for two different *P. falciparum* isolates, 3D7 and MISA011, respectively. C represents the differential expression of erythrocyte receptors assessed in A and B.

3.2.4.5. *P. falciparum* invasion phenotype is independent of the ABO blood group antigen or Hb genotype

Protection against malaria clinical manifestations has for long been associated with erythrocyte surface antigens such as those associated with the ABO blood group system, as well as erythrocyte hemoglobin defects (e.g. sickle cell trait, thalassemia) (Egan, 2018; Egan et al., 2018; Leffler et al., 2017; Sironi et al., 2018; Williams, 2006). To ascertain the relative contribution of donor blood group and/or hemoglobin genotype in the observed variation in invasion phenotype, we performed a Kruskal Wallis test followed by the Dunn's multiple comparison tests as post hoc analysis. As shown in figure 3.10, there were no significant differences in invasion phenotype associated with either the donor blood group or the host hemoglobin genotype. This further suggests that the observed differences may solely be due to intrinsic characteristics specific to each individual donor rather than commonly shared erythrocyte features.

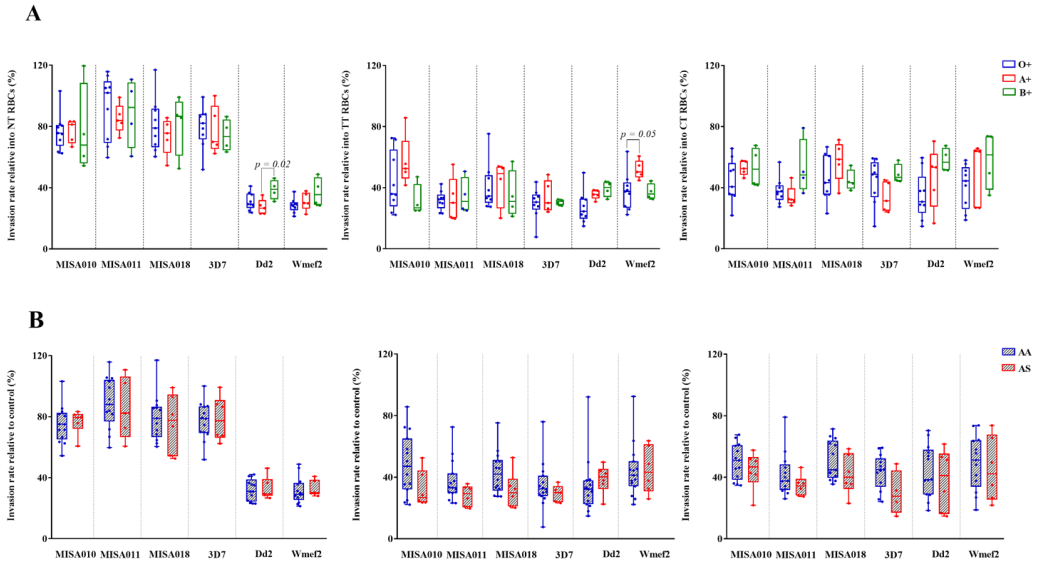

Figure 3. 10: Relationship between blood group or hemoglobin genotype and invasion into enzyme-treated erythrocytes. Erythrocytes from donors of different (A) blood groups (O^+ = 10, A^+ = 5 and B^+ = 4) or (B) hemoglobin genotypes (AA = 14, AS/AC = 5) were treated with different enzymes and coincubated with schizont-infected *P. falciparum* isolates for 18-24h. For each set of donor erythrocytes, the invasion efficiency was assessed using flow cytometry and compared to that of mock-treated control erythrocytes. The data were analysed using GraphPad Prism v.7.01 and statistical significance was assessed by the Kruskal Wallis and pairwise comparisons were performed with the Dunn's multiple comparison test. None of the observed differences was statistically significant when comparing invasion efficiency into erythrocytes with different hemoglobin genotype.

3.2.5. Discussion

This study was undertaken to investigate the effect of blood donor variability in *P. falciparum* IPAs. *P. falciparum* invasion of erythrocytes is a multistep process which necessitates a tightly regulated interaction between the parasite-derived ligands and specific receptors on the host cell surface. These interactions occur in a functionally redundant manner and therefore define the parasites invasion pathway.

Here, we present results from preliminary investigations of the effect of key erythrocyte phenotypic attributes in *P. falciparum* IPAs. Using erythrocytes from twenty unrelated donors with different blood groups and hemoglobin genotypes, we showed that both *P. falciparum* laboratory lines and clinical isolates differently invade enzyme-treated erythrocytes from distinct donors. Across all isolates, the invasion efficiency significantly differs from donor to donor. Although invasion phenotypes did not vary with regards to the use of SA residues, there was a more pronounced variation in invasion profiles, across isolates, following treatment with either trypsin or chymotrypsin as compared to neuraminidase. This could partially be as a result of the mode of action of the individual enzymes, given that trypsin and chymotrypsin are more promiscuous than neuraminidase and could affect a wider range of receptors with unknown function during the invasion but also as a result of a small number of binding sites still present following enzyme treatment.

As we found that individual donor erythrocytes presented a different level of sensitivity to enzyme treatment, our data suggest that other host-related factors play a significant role in the observed invasion efficiency. We postulate that erythrocyte receptors are differentially expressed on the surface of individual donor cells, thus driving the sensitivity to enzyme treatment. Nevertheless, although the expression level of erythrocyte receptors varies from donor to donor, we observed no relationship between receptor density and sensitivity to enzyme

treatment. Moreover, in this study, all parasites were maintained in a uniform culture environment and the only major variable factor was the erythrocytes from different donors.

Differences in the expression of different erythrocyte surface receptors might have accounted for the differential invasion efficiency into individual donor erythrocytes. Knockdown experiments of both basigin and CR1 have previously shown a linear relationship between receptor density and invasion efficiency into erythrocytes (Bei, Brugnara, et al., 2010; Crosnier et al., 2011). Here, there is a possibility that the absence of a relationship between receptor density and invasion efficiency was masked by the effect of enzyme treatment as a result of changes in the erythrocytes biophysical properties as previously reported (Yang Y, 2009).

To rule out any effect of enzyme treatment, erythrocytes from five different donors were used in an antibody-dependent invasion inhibition assay without any prior enzyme treatment. Increasing concentrations of antibodies limit the number of receptors available for parasite invasion, therefore mimicking the effect of receptor knockdown at the individual level. In the case of a positive linear relationship between these two variables, one would expect higher invasion rates across all dilutions in individuals with a higher level of a given receptor. Although there was an evident dose-dependent inhibition of all isolates when donors were taken individually, there was no apparent linear relationship between receptor density and invasion efficiency into erythrocytes from different donors. This, therefore, suggest that receptor density solely is not the absolute driving mechanism of invasion efficiency into erythrocytes of different origin.

The relationship between *P. falciparum* and the ABO blood group system or hemoglobin genotypes remains a fascinating subject for researchers. Despite the small number of donors included in this study, we sought to investigate a possible relation between the observed invasion phenotype and the donor blood group or hemoglobin genotype. Overall, across all strains, invasion into erythrocytes of different blood groups or hemoglobin genotypes did not

differ significantly. These data are partially in line with previous works with regards to both factors. Majority of the hemoglobin variants conferring protection against malaria have been shown not to significantly affect erythrocytes invasion *in vitro* (Lelliott, McMorran, Foote, & Burgio, 2015). However, several studies have reported the parasite preference for O^+ blood group *in vitro*. Pathak and colleagues, reported similar invasion rates during the first replicative cycle when parasites were cultured in erythrocytes of different blood groups (Pathak, Colah, & Ghosh, 2016). However, there were marked differences in parasitemia when parasites were allowed to grow beyond the second replicative cycle, with O^+ blood group being more susceptible to invasion as compared to others blood groups (Pathak et al., 2016). This observation is consistent with recently published data regarding the *in vitro* preference for O^+ blood group by parasites of different background (Theron, Cross, Cawkill, Bustamante, & Rayner, 2018). More recently, different *P. falciparum* strains have been shown to differentially invade erythrocytes of the same blood group from thirty different donors (Vimonpatranon et al., 2019), suggesting that variation in invasion efficiency could be driven by host-specific features rather than commonly shared ones.

Understanding the interplay between merozoite attachment and the changes in the erythrocyte biophysical properties would add complementary information with regard to the host cell contribution to invasion. Koch *et al*. reported the occurrence of biophysical changes in the host cell upon binding of a recombinant EBA-175 to its GYPA counterpart (Koch et al., 2017). The erythrocyte tension has particularly been shown to be affected by this interaction in a concentration-dependent manner, in both untreated and neuraminidase treated cells, while the bending modulus (defined as the energy necessary to cause bending of the lipid bilayer) was only affected in untreated erythrocytes. However, erythrocyte tension resulting from this interaction was not required for successful invasion, while the resulting decrease in bending

modulus was strongly correlated with invasion of both SA-dependent and independent *P. falciparum* isolates (Koch et al., 2017).

In summary, if signalling pathways in the host cell upon primary contact with external ligands alter the biophysical properties of the host cell as previously reported (Karnchanaphanurach et al., 2009; Khoory et al., 2016; Koch et al., 2017), this suggest a more or less active contribution of the host cell to the invasion efficiency, through activation of downstream signaling pathways following the primary contact with the invading merozoite. Besides, this emphasizes the need for more robust assays to pinpoint the actual contribution of the host cell during *P. falciparum* invasion.

3.3. CELL TRACE FAR-RED IS A SUITABLE ERYTHROCYTE DYE FOR MULTI-COLOUR *PLASMODIUM FALCIPARUM* INVASION PHENOTYPING ASSAYS

Cell trace far-red is a suitable erythrocyte dye for multi-colour *P. falciparum* invasion phenotyping assays

Laty G. Thiam[1, 2], Yaw Aniweh[1, 2*], Evelyn B. Quansah[1, 2], Jacob K. Donkor[2], Theresa M. Gwira[1, 2], Kwadwo A. Kusi[1, 2, 3], Makhtar Niang[4] and Gordon A. Awandare[1, 2*]

[1]West African Centre for Cell Biology of Infectious Pathogens, College of Basic and Applied Sciences, University of Ghana, Legon, P.O. Box LG 54, Legon, Accra

[2]Department of Biochemistry, Cell and Molecular Biology, College of Basic and Applied Sciences, University of Ghana, Legon, P.O. Box LG 54, Legon, Accra

[3]Department of Immunology, Noguchi Memorial Institute for Medical Research, University of Ghana, Legon, P.O. Box LG 581 Legon, Accra

[4]Unité d'Immunologie, Institut Pasteur de Dakar, Senegal, P. O. Box 220, Pasteur Avenue, Dakar, Senegal

Running title: Using cell trace far red as a dye for invasion assays

This manuscript has been published in the journal Experimental Biology and Medicine and is reproduced in this thesis with the permission from the journal editorial board.

3.3.1. Abstract

P. falciparum erythrocyte invasion phenotyping assays are a very useful tool for assessing the parasite diversity and virulence, and for characterizing the formation of ligand-receptor interactions. However, such assays need to be highly sensitive and reproducible, and the selection of labelling dyes for differentiating donor and acceptor erythrocytes is a critical factor. We investigated the suitability of Cell Trace Far-Red (CTFR) as a dye for *P. falciparum* invasion phenotyping assays. Using the dyes carboxyfluorescein diacetate succinimidyl ester (CFDA-SE) and dichloro dimethyl acridin one succinimidyl ester (DDAO-SE) as comparators, we used a dye-dilution approach to assess the limitations and specific staining procedures for the applicability of CTFR in *P. falciparum* invasion phenotyping assays. Our data show that CTFR effectively labels acceptor erythrocytes and provides a stable fluorescent intensity at relatively low concentrations. CTFR also yielded a higher fluorescence intensity relative to DDAO-SE and with a more stable fluorescence intensity over time. Furthermore, CTFR did not affect merozoites invasion of erythrocytes and was not toxic to the parasite's intraerythrocytic development. Additionally, CTFR offers flexibility in the choice of combinations with several other DNA dyes, which broaden its usage for *P. falciparum* erythrocyte invasion assays considering a wider range of flow cytometers with various laser settings.

Keywords: Cell Trace Far-Red, Flow cytometry, *Plasmodium falciparum*, Erythrocyte invasion

3.3.2. Statement of impact

In recent years, flow cytometry has become a cornerstone in investigating *P. falciparum* phenotypic diversity using multiple dyes to discriminate between donor and acceptor erythrocytes. To broaden the applicability of such assays, we optimized the staining conditions of a newly developed cytoplasmic dye, Cell Trace Far-Red (CTFR), and assessed its suitability for use in *P. falciparum* invasion phenotyping assays. We showed that CTFR has a very narrow emission peak excited by red lasers. Furthermore, CTFR labelling of target erythrocytes, achieved even at low concentrations, is stable over time and did not impair parasite development. *P. falciparum* erythrocyte invasion phenotyping assays revealed that CTFR is suitable for use in combination with several DNA dyes in multiplex assays. This will allow for high throughput phenotyping of parasites as well as facilitate the evaluation of preference of erythrocytes by merozoites. Altogether, these make screening for potential invasion-blocking interventions possible.

3.3.3. Introduction

Erythrocyte invasion is critical for *P. falciparum* establishment, multiplication and transmission. The process of merozoite invasion is complex and well regulated, involving an array of interactions between parasite ligands and erythrocyte receptors (Cowman & Crabb, 2006). In response to immune pressure or natural genetic variation, *P. falciparum* alters the usage of these ligand-receptor interactions to successfully invade the host cells (Duraisingh, Triglia, et al., 2003; Gaur et al., 2004). Collectively, these interactions define distinct invasion pathways, hence, the parasite invasion phenotype. Invasion phenotyping assays have traditionally been monitored using microscopy (Baum, Pinder, & Conway, 2003a; Deans et al., 2007), which is time-consuming and requires technical expertise. As an alternative, early flow cytometry-based approaches made use of DNA labelling dyes such as SYBR Green I to assess

the parasite invasion efficiency (Bei, Desimone, et al., 2010). Nevertheless, this approach does not distinguish acceptor erythrocytes from culture or patient-derived uninfected erythrocytes. Screening large numbers of *P. falciparum* clinical isolates is necessary for vaccine candidate prioritization, therefore, requiring high throughput assay system with different levels of discrimination. Recent progress in flow cytometry applications has entrenched its wider usage in *P. falciparum* erythrocyte invasion phenotyping assays. So far, the commonly used flow cytometry-based assay employs a dual-dye combination approach requiring an amine-reactive cytoplasmic dye to be used in combination with fluorescent DNA dye to label the cytoplasm of acceptor erythrocytes and the parasite's DNA, respectively (Theron et al., 2010). Advantages and disadvantages of the most commonly used dye-combinations have earlier been assessed, and as a result, an adaptable flow cytometry-based assay has been proposed (Theron et al., 2010). Given their ability to passively diffuse through the lipid bilayer of different cell types, amine-reactive dyes have been preferred over lipophilic dyes that bind to the plasma membrane (Wallace et al., 2008). Furthermore, lipophilic dyes may alter the nature of ligand-receptor interactions during merozoites invasion. Consequently, the most commonly used cytoplasmic dyes are carboxyfluorescein diacetate succinimidyl ester (CFDA-SE) and 7-hydroxy-9H-(1,3-dichloro-9,9-dimethylacridin-2-one) succinimidyl ester (DDAO-SE). First used in tracking lymphocyte migration (Lyons & Parish, 1994), CFDA-SE has since been used in a wide range of applications (Brusko, Hulme, Myhr, Haller, & Atkinson, 2007; Gett & Hodgkin, 2000; Krupnick et al., 2001) and has been shown to be non-toxic to *P. falciparum* (Joanny, Held, & Mordmuller, 2012). Despite being extremely bright and readily affordable, CFDA-SE is limited by its poor spectral properties, preventing its usage in multi-colour assays involving dyes that emit through the green channel (Zhou et al., 2016). DDAO-SE, which is a red laser-excitable dye, has been found to be an excellent alternative for CFDA-SE in *P. falciparum* erythrocyte invasion phenotyping assays (Theron et al., 2010). However, despite its numerous properties,

DDAO-SE has recently been discontinued (Thermo Fisher Scientific, United Kingdom), hence the need for an alternative dye that might help free up the green channel for multi-colour assays. Cell Trace Far-Red (CTFR), a newly developed amine-reactive dye (Thermo Fisher Scientific, United Kingdom), is excited by the red channel at 640 nm and can be used in red-laser equipped flow cytometers. CTFR has been proposed as a candidate for monitoring early events of bacterial invasion (Atwal, Giengkam, VanNieuwenhze, & Salje, 2016), but also, as an alternative to dyes with limited spectral properties such as CFDA-SE in cell proliferation assays (Zhou et al., 2016). However, the use of CTFR in flow cytometry-based *P. falciparum* assays, and particularly the effect of the dye on the parasites' invasion or subsequent intraerythrocytic development is yet to be reported. In this study, we used a dye-dilution approach to assess the applicability and limitations of erythrocyte staining with CTFR in *P. falciparum* erythrocyte invasion phenotyping assays. Using both DDAO-SE and CFDA-SE as comparators, the suitability of CTFR was evaluated by assessing the strengths and weaknesses of the dye with regards to its spectral properties, the persistence of staining as well as toxicity to *P. falciparum* invasion and development.

3.3.4. Materials and methods

3.3.4.1. Ethics statement

The use of human blood for this study was approved by the Institutional Review Board of Noguchi Memorial Institute for Medical Research, University of Ghana and the Ghana Health Services Ethical Review Committee. Blood samples were obtained from healthy donors after they have endorsed a written informed consent form.

3.3.4.2. Labelling dyes

The properties of the different dyes used in this study are summarized in Table 1. Except for DDAO-SE, a generous gift from Dr Amy K. Bei, all dyes were purchased from Thermo Fisher Scientific, United Kingdom. CTFR (cat# C34564) and CFDA-SE (cat# V122883) were obtained in 15 and 50 µg lyophilized vials, respectively. Stock concentrations of 1 and 5 mM were respectively made by the addition of 20 and 180 µL dimethyl sulphoxide (DMSO), according to manufacturer's recommendations. DDAO-SE was also received in a 50µg lyophilized vial and was reconstituted into 19.8 µL DMSO to obtain 5 mM initial concentration. Nucleic acid dyes, SYBR Green I (cat# 668120) and Hoechst 33342 (cat# 62249), were purchased in solutions of 10,000X and 20 mM concentrations, respectively. For all dyes, working concentrations were made by the addition of adequate volumes of either RPMI 1640 or 1X phosphate buffer saline (PBS).

3.3.4.3. Staining with DDAO-SE and CFDA-SE

DDAO-SE and CFDA-SE staining procedures were adapted from (Theron et al., 2010). Briefly, freshly washed O^+ erythrocytes were suspended at 4% hematocrit with either 10 µM DDAO-SE or 20 µM CFDA-SE in RPMI 1640. The suspension was protected from any source of light and incubated at 37 ºC in a shaking incubator (150 rpm) for two hours. The cells were subsequently pelleted by centrifugation at 2000 rpm and incubated for 10 minutes at room temperature in complete parasite medium (CPM), RPMI 1640 medium supplemented with 0.5% Albumax II (Gibco, Life Technologies, New Zealand), two mg/mL Sodium bicarbonate and 50 µg/mL Gentamycin (Sigma, United Kingdom) and 2% normal human serum (NHS), to quench the excess of the dyes. The pellets were finally washed three times at 2000 rpm for 3 minutes with RPMI 1640, suspended at 25% hematocrit in CPM (without NHS) and stored at 4 ºC until use.

3.3.4.4. Staining with Cell Trace Far-Red

CTFR was serially diluted with either RPMI 1640 or PBS to obtain working concentrations of 1, 2 and 5 µM (Table 1). Erythrocytes were suspended with the CTFR staining solution and incubated at 37 ºC in a shaking incubator (150 rpm). Cells were subsequently pelleted by centrifugation at 2000 rpm for 3 minutes, suspended in CPM containing 2% NHS and incubated at room temperature for 10 minutes. The suspension was then centrifuged for 3 minutes at 2000 rpm and the pellet washed thrice with RPMI 1640 or PBS. The resulting pellets were finally suspended in CPM (without NHS) and stored at 4 ºC until use. To optimize the staining conditions, parameters such as the hematocrit and the incubation time were varied in the preliminary experiments.

3.3.4.5. Assessment of dye stability

To assess the stability of CTFR-derived fluorescent intensity, the mean fluorescent intensities (MFIs) of erythrocytes labelled 20 µM of CFDA-SE, 10 µM 0f DDAO-SE or with different concentrations of CTFR in either PBS or RPMI 1640 were compared to those of unlabelled erythrocytes over time. Both labelled and unlabelled erythrocytes were kept at 4°C in separate tubes after processing. For each measured time point (days 1, 5, 10 and 15 post staining), equal volumes of labelled and unlabelled erythrocytes were mixed together and incubated at 37°C for 24 hours. The resulting MFI of each erythrocyte population was assessed by flow cytometry and the stain index of labelled erythrocytes was assessed accordingly.

3.3.4.6. *In vitro* culturing and invasion assay set up

P. falciparum laboratory-adapted strains, 3D7 and Dd2, were maintained in culture at 4% hematocrit in complete parasite media and incubated under an atmosphere of 2% O_2, 5.5% CO_2 and 92.5% N_2. The parasites' growth patterns in labelled versus unlabelled erythrocytes were

assessed throughout two successive asexual replication cycles. The parasitemias in culture aliquots, taken at 24 hours intervals were assessed daily using flow cytometry after Hoechst 33342 staining. For the invasion assays, CTFR labelled erythrocytes were suspended at 50% hematocrit in different tubes for enzyme treatments with either 250 mU/mL of neuraminidase (*Vibrio cholerae*; Sigma, United Kingdom), 1 mg/mL of trypsin or chymotrypsin (Sigma, United Kingdom). Invasion assays were performed as described earlier (H. E. Mensah-Brown et al., 2015) for two both parasite strains. Briefly, schizont-infected erythrocytes were mixed with equal volumes of either enzyme-treated or untreated CTFR-labelled erythrocytes at 2% hematocrit in CPM. All assays were performed in triplicates in 96-well plates and incubated in blood gas atmosphere of 2% O_2, 5.5% CO_2 and 92.5% N_2. Parasites were left to grow at 37°C for 18 to 24 hours, after which the plates were centrifuged at 1500 rpm for 3 minutes and the supernatant was discarded. Parasite DNA was then labelled by adding 100 µL of either 1X SYBR Green I or 1 µM Hoechst 33342 and incubated at 37 ºC in a shaking incubator for an hour. The plates were once more centrifuged, and cells washed with 1X PBS after removal of the supernatant. The cells were finally suspended into1X PBS and the invasion efficiency was determined by flow cytometry. The percentage of erythrocytes positive for CTFR and either SYBR Green I of Hoechst 33342 was recorded as invasion rate.

3.3.4.7. Microscopy imaging

To ascertain the normal parasite development in labelled erythrocytes, *P. falciparum* culture aliquots, collected at different time-points for two complete asexual replication cycles, were smeared on glass microscope slides, fixed with 100% methanol and stained with 10% Giemsa. The parasites morphologies were assessed using a Cole Palmer light microscope (Vernon Hills, Illinois 60061, USA) and coupled to a MoticamBTW8 camera (Motic China Group Co., Ltd). For the confocal imaging, schizont-infected erythrocytes were co-incubated with CTFR-

labelled erythrocytes for 48 hours in CPM at 37 ºC. Small aliquots of culture, taken at different time-points, were fixed with 4% paraformaldehyde, stained with SYBR Green I then smeared on glass microscope slides. Microscope slides were viewed under oil immersion (40X) on an LSM 800 confocal laser scanning microscope and images were acquired using ZEN 2.6 Blue Software (Carl Zeiss, Germany). All images were processed using Fiji ImageJ 1.52i (National Institutes of Health, USA).

3.3.4.8. Flow cytometry data acquisition

Labelled erythrocytes were analyzed using a BD LSR Fortessa™ X-20 (BD Biosciences, Belgium). CFDA-stained erythrocytes were excited with a blue laser (488 nm) and detected with a 530/30 (505LP) filter set, while both DDAO and CTFR-stained cells were analyzed with a red laser (640 nm) and detected with 670/30 filter set. SYBR Green I was detected with the blue laser associated to a 530/30 (505LP) filter set and Hoechst 33342 was excited by a UV laser (355 nm) associated to a 450/50 (410LP) filter set (Table 1). No compensation was necessary since the dyes were used separately. Data were acquired with the BD FACSDiva v.8.0 software (BD Biosciences, Oxford, United Kingdom). Total erythrocytes were gated using 125 and 203 FSC and SSC voltages, respectively, with a threshold of 5,000 on the FSC-A. Single erythrocytes were further gated using the forward scatter high (FSC-H) versus the forward scatter area (FSC-A). Data were acquired in triplicates and 100,000 events were recorded for each replicate using a low sample flow rate (12 µL/minute).

3.3.4.9. Data analysis

Flow cytometry data were acquired with the FACS Diva software (BD Biosciences) and exported as FCS files for analysis with FlowJo v10.5.0 (FlowJo, LLC, Ashland OR). A similar gating strategy was applied to all data sets to identify acceptor erythrocytes and to distinguish

positive and negative populations. The data was displayed on a logarithmic scale and total erythrocytes population was gated in FSC-A vs. SSC-A plot as the events falling between 0 and 10^5 on both sides. Single cells were gated using the FSC-H vs. FCS-A, from which acceptor erythrocytes were gated based on the fluorescence intensity of the corresponding dye. Data were primarily expressed as median fluorescent intensity (MFI) from which, the stain index (SI) was calculated for each dye. SI is a normalized sensitivity metric, used for quantitating the brightness of immunofluorescent reagents through estimation of signal detection over the background. Here, the SI was calculated using the following formula:

$$SI\ nonparametric = \frac{3.29 \times (50th\ positive - 50th\ negative)}{95th\ negative - 5th\ negative}$$

To acquire data from invasion phenotyping assays, parasitized erythrocytes were further gated from DDAO-SE or CTFR-labelled cells based on either SYBR Green I or Hoechst 33342 fluorescent intensity. Each condition was tested three times and the data were presented as the mean plus or minus the standard error from the different replicates. Additional calculations and graphs were generated using GraphPad Prism v.7.01 (GraphPad Software, Inc.).

3.3.5. Results

3.3.5.1. Gating strategy for the selection of CTFR-labelled erythrocytes

Although CTFR has a well-defined emission peak (661 nm; Table 3.5), its fluorescent signal can be detected with a wide range of filter sets. Here we used filters designed to acquire wavelength derived from Alexa Fluor 647 fluorochrome to detect CTFR-associated signal. Total erythrocytes were primarily gated using the FSC-A and SSC-A parameters (Figure 3.11A) and single erythrocytes (Figure 3.11B) were used to further gate CTFR positive population (Figure 3.11C-D)

207 Table 3.5: Dye properties and their associated flow cytometer settings

Staining parameters					Flow cytometer settings				
Dyes (Form)	Diluent	Stock concentration	Working concentration	Staining properties	Excitation (nm)	Emission (nm)	Laser line (nm)	Filter sets	PMT*** (Volts)
CFDA-SE (Lyophilised)	DMSO	5 mM	20 µM	Cytoplasmic	492	517	Blue (488)	530/30 (505LP)	452
DDAO-SE (Lyophilised)	DMSO	5 mM	10 µM	Cytoplasmic	648	657	Red (640)	670/30	505
CT Far-Red (Lyophilised)	DMSO	1 mM	1, 2 or 5 µM	Cytoplasmic	633	661	Red (640)	670/30	505
Hoechst 33342 (Solution)	-	20 mM	1 µM	Nuclear	361	497	UV (355)	450/30 (410LP)	300
SYBR Green I (Solution)	-	10,000X	1X	Nuclear	NA	NA	Blue (488)	530/30 (505LP)	350

208 *** These settings should be optimized when using a different flow cytometer model

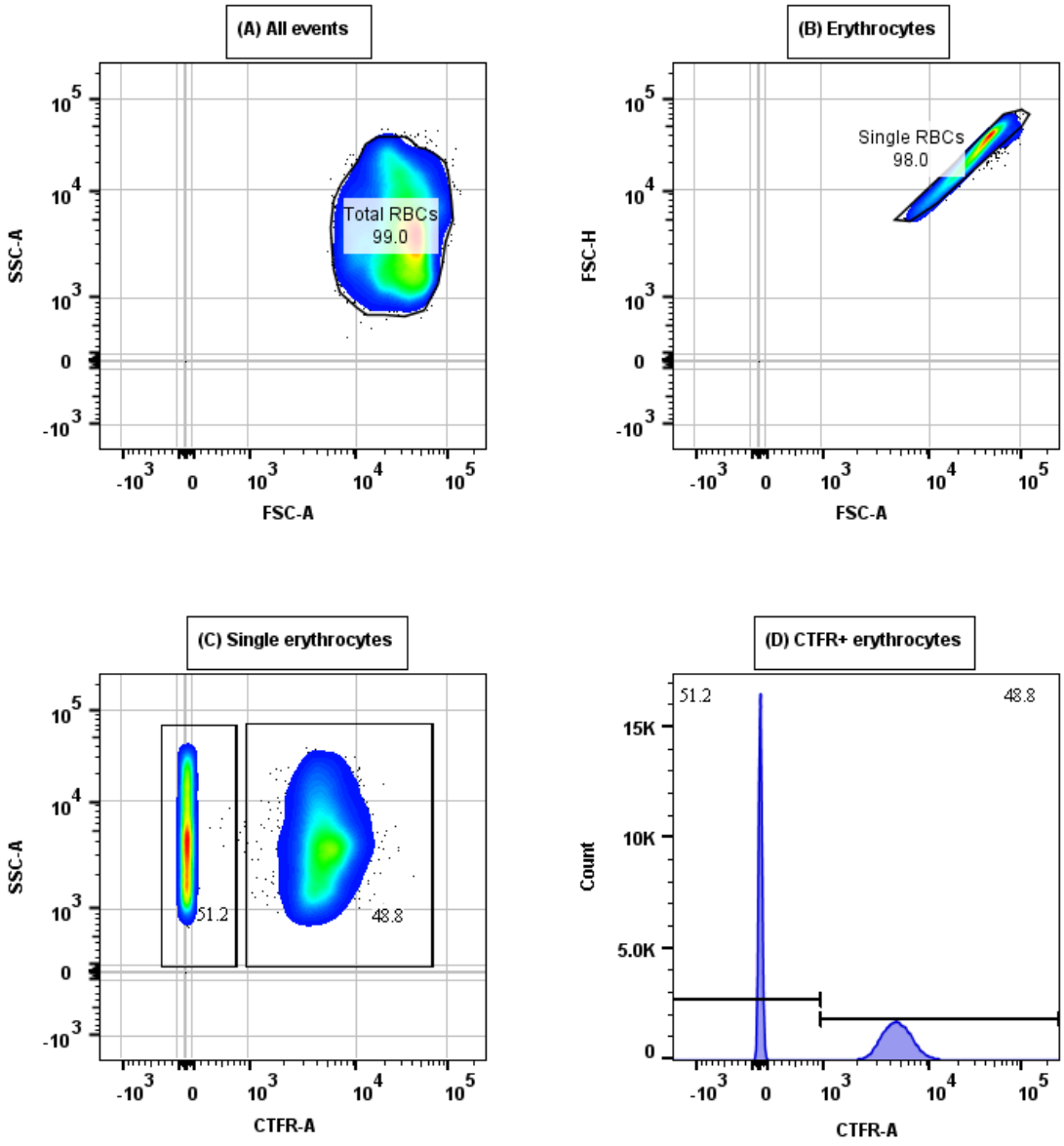

Figure 3.11: Gating strategy of data generated by CTFR staining. (A): Pseudocolor plot of all events gated in the forward scatter area (FSC-A) by side scatter area (SSC-A). (B): Selection of single erythrocytes using forward scatter hight (FSC-H) by the FSC-A. (C-D): Dot plot and histogram plot showing CTFR fluorescent intensity by the SSC-A and number of erythrocytes count, respectively. PMT voltages were adjusted so that CTFR stained erythrocytes register between 10^3 and 10^5 on the logarithmic scale. Black dots represent outliers.

3.3.5.2. CTFR labelling requires minimal dye concentration and short incubation time

The first step for assessing the applicability of CTFR in *P. falciparum* phenotyping assays was to determine the optimal concentration to effectively distinguish the staining intensity over the autofluorescence background. Dye concentrations of 1, 2 and 5 µM were used and the resulting stain index (SI) was compared to that of CFDA-SE and DDAO-SE. Prior to data acquisition, labelled erythrocytes were pre-incubated with mock-labelled erythrocytes (negative control) at 37° C for at least 24 hours. As expected, fluorescent intensity shows a dose-dependency with dye concentration, with 5 µM CTFR yielding a higher fluorescent intensity as compared to 1 and 2 µM, which nevertheless, yielded distinct fluorescent peaks relative to the negative control (Figure 3.12A-D). Additionally, staining erythrocytes at 4% hematocrit yielded a better resolution between positive and negative populations (Figure 3.12A, C) relative to 8% hematocrit (Figure 3.12B, D). To prepare working concentrations from CTFR stock, we assessed the effectiveness of two different diluents, RPMI 1640 and PBS, to uniformly stain erythrocytes. Overall, similar staining patterns were observed when erythrocytes were stained in either labelling solution at the same dye or cell concentration (Figure 3.12). However, the data show that staining with RPMI at lower hematocrit gives a better resolution with minimal overlap between different concentrations of dye (Figure 3.12).

Furthermore, we assessed the minimal incubation time needed to allow the dye to penetrate the cells and develop a detectable positive signal. Strong and relatively similar fluorescent intensities were observed after 20, 40 and 60 minutes of incubation and a slightly higher MFI observed after 2 hours of incubation (Figure 3.A7).

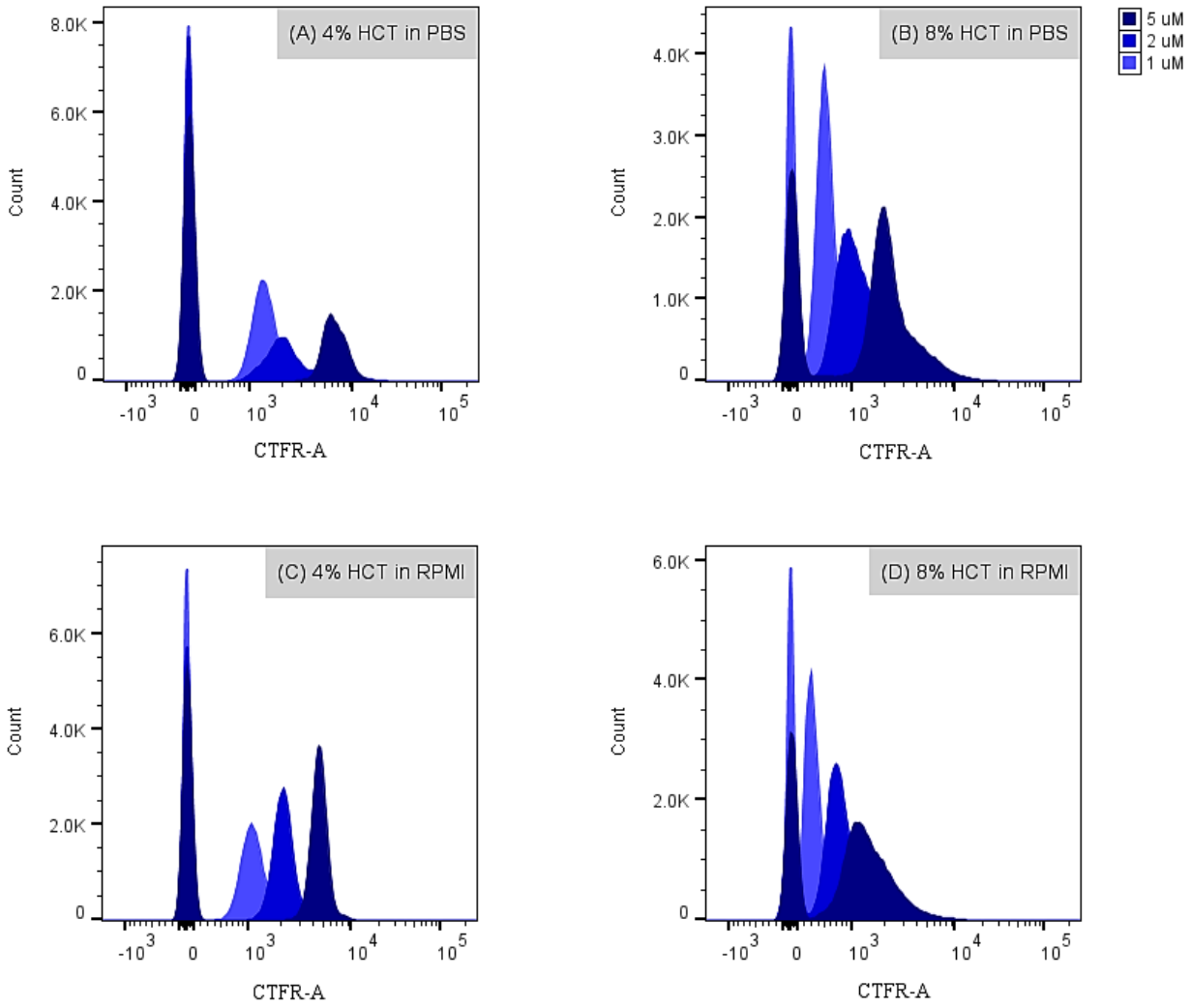

Figure 3.12: Labelling conditions of acceptor erythrocytes with CTFR. Erythrocytes were labelled using different concentrations of CTFR diluted in different solvents – 1X PBS (A-B) or RPMI 1640 (C-D) - at different hematocrits - 4% (A and C) or 8% (B and D) - and incubated at 37 ºC for 2 hours in a shaking incubator. Labelled erythrocytes were further mixed with unlabelled erythrocytes and analyzed by flow cytometry.

3.3.5.3. CTFR labels erythrocytes with a stable fluorescent intensity

Conducting *P. falciparum* invasion phenotyping assays requires the co-incubation of the acceptor (labelled) with donor erythrocytes (unlabelled), hence the stability of CTFR within stained cells was of interest. Passive dye-transfer from labelled to unlabelled cells has been reported in cell proliferation studies involving both membrane and cytoplasmic dyes (Begum et al., 2013; Filby, Begum, Jalal, & Day, 2015; Lassailly, Griessinger, & Bonnet, 2010; Quah & Parish, 2012). Here, the stability of CTFR stain index was monitored for a period of two weeks and compared to that of DDAO-SE or CFDA-SE stained cells. Overall, all dyes showed a decrease of SI, which seemed to be progressive over time and irrespective to cell concentration or staining solution in the case of CTFR (Figure 3.13).

However, staining with 1 µM CTFR in RPMI at 4% hematocrit yielded a more stable SI relative to the rest of the conditions (Figure 3.13, Figure 3.A8). Given the relatively stable background fluorescence observed in unlabelled cells, which, overall does not seem to increase over time as expected in case of dye transfer (Table 3.A8), our data suggest that the observed variations might be due to other erythrocyte intrinsic properties than to passive dye transfer between cells. This, therefore, indicates that CTFR could be appropriate for labelling of acceptor erythrocytes for invasion phenotyping assays.

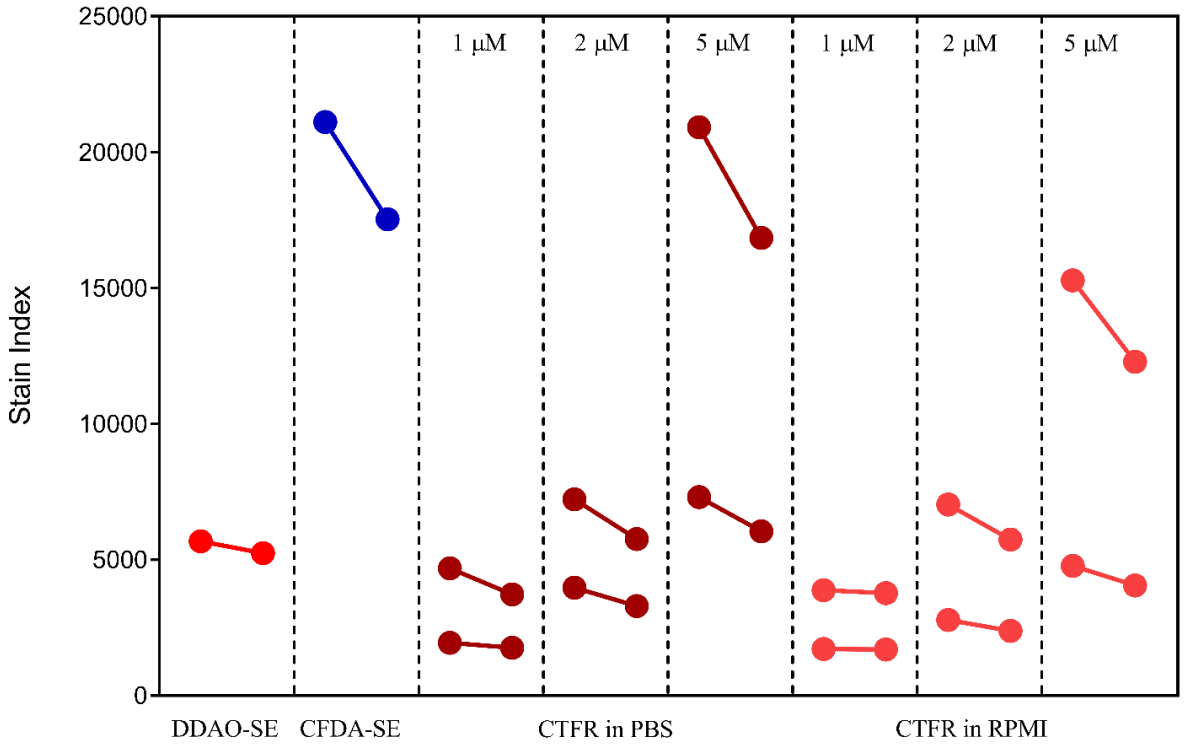

Figure 3.13: Graph showing the variation of CTFR stain index at two-time points, day 0 and day 15 post-staining. To monitor the stability of CTFR, labelled erythrocytes were co-incubated with unlabelled erythrocytes for at least 24 hours prior to data acquisition by flow cytometry. CTFR SI was monitored for 15 days and compared to that of CFDA-SE and DDAO-SE.

3.3.5.4. CTFR labelling does not impair erythrocyte invasion or normal parasite growth

Amine-reactive dyes, such as DDAO-SE and CFDA-SE, have been preferred over membrane dyes because they do not impair parasite invasion (Theron et al., 2010). To test whether CTFR affects parasite invasion or early intraerythrocytic development, erythrocytes from tightly synchronized 3D7 and Dd2 cultures were co-incubated with erythrocytes labelled with CFDA-SE, DDAO-SE or CTFR for two complete asexual cycles. Culture aliquots collected at different time points were analyzed by both flow cytometry and microscopy to assess the invasion rate

and parasite morphology, respectively, in both labelled and unlabelled erythrocytes. Overall, there was no significant difference in the parasites' invasion rates into CTFR labelled and unlabelled erythrocytes (Figure3.14A). There was also no significant difference in the parasites' growth rates in CTFR labelled erythrocytes relative to those in CFDA-SE or DDAO-SE labelled erythrocytes (Figure 3.14A). Across all assays, the ratio of invasion into labelled/unlabelled erythrocytes was not significantly different from 1 (Figure 3.A9), therefore suggesting that none of the dyes tested here, particularly CTFR, significantly affects parasite invasion relative to unlabelled erythrocytes. Besides, our data also showed that parasites were able to develop normally within both erythrocyte subpopulations, as they underwent complete intraerythrocytic development with no apparent morphological changes (Figure 3.14B, Figure 3.A10). This result mimics early reports regarding the nontoxic effect of CTFR when used to study other cell types (Atwal et al., 2016; Zhou et al., 2016), but also confirms previous reports regarding the use of amine-reactive dyes in invasion phenotyping assays (Theron et al., 2010).

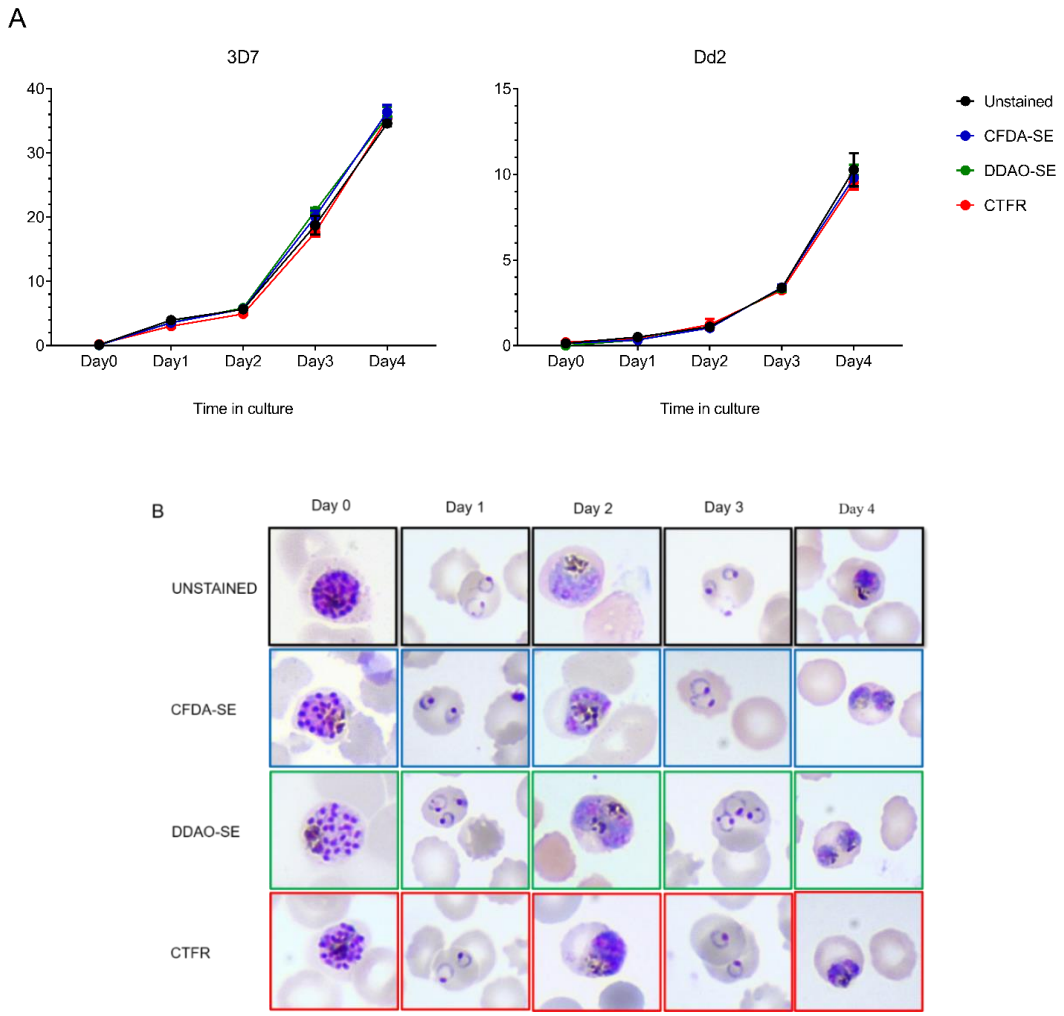

Figure 3.14: CTFR labelling does not impair *P. falciparum* erythrocyte invasion and normal parasite growth. Erythrocytes labelled with either CFDA-SE (20 µM), DDAO-SE (10 µM) or CTFR (2 µM) were individually incubated with equal volumes of schizont-infected erythrocytes from 3D7 and Dd2 parasite cultures under normal *P. falciparum* culturing conditions. (A) Graphs showing the parasite growth patterns for two successive asexual replication cycles in labelled erythrocytes relative to the unlabelled control erythrocytes. (B) Giemsa-stained parasites showing the parasite morphology in unstained (black squares), CFDA-SE-stained (blue squares), DDAO-SE-stained (green squares) and CTFR-stained erythrocytes (red squares). Culture aliquots, harvested at regular time intervals were fixed with 100% methanol and stained with 10% Giemsa on glass microscope slides. Images were taken with a Cole Palmer light microscope (Vernon Hills, Illinois 60061, USA) coupled with a MoticamBTW8 camera (Motic China Group Co., Ltd).

3.3.5.6. A CTFR-based dual-dye flow cytometry assay for *P. falciparum* invasion phenotyping assays

Appropriate discrimination between infected and uninfected erythrocytes is key for developing a highly sensitive flow cytometry-based *P. falciparum* invasion assay. Based on the previously described approach (Theron et al., 2010), we assessed the sensitivity of SYBR Green I and Hoechst 33342, two nucleic acid dyes in differentiating infected and uninfected erythrocytes and showed that both were able to similarly detect infected erythrocytes, with however Hoechst 33342 yielding a relatively lower level of background staining with uninfected erythrocytes (Figure 3.A11). To further confirm the suitability of CTFR for *P. falciparum* invasion phenotyping assays, we used it to assess the invasion phenotypes of two *P. falciparum* laboratory strains, 3D7 and Dd2, with known invasion phenotypes (Duraisingh, Maier, Triglia, & Cowman, 2003; Gaur, Storry, Reid, Barnwell, & Miller, 2003; Persson et al., 2008). Schizont-infected erythrocytes were co-incubated with either DDAO-SE or CTFR-labelled and enzyme-treated erythrocytes for 24 hours, and infected cells were then labelled post-incubation with either SYBR Green I or Hoechst 33342 to determine the parasitemia. Mock-treated erythrocytes were used as positive controls to estimate the invasion efficiency wherein the observed parasitemia of a given treatment group was expressed as a percentage of the former one. The effect of enzyme treatment was assessed for each isolate using DDAO-SE or CTFR-labelled erythrocytes. As expected, both isolates retained similar invasion phenotypes following staining with either SYBR Green I or Hoechst 33342, irrespective of the erythrocyte dye (Figure 5). *P. falciparum* 3D7 invaded neuraminidase treated erythrocytes with higher invasion efficiency (> 50%) relative to that of Dd2 (< 50%), therefore, confirming previously published data regarding the degree of sialic acid dependency of these isolates (Figure 3.15). We also assessed invasion

rates into trypsin and chymotrypsin treated erythrocytes by both *P. falciparum* isolates. Both isolates showed a relatively high invasion of chymotrypsin-treated erythrocytes (> 50%) while 3D7 invaded trypsin-treated cells with less efficiency (< 50%) relative to Dd2, which showed invasion rates of above 60% (Figure 3.15).

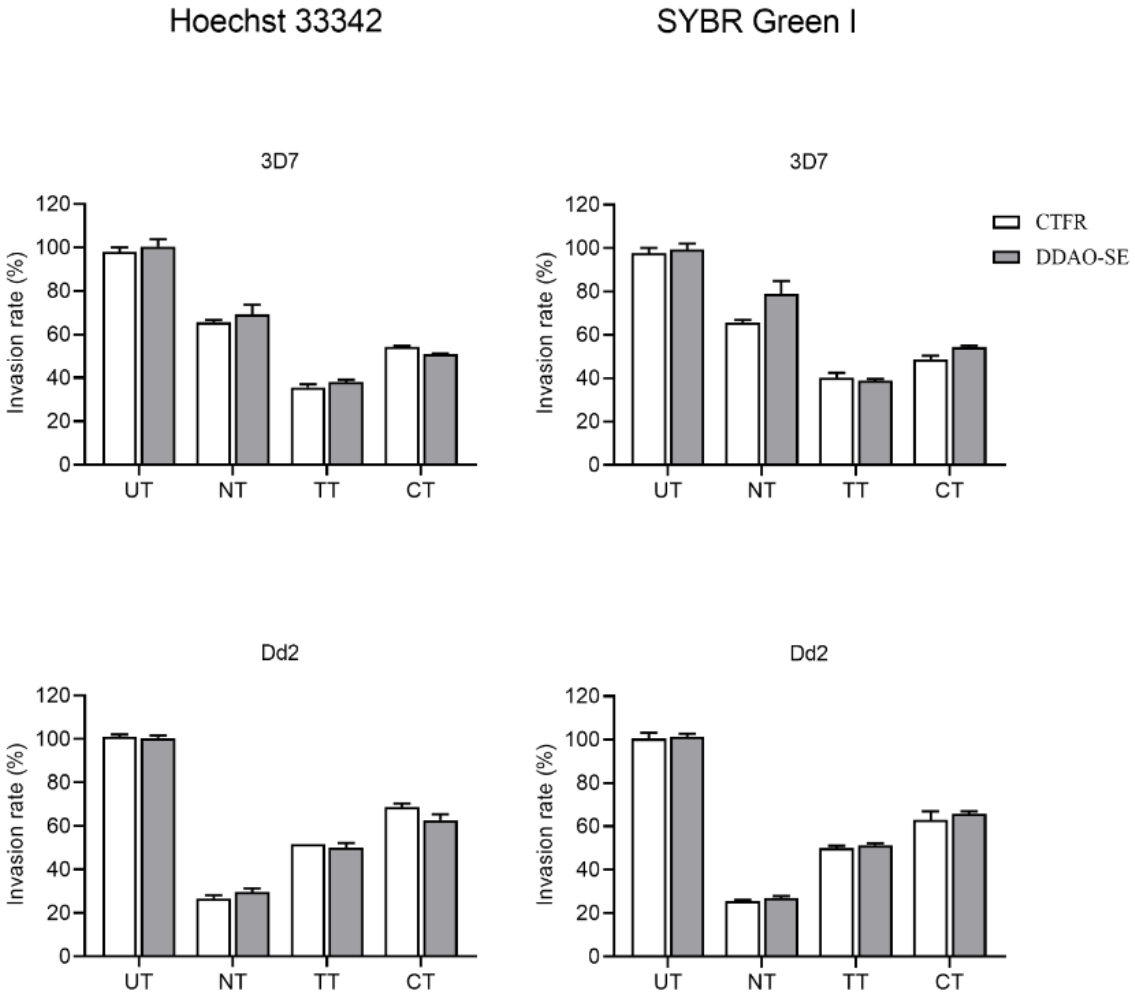

Figure 3.15: Invasion phenotypes of two *P. falciparum* laboratory strains: 3D7 and Dd2 into enzyme-treated erythrocytes. Schizont-infected unlabelled erythrocytes were co-incubated in a 1:1 ratio with either DDAO-SE or CTFR-labelled erythrocytes, at 37 ºC for 18-24 hours. Following incubation, parasites were stained with either Hoechst 33342 or SYBR Green I and final parasitemias in the target populations were determined by gating on the fluorescently labelled erythrocyte population using flow cytometry. Invasion efficiencies were determined as a percentage of the final parasitemia of a mock-treated and labelled positive control erythrocyte population. The data are presented as the mean ± standard error of the mean of two independent experiments conducted in triplicates. UT, untreated; NT, neuraminidase treatment; TT, trypsin treatment; CT, chymotrypsin treatment.

3.3.6. Discussion

The pathogenic phase associated with *P. falciparum* infection is initiated following erythrocyte invasion by the merozoite form of the parasite. Erythrocyte invasion is a very complex process and its molecular mechanisms need further understanding, particularly the specific ligand-receptor interactions involved. The development of new flow cytometry-based approaches offers higher sensitivity, specificity and speed compared to other routinely used technologies such as microscopy (Bei, Desimone, et al., 2010). Furthermore, flow-cytometry based approaches have enabled the easy investigation of *P. falciparum* invasion phenotypes in the field of malaria research. One of the advantages of flow cytometry is its ability to provide a platform for high throughput data generation. This study describes a flow cytometry-based assay to assess the suitability of CTFR, a newly developed red excited cytoplasmic dye, for *P. falciparum* erythrocyte invasion phenotyping assays. CTFR can passively diffuse through the plasma membrane, to covalently bind to cell cytoplasm and to develop a stable fluorescence (Zhou et al., 2016). Besides, CTFR has a very narrow emission band 633-661 nm, which allows its usage in multiplex experiments with minimal risk of spectral overlap (Zhou et al., 2016). To our knowledge, this is the first study that assessed the applicability of CTFR for labelling erythrocytes for merozoites invasion assays. For parasite quantification, previously described DNA dyes, namely SYBR Green I and Hoechst 33342 (Theron et al., 2010), were used to distinguish between infected and uninfected erythrocytes. To minimize the effect on cell integrity or metabolism, if any, a good cytoplasmic dye should be able to brightly label the acceptor cells with relatively low concentrations. Consequently, we have shown that, even at low concentrations (1 µM), CTFR is able to yield high fluorescence upon excitation with the red laser and this is consistent with a previous report on the labelling of other cell types (Zhou

et al., 2016). Routine *P. falciparum* phenotyping assays involve co-incubation of labelled acceptor erythrocytes with unlabelled donor erythrocytes from the starting culture and therefore necessitates a clear distinction between these two populations of erythrocytes. Confounders, such as dye-transfer between co-incubated positive and negative cells, have previously been shown to affect the sensitivity of cell proliferation assays using cytoplasmic dyes (Begum et al., 2013; Filby et al., 2015). However, such variations were not observed in our study which shows that the dye was well retained in erythrocytes which is in agreement with the dye being carried in mammalians cells for several generations (Miao et al., 2017; Tario, Conway, Muirhead, & Wallace, 2018) and therefore, suggesting its stable binding to the free amino groups of intracellular macromolecules. Moreover, the preference of cytoplasmic dyes over membrane dyes is determined by their ability to not impair erythrocyte invasion. We showed that CTFR has the ability to efficiently stain erythrocytes without impairing the parasite invasion or development. Furthermore, we also showed that combination of CTFR with either SYBR Green I or Hoechst 33342 reveals some common features of the CTFR with DDAO-SE in terms of spectral properties as previously reported (Theron et al., 2010). Besides, our study also reports similar rates of merozoites invasion between CTFR and DDAO-SE. This further reiterates the ability of CTFR to be used as an alternative for DDAO-SE in flow cytometry-based *P. falciparum* invasion assays. Our assay is optimized for utilization with instruments that are not equipped to simultaneously excite CFDA-SE and Hoechst 33342, but, also for experiments where there is the need to free-up the green channel (e.g. experiments requiring SYBR Green or GFP detection). In conclusion, we have optimized a sensitive CTFR-based dual-dye flow cytometry assay for assessing the invasion phenotypic diversity of *P. falciparum* and providing highly reliable and reproducible data comparable to existing assays. Also, given the ability of

CTFR to stain acceptor erythrocytes at relatively low concentrations, combined to its narrow emission peak, it would be a dye of choice to consider for more complex experimental designs, such as, the recently developed erythrocyte preference assay (Theron et al., 2018), that requires dyes able to provide scalable assay design.

CHAPTER FOUR: SPECIFIC AIM TWO

4.1. PHENOTYPIC AND GENOTYPIC INVASION DIVERSITY OF *P. FALCIPARUM* CLINICAL ISOLATES FROM FOUR ENDEMIC AREAS IN GHANA

Hypothesis 1: The use of standardized approaches provides more relevant data with regards to the parasite phenotypic and genotypic invasion diversity and will help in designing transient invasion blocking vaccines.

To ascertain this hypothesis, *P. falciparum* clinical isolates were collected from children of age 2 to 14 years from four areas of varying transmission intensity across Ghana. The parasites' invasion phenotypes were assessed using enzyme-treated erythrocytes as well as anti-CR1 antibodies to ascertain the contribution of PfRh4-CR1 mediated invasion pathways in Ghanaian clinical isolates. The expression levels of known *P. falciparum* invasion-related genes were also determined to assess their relationship with the parasite's invasion pathways. Results from these investigations were used to draw comparisons with previous studies conducted in our laboratory.

4.1.1. Abstract

Erythrocyte invasion by *P. falciparum* occurs in four distinct steps involving functionally overlapping interactions between the parasite's ligands and the erythrocyte surface receptors. While some *P. falciparum* isolates necessarily engage the sialic acid (SA) moieties of the erythrocytes during the invasion, others use ligands whose binding is independent of the presence of SA for a successful invasion. It has been hypothesized that the combinatory usage of some sets of parasites ligands is dictated by the level of immunity of the infected host, which in turn is as a result of transmission intensity. Invasion phenotype was assessed using enzyme-treated erythrocytes along with anti-CR1 antibodies to determine the relative contribution of the PfRh4-CR1 interaction in Ghanaian *P. falciparum* clinical isolates. Complete invasion data from 156 isolates, from four different transmission areas, showed the predominance of SA-independent pathways in Ghanaian clinical isolates. Moreover, there was no significant difference in the parasite's sensitivity to neuraminidase treatment across all study sites. Overall, there was a strong positive correlation between the parasites' sensitivity to trypsin and chymotrypsin. Additionally, our data also confirmed that the PfRh4-CR1 mediated alternative pathway is important in Ghanaian clinical isolates. Furthermore, the transcript levels of ten invasion-related genes obtained in the study showed little variations in gene expression profiles within and between parasite populations across sites. In conclusion, our data suggest a low level of variation of phenotypic and genotypic diversity in Ghanaian clinical isolates across areas of varying endemicity. This is of great interest in the quest for new intervention strategies, such as the investigation of blood-stage vaccine targets, particularly those targeting specific pathways that require the stimulation of broadly neutralizing invasion antibodies.

4.1.2. Introduction

Despite tremendous efforts that led to the drastic reduction of the malaria burden (WHO, 2015), *P. falciparum* malaria continues to be a major public health concern, claiming more than 400,000 deaths in 2017, with the sub-Saharan region of Africa being the most afflicted worldwide (WHO, 2018b). Thus, the development of an affordable, yet efficient malaria vaccine remains one of the last resorts to achieve the goal of elimination. The clinical manifestations of malaria only occur during the asexual replication of the parasites in the host erythrocytes.

Erythrocyte invasion by *P. falciparum* is a very rapid and complex process which involves the sequential release of an arsenal of parasite antigens (ligands) from the merozoite's secretory organelles (Farrow et al., 2011), which subsequently bind to specific receptors on the surface of the host erythrocyte to mediate invasion (reviewed in (Cowman et al., 2017)). *P. falciparum* invasion-related ligands include members of the *P. falciparum* erythrocytes binding antigens (PfEBAs), namely PfEBL1, PfEBA175, PfEBA140, PfEBA181 and PfEBA165, as well as members of the *P. falciparum* reticulocyte binding-like homologue (PfRh) family proteins, including PfRh1, PfRh2a, PfRh2b, PfRh4 and PfRh5 (Tham et al., 2012). Taken together, PfEBL and PfRh proteins are essential for the survival of the parasite, however, with the exception of Rh5, *P. falciparum* ligands are functionally redundant (reviewed in (Tham et al., 2012). Besides, SA residues, present on the erythrocyte glycoproteins, have also been shown to be a major determinant of *P. falciparum* invasion (Adams et al., 1992; Malpede, Lin, & Tolia, 2013). Consequently, *P. falciparum* invasion pathways are classified as SA-dependent or SA-independent.

Of the five *P. falciparum* ligand-receptor interactions known to be involved in invasion, three mediate the SA-dependent pathway (PfEBA175/glycophorin A, PfEBL1/glycophorin B and PfEBA140/glycophorin C), whereas the PfRh4/complement receptor 1 mediate the SA-independent pathway (Cowman et al., 2017). It is widely accepted that *P. falciparum* uses the mechanism of phenotypic variation to circumvent the host immune response during acute malaria infection (Persson et al., 2008; Stubbs et al., 2005; Wright & Rayner, 2014). Therefore, characterizing the phenotypic invasion diversity of *P. falciparum* clinical isolates would provide relevant data with regards to the major invasion pathways used by these parasites during natural infections. This, in turn, could be exploited as a key resource in the quest of an efficient malaria vaccine.

Pioneering studies on the invasion diversity of *P. falciparum* clinical isolates reported distinct invasion pathways used by isolates from different geographical locations. For instance, clinical isolates from both The Gambia (Baum et al., 2003b) and Brazil (Lobo et al., 2004) have been shown to preferentially use the SA-dependent pathway, while isolates from India (Okoyeh et al., 1999), Ghana (H. E. Mensah-Brown et al., 2015), and Senegal (Jennings et al., 2007; Lantos et al., 2009) predominantly use the SA-independent pathway. This led to the hypothesis that *P. falciparum* phenotypic diversity is influenced by the level of natural immunity against the circulating parasite populations, which in turn is as a result of the transmission intensity (Bowyer et al., 2015; H. E. Mensah-Brown et al., 2015).

Previous reports from our group showed that *P. falciparum* clinical isolates from three endemic areas in Ghana used SA-independent invasion pathway. However, while there was a significant difference in the invasion efficiency into neuraminidase treatment, which was inversely

proportional to transmission intensity, such a trend was not observed in the sensitivity to trypsin and chymotrypsin treatment (H. E. Mensah-Brown et al., 2015).

In this study, we included a larger number of *P. falciparum* clinical isolates from four endemic areas in Ghana to assess their phenotypic invasion diversity. Given the earlier reports on the use of CR1 as a key receptor for invasion in Ghanaian clinical isolates (Bowyer et al., 2015; H. E. Mensah-Brown et al., 2015), we also tested the contribution of the CR1-mediated pathways in our study population. Furthermore, we tested for the differential expression of invasion-related genes with regards to the PfEBA and PfRh family proteins in selected isolates from our study sites.

4.1.3. Materials and Methods

4.1.3.1. Sample collection

This study was approved by Ethics Committees of the Ghana Health Service, the Kintampo Health Research Centre, the Navrongo Health Research Centre and the Noguchi Memorial Institute for Medical Research, University of Ghana, Legon. *P. falciparum* clinical isolates used in this study were collected from children aged between 2 to 14 years, presenting a clinically diagnosed malaria infection visiting the LEKMA municipal hospital (Accra), the Hohoe municipal hospital (Hohoe), the Kintampo health research centre (Kintampo) or the Navrongo health research centre (Navrongo) between 2011 and 2016. According to the most recent data regarding the transmission intensity, Kintampo has the highest transmission rate with an estimated entomological inoculation rate (EIR) of >250 infective mosquito bites per person/year, followed by Navrongo with <250 infective mosquito bites per person/year, while Hohoe and Accra have the lowest transmission rates with 65 and <50 infective mosquito bites

per person/year, respectively (Kasasa et al., 2013; Klinkenberg, McCall, Wilson, Amerasinghe, & Donnelly, 2008; Kweku et al., 2008; Owusu-Agyei et al., 2009). For all participants, written consent was obtained from the parent or guardian prior to sample collection and additional assent was sought from children older than 10 years. *P. falciparum* infections were confirmed by microscopy following a positive rapid diagnostic test (RDT). For each patient, the parasitemia was estimated as previously described (H. E. Mensah-Brown et al., 2015). Samples were collected in acid citrate dextrose (ACD) vacutainers and parasitized erythrocytes were cryopreserved in liquid nitrogen until use.

4.1.3.2. *P. falciparum in vitro* culturing and invasion assays

Cryopreserved *P. falciparum* clinical isolates were thawed using NaCl solutions and suspended at 4% haematocrit in complete parasite medium, RPMI 1640 medium (Sigma, UK), supplemented with 0.5% Albumax II (Gibco), 2% normal human serum (PAN Biotech, UK), 50 µg/mL Gentamicin and 2 mg/mL sodium bicarbonate. Cultures were incubated at 37º C in an atmosphere of 2% O_2, 5% CO_2 and balanced with N_2. Human erythrocytes of blood group O^+ were used for all invasion assays. Upon collection, blood samples were spun at 2000 rpm for 10 minutes and the erythrocyte pellets were further washed with RPMI 1640 medium and suspended at 50% haematocrit. Erythrocytes used in invasion assays were treated with either neuraminidase (250 mU/mL), trypsin (1 mg/mL) or chymotrypsin (1 mg/mL) for an hour at 37º C with gentle shaking, washed thrice with RPMI 1640 and labelled with 20 µM carboxyfluorescein diacetate succinimidyl ester (CFDA-SE) for two hours at 37º C. Invasion assays were set as previously described (H. E. Mensah-Brown et al., 2015). Briefly, parasites were allowed to grow for at least 36 hours following thawing and all assays were conducted in

triplicates in 96 well plates. Additionally, to determine the relative dependence of clinical isolates on the CR1-mediated pathway, assays were set with the presence of 12 µg/mL of chicken anti-human CR1 antibodies or control immunoglobulin Y (IgY, Gallus Immunotech, Fergus, Canada). Culture-derived infected erythrocytes were seeded with equal volumes of target labelled cells and incubated at 37º C for approximately 24 hours. Plates were subsequently removed from the incubator and spun at 2000 rpm for 3 minutes and the medium replaced with 1 mM Hoechst 33342 solution to label the parasites' DNA. Invasion rates were determined using a BD LSR Fortessa X-20 cytometer (BD Biosciences, Belgium).

4.1.3.3. Gene expression analysis

For isolates that grew well, schizont-infected erythrocytes were pelleted and stored at -80º C in Trizol reagent (Ambion, Life Technologies, Carlsbad, CA). For each sample, both RNA and DNA were extracted using the All Prep DNA/RNA Mini Kit (Qiagen) following the manufacturer's instructions. The expression level of selected invasion-related genes was assessed using the Luna Universal One-Step RT qPCR Kit (New England Biolabs, Inc.). Experiments were run using a Quant Studio 5 Real-Time PCR System (Applied Biosystems), following manufacturer's instructions. For each isolate, the transcript level of each gene was determined as the percentage of the sum of transcript levels of individual genes following normalization using the 60S ribosomal protein L18 and the apical membrane antigen 1 (AMA1) as endogenous control and parasites maturation marker, respectively.

4.1.3.4. Statistical analysis

All statistics were performed using GraphPad Prism v.8.01. The Chi-square test was used to compute for differences between categorical variables. One-way ANOVA or Kruskal Wallis was used to assess for differences between distinct groups and where significant, the Tukey's or the Dunn's multiple comparison test was used for pairwise comparisons, respectively. The Spearman rank correlation or the Pearson correlation was used to assessing relationships between variables. For all analysis, a *p-value* of at least 0.05 was considered as significant.

4.1.4. Results

4.1.4.1. Characteristics of study participants

Participants for this study were children aged between 2 to 14 years, presenting symptomatic *P. falciparum* infection, recruited from areas of varying transmission Accra: (N = 42) < Hohoe (N = 36) < Navrongo (N = 38) < Kintampo (N = 40). The demographic and haematological characteristics of the study participants are summarized in table 4.1. Overall, there was no significant difference in terms of sex ratio across the four study sites (Chi-square, P = 0.97), however, there was a significant difference in the mean age (ANOVA, P = 0.008), with children from Navrongo being the youngest (mean age, 4.67 years), while the oldest children were from Hohoe (mean age, 7 years). With respect to the parasite density, children from Kintampo reported the highest parasite burden (144,811 parasites/µL), while those from Navrongo were found to harbour the lowest number of parasites (52,170 parasites/µL). There was a significant difference in the parasite burden in children from Kintampo compared to those from Accra (P = 0.002), Hohoe (P = 0.0003) and Navrongo (P = 0.0001), while no significant difference was

observed between the three other sites. Furthermore, no significant variation was observed with the hemoglobin levels (Table 4.1), or with the other haematological indices (e.g. white blood cell counts, platelet counts) (data not shown).

Table 4. 1: Clinical and demographic data of study participants from Accra, Hohoe, Navrongo and Kintampo.

Characteristics	**Accra**	**Hohoe**	**Navrongo**	**Kintampo**	***P-value*** [a]
Donors, No.	42	36	38	40	
Demographic data					
Sex ratio (Male/Female)	1.25	1.18	1.19	1.44	0.97[b]
Age (Years), Mean ± SEM,	5.75 ± 0.54	7 ± 0.56	4.67 ± 0.46	4.89 ± 0.49	0.008
Haematological indices					
Parasite density (Parasites/uL), Mean ± SEM,	69872 ± 7866	58333 ± 7988	52170 ± 4966	144811 ± 25688	<0.0001
Hemoglobin level (g/dL), Mean ± SEM	10.31 ± 0.29	10.79 ± 0.17	10.35 ± 0.29	9.70 ± 0.31	0.051

SEM: standard error of the mean

[a] indicates analysis performed with One-way ANOVA

[b] indicates test performed using Chi-square

4.1.4.2. Invasion pathways of Ghanaian *P. falciparum* clinical isolates

To investigate the major invasion pathways used by Ghanaian *P. falciparum* clinical isolates, parasites were first tested for their propensity to invade enzyme-treated erythrocytes. Target erythrocytes were treated with either neuraminidase, which removes the SA residues of glycoproteins, or trypsin or chymotrypsin, which cleave the peptide backbones of receptors such as GYPA, GYPB, GYPC and CR1. Across all sites, the invasion rate into neuraminidase-treated erythrocytes varied from 37.14 to 100% relative to untreated cells. Overall, the mean invasion rate into neuraminidase-treated erythrocytes was 74.85%, therefore confirming earlier reports on the predominance of the SA-independent pathway in Ghanaian clinical isolates (Bowyer et al., 2015; H. E. Mensah-Brown et al., 2015). Expectedly, there were differences in the invasion of neuraminidase-treated cells when comparing isolates across the different study sites (Figure 4.1A). Isolates from Navrongo showed the highest invasion rates into neuraminidase treated cells as compared to the rest of the study sites, however, this variation in invasion efficiency was only significant when comparing between isolates from Kintampo and Navrongo (P=0.02, Figure 4.1A). There was also wide variation in invasion rates following trypsin (mean, 28.92%) and chymotrypsin (mean, 35.87%) treatment, ranging from 5.97 to 71.11% and 9.09 to 68.89%, respectively (Figure 4.1B-C).

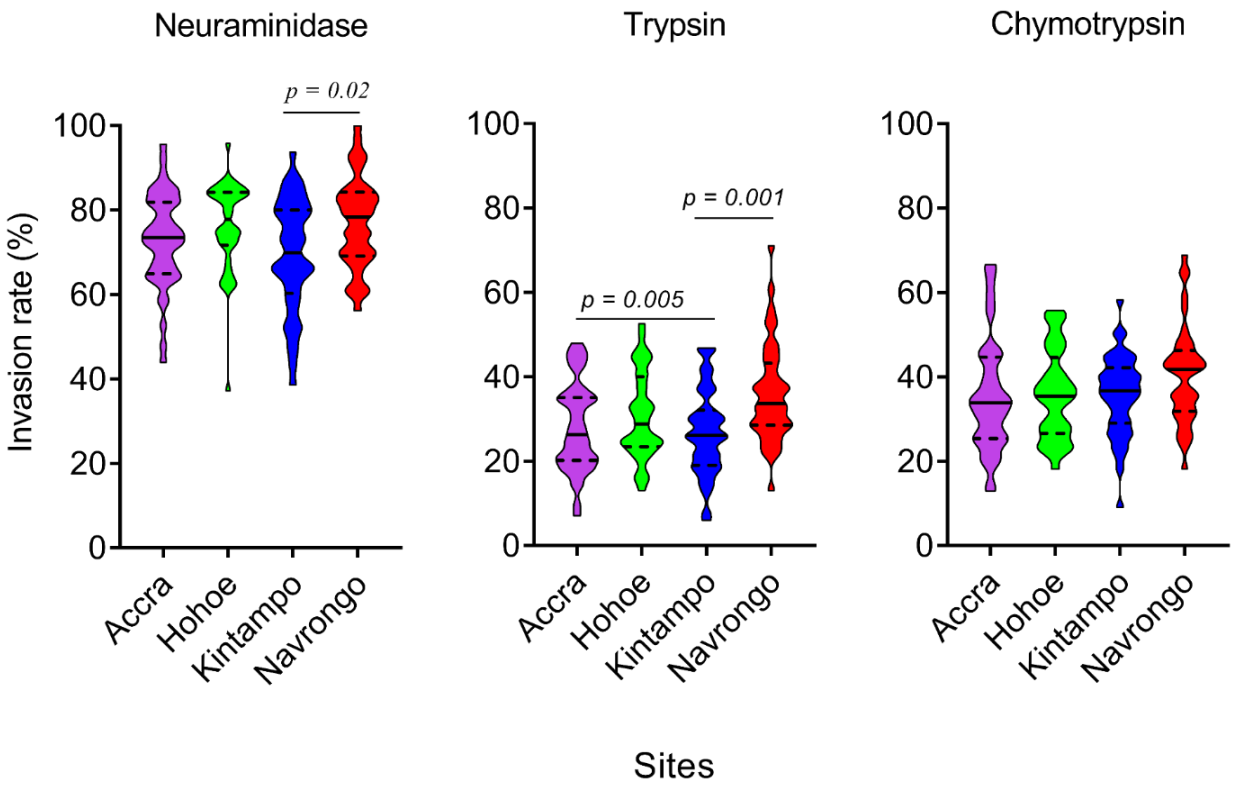

Figure 4. 1: Violin plots showing the invasion phenotypes of *P. falciparum* clinical isolates from areas of varying transmission intensity Accra (N = 42) < Hohoe (N = 36) < Navrongo (N = 38) < Kintampo (N = 40). Invasion efficiency was determined by the parasite invasion efficiency into neuraminidase (A), trypsin (B) or chymotrypsin (C) treated erythrocyte relative to the untreated control. Pairwise comparisons computed using the Tukey's multiple comparison test showed differences in the invasion efficiency of parasites from Navrongo and Kintampo following neuraminidase treatment (P = 0.02) and between Navrongo and Accra or Kintampo following trypsin treatment (P = 0.002 and P = 0.005, respectively).

Overall, isolates from Navrongo were less sensitive to treatment with trypsin or chymotrypsin. There was a significant difference in invasion into trypsin-treated cells only when comparing between isolates from Navrongo to those from Accra (P = 0.001, Figure 4.1B) or Kintampo (P = 0.005, Figure 4.1B). However, no significant difference was observed in the invasion into chymotrypsin treated cells across all study sites (P = 0.15, Figure 4.1C).

Furthermore, invasion into neuraminidase-treated erythrocytes did not correlate with invasion into of trypsin or chymotrypsin-treated erythrocytes (Figure 4.2A and B). However, there was a moderate to strong positive correlation in invasion efficiency between trypsin and chymotrypsin-treated erythrocytes across all sites (Figure 4.2C).

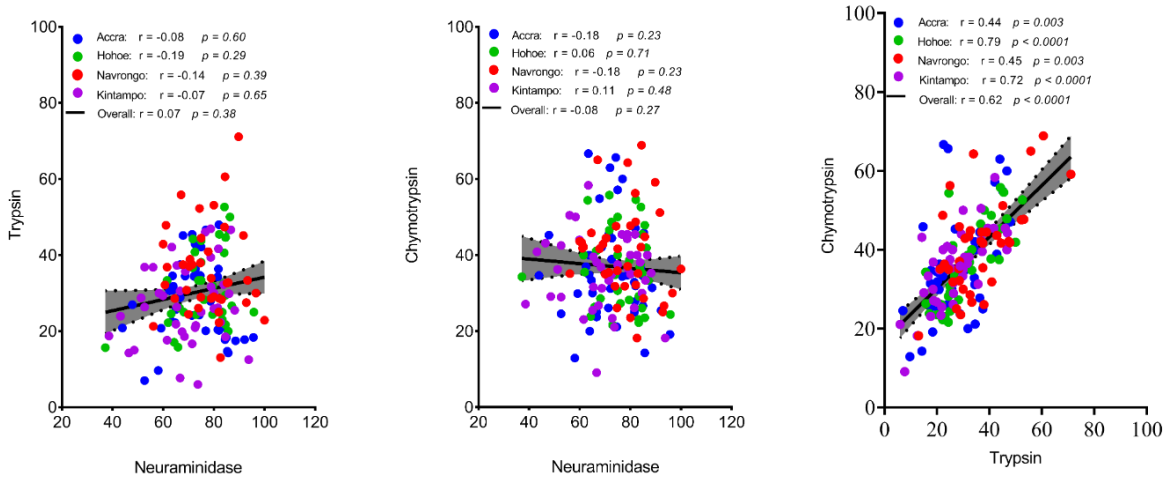

Figure 4. 2: Scatter plots showing the pairwise correlations of the parasite invasion efficiency into enzyme-treated erythrocytes. The Pearson correlation was used to compute the coefficients of correlation between invasion efficiency into neuraminidase and trypsin treated erythrocytes (B), that between trypsin neuraminidase and chymotrypsin treated erythrocyte (B) or that of the trypsin and chymotrypsin treated erythrocytes (C). Graphs were generated from invasion phenotypic data of 156 *P. falciparum* collected from areas of varying transmission intensities Accra (N = 42) < Hohoe (N = 36) < Navrongo (N = 38) < Kintampo (N = 40).

4.1.4.3. Phenotypic diversity of Ghanaian *P. falciparum* clinical isolates

To assess the phenotypic diversity of our isolates, we investigated the combined effect of the three different enzymes, also defined as invasion profiles (Lopez-Perez et al., 2012), on the parasites' invasion efficiency. A cut-off of 50% invasion efficiency relative to control erythrocytes was used to define sensitivity to a given treatment, consequently isolates were classified as sensitive (s, <50% invasion) or resistant (r, >50% invasion) to neuraminidase (N), trypsin (T) or chymotrypsin (C). Overall, five different profiles were observed across all sites, namely NsTsCs, NrTsCs, NrTsCr, NrTrCs and NrTrCr (Figure 4.3). Isolates from Hohoe and Navrongo presented the highest diversity with five and four different profiles, respectively (Figure 4.3). Across all sites, the NsTsCs profile was the least common, while the NrTsCs profile was the commonest, present in all study sites (Figure 4.3). This confirms an earlier report from our group regarding the preference of SA-independent pathways in Ghanaian clinical isolates (H. E. Mensah-Brown et al., 2015) and suggests that these isolates might be using alternative pathways mediated by receptors sensitive to both trypsin and chymotrypsin proteases.

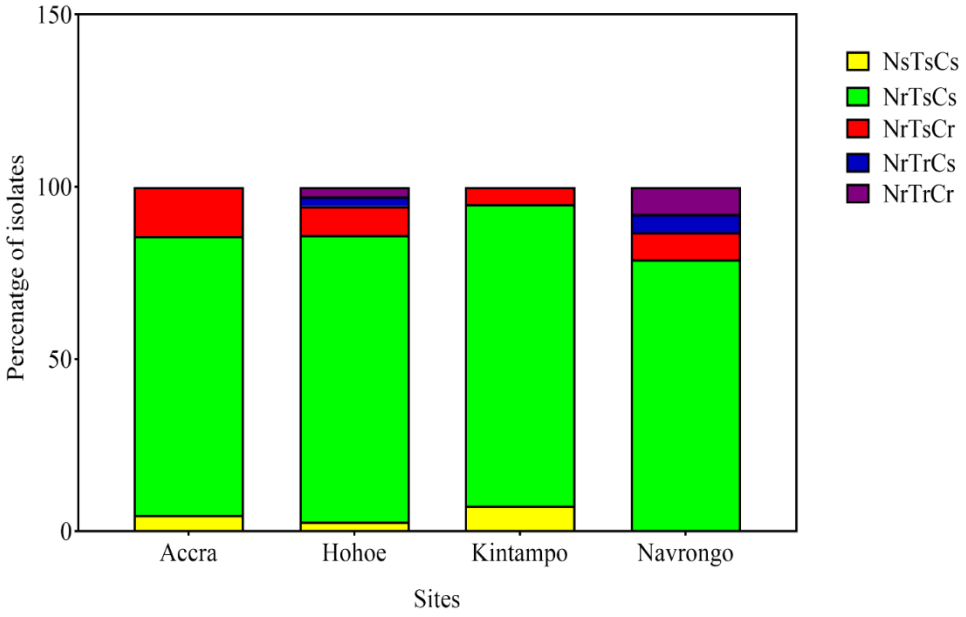

Figure 4. 3: Invasion profiles of Ghanaian *P. falciparum* clinical isolates for areas of varying transmission intensity. The graph shows the proportion of a given profile within the parasite population from a given area. For each the parasites, the invasion profile was determined as the combination of sensitivity to the three enzymes using a cut-off of 50% as a threshold to classify the observed profile as sensitive (≤50%) or resistance (>50%) for each given treatment.

4.1.4.4. CR1 is a major receptor mediating SA-independent pathway in Ghanaian *P. falciparum* clinical isolates

Given the preference for SA-independent pathways across all isolates and the role of CR1 as a major receptor mediating this particular pathway, we sought to assess the contribution of CR1 in the invasion efficiency of Ghanaian clinical isolates. *P. falciparum* clinical isolates from the different study sites were cultured at the schizont stage and used in invasion phenotyping assays to assessed the relative contribution of the human CR1receptor on the alternative invasion pathways used by Ghanaian clinical isolates. Parasites were incubated with either untreated or neuraminidase treated erythrocytes in the presence of either aniti-CR1 antibodies or IgY isotope

control. Invasion efficiency in each target group was then compared to that of the untreated erythrocyte control. Overall, there was no significant effect of anti-CR1 antibodies on the parasites' invasion efficiency into untreated cells, while the invasion efficiency into neuraminidase treated cells was drastically reduced by the addition anti-CR1 antibodies (mean, 22.67%) as compared to IgY control (Figure 4.4).

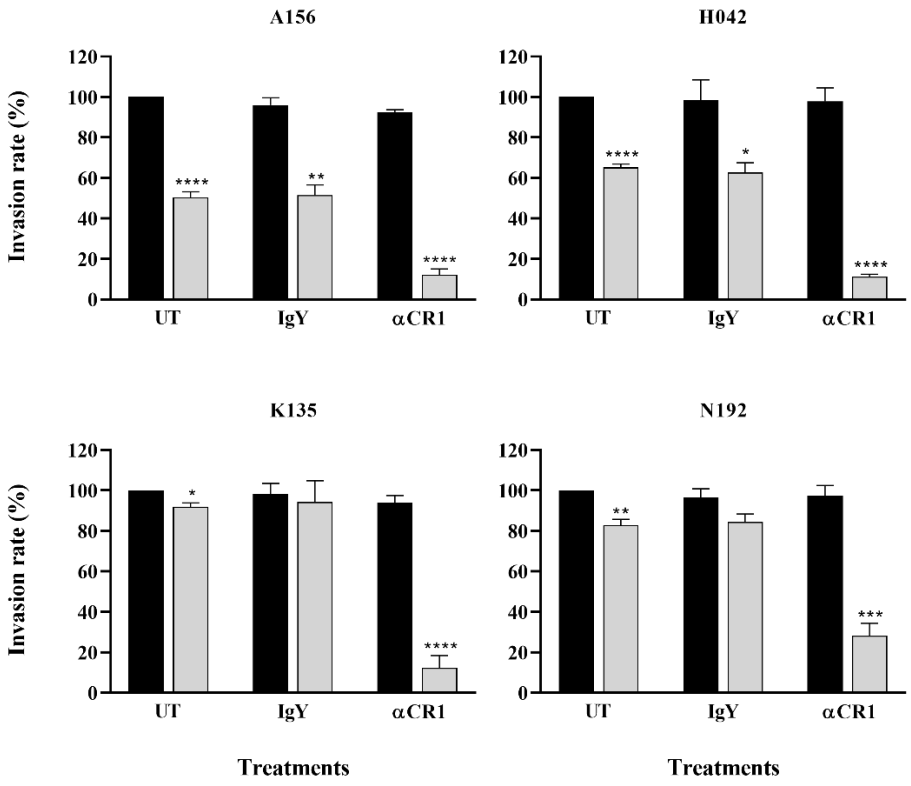

Figure 4. 4: Representative graphs showing the importance of CR1 as an alternative receptor for the invasion in Ghanaian *P. falciparum* clinical isolates. Invasion efficiency into untreated and neuraminidase treated erythrocytes was determined in the presence of 12 µg/mL of either αCR1 antibodies of IgY isotype control and expressed as the percentage of invasion into untreated control erythrocytes. Graphs represent the means ± standard errors of three independent experiment performed in duplicates. Statistical tests were performed using the Mann Whitney U test (*p = 0.03 (*), p = 0.002 (**), p = 0.0002 (***), p < 0.0001 (****)*).

Across all isolates, the invasion rate into neuraminidase-treated erythrocytes ranged from 1.15 to 76.27% following the addition of anti-CR1 antibodies as compared to untreated erythrocytes. Although invasion efficiency into neuraminidase-treated cells in the presence of anti-CR1 antibodies varied across isolates, these differences were not statistically significant ($p = 0.11$, data not shown). In addition, there was a moderate to strong positive correlation between the effect of anti-CR1 antibodies and that of trypsin and chymotrypsin treatment in the parasites' invasion efficiency (Figure 4.5A-B), while a very modest positive correlation was observed following neuraminidase treatment (Figure 4.5C). Given the sensitivity of CR1 to both trypsin and chymotrypsin, this further emphasize the possible involvement of the PfRh4-CR1-mediated pathway in the observed SA-independent pathway.

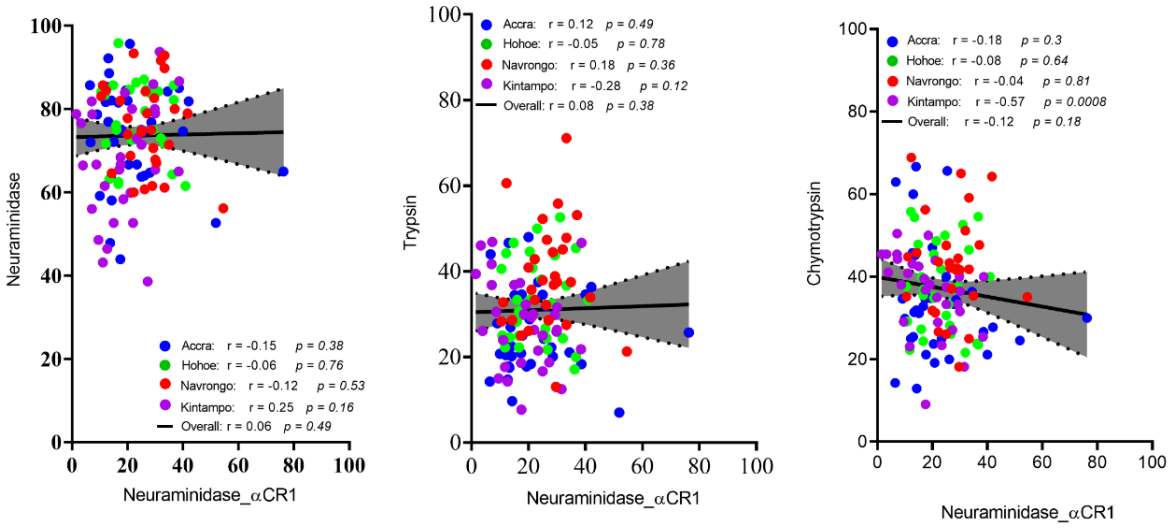

Figure 4. 5: Scatter plots showing the pairwise correlations of the parasite invasion efficiency into enzyme-treated erythrocytes. The Pearson correlation was used to compute the coefficients of correlation between invasion efficiency into neuraminidase treated erythrocyte and, in the presence, or absence of αCR1 antibodies (A), that between trypsin treated and neuraminidase in the presence of αCR1 (B) or that of the former and chymotrypsin treated erythrocytes (C). The data was generated from 124 isolates from Accra (N = 34), Hohoe (N = 30), Navrongo (N = 29) and Kintampo (N = 31).

4.1.4.5. Expression levels of invasion ligands in Ghanaian *P. falciparum* clinical isolates

For all isolates that grew well, schizont-infected erythrocytes were collected and stored in Trizol reagent for RNA extraction. Gene expression analysis was performed for 10 different invasion-related genes (PfEBA175, PfEBA140, PfEBA181, PfEBA165, PfEBL1, PfRh1, PfRh21, PfRh2b, PfRh4 and PfRh5) in a total of 44 isolates for which invasion data were also available (Accra = 13, Hohoe = 7, Kintampo = 14 and Navrongo = 10). Across all isolates, the PfEBAs expression was highly abundant as compared to the PfRh genes (Figure 4.6). With regards to the PfEBA genes, PfEBA175 was the most abundant (mean expression level 32.86% of all ten genes), followed by PfEBA140 (18.15%) and PfEBA181 (9.83%), while PfRh5 was the most abundant (8.08%) of the PfRh genes. Moreover, the pattern of gene expression was relatively similar and there was almost no difference in the relative expression of individual genes across all study sites (Figure 4.6). Taken individually, the expression level of PfEBA175 was highest in isolates from Accra (34.68%), while isolates from Hohoe had the lowest transcript level of PfEBA175 (28.29%). Moreover, isolates from Hohoe presented the highest transcript levels for PfEBA140 (mean, 19.17%), PfEBL1 (mean, 8.94%), PfEBA165 (mean, 5.37%), Rh1 (mean, 4.62.17%), PfRh2a (mean, 7.51%), PfRh2b (mean, 8.5%) and PfRh4 (mean, 9.11%), while those of PfEBA181 and PfRh4 were higher in isolates from Accra (mean, 13.2%) and Navrongo (mean, 10.58%), respectively. Furthermore, with the exception of PfEBA140, there was a moderate to strong negative correlation between the expression level of PfEBA175, the most abundant transcript, with that of the rest of the ligands tested here (Figure 4.7).

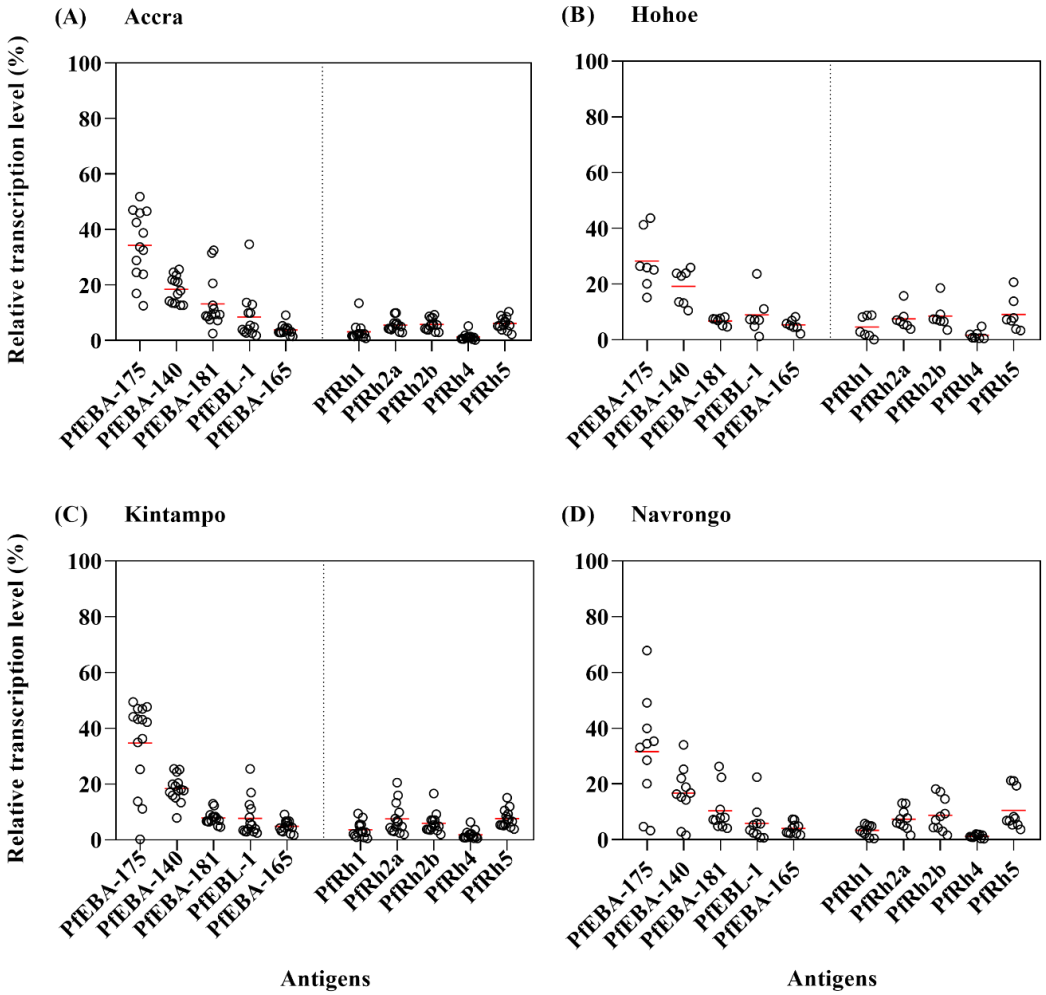

Figure 4. 6: relative transcript levels of invasion-related genes in Ghanaian *P. falciparum* clinical isolates. The transcript level of each gene was determined by RT qPCR in a total of 44 isolates from (A) Accra, N = 13, (B) Hohoe N=7, (C) Navrongo, N = 10 and (D) Kintampo, N = 14. The transcript level of each gens was expressed as a proportion of the total transcript level of the ten genes following normalization to that of the 60S ribosomal L18 protein and that of AMA1, respectively used as endogenous control and late-stage parasite marker.

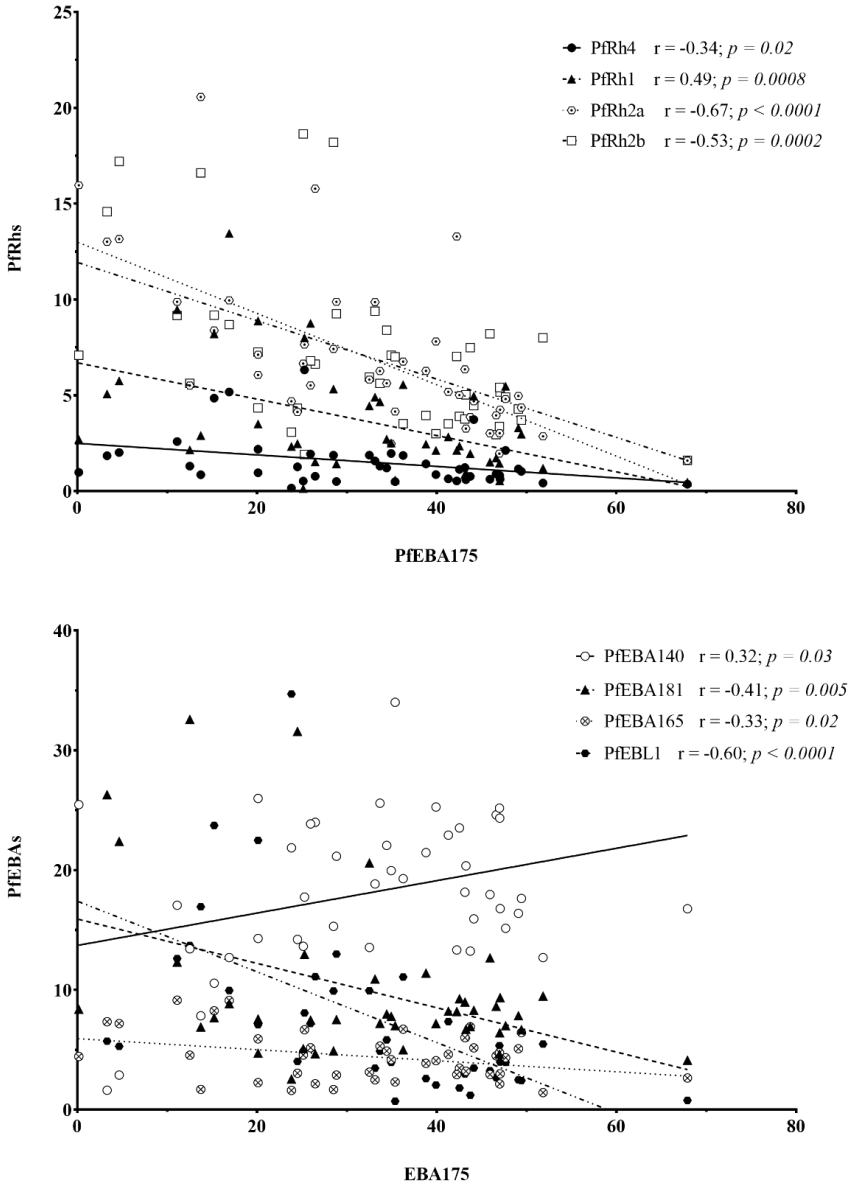

Figure 4. 7: Correlation of the transcript level of EBA175 with other invasion related genes. (A) The high transcript level of EBA175 is associated with low levels of Rh genes. (B) Transcript levels of EBA genes are negatively correlated with the transcript level of EBA175, except for EBA140, the only invasion-related ligand to show a moderated positive correlation with EBA175.

4.1.5. Discussion

P. falciparum clinical isolates used in this study were collected from Ghanaian children of age 2-14 years residing in four endemic areas. This age group constitutes a good cohort for understanding the dynamics of malaria transmission and the development of antimalarial immunity in exposed individuals. The data presented in this study showed that children from Kintampo and Navrongo were younger as compared to those from Accra and Hohoe. This trend confirms previous reports in Ghanaian children from areas of varying transmission (Ademolue, Aniweh, Kusi, & Awandare, 2017; H. E. Mensah-Brown et al., 2015) and suggest that the age of vulnerability shifts higher in low transmission areas. Besides, there was a significantly higher parasite density in children from Kintampo as compared to the rest of the study sites. This is in agreement with reports suggesting a higher threshold parasitaemia for symptomatic malaria in individuals from high transmission settings (Galatas, Bassat, & Mayor, 2016; Goncalves, Fried, & Duffy, 2014; H. E. Mensah-Brown et al., 2015).

In this study, *in vitro* invasion phenotyping data of 156 *P. falciparum* clinical isolates from four endemic areas in Ghana were compared and found to form a homogenous population in their use of the SA-independent invasion pathway. This study is the second study reporting on the invasion phenotype of *P. falciparum* clinical isolates from different endemic areas within Ghana. Overall, there was a slight difference in the parasites' sensitivity to neuraminidase treatment, which was only significant when comparing isolates from Kintampo and Navrongo, the two sites with the highest transmission intensity. This data contradicts earlier reports from the Gambia, where the majority of the isolates tested showed a SA-dependent invasion pathway (Baum et al., 2003b). Our result also contradicts previous reports from our group, which showed

a significant inverse relationship between the sensitivity to neuraminidase treatment and the transmission intensity (H. E. Mensah-Brown et al., 2015), while in agreement with other findings from a collaborative team which reported no significant differences in the sensitivity of neuraminidase treatment when comparing isolates from across different endemic countries (Bowyer et al., 2015).

Although this current study used similar protocols as previously reported in our group, there was a notable variation with regards to the reagents and protocols for invasion assays relative to other studies, therefore, suggesting their possible effect on the measured outcomes. Also, another possible cause of the discrepancies of the individual results could be the differences in the number of isolates assayed in each study. The earlier studies included 38, 52 and 67 isolates respectively while ours involved the largest sample size (156 isolates), therefore providing more power for significant statistical analysis. While no significant differences were observed with regards to the sensitivity to chymotrypsin treatment, our data showed significant differences in the sensitivity to trypsin treatment when comparing isolates from Navrongo to those from Accra or Kintampo, once again contradicting previous results where no significant difference was observed across sites following trypsin treatment (Bowyer et al., 2015; H. E. Mensah-Brown et al., 2015). A possible explanation of these contradicting data could be as a result of batch to batch variation in the reagents used (e.g. enzymes) or the storage conditions, two major factors that may affect the effectiveness of the enzymes used to treat target erythrocytes in the respective studies. Furthermore, our data showed the predominance of the NrTsCs invasion profile across all isolates, but also a strong positive correlation between sensitivity to trypsin and chymotrypsin treatment while that of neuraminidase was not correlated with trypsin or chymotrypsin treatment. This data are in agreement with the most recent reports on the field (Bowyer et al.,

2015; H. E. Mensah-Brown et al., 2015), although previous stuies reported NrTsCr as the predominant profiles in Senegalese isolates (Jennings et al., 2007), while NrTrCr was the most common profile reported in Colombian and Peruvian isolates (Lopez-Perez et al., 2012).

Given the strong positive correlation between the sensitivity to trypsin and chymotrypsin treatment, we sought to test the contribution of CR1, which as previously reported is a major receptor driving the SA-independent invasion pathway (Awandare, Nyarko, Aniweh, Ayivor-Djanie, & Stoute, 2018; H. E. Mensah-Brown et al., 2015; Spadafora et al., 2010). Using a similar approach, our data perfectly matched previous reports from our group which showed that Ghanaian *P. falciparum* clinical isolates rely on PfRh4-CR1 interaction as alternative invasion pathway (H. E. Mensah-Brown et al., 2015). Altogether, these data show that Ghanaian clinical isolates can use various invasion pathways to achieve successful invasion. Consistent with previous findings, none of the receptors affected by the three enzymes is unanimously used by clinical isolates from a given area (Bowyer et al., 2015; Jennings et al., 2007; Lopez-Perez et al., 2012; H. E. Mensah-Brown et al., 2015).

Here, we also tested for the relative expression levels of known invasion-related genes and our data, once again, are in agreement with previous reports on Ghanaian clinical isolates (Bowyer et al., 2015; H. E. Mensah-Brown et al., 2015). There was higher expression of PfEBA175 across all isolates (Bowyer et al., 2015; H. E. Mensah-Brown et al., 2015; Nery et al., 2006). There was also a strong negative correlation between the expression levels of PfEBA175 and PfRh4 found in this study, similarly to earlier reports (H. E. Mensah-Brown et al., 2015). The higher transcript level of PfEBA175 in isolates from Accra, although not significant, is in

agreement with suggestions regarding the use of this ligand in non-immune individuals (Bowyer et al., 2015), since Accra represents the lowest transmission setting.

To sum up, our findings indicate that Ghanaian *P. falciparum* clinical isolates predominantly invade erythrocytes through a SA-independent pathway, irrespective of the level of transmission intensity. Additionally, across all isolates, the NrTsCs was the most predominant profile, therefore suggesting a major contribution of the PfRh4-CR1 interaction during invasion of Ghanaian clinical isolates.

CHAPTER FIVE: SPECIFIC AIM THREE

5.1. SYSTEMATIC SCREENING OF THE INVASION INHIBITION POTENTIAL OF ANTIBODIES AGAINST TWO NOVEL *P. FALCIPARUM* ANTIGENS

Hypothesis 1: Antibodies against functionally conserved blood-stage antigens will provide strain transcendent invasion blocking activity, if any, and constitute a great value in both efficacy and cost-effectiveness as potential vaccine candidates.

To ascertain this hypothesis, peptide-specific antibodies against two candidate genes (PF3D7_0210600 and PF3D7_1136200, GenScript, USA) were used in growth inhibitory assays against four *P. falciparum* isolates. The antibody inhibitory activities were tested for all individual antibodies, but also as combinations of antibody pairs to assess their synergistic effect. Furthermore, plasma samples from children presenting an acute malaria illness were used to assess the naturally-derived antibody responses against both antigens using enzyme-linked immunosorbent assays (ELISAs). Results from these investigations are presented below.

5.1.1. Abstract

With the occurrence of resistance to the frontline antimalarial therapies, the development of a highly efficient malaria vaccine would be of utmost importance in the malaria control toolbox. The first step towards developing an effective malaria vaccine is to find a target which can trigger the production of broadly neutralizing antibodies and/or efficient cell-mediated immune response that prevents subsequent parasite multiplication. Currently, no such vaccine is available, and out of the thousands of parasite antigens exposed to the immune system at a given stage, only a handful are being assessed as potential vaccine candidates. Given the high polymorphism rates that precluded the bulk of the malaria vaccine candidates, we opted for a reverse vaccinology approach whereby peptide-specific antibodies against two candidate genes were first tested for their ability to neutralize merozoites invasion in both *P. falciparum* laboratory and clinical isolates. We also assessed the peptide-specific naturally derived antibody responses in both malaria symptomatic children and healthy malaria-exposed adults from Ghana. Testing antibodies in growth inhibition assays showed a dose-dependent inhibitory activity in both *P. falciparum* laboratory and clinical isolates. Also, antibodies in combination revealed an antagonistic inhibitory effect at high concentrations. Data from enzyme linked immunosorbent assays (ELISAs) showed that both candidates were targets of naturally-derived antibody responses in both symptomatic children and exposed adults. Further analysis revealed an increasing seroprevalence against the antigens as transmission intensity increases. Overall, this study reports the preliminary data relative to two novel *P. falciparum* antigens that have the potential to be considered for either *in vitro* and *in vivo* functional assays as potential diagnostic or vaccine candidates.

5.1.2. Introduction

Over the last two decades, the malaria burden has considerably declined as a result of combined preventive and therapeutic approaches (Bhatt et al., 2015; WHO, 2018a). However, the sustainability of such measures is threatened by the emergence and spread of parasites that are resistant to the first-line antimalarial drug regimens (Ashley et al., 2014). For the past three years, the decline witnessed over the decade on malaria cases had been stalled (WHO, 2018b). With the global aim of achieving high malaria control towards elimination by 2035, new interventions are needed to drive greater impact. This emphasizes the need to strengthen efforts towards the development of new preventive and intervention tools to further drive the gains achieved over the years.

With this in mind, one major development of priority is the development of an efficient vaccine to complement existing control strategies. So far, malaria vaccine development has been thwarted by two main challenges, the complexity of the parasite life cycle, involving an arsenal of antigenically diverse immune targets, and the genetic polymorphism within individual parasite antigens (Arama & Troye-Blomberg, 2014; Hoffman, Vekemans, Richie, & Duffy, 2015b). This lapse has made all effort in vaccine development to be limited by strain-specific protection against the circulating parasite populations (Neafsey et al., 2015), instead of a strain-transcending impact.

The development of multicomponent vaccines that are able to trigger an efficient and strain-transcending immune response is therefore of great interest for efforts towards malaria elimination. The development of such a vaccine has also been impeded by lack of functionality to over 60% of the proteins coding genes in the genome. This has limited the number of

candidates being evaluated for their potential as vaccine candidates (Conway, 2015). The malaria-associated high mortality rate is attributed to the parasite's asexual replication within the host erythrocytes. Invasion of human erythrocytes by *P. falciparum* has over the years been shown to be a complex yet essential step for the parasite survival and transmission. The blood-stage has also been shown to be a critical step that could be targeted for intervention as it directly encounters the immune system (Cowman et al., 2017; Wright & Rayner, 2014).

Erythrocyte invasion by *P. falciparum* involves hundreds of parasite proteins, including both surface and membrane-associated proteins as well as secreted proteins from the parasite apical organelles (Beeson et al., 2016; Cowman et al., 2017). The abundance of *P. falciparum* surface and membrane-associated proteins has been shown to positively correlate with antibody reactivity in naturally exposed individuals (Osier et al., 2008). Besides, antibodies against secreted proteins have also been reported to induce strong invasion inhibitory activities in both *in vivo* and *in vitro* studies (Chiu et al., 2014; Chiu et al., 2015; Osier et al., 2008; Reiling et al., 2012; Richards et al., 2010; Tran et al., 2014). Therefore, vaccines targeting this crucial stage of the parasite's life cycle are among the most promising strategies currently sought after. In recent years, the use of reverse vaccinology approach has gained interest in the identification of potential malaria vaccine candidates (Bustamante et al., 2017). On-going research with the focus on the identification, selection and assessment of the invasion inhibitory activities of antibodies against potential malaria vaccine targets (Amlabu et al., 2018) is helping delineate a few for further validation.

Here, we tested the invasion inhibitory activities of antibodies against two novel *P. falciparum* antigens (PF3D7_0210600 and PF3D7_1136200), as well as, their naturally occurring antibody

responses in both malaria symptomatic children and exposed adults from areas of varying levels of endemicity across Ghana.

5.1.3. Materials and methods

5.1.3.1. Ethical approval

The use of plasma samples in this study was approved by ethics committees of the Ghana Health Service, the Kintampo Health Research Centre, the Navrongo Health Research Centre and the Noguchi Memorial Institute for Medical Research, University of Ghana, Legon. Informed consent was obtained from participating adults, and from parents or guardians of all children included in this study.

5.1.3.2. *In silico* screening, peptide synthesis and antibody generation for candidate genes

Screening for candidate genes was performed as previously described (Amlabu et al., 2018) and for each selected candidate, peptides spanning three different regions were synthesized using the 3D7 amino acid sequence as a template. Peptide selection was based on the prediction of sequence antigenicity, surface exposure and hydrophobicity scores. For both candidate genes, peptide-specific polyclonal antibodies were raised from two New Zeland Rabbits (GenScript, US). The immune sera were titrated serially with the peptides and the final limit of dilution determined to be 1:512,000 (1.95 ng/mL) by ELISA and further purified over a bed of A/G coupled protein beads. Purified antibodies were finally concentrated (using Amicon 30 kDa) or diluted to the required concentration for use in the different assays they were intended.

5.1.3.3. *P. falciparum in vitro* culturing

Two *P. falciparum* laboratory lines 3D7 and Dd2 and two clinical isolates MISA011 and MISA031 were used in this study. Laboratory lines were cultured in complete parasite medium containing RPMI 1640 (Sigma, UK), supplemented with 0.5% Albumax II (Gibco), 50 ug/mL Gentamicin and 2 mg/mL sodium bicarbonate. The complete parasite medium was further supplemented with 2% normal human serum (PAN Biotech, UK) to allow the growth of clinical isolates. Parasites were grown in O^+ human erythrocytes and cultures were incubated at 37º C in an atmosphere of 2% O_2, 5% CO_2 and balanced with N_2. Routine culture synchronization was performed using 5 % D-Sorbitol (Sigma).

5.1.3.4. Growth inhibition assays

In vitro growth inhibition assays were conducted as described earlier (Amlabu et al., 2018). Briefly, target O^+ erythrocytes, labelled with 20 µM carboxyfluorescein diacetate succinimidyl ester (DDAO-SE), were used to distinguish newly invaded erythrocytes to those present in the donor cultures. Schizont-infected erythrocytes were incubated with labelled erythrocytes in a 1:1 ratio in complete parasite medium containing increasing concentrations (0-250 mg/mL) of antibodies against PF3D7_0210600 and PF3D7_1136200 specific peptides. Besides, anti-human CR1 antibodies (clone J3D3, Santa Cruz Biotech, US) and anti-human basigin antibodies (clone MEM-M6/6, Thermo Scientific, UK), with known invasion inhibitory activities were used at 12 µg/mL as a positive control. Assays were set up in flat bottom 96-well plates in a total volume of 50 µL and incubated at 37º C for approximately 24 hours. Plates were subsequently removed from the incubator and spun at 2000 rpm for 3 minutes and the medium

replaced with 1 mM Hoechst 33342 solution to label the parasites' DNA. Invasion rates were determined using a BD LSR Fortessa X-20 cytometer (BD Biosciences, Belgium).

5.1.3.5. Enzyme-linked immunosorbent assays

The presence of naturally acquired antibodies against PF3D7_0210600 and PF3D7_1136200 was assessed using indirect enzyme-linked immunosorbent assays (ELISAs). Samples tested in this study were collected from children living in areas of varying transmission intensity in Ghana (Accra<Hohoe<Navrongo<Kintampo) and presenting acute malaria episodes, but also from semi-immune adults living in a malaria-endemic area. Briefly, MaxiSorp ELISA plates (NUNC, Denmark) were coated with 2 µg concentrations of the respective antigen and incubated at 4° C overnight and blocked for an hour at room temperature (RT). Samples to be tested were diluted at 1:400 and incubated with washed plates for 2 hours at RT. Plates were washed and antibody reactivity was detected using a horseradish peroxidase-conjugated anti-human IgG incubated for an hour at RT and protected from light exposure. Plates were finally washed and incubated with the 3, 3′, 5, 5′-Tetramethylbenzidine (TMB) and the color development stopped with 2 N sulfuric acid. The resulting absorbance was read at 450 nm on a Varioskan™ LUX multimode microplate reader (Thermo Scientific, Waltham, Massachusetts, USA). For data comparison, each plate included serially diluted standard pooled sera sample collected from semi-immune adults as well as a naïve European adult sample. The standard sample was used to convert optical density values (ODs) into arbitrary units (AU) using the four-parameter logistic curve fitting program known as ADAMSEL (Edmond J. Remarque®).

5.1.3.6. Data analysis

All statistics were performed using GraphPad Prism v.8.01. One-way ANOVA was used to assess for differences between distinct groups and where significant, the Tukey's multiple comparison tests were used for pairwise comparisons. The Mann Whitney U test was used to compute for differences in antibody reactivity between different age groups. The Spearman rank correlation was used to assess relationships between variables. The Chi-square test was used to compute for differences between categorical variables. For all analysis, a *p-value* of at least 0.05 was considered as significant.

5.1.4. Results

5.1.4.1. Characteristics of selected candidate genes

The genes were selected based on their timing of expression and genes with which they are co-expressed, as a way of assigning putative functions. The PF3D7_0210600 gene is conserved across all plasmodia. The gene encodes for a predicted 446 amino acid protein at 53.7 kDa in size. The gene is predominantly expressed at the late schizont stages of development with no transmembrane (TM) domain but has a signal peptide (Fig 5.1A, C). In a recent large-scale gene knock-out analysis using the piggyBac insertion mutagenesis, the gene was classified as being essential to the parasite development. The PF3D7_1136200 gene, which is conserved across the genus, encodes for 679 aa, 76.57 kDa protein having a signal peptide and no TM (Fig 5.1B, D). It is expressed at late schizont stages and shown to be possibly non-essential. Both genes lack any classical domains as well as GPI anchor signal residues.

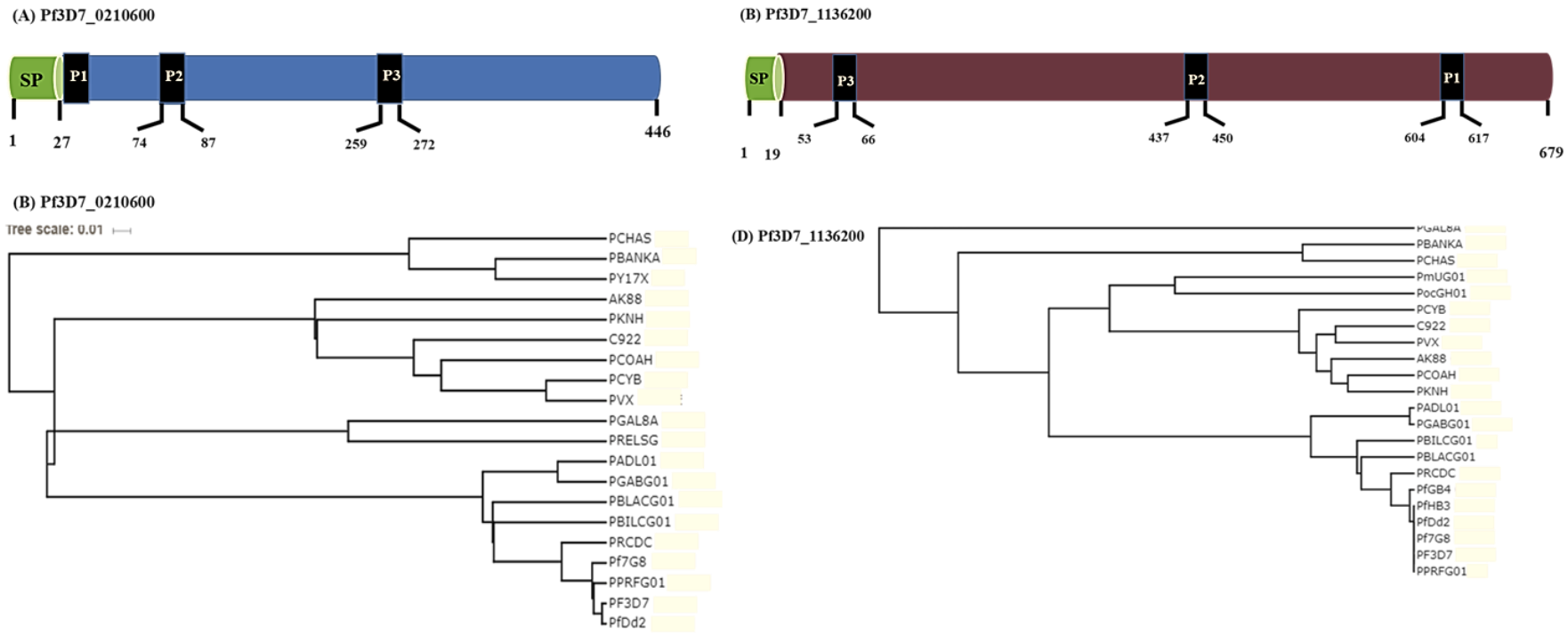

Figure 5. 1: Summary of PF3D7_0210600 and PF3D7_1136200 protein characteristics and phylogenetic trees of the protein sequences of the two antigens. (A-B) Cartoons of PF3D7_0210600 and PF3D7_1136200 proteins highlighting the size and location of the signal peptides on the respective sequences. (C-D) phylogenetic trees of the full-length amino acid sequences of PF3D7_0210600 (C) and PF3D7_1136200 (D). Sequence alignments were generated using Clustal Omega (PMID: 21988835), using *P. gallinaceum* as reference.

5.1.4.2. Peptide-specific antibodies inhibit erythrocyte invasion in a dose-dependent manner

Growth inhibition assays (GIAs) were used to assess the effect of peptide-specific antibodies against both PF3D7_0210600 and PF3D7_1136200 on invasion. Late-stage cultures of the *P. falciparum* laboratory line 3D7 and clinical isolate MISA031 were incubated for 24 hours in the presence of increasing concentrations of individual antibodies for each candidate gene, and the parasitemia was measured by flow cytometry, as earlier described (Amlabu et al., 2018). Pre-immune sera were used at similar dilutions as a negative control. Overall, all antibodies used in this study inhibit invasion in a dose-dependent manner relative to pre-immune control sera (Figure 5.2). At the highest concentration (250 µg/mL), peptide-specific antibodies against PF3D7_0210600 inhibited invasion by 51.37 to 77.82%, while the inhibition by antibodies against PF3D7_1136200 ranged from 36.96 to 81.22% (Figure 5.2). For both candidate genes, invasion inhibitory activity was more pronounced when parasites were incubated in the presence of antibodies targeting the peptide 3 of the respective genes (Figure 5.2).

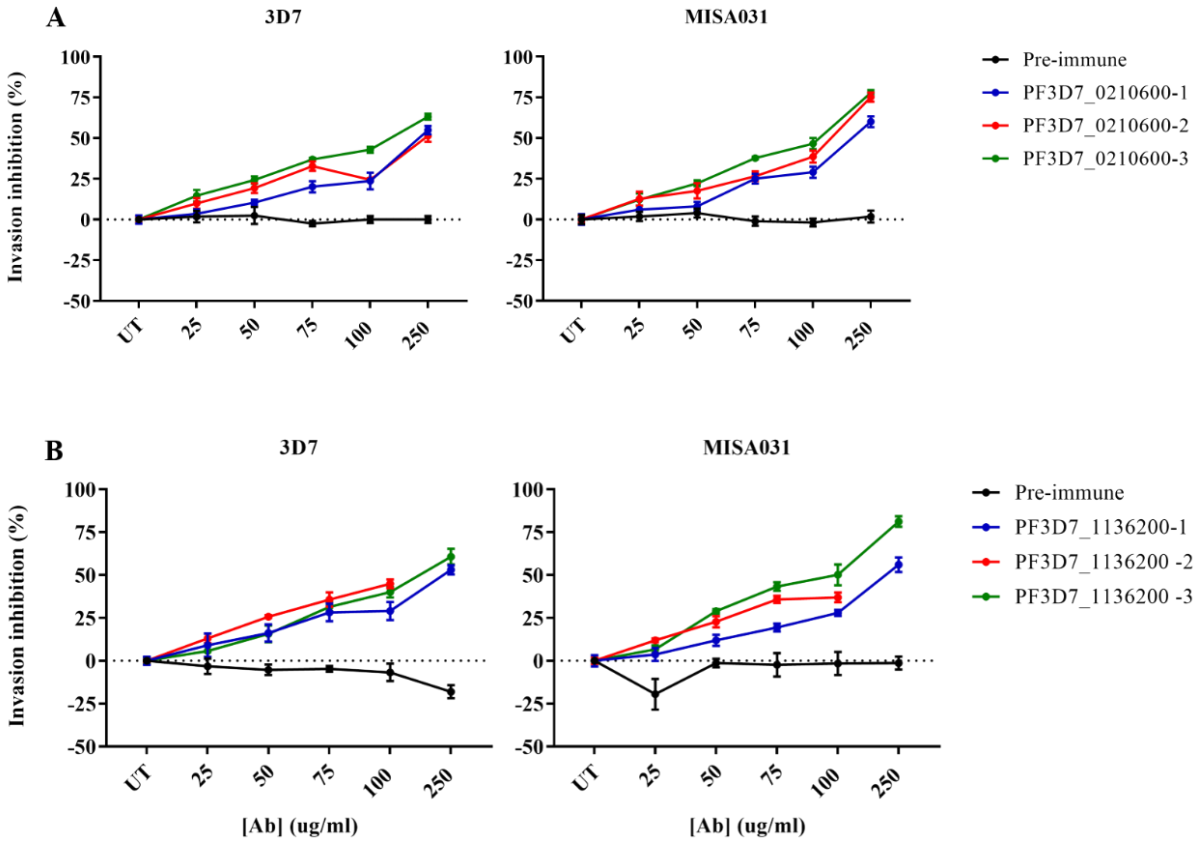

Figure 5. 2: Invasion inhibitory activity of αPF3D7_0210600 and αPF3D7_1136200 antibodies against *P. falciparum* isolates. The invasion inhibitory activities of six different antibodies against two *P. falciparum* antigens PF3D7_0210600 (A) and PF3D7_1136200 (B) were tested at different concentrations (25-250 µg/mL). Assays were set up in a total volume of 50 µL in flat bottom 96 well plates four two *P. falciparum* laboratory strain (3D7) and one clinical isolate (MISA031) and the parasitemia was quantified using a BD LSR Fortessa Flow cytometer. Error bars represent the standard errors of the means from two independent performed in duplicated wells.

Besides, across all antibodies, the invasion inhibitory activity was slightly higher in MISA031 relative to 3D7. Furthermore, to test for cross-strain invasion inhibition activities, antibodies were tested at 250 µg/mL in separate experiments using four different *P. falciparum* isolates. Antibodies against the human basigin (BSG) and complement receptor 1 (CR1) were used as comparators in these experiments. Overall, invasion inhibition activities significantly varied over the different antibodies (Figure 5.3). Across all isolates, antibodies against PF3D7_0210600-2 and PF3D7_1136200-1 (against the peptides 2 and 1 of the respective genes) were less potent in inhibiting invasion (Figure 5.3). Of all isolates, Dd2 was the least susceptible to inhibition across all antibodies, while the clinical isolates MISA011 and MISA031 were more susceptible to invasion inhibition. Unlike Dd2, there was no significant difference in the efficacy against 3D7 relative to the clinical isolates (Figure 5.3). However, consistent with previous reports (Awandare et al., 2018; Spadafora et al., 2010), antibodies against BSG and CR1 showed similar invasion inhibition activities across all isolates.

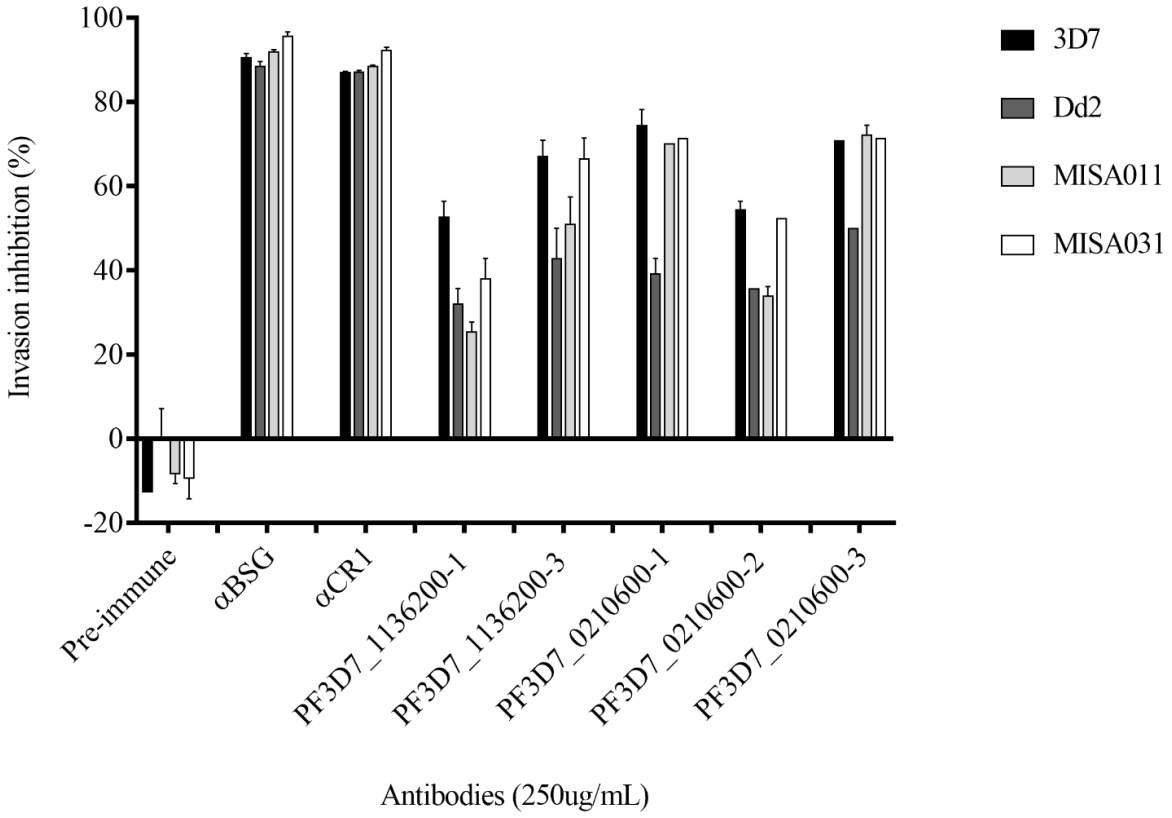

Figure 5. 3: Screening of αPF3D7_0210600 and αPF3D7_1136200 antibodies for cross-strain inhibitory activity against *P. falciparum* isolates. For both antigens, antibody inhibitory activity was tested against two *P. falciparum* laboratory strains, 3D7 (black bars) and Dd2 (dark grey bars) and two clinical isolates, MISA011 (light grey bars) and MISA031 (white bars). Schizont-infected parasites were grown for 24 hours in the presence of 250 µg/mL concentration of five different antibodies against PF3D7_0210600 and PF3D7_1136200. Monoclonal antibodies against the human basigin (BSG) and complement receptor 1 (CR1) receptors were used at 12 µg/mL as positive control and the rabbit pre-immune sera as a negative control.

5.1.4.3. Antibody combinations show different levels of synergy

Given the relatively low invasion inhibitory activity of individual antibodies at lower concentrations, we sought to test the synergistic effect of combined antibodies against the same antigen. Peptide-specific antibodies against both antigens were tested in combination at 50 µg/mL and the resulting invasion inhibition of each combination was compared to that of the individual antibodies. Overall, there was no synergistic effect of the antibody combinations relative to individual antibodies and this was consistent across all isolates (Figure 5.4). Besides, a similar trend in the parasite susceptibility to inhibition was observed with Dd2 still being the least susceptible isolate across all antibody combinations (Figure 5.4). Furthermore, we also tested the synergistic effect of the combination of antibodies against different antigens in inhibiting parasite invasion. Antibody pairs against different antigens were simultaneously tested at 50 and 250 µg/mL, and their invasion inhibitory activities were compared to that of corresponding antibodies tested individually at similar concentrations in the same assays. This analysis showed no specific effect when antibodies were used at low concentration (50 µg/mL) (data not shown), while, a different trend was observed when antibodies were incubated at a higher concentration (250 µg/mL). Combinatorial screening of antibody pairs at 250 µg/mL revealed an antagonistic effect between antibodies targeting different antigens. Taken individually, antibodies to PF3D7_0210600 showed higher inhibition activities relative to antibodies against PF3D7_1136200 (Figure 5.5). However, across all isolates, there is a significant decrease in invasion inhibition activity when parasites were incubated in the presence of antibodies against the different antigens, relative to that obtained in the presence of antibodies against PF3D7_0210600 alone (Figure 5.5).

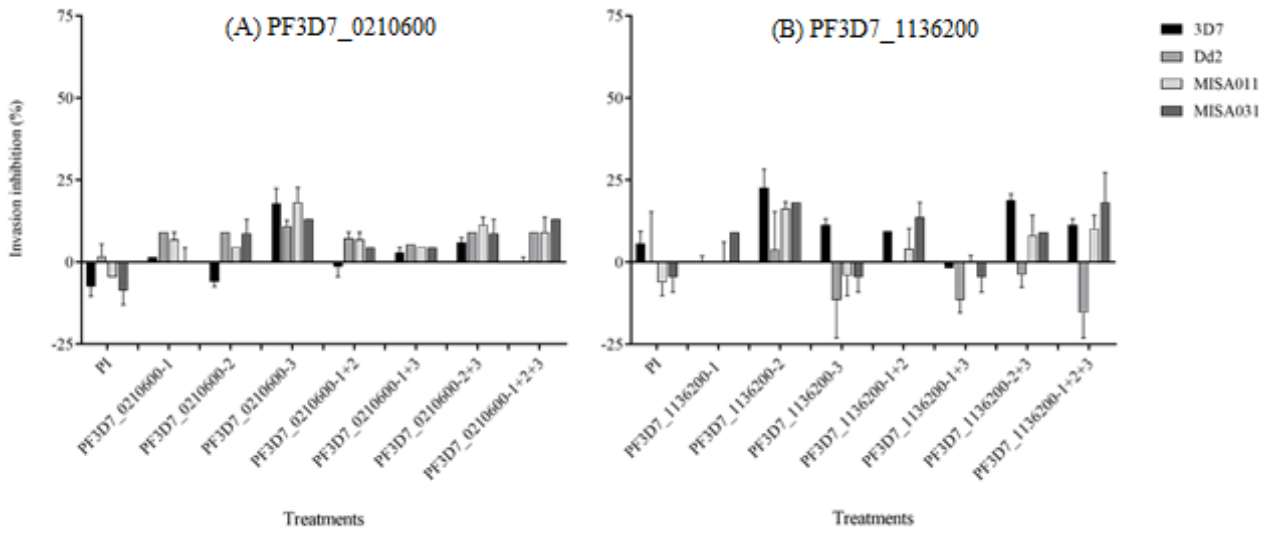

Figure 5. 4: Screening of isogenic antibody combinations reveals no additive effect in invasion inhibitory activities. Bars graphs showing the combined inhibitory activities of antibodies against different peptides of the same antigens (A) PF3D7_0210600 and (B) PF3D7_1136200. In each assay, single antibodies were incubated at 50 µg/mL and the resulting invasion inhibitory activity was compared to that resulting from its combination with other antibodies targeting different epitopes of the same antigen. All assays were performed in duplicates and the data are presented as means and standard errors of the means from two independent experiments.

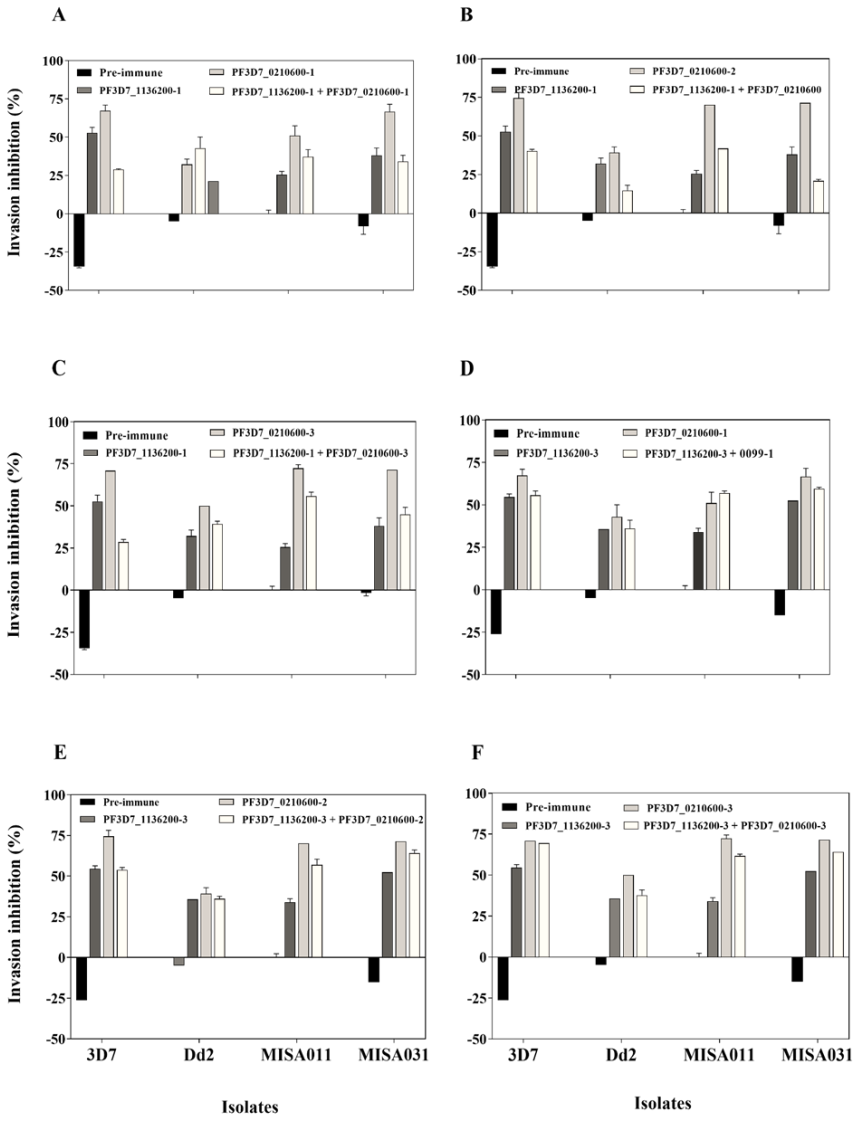

Figure 5. 5: Combinatorial screening reveals antibody pairs with antagonistic invasion inhibitory activities. Bar graphs showing the effect of antibody combination on *P. falciparum* erythrocyte invasion. In each assay, antibodies were used individually or in combinations with a non-isogenic antibody at 250 µg/mL and coincubated with different *P. falciparum* strains for 24 hours. Parasites were then labelled with Hoechst 33342 and the invasion inhibitory effect of single antibodies were compared to that of combined antibody pairs.

5.1.4.4. Natural antibody responses to PF3D7_0210600 and PF3D7_1136200 domains

Antibody responses against different peptides of both PF3D7_0210600 and PF3D7_1136200 were measured on a set of 156 serum samples from children presenting with acute malaria and at hospitals in different endemic areas in Ghana (39 samples pers site): Accra (mean 8.1, min-max 1-14 years), Hohoe (mean 6.9, min-max 1-14 years, Navrongo (mean 4.6, min-max 2-10 years) and Kintampo (mean 5.5, min-max 2-13 years). In addition, 31 samples from semi-immune adults living in a low transmission area (Accra) were examined. Peptides corresponding to the antibodies with the highest invasion inhibitory activities (PF3D7_0210600-1, 3 and PF3D7_1136200-3) were chosen and the naturally-derived antibody titers were measured using an indirect ELISA assay. Overall, all three peptides were recognized by sera samples from both adults and children, with a similar trend in the level of antibody response across the study sites (Figure 5.6). For all peptides, patterns of antibody responses in symptomatic children, expressed as arbitrary units, increased as transmission intensity increased, with samples from Kintampo and Navrongo showing the highest mean antibody titers relative to Accra and Hohoe (Figure 5.6). Besides, for PF3D7_0210600-3 and PF3D7_1136200-3 peptides, antibody reactivity in adult samples was higher than that observed in children from lower endemic areas (Accra and Hohoe), but lower than that of children from high transmission areas (Navrongo and Kintampo). However, antibody levels did not vary significantly across the different study sites (Tukey's multiple comparison tests, Figure 5.6).

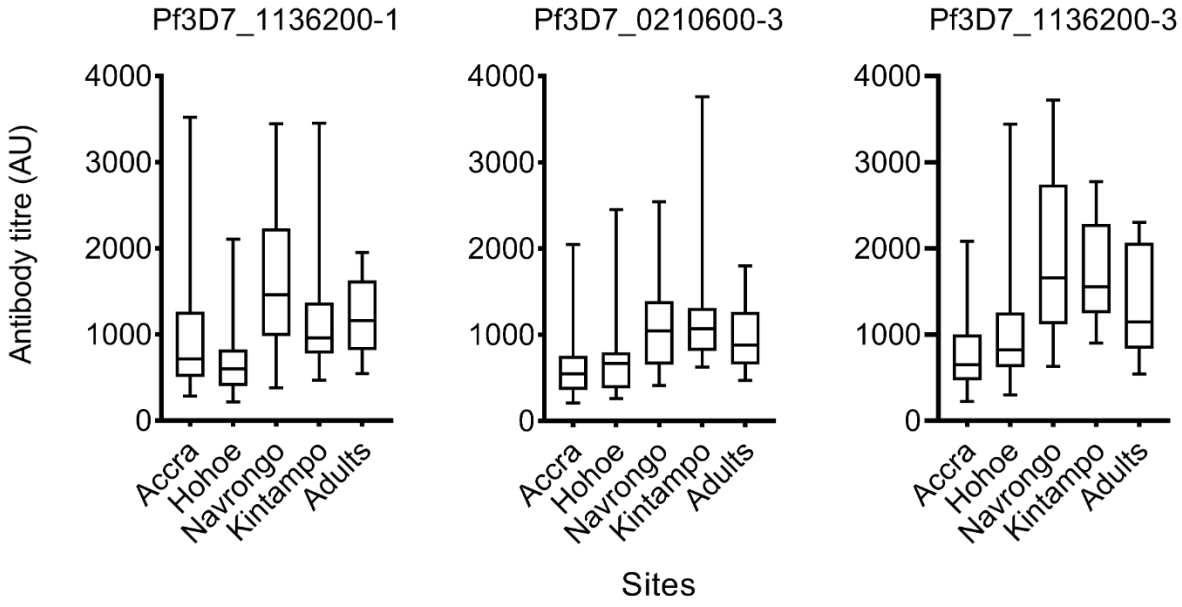

Figure 5. 6: PF3D7_0210600 and PF3D7_1136200 are targets of natural antibody responses. IgG reactivity against two peptides of PF3D7_0210600 (A and B) and one peptide of PF3D7_1136200 (C) in adults (31 samples) children plasma samples from across various endemic areas in Ghana (39 samples per site) is shown as arbitrary units (AU) resulting from background subtraction of actual values converted from optical density (450 nm) values by ELISA. Boxes show interquartile range with central lines with medians denoted by central lines. Whiskers indicate the 5-95 percentile and dots represent outliers. AU values were extrapolated from a standard curved generated form a serially diluted standard sample (pooled plasma samples with high OD values relative to naïve European donor).

Given the earlier reported positive correlation between transmission intensity and the parasite density in children residing in different endemic areas (H. E. Mensah-Brown et al., 2015) as well as the observed differences in antibody responses across sites, we sought to investigate the relationship between parasite density and the level of antibody response against all three peptides

tested here. Surprisingly, no relationship was observed between these two parameters across all study sites (Pearson's correlation, Figure 5.7A). We further investigated the relationship between antibody response and age of children from the different study sites and showed no correlation between antibody response and age (data not shown). Furthermore, there were no statistical differences between the different age groups when children were categorized into two groups, ≤6 and >6 years old (Mann Whitney U test, Figure 5.8).

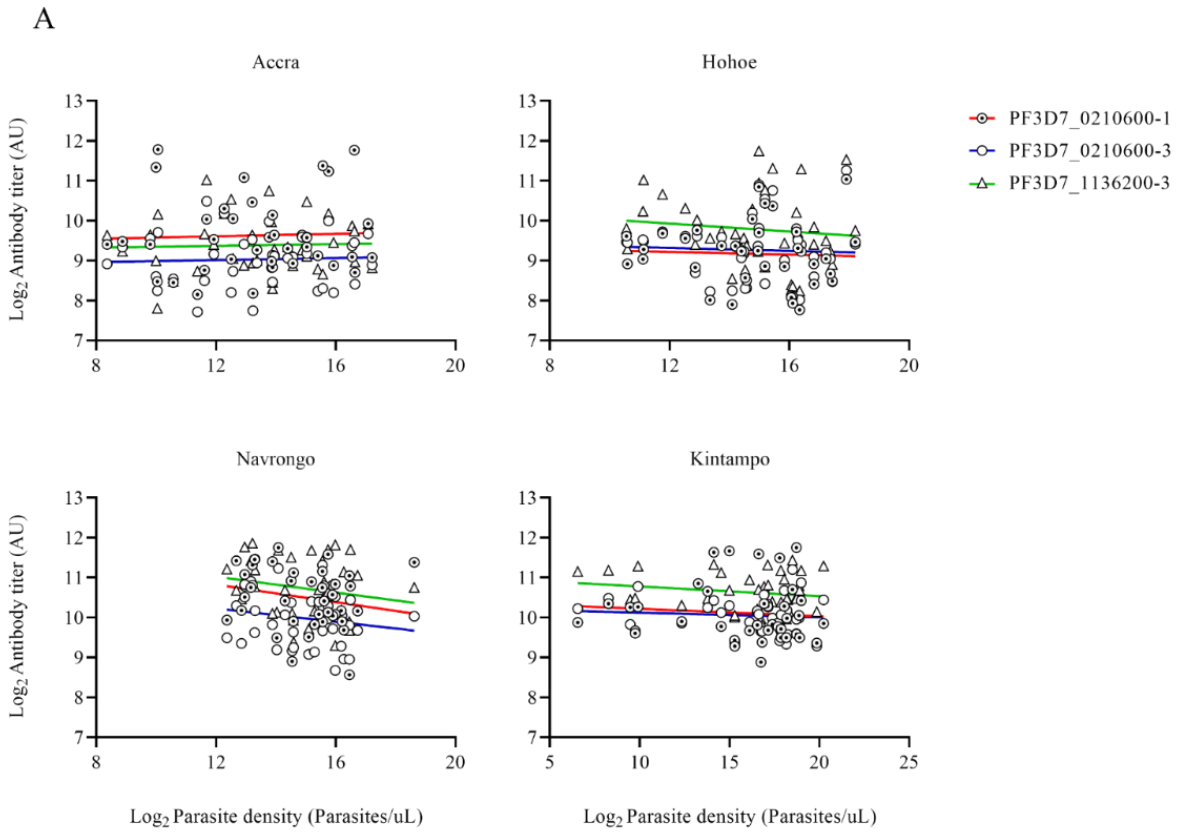

Figure 5. 7: Relationship between antibody titers and parasite density or age. There is no relationship between antibody reactivity and parasite density. Dot plots showing the correlation between parasite density and antibody titers in the plasma of children diagnosed with clinical malaria.

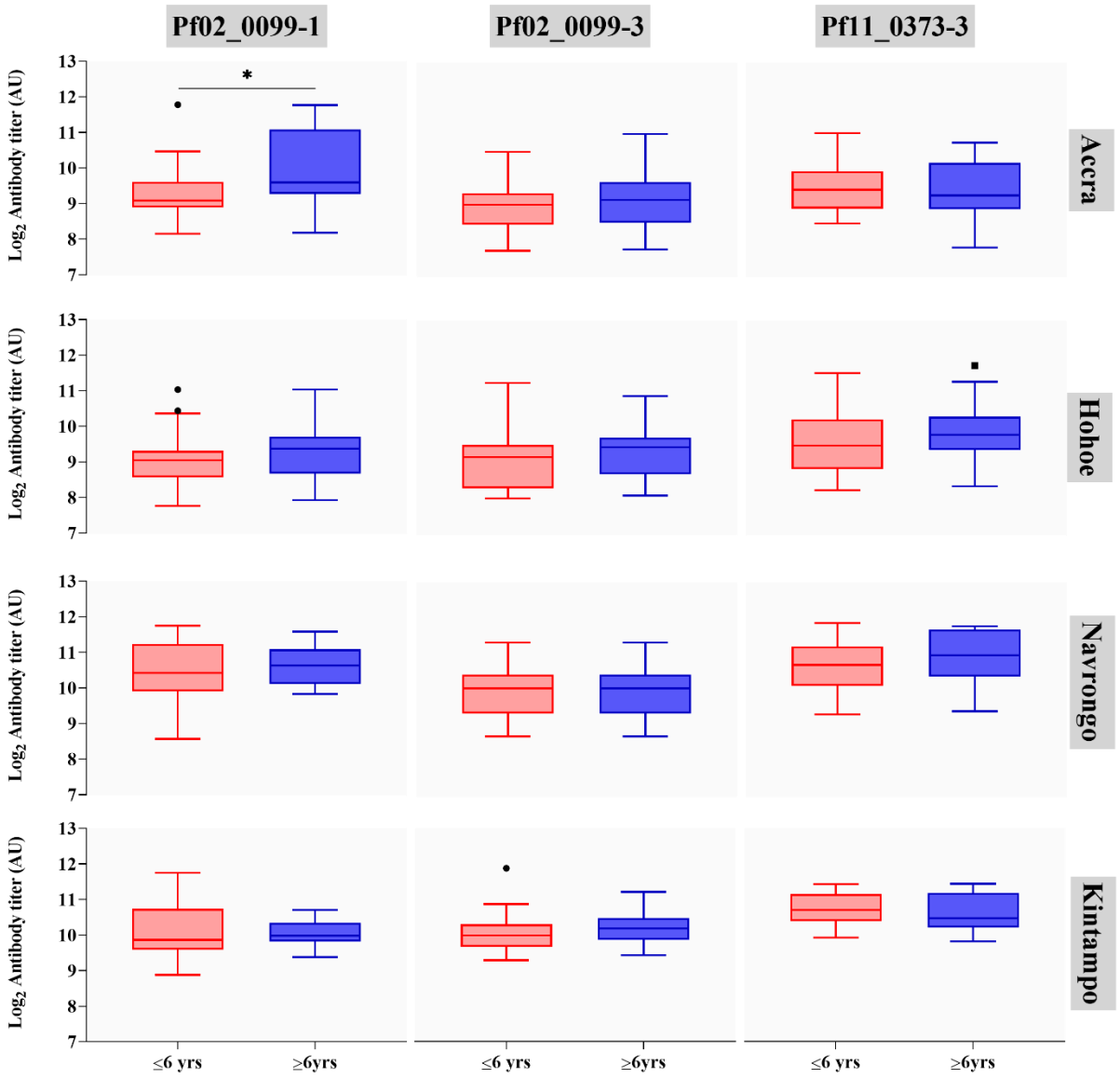

Figure 5. 8: Antibody reactivity does not vary between age groups. Boxes show interquartile range with central lines with medians denoted by central lines. Whiskers indicate the 5-95 percentile and dots represent outliers. Mann-Whitney U test to assess statistical differences.

5.1.4.5. Malaria transmission dynamics is associated with antibody seroprevalence

Given the wide range of variation, yet non-significantly different antibody titers across the various sites, we sought to eliminate any cofounders (e.g. cross reactivity) that may arrive during experimental setup. A naïve European plasma sample, run across all plates, was used to categorize the samples as seropositive or seronegative for antibodies against a given peptide. Seropositivity was defined as any sample presenting a mean antibody titer value greater than that of the mean plus or minus three standard deviations of the naïve control plasma. We performed a multiple linear regression analysis to assess the contribution of age, parasite density and transmission intensity in the level of antibody response in seropositive individuals. Relative antibody titers against PF3D7_0210600-1 was strongly associated with transmission intensity ($F = 4.305$, $P < 0.0001$, Table 1), while both age and parasite density also showed an association with antibody titers, though to a lesser extent ($F = 2.085$, $P = 0.401$ and $F = 2.339$, $P = 0.0217$, respectively, Table 5.1). However, antibody titers against PF3D7_0210600-3 were only associated with parasite density ($F = 2.500$, $P = 0.0143$, Table 5.1). On the other hand, antibody response against PF3D7_1136200-3 was found to be strongly associated with transmission intensity ($F = 8.372$, $P < 0.0001$, Table 1), while no association was observed with age or parasite density (Table 5.1).

Table 5. 1 Multiple linear regression analysis of clinical and demographic factors associated with relative antibody responses in seropositive samples

	PF3D7_0210600-1		**PF3D7_0210600-3**		**PF3D7_1136200-3**	
	F	**P-value**	**F**	**P-value**	**F**	**P-value**
Age	2.085	0.0401	0.7935	0.4297	0.9119	0.3671
Parasite density	2.339	0.0217	2.500	0.0143	0.7752	0.4425
Sites	4.305	<0.0001	0.9210	0.3597	8.372	<0.0001

We also performed a Chi-square test to assess the statistical difference in the prevalence of seropositive sample across the different study groups. Notably, for both antigens, there were significant differences in the relative antibody response in children from across the different study sites. Overall, children from Navrongo recorded a higher sample seroprevalence against PF3D7_0210600-1 compared to those from Accra and Hohoe ($P < 0.0001$, $P < 0.007$, respectively, Figure 5.9, Table 5.A1), while no significant difference was observed between Navrongo and Kintampo ($P = 0.179$). A similar trend, yet associated with a wider range of variation across sites was observed with the sample seroprevalence against PF3D7_1136200-3. Overall, the relative sample seroprevalence against PF3D7_0210600-3 was significantly different across the study groups, except for samples from Accra and Hohoe ($P = 0.556$, Figure 8, Table 5.A9). Interestingly, no positive responder was detected against PF3D7_1136200-3 in samples from Accra, while only a handful number of samples from Hohoe were seropositive against this antigen (Figure 5.9), and

expectedly, there were significant differences in the seroprevalence of samples from low (Accra and Hohoe) and high (Navrongo and Kintampo) transmission areas (Table 5.A9). Besides, for all tested antigens, there was a relatively similar trend of antibody response between the adult samples and those from Accra and Hohoe (Figure 5.9, Table 5.A9).

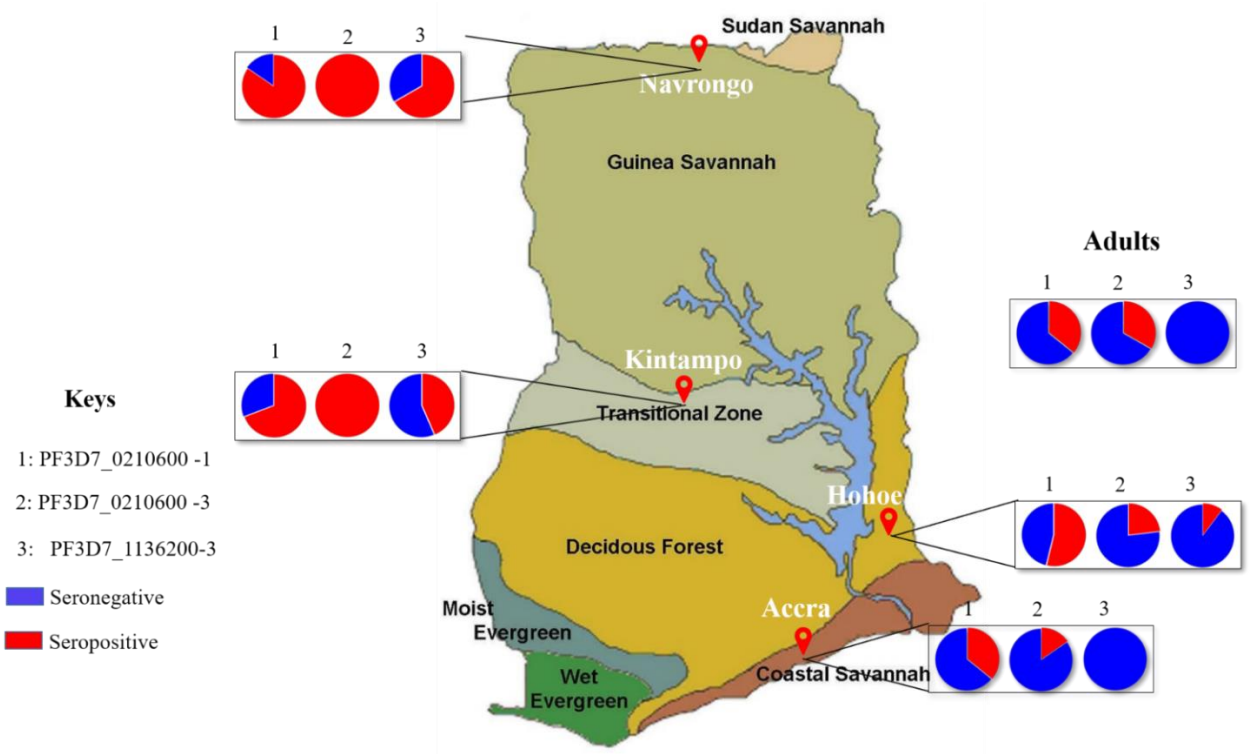

Figure 5. 8: Seroprevalence of positive responders across different endemic areas. Represented is the map of Ghana showing the different ecological zones and the sample collection sites. For each antigen tested here, graphs are showing the distribution of seropositive samples across the various endemic areas as well as the adult samples. Seropositivity was defined as any sample tested with a mean AU greater than that of the naïve European donor plus three standard deviations.

5.1.5. Discussion

Malaria vaccine development strategies have for long been precluded by both the complexity of the parasite's life cycle and the development of strain-specific immunity against different parasite populations (Arama & Troye-Blomberg, 2014). Therefore, the quest for an effective vaccine would necessarily involve the early consideration of the specific stage of the parasite's life cycle to be tackled, also the extent of the genetic polymorphism of the parasite's antigens to be considered as potential vaccine candidates.

The erythrocytic phase of *P. falciparum* has, for long, been considered as a primary target for vaccine development strategies. However, given the phenotypic plasticity of this stage, targeting single antigens as vaccine candidate has so far been unsuccessful (Arama & Troye-Blomberg, 2014; Crompton, Pierce, et al., 2010), hence the new paradigm of shifting to a multicomponent malaria vaccine strategy (Bustamante et al., 2013). Therefore, the identification of specific vaccine targets that mediate both high invasion inhibitory activities and high antibody response in naturally exposed individuals, would be of utmost importance in the development of an efficient malaria vaccine.

Herein, we assessed the growth inhibition potential of antibodies against two novel *P. falciparum* antigens (PF3D7_0210600 and PF3D7_1136200) as well as the breadth of naturally derived antibodies in both malaria-exposed adults and symptomatic children from areas of varying transmission intensity. Both candidate genes tested here were identified through combinatory screenings of publicly available databases as previously described (Amlabu et al., 2018) and found to be conserved within the genus. Using increasing concentrations of antibodies against different peptides of each antigen, we showed that both the *P. falciparum*

laboratory line 3D7 and clinical isolate MISA031 were susceptible to invasion inhibition in a dose-dependent manner.

Given the major challenges associated to malaria vaccine development, notably antigen polymorphism, we tested the transient growth inhibitory activity of antibodies against our target antigens in both laboratory and clinical *P. falciparum* isolates. We showed that across all isolates, antibodies targeting different peptides of the same antigen had different invasion inhibitory activities at the same concentration. Besides, of all isolates, Dd2 was the least susceptible to invasion inhibition across all antibodies. This is consistent with previous reports showing a significant reduction of the invasion inhibitory activities of three different invasion-related genes (PfEBA181, PfCyRPA and PfRAMA) in Dd2 relative to the 3D7 strain (Bustamante et al., 2017).

Based on these data, we sought to assess the invasion inhibitory activity of combinations of antibody pairs at different concentrations and showed no additive effect of antibody combinations when antibodies against the same antigen were used at low concentration (50 µg/mL). However, there was an antagonistic effect when antibodies targeting different antigens were used in combinations at a higher concentration (250 µg/mL). This again is in agreement with previous reports relative to the antagonistic inhibitory effect of some antibody pair combinations such as anti-PfEBA181/PfCyRPA or anti-PfEBA181/PfSERA9, while emphasizing on the need to consider different antibody ratios to ascertain their synergistic effect (Bustamante et al., 2017). However, because of the limited quantity of antibodies available for this study, we could not consider using different antibody ratios while assessing their synergistic inhibitory effect.

To further investigate the immunogenicity of our target antigens, we assessed the levels of naturally acquired antibodies against selected peptides of each gene. Only peptides corresponding to the antibodies with the highest invasion inhibitory activity were selected and plasma samples from children with clinical malaria were used in this experiment. The data showed that, across all sites, there were no significant differences in the antibody responses against the selected three peptides. Antibody responses against *P. falciparum* merozoite surface antigens have recently been shown to positively correlate with age in Ghanaian children presenting symptomatic malaria (Henrietta E Mensah-Brown et al., 2019). Besides, the same study reported a negative correlation between antibody responses and parasite density in the same populations. Interestingly, antibody response did not correlate with age or parasites density in our study. However, the stratification of the data based on the samples seropositivity relative to the naïve control showed a similar, yet significant trend in the levels of antibody titers across sites. Levels of antibody titers against PF3D7_0210600-1 were significantly associated with age, parasite density and transmission intensity, while that against PF3D7_0210600-3 was only associated with parasite density. This data suggesting that different epitopes of a given antigen may present different levels of immunogenicity, similar to results for SERA5 (Aoki et al., 2002). Besides, antibody titers against PF3D7_1136200 were only significantly associated with transmission intensity. Interestingly, no positive responders were found in the Accra and adult samples. Moreover, there were non-significant differences in the sample seropositivity when comparing Hohoe, Navrongo and Kintampo.

Although the data summarized in this study shows the potential consideration of these two antigens as diagnostic or vaccine candidates, further functional assays are required to confirm the invasion inhibitory activities of these two candidate genes as well as their potential

contribution in the invasion, if any. Besides, a better sero-epidemiological study design, possibly involving a cohort of participants, could shed light on the functional role of naturally acquired antibodies against these antigens.

CHAPTER SIX: DISCUSSION

Despite the complexity of the life cycle, the pathogenic phase of malaria only occurs during the asexual replication of the parasites in the host erythrocytes. The mechanism of erythrocyte invasion by *P. falciparum*, responsible for the most severe forms of malaria, is very coordinated and complex, and so far, it appears to be only partially understood. Erythrocyte invasion by *P. falciparum* involves an array of protein-protein interactions between the parasite's ligands and the erythrocytes' receptors (Beeson et al., 2016; Cowman et al., 2017).

P. falciparum merozoites, the blood-stage invasive form of the parasite, are covered in a fibrillar coat of surface proteins and harbour an apical invasion machine, involving Apicomplexan specific secretory organelles, such as the rhoptries and the micronemes (Bannister et al., 2003; Counihan et al., 2013; Lal et al., 2009). Throughout the active phase of erythrocyte invasion, both surface and secreted proteins are exposed on the surface of the invading merozoite and therefore targeted by the immune system (Wright & Rayner, 2014). Targeting antigens involved in the blood stage of the parasite replication as vaccine candidates would not only reduce the disease occurrence in the vaccine recipient but would also have a great impact on the subsequent transmission of the parasite. Besides, there are reports of naturally-derived antibody responses against numerous blood-stage antigens being assessed as potential vaccines candidates (Crompton, Kayala, et al., 2010; Henrietta E Mensah-Brown et al., 2019; Partey et al., 2018). However, coordinated *in vitro* investigation and down-selection of malaria vaccine candidates is hampered by the lack of consensus in the assay protocols, which further influence cross-study comparison of data from different groups (WAMIN, 2016).

Given the importance of *P. falciparum* erythrocyte invasion phenotyping assays in the quest for potential vaccine candidates, we hypothesized that the use of different protocols in investigating *P. falciparum* invasion diversity may not reflect the true biological differences in isolates from different endemic areas. In support of this hypothesis, available data on the handful number of studies reporting on the major invasion phenotypes in circulating *P. falciparum* clinical isolates showed a wide range of variation in protocols across study sites, sometimes even within the same research group (WAMIN, 2016).

This study was designed to investigate the contribution of some potential sources of variation (e.g. cryopreservation and freeze-thaw protocols and blood donor variability) in the outcome of *P. falciparum* erythrocyte invasion phenotyping assays. Additionally, the invasion phenotypes of circulating Ghanaian *P. falciparum* clinical isolates, assessed in this study, were compared to existing data from the same study sites. Finally, we assessed the invasion inhibitory activities of antibodies against two novel *P. falciparum* antigens as potential candidates for prioritization.

To investigate the effect of cryopreservation and freeze-thaw protocols as well as the effect of short-term culture adaptation in *P. falciparum* erythrocyte invasion phenotype, freshly collected *P. falciparum* clinical isolates were phenotyped prior to and following cryopreservation or short-term culture adaptation. Results from these investigations revealed that there is a fitness cost associated with the *in vitro* culture-adaptability of freshly collected *P. falciparum* clinical isolates, as shown by the parasites' multiplication rates during the first *in vitro* replicative cycles, and by the loss of specific parasite clones following short-term culture adaptation. These findings are in agreement with previous reports relative to the parasite multiplication rates (Lantos et al., 2009) and the on-going clonal selection in freshly culture-adapted clinical isolates

(Chaorattanakawee et al., 2015; Sondo et al., 2019), respectively. Additionally, our data also revealed a significant change in the invasion phenotype of some isolates following culture-adaptation relative to the uncultured isogenic parental isolates. This change may be a result of the potential influence of culture-adaptation of the ongoing clonal selection, but also as a result of technical variations during assay set up. However, given the limited number of isolates involved here, such finding necessitates further validation with a larger sample size. Furthermore, our data also showed that short-term cryopreservation or thawing protocols have minimal effect on the parasite's invasion phenotype relative to the fresh isogenic parental isolate, despite the decrease in the PMR observed following cryopreservation.

Another potential source of variation in *P. falciparum* invasion phenotyping assays investigated in this study was the effect of blood donor variability. Given the lack of an appropriate erythroid cell line capable of supporting large-scale *in vitro* phenotyping of *P. falciparum*, such assays mostly rely on the use of erythrocytes of different background. As such, we hypothesized that blood donor variability may be a modulator of *P. falciparum* invasion phenotype. To assess this hypothesis, erythrocytes from twenty unrelated donors presenting different phenotypes relative to their blood groups, hemoglobin genotypes and receptor density were used to assess the invasion phenotypes of six different *P. falciparum* isolates.

Our findings revealed that, across all isolates, invasion efficiency into enzyme-treated erythrocytes varied from one donor to another. However, there was no association between invasion efficiency and sensitivity to enzyme treatment across all donors. As such, we further hypothesized that the difference in invasion efficiency may be driven by the abundance of receptors available on the surface of target erythrocyte as previously reported (Bei, Brugnara, et

al., 2010; Crosnier et al., 2011). Surprisingly, no such relationship was observed between invasion efficiency and receptor density on the surface of target erythrocytes, even in the absence of enzyme treatment. Besides, we found no relationship between invasion efficiency and blood group, hence contradicting previous reports regarding the parasites' preference of O^+ blood group in *in vitro* culture systems (Pathak et al., 2016; Theron et al., 2018). Likewise, and in agreement with previous reports (Lelliott et al., 2015), no relationship was found between invasion efficiency and hemoglobin genotype.

Given the lack of correlation between invasion efficiency and the majority of erythrocyte phenotypic features, a potential source of variation in invasion efficiency could be driven by other intrinsic properties of the erythrocyte itself. On top of the list of potential erythrocyte properties being investigated as potential factors facilitating invasion by *P. falciparum* are the erythrocyte tension and bending modulus as recently suggested (Koch et al., 2017). Interestingly, while bending modulus has been shown to greatly influence erythrocyte invasion by *P. falciparum*, the involvement of the erythrocyte's membrane tension is yet to be fully defined (Koch et al., 2017). Besides, given the potential activation of downstream signaling pathways upon establishment of the ligand-receptor interaction during invasion (Karnchanaphanurach et al., 2009; Khoory et al., 2016; Koch et al., 2017), there is a need to design more robust experiments able to decipher the actual contribution of the host cell during *P. falciparum* invasion.

In the recent years, flow cytometry has become a cornerstone in investigating the phenotypic diversity of *P. falciparum* invasion pathways (Bei, Desimone, et al., 2010; Theron et al., 2018; Theron et al., 2010), as a result of its high sensitivity, specificity and speed relative to routinely

used technologies such as microscopy (Bei, Desimone, et al., 2010). Flow cytometry-based invasion phenotyping assays involve the use of cytoplasmic dye to differentiate target erythrocytes from culture-derived uninfected erythrocytes. As such, CFDA-SE and DDAO-SE have so far been the most commonly used dyes in such experiments. However, given the recent discontinuation of DDAO-SE manufacturing, and the limited spectral properties of CFDA-SE, there was the need to assess the suitability of other cytoplasmic dyes in order to broaden the range of flow cytometry instruments to be used in such experiments. Here, we assessed the suitability of a newly developed cytoplasmic dye, Cell Trace Far Red (CTFR), for use in flow-cytometry-based assays for investigating the phenotypic diversity of *P. falciparum*. Using a dye-dilution approach, we showed that CTFR yields a bright and stable fluorescent intensity in target erythrocytes at relatively low concentrations, therefore supporting previous reports about the labelling of other cell types (Zhou et al., 2016). Besides, our data revealed that CFTR was not toxic to invasion efficiency and subsequent intra erythrocytic growth. We also showed that CTFR could be used in combination with either SYBR Green I or Hoechst 33342 in *P. falciparum* erythrocyte invasion phenotyping assays. Along with its ability to stain target erythrocytes at relatively low concentrations, the narrowed emission peak associated with CTFR makes it a dye of choice for more complex flow cytometry-based assays such as the recently developed erythrocyte preference assay (Theron et al., 2018).

The second objective of our study was achieved through the investigation of the phenotypic diversity of *P. falciparum* invasion pathways in Ghanaian clinical isolates. Previous studies implicating *P. falciparum* clinical isolates have reported contradictory results relative to the relationship between erythrocyte invasion phenotype and transmission intensity (Bowyer et al., 2015; H. E. Mensah-Brown et al., 2015). In this study, we assessed the erythrocytes invasion

diversity of *P. falciparum* clinical samples collected from children of age 2 to 14 years residing in four different endemic areas in Ghana. The analysis of socio-demographic data from our study participants revealed a similar trend on age and transmission intensity (Ademolue et al., 2017; H. E. Mensah-Brown et al., 2015), with the age of the patients decreasing as transmission intensity increases. However, a different trend was observed with parasite density, which overall increases alongside transmission intensity. These findings suggest that, unlike children living in low transmission areas, in high transmission areas, children develop malaria-related symptoms only when the parasites density is beyond a threshold limit as previously reported (Galatas et al., 2016; Goncalves et al., 2014; H. E. Mensah-Brown et al., 2015). The data from the erythrocyte invasion phenotyping experiments conducted in this study confirmed the predominance of the SA-independent invasion pathway in Ghanaian clinical isolates (Bowyer et al., 2015; H. E. Mensah-Brown et al., 2015), with a slight difference in the parasites' susceptibility to neuraminidase treatment across study sites. This finding was however different to an earlier report from the Gambia which showed the predominance of the SA-dependent pathway (Baum et al., 2003b). However, there were discrepancies in the relationship between SA-dependency and transmission intensity. While our data confirmed previous reports showing no correlation between these two factors (Bowyer et al., 2015), the results were contradictory to our previous observations of such a correlation (H. E. Mensah-Brown et al., 2015). Besides, we also showed significant differences in the invasion efficiency into trypsin-treated erythrocytes across sites, once again contradicting earlier reports which showed no significant differences across sites (Bowyer et al., 2015; H. E. Mensah-Brown et al., 2015). However, results from these different studies were individually generated using different protocols and reagent batches, which, along with the number of isolates assayed in each study, could partly explain the

observed variation. Across all isolates, the NrTsCs invasion profile was the most predominant one, while across all sites invasion into trypsin-treated erythrocytes was positively correlated to that of chymotrypsin-treated erythrocytes, therefore confirming earlier reports (Bowyer et al., 2015; H. E. Mensah-Brown et al., 2015). Furthermore, our data also revealed the predominance of the CR1/Rh4- mediated invasion pathway in Ghanaian clinical isolates (Bowyer et al., 2015; H. E. Mensah-Brown et al., 2015; Nery et al., 2006). Finally, we assessed the relative expression levels of *P. falciparum* invasion-related genes and showed that, across all isolates EBA175 was the most predominantly expressed antigen and was negatively correlated to the expression of Rh4, as previously reported (Bowyer et al., 2015; H. E. Mensah-Brown et al., 2015; Nery et al., 2006). In sum, many findings from these experiments indicate that Ghanaian *P. falciparum* clinical isolates preferably invade erythrocytes through a SA-independent pathway and may predominantly involve the CR1/Rh4 interaction.

The third and last objective of this study was to assess the invasion inhibitory activities of antibodies against two novel *P. falciparum* antigens and to test the levels of naturally-derived antibody responses against them in symptomatic children from areas of different transmission intensity. Candidate genes were selected based on specific features such as the prediction of sequence antigenicity, surface exposure and hydrophobicity scores. We performed growth inhibitory assays using peptide-specific antibodies against different epitopes of the respective antigens and showed a dose-dependent inhibitory activity of the individual antibodies in both *P. falciparum* laboratory and clinical isolates.

Given the previously reported strain-specific invasion inhibitory activity that precluded the majority of blood-stage vaccines candidates (reviewed in (Arama & Troye-Blomberg, 2014)),

we tested for the strain transcending inhibitory activities of the respective antigens and showed similar invasion inhibition patterns across all isolates tested here. Consistent with previous reports, of all isolates tested here, Dd2 was the least susceptible isolate (Bustamante et al., 2017), while the *P. falciparum* clinical isolates were more susceptible to inhibition across all antibodies. This finding is of a particular interest given that *P. falciparum* clinical isolates are the parasites population to be targeted by any malaria vaccine to be developed. Additionally, given the growing interest in designing multiplex vaccine candidates, we sought to assess the invasion inhibitory potential of the combinations of antibodies against peptides of the same or different antigens in growth inhibition assays. While the combination of antibody pairs targeting the same antigen showed no additive effect relative to the invasion inhibition activity of individual antibodies, there was an antagonistic effect in combinations of antibody pairs targeting different antigens. Similar results had earlier been reported when antibodies against PfEBA181 were combined with antibodies targeting PfCyRPA of PfSERA9. However, the same study emphasized the importance of considering different combination ratios while assessing the synergic effects of different antibodies (Bustamante et al., 2017), which we could not assess here given the limited quantity of antibodies at our disposal. Furthermore, we tested the levels of naturally-derived antibody responses against our target antigens in children from different transmission areas. Our data revealed an increased antibody level as transmission intensity increases, however, there was no significant difference in the observed variation across sites. We also performed a Pearson correlation and showed that, across all sites, the antibody response was not correlated with parasite density or age of the children. However, our recent study assessing the levels of natural antibody responses against different merozoite surface proteins, showed a positive correlation between antibody response and age, while that between antibody

response and parasite density was found to be negative in children with symptomatic malaria (Henrietta E Mensah-Brown et al., 2019). We, therefore, stratified our data into seropositive and seronegative groups using a malaria-naïve European plasma sample to control for antibody cross-reactivity. We then performed a multiple linear regression analysis using age, parasite density and transmission intensity as covariates and showed a very strong relationship between antibody titers and transmission intensity in two of the three peptides tested here. Antibody titer was found to be associated with parasite density for both peptides from PF3D7_0210600 antigen, while the association between antibody titer and age was restricted to the peptide PF3D7_1136200. As previously reported in the case of PfSERA5 (Aoki et al., 2002), this could be as a result of different levels of antigenicity of specific peptides with regards to their sequence or position. Interestingly, our data showed significant differences in the prevalence of positive responders across the different study sites, but similar patterns of antibody responses in adults and children from low transmission settings. Altogether, these findings showed that these two candidate genes could be considered for down-selection for a more thorough investigation of their potentials as a vaccine candidates or diagnostic markers.

REFERENCES

Adams, J. H., Sim, B. K., Dolan, S. A., Fang, X., Kaslow, D. C., & Miller, L. H. (1992). A family of erythrocyte binding proteins of malaria parasites. *Proc Natl Acad Sci U S A, 89*(15), 7085-7089. Retrieved from http://www.ncbi.nlm.nih.gov/pubmed/1496004

Ademolue, T. W., Aniweh, Y., Kusi, K. A., & Awandare, G. A. (2017). Patterns of inflammatory responses and parasite tolerance vary with malaria transmission intensity. *Malar J, 16*(1), 145. doi:10.1186/s12936-017-1796-x

Alexander, D. L., Arastu-Kapur, S., Dubremetz, J. F., & Boothroyd, J. C. (2006). *Plasmodium falciparum* AMA1 binds a rhoptry neck protein homologous to TgRON4, a component of the moving junction in Toxoplasma gondii. *Eukaryot Cell, 5*(7), 1169-1173. doi:10.1128/EC.00040-06

Alexander, D. L., Mital, J., Ward, G. E., Bradley, P., & Boothroyd, J. C. (2005). Identification of the moving junction complex of Toxoplasma gondii: a collaboration between distinct secretory organelles. *PLoS Pathog, 1*(2), e17. doi:10.1371/journal.ppat.0010017

Amlabu, E., Mensah-Brown, H., Nyarko, P. B., Akuh, O. A., Opoku, G., Ilani, P., . . . Awandare, G. A. (2018). Functional Characterization of *Plasmodium falciparum* Surface-Related Antigen as a Potential Blood-Stage Vaccine Target. *J Infect Dis, 218*(5), 778-790. doi:10.1093/infdis/jiy222

Anand, G., Reddy, K. S., Pandey, A. K., Mian, S. Y., Singh, H., Mittal, S. A., . . . Gaur, D. (2016). A novel *Plasmodium falciparum* rhoptry associated adhesin mediates erythrocyte invasion through the sialic-acid dependent pathway. *Sci Rep, 6*, 29185. doi:10.1038/srep29185

Aniweh, Y., Gao, X., Gunalan, K., & Preiser, P. R. (2016). PfRH2b specific monoclonal antibodies inhibit merozoite invasion. *Mol Microbiol*. doi:10.1111/mmi.13468

Antinori, S., Galimberti, L., Milazzo, L., & Corbellino, M. (2012). Biology of human malaria plasmodia including *Plasmodium* knowlesi. *Mediterr J Hematol Infect Dis*, *4*(1), e2012013. doi:10.4084/MJHID.2012.013

Antinori, S., Galimberti, L., Milazzo, L., & Corbellino, M. (2013). *Plasmodium* knowlesi: the emerging zoonotic malaria parasite. *Acta Trop, 125*(2), 191-201. doi:10.1016/j.actatropica.2012.10.008

Aoki, S., Li, J., Itagaki, S., Okech, B. A., Egwang, T. G., Matsuoka, H., . . . Horii, T. (2002). Serine repeat antigen (SERA5) is predominantly expressed among the SERA multigene family of *Plasmodium falciparum*, and the acquired antibody titers correlate with serum inhibition of the parasite growth. *J Biol Chem, 277*(49), 47533-47540. doi:10.1074/jbc.M207145200

Arama, C., & Troye-Blomberg, M. (2014). The path of malaria vaccine development: challenges and perspectives. *J Intern Med, 275*(5), 456-466. doi:10.1111/joim.12223

Arastu-Kapur, S., Ponder, E. L., Fonovic, U. P., Yeoh, S., Yuan, F., Fonovic, M., . . . Bogyo, M. (2008). Identification of proteases that regulate erythrocyte rupture by the malaria parasite *Plasmodium falciparum*. *Nature chemical biology, 4*(3), 203-213. doi:10.1038/nchembio.70

Ashley, E. A., Dhorda, M., Fairhurst, R. M., Amaratunga, C., Lim, P., Suon, S., . . . Tracking Resistance to Artemisinin, C. (2014). Spread of artemisinin resistance in *Plasmodium falciparum* malaria. *N Engl J Med, 371*(5), 411-423. doi:10.1056/NEJMoa1314981

Atwal, S., Giengkam, S., VanNieuwenhze, M., & Salje, J. (2016). Live imaging of the genetically intractable obligate intracellular bacteria Orientia tsutsugamushi using a panel of fluorescent dyes. *J Microbiol Methods, 130*, 169-176. doi:10.1016/j.mimet.2016.08.022

Awandare, G. A., Nyarko, P. B., Aniweh, Y., Ayivor-Djanie, R., & Stoute, J. A. (2018). *Plasmodium falciparum* strains spontaneously switch invasion phenotype in suspension culture. *Sci Rep, 8*(1), 5782. doi:10.1038/s41598-018-24218-0

Awandare, G. A., Spadafora, C., Moch, J. K., Dutta, S., Haynes, J. D., & Stoute, J. A. (2011). *Plasmodium falciparum* field isolates use complement receptor 1 (CR1) as a receptor for invasion of erythrocytes. *Mol Biochem Parasitol, 177*(1), 57-60. doi:10.1016/j.molbiopara.2011.01.005

Badiane, A. S., Bei, A. K., Ahouidi, A. D., Patel, S. D., Salinas, N., Ndiaye, D., . . . Duraisingh, M. T. (2013). Inhibitory humoral responses to the *Plasmodium falciparum* vaccine candidate EBA-175 are independent of the erythrocyte invasion pathway. *Clin Vaccine Immunol, 20*(8), 1238-1245. doi:10.1128/CVI.00135-13

Bannister, L. H., Butcher, G. A., Dennis, E. D., & Mitchell, G. H. (1975). Studies on the structure and invasive behaviour of merozoites of *Plasmodium* knowlesi. *Transactions of the Royal Society of Tropical Medicine and Hygiene, 69*(1), 5. Retrieved from http://www.ncbi.nlm.nih.gov/pubmed/807001

Bannister, L. H., Hopkins, J. M., Dluzewski, A. R., Margos, G., Williams, I. T., Blackman, M. J., . . . Mitchell, G. H. (2003). *Plasmodium falciparum* apical membrane antigen 1 (PfAMA-1) is translocated within micronemes along subpellicular microtubules during merozoite development. *J Cell Sci, 116*(Pt 18), 3825-3834. doi:10.1242/jcs.00665

Bannister, L. H., Hopkins, J. M., Fowler, R. E., Krishna, S., & Mitchell, G. H. (2000). Ultrastructure of rhoptry development in *Plasmodium falciparum* erythrocytic schizonts. *Parasitology, 121 (Pt 3)*, 273-287. Retrieved from https://www.ncbi.nlm.nih.gov/pubmed/11085247

Baum, J., Chen, L., Healer, J., Lopaticki, S., Boyle, M., Triglia, T., . . . Cowman, A. F. (2009). Reticulocyte-binding protein homologue 5 - an essential adhesin involved in invasion of human erythrocytes by *Plasmodium falciparum*. *Int J Parasitol, 39*(3), 371-380. doi:10.1016/j.ijpara.2008.10.006

Baum, J., Pinder, M., & Conway, D. J. (2003a). Erythrocyte invasion phenotypes of *Plasmodium falciparum* in The Gambia. *Infect Immun, 71*(4), 1856-1863. Retrieved from http://www.ncbi.nlm.nih.gov/pubmed/12654801

Baum, J., Pinder, M., & Conway, D. J. (2003b). Erythrocyte Invasion Phenotypes of *Plasmodiumfalciparum* in The Gambia. *Infect Immun, 71*(4), 1856-1863. doi:10.1128/iai.71.4.1856-1863.2003

Baum, J., Richard, D., Healer, J., Rug, M., Krnajski, Z., Gilberger, T. W., . . . Cowman, A. F. (2006). A conserved molecular motor drives cell invasion and gliding motility across malaria

life cycle stages and other apicomplexan parasites. *The Journal of biological chemistry, 281*(8), 5197-5208. doi:10.1074/jbc.M509807200

Beeson, J. G., Drew, D. R., Boyle, M. J., Feng, G., Fowkes, F. J., & Richards, J. S. (2016). Merozoite surface proteins in red blood cell invasion, immunity and vaccines against malaria. *FEMS Microbiol Rev, 40*(3), 343-372. doi:10.1093/femsre/fuw001

Begum, J., Day, W., Henderson, C., Purewal, S., Cerveira, J., Summers, H., . . . Filby, A. (2013). A method for evaluating the use of fluorescent dyes to track proliferation in cell lines by dye dilution. *Cytometry A, 83*(12), 1085-1095. doi:10.1002/cyto.a.22403

Bei, A. K., Brugnara, C., & Duraisingh, M. T. (2010). In vitro genetic analysis of an erythrocyte determinant of malaria infection. *J Infect Dis, 202*(11), 1722-1727. doi:10.1086/657157

Bei, A. K., Desimone, T. M., Badiane, A. S., Ahouidi, A. D., Dieye, T., Ndiaye, D., . . . Duraisingh, M. T. (2010). A flow cytometry-based assay for measuring invasion of red blood cells by *Plasmodium falciparum*. *Am J Hematol, 85*(4), 234-237. doi:10.1002/ajh.21642

Bei, A. K., & Duraisingh, M. T. (2012). Functional analysis of erythrocyte determinants of *Plasmodium* infection. *Int J Parasitol, 42*(6), 575-582. doi:10.1016/j.ijpara.2012.03.006

Bei, A. K., Membi, C. D., Rayner, J. C., Mubi, M., Ngasala, B., Sultan, A. A., . . . Duraisingh, M. T. (2007). Variant merozoite protein expression is associated with erythrocyte invasion phenotypes in *Plasmodium falciparum* isolates from Tanzania. *Mol Biochem Parasitol, 153*(1), 66-71. doi:10.1016/j.molbiopara.2007.01.007

Besteiro, S., Michelin, A., Poncet, J., Dubremetz, J. F., & Lebrun, M. (2009). Export of a Toxoplasma gondii rhoptry neck protein complex at the host cell membrane to form the moving junction during invasion. *PLoS Pathog, 5*(2), e1000309. doi:10.1371/journal.ppat.1000309

Bhatt, S., Weiss, D. J., Cameron, E., Bisanzio, D., Mappin, B., Dalrymple, U., . . . Gething, P. W. (2015). The effect of malaria control on *Plasmodium falciparum* in Africa between 2000 and 2015. *Nature, 526*(7572), 207-211. doi:10.1038/nature15535

Black, C. G., Wang, L., Hibbs, A. R., Werner, E., & Coppel, R. L. (1999). Identification of the *Plasmodium* chabaudi homologue of merozoite surface proteins 4 and 5 of *Plasmodium falciparum*. *Infect Immun, 67*(5), 2075-2081. Retrieved from http://www.ncbi.nlm.nih.gov/pubmed/10225857

Black, C. G., Wang, L., Wu, T., & Coppel, R. L. (2003). Apical location of a novel EGF-like domain-containing protein of *Plasmodium falciparum*. *Mol Biochem Parasitol, 127*(1), 59-68. Retrieved from http://www.ncbi.nlm.nih.gov/pubmed/12615336

Bowyer, P. W., Stewart, L. B., Aspeling-Jones, H., Mensah-Brown, H. E., Ahouidi, A. D., Amambua-Ngwa, A., . . . Conway, D. J. (2015). Variation in *Plasmodium falciparum* erythrocyte invasion phenotypes and merozoite ligand gene expression across different populations in areas of malaria endemicity. *Infect Immun, 83*(6), 2575-2582. doi:10.1128/IAI.03009-14

Boyle, M. J., Langer, C., Chan, J. A., Hodder, A. N., Coppel, R. L., Anders, R. F., & Beeson, J. G. (2014). Sequential processing of merozoite surface proteins during and after erythrocyte invasion by *Plasmodium falciparum*. *Infect Immun, 82*(3), 924-936. doi:10.1128/IAI.00866-13

Brusko, T. M., Hulme, M. A., Myhr, C. B., Haller, M. J., & Atkinson, M. A. (2007). Assessing the in vitro suppressive capacity of regulatory T cells. *Immunol Invest, 36*(5-6), 607-628. doi:10.1080/08820130701790368

Bustamante, L. Y., Bartholdson, S. J., Crosnier, C., Campos, M. G., Wanaguru, M., Nguon, C., . . . Rayner, J. C. (2013). A full-length recombinant *Plasmodium falciparum* PfRH5 protein induces inhibitory antibodies that are effective across common PfRH5 genetic variants. *Vaccine, 31*(2), 373-379. doi:10.1016/j.vaccine.2012.10.106

Bustamante, L. Y., Powell, G. T., Lin, Y. C., Macklin, M. D., Cross, N., Kemp, A., . . . Rayner, J. C. (2017). Synergistic malaria vaccine combinations identified by systematic antigen screening. *Proc Natl Acad Sci U S A, 114*(45), 12045-12050. doi:10.1073/pnas.1702944114

Cao, J., Kaneko, O., Thongkukiatkul, A., Tachibana, M., Otsuki, H., Gao, Q., . . . Torii, M. (2009). Rhoptry neck protein RON2 forms a complex with microneme protein AMA1 in *Plasmodium falciparum* merozoites. *Parasitol Int, 58*(1), 29-35. doi:10.1016/j.parint.2008.09.005

Carruthers, V. B., & Tomley, F. M. (2008). Microneme proteins in apicomplexans. *Sub-cellular biochemistry, 47*, 33-45. Retrieved from http://www.ncbi.nlm.nih.gov/pubmed/18512339

Chaorattanakawee, S., Lanteri, C. A., Sundrakes, S., Yingyuen, K., Gosi, P., Chanarat, N., . . . Saunders, D. L. (2015). Attenuation of *Plasmodium falciparum* in vitro drug resistance phenotype following culture adaptation compared to fresh clinical isolates in Cambodia. *Malar J, 14*, 486. doi:10.1186/s12936-015-1021-8

Chen, K., Sun, L., Lin, Y., Fan, Q., Zhao, Z., Hao, M., . . . Yang, Z. (2014). Competition between *Plasmodium falciparum* strains in clinical infections during in vitro culture adaptation. *Infect Genet Evol, 24*, 105-110. doi:10.1016/j.meegid.2014.03.012

Chen, L., Lopaticki, S., Riglar, D. T., Dekiwadia, C., Uboldi, A. D., Tham, W. H., . . . Cowman, A. F. (2011). An EGF-like protein forms a complex with PfRh5 and is required for invasion of human erythrocytes by *Plasmodium falciparum*. *PLoS Pathog, 7*(9), e1002199. doi:10.1371/journal.ppat.1002199

Chiu, C. Y., Healer, J., Thompson, J. K., Chen, L., Kaul, A., Savergave, L., . . . Hansen, D. S. (2014). Association of antibodies to *Plasmodium falciparum* reticulocyte binding protein homolog 5 with protection from clinical malaria. *Front Microbiol, 5*, 314. doi:10.3389/fmicb.2014.00314

Chiu, C. Y., Hodder, A. N., Lin, C. S., Hill, D. L., Li Wai Suen, C. S., Schofield, L., . . . Hansen, D. S. (2015). Antibodies to the *Plasmodium falciparum* Proteins MSPDBL1 and MSPDBL2 Opsonize Merozoites, Inhibit Parasite Growth, and Predict Protection From Clinical Malaria. *J Infect Dis, 212*(3), 406-415. doi:10.1093/infdis/jiv057

Chiu, C. Y., White, M. T., Healer, J., Thompson, J. K., Siba, P. M., Mueller, I., . . . Hansen, D. S. (2016). Different Regions of *Plasmodium falciparum* Erythrocyte-Binding Antigen 175 Induce Antibody Responses to Infection of Varied Efficacy. *J Infect Dis, 214*(1), 96-104. doi:10.1093/infdis/jiw119

Conway, D. J. (2015). Paths to a malaria vaccine illuminated by parasite genomics. *Trends Genet, 31*(2), 97-107. doi:10.1016/j.tig.2014.12.005

Cortés, A. (2008). Switching *Plasmodium falciparum* genes on and off for erythrocyte invasion. *Trends Parasitol, 24*(11), 517-524. doi:10.1016/j.pt.2008.08.005

Counihan, N. A., Chisholm, S. A., Bullen, H. E., Srivastava, A., Sanders, P. R., Jonsdottir, T. K., . . . de Koning-Ward, T. F. (2017). *Plasmodium falciparum* parasites deploy RhopH2 into the host erythrocyte to obtain nutrients, grow and replicate. *Elife, 6*. doi:10.7554/eLife.23217

Counihan, N. A., Kalanon, M., Coppel, R. L., & de Koning-Ward, T. F. (2013). *Plasmodium* rhoptry proteins: why order is important. *Trends Parasitol, 29*(5), 228-236. doi:10.1016/j.pt.2013.03.003

Cowman, A. F., Berry, D., & Baum, J. (2012). The cellular and molecular basis for malaria parasite invasion of the human red blood cell. *The Journal of cell biology, 198*(6), 961-971. doi:10.1083/jcb.201206112

Cowman, A. F., & Crabb, B. S. (2006). Invasion of red blood cells by malaria parasites. *Cell, 124*(4), 755-766. doi:10.1016/j.cell.2006.02.006

Cowman, A. F., Tonkin, C. J., Tham, W. H., & Duraisingh, M. T. (2017). The Molecular Basis of Erythrocyte Invasion by Malaria Parasites. *Cell Host Microbe, 22*(2), 232-245. doi:10.1016/j.chom.2017.07.003

Crompton, P. D., Kayala, M. A., Traore, B., Kayentao, K., Ongoiba, A., Weiss, G. E., . . . Pierce, S. K. (2010). A prospective analysis of the Ab response to *Plasmodium falciparum* before and after a malaria season by protein microarray. *Proc Natl Acad Sci U S A, 107*(15), 6958-6963. doi:10.1073/pnas.1001323107

Crompton, P. D., Pierce, S. K., & Miller, L. H. (2010). Advances and challenges in malaria vaccine development. *J Clin Invest, 120*(12), 4168-4178. doi:10.1172/JCI44423

Crosnier, C., Bustamante, L. Y., Bartholdson, S. J., Bei, A. K., Theron, M., Uchikawa, M., . . . Wright, G. J. (2011). Basigin is a receptor essential for erythrocyte invasion by *Plasmodium falciparum*. *Nature, 480*(7378), 534-537. doi:10.1038/nature10606

Crosnier, C., Iqbal, Z., Knuepfer, E., Maciuca, S., Perrin, A. J., Kamuyu, G., . . . Wright, G. J. (2016). Binding of *Plasmodium falciparum* Merozoite Surface Proteins DBLMSP and DBLMSP2 to Human Immunoglobulin M Is Conserved among Broadly Diverged Sequence Variants. *J Biol Chem, 291*(27), 14285-14299. doi:10.1074/jbc.M116.722074

Culvenor, J. G., Day, K. P., & Anders, R. F. (1991). *Plasmodium falciparum* ring-infected erythrocyte surface antigen is released from merozoite dense granules after erythrocyte invasion. *Infection and immunity, 59*(3), 1183-1187. Retrieved from http://www.ncbi.nlm.nih.gov/pubmed/1997422

Dankwa, S., Chaand, M., Kanjee, U., Jiang, R. H. Y., Nobre, L. V., Goldberg, J. M., . . . Duraisingh, M. T. (2017). Genetic Evidence for Erythrocyte Receptor Glycophorin B Expression Levels Defining a Dominant *Plasmodium falciparum* Invasion Pathway into Human Erythrocytes. *Infect Immun, 85*(10). doi:10.1128/IAI.00074-17

Das, S., Hertrich, N., Perrin, A. J., Withers-Martinez, C., Collins, C. R., Jones, M. L., . . . Blackman, M. J. (2015). Processing of *Plasmodium falciparum* Merozoite Surface Protein MSP1 Activates a Spectrin-Binding Function Enabling Parasite Egress from RBCs. *Cell Host Microbe, 18*(4), 433-444. doi:10.1016/j.chom.2015.09.007

Deans, A. M., Nery, S., Conway, D. J., Kai, O., Marsh, K., & Rowe, J. A. (2007). Invasion pathways and malaria severity in Kenyan *Plasmodium falciparum* clinical isolates. *Infect Immun, 75*(6), 3014-3020. doi:10.1128/IAI.00249-07

Debrabant, A., & Delplace, P. (1989). Leupeptin alters the proteolytic processing of P126, the major parasitophorous vacuole antigen of *Plasmodium falciparum*. *Mol Biochem Parasitol, 33*(2), 151-158. Retrieved from https://www.ncbi.nlm.nih.gov/pubmed/2657420

Dent, A. E., Nakajima, R., Liang, L., Baum, E., Moormann, A. M., Sumba, P. O., . . . Kazura, J. W. (2015). *Plasmodium falciparum* Protein Microarray Antibody Profiles Correlate With Protection From Symptomatic Malaria in Kenya. *J Infect Dis, 212*(9), 1429-1438. doi:10.1093/infdis/jiv224

Dias, J., Gumenyuk, M., Kang, H., Vodyanik, M., Yu, J., Thomson, J. A., & Slukvin, II. (2011). Generation of red blood cells from human induced pluripotent stem cells. *Stem Cells Dev, 20*(9), 1639-1647. doi:10.1089/scd.2011.0078

Diouf, B., Diop, F., Dieye, Y., Loucoubar, C., Dia, I., Faye, J., . . . Toure-Balde, A. (2019). Association of high *Plasmodium falciparum* parasite densities with polyclonal microscopic infections in asymptomatic children from Toubacouta, Senegal. *Malar J, 18*(1), 48. doi:10.1186/s12936-019-2684-3

Dluzewski, A. R., Ling, I. T., Hopkins, J. M., Grainger, M., Margos, G., Mitchell, G. H., . . . Bannister, L. H. (2008). Formation of the food vacuole in *Plasmodium falciparum*: a potential role for the 19 kDa fragment of merozoite surface protein 1 (MSP1(19)). *PLoS One, 3*(8), e3085. doi:10.1371/journal.pone.0003085

Douglas, A. D., Williams, A. R., Illingworth, J. J., Kamuyu, G., Biswas, S., Goodman, A. L., . . . Draper, S. J. (2011). The blood-stage malaria antigen PfRH5 is susceptible to vaccine-inducible cross-strain neutralizing antibody. *Nat Commun, 2*, 601. doi:10.1038/ncomms1615

Draper, S. J., Angov, E., Horii, T., Miller, L. H., Srinivasan, P., Theisen, M., & Biswas, S. (2015). Recent advances in recombinant protein-based malaria vaccines. *Vaccine, 33*(52), 7433-7443. doi:10.1016/j.vaccine.2015.09.093

Duraisingh, M. T., Maier, A. G., Triglia, T., & Cowman, A. F. (2003). Erythrocyte-binding antigen 175 mediates invasion in *Plasmodium falciparum* utilizing sialic acid-dependent and -independent pathways. *Proc Natl Acad Sci U S A, 100*(8), 4796-4801. doi:10.1073/pnas.0730883100

Duraisingh, M. T., Triglia, T., Ralph, S. A., Rayner, J. C., Barnwell, J. W., McFadden, G. I., & Cowman, A. F. (2003). Phenotypic variation of *Plasmodium falciparum* merozoite proteins directs receptor targeting for invasion of human erythrocytes. *EMBO J, 22*(5), 1047-1057. doi:10.1093/emboj/cdg096

Egan, E. S. (2018). Beyond Hemoglobin: Screening for Malaria Host Factors. *Trends Genet, 34*(2), 133-141. doi:10.1016/j.tig.2017.11.004

Egan, E. S., Jiang, R. H., Moechtar, M. A., Barteneva, N. S., Weekes, M. P., Nobre, L. V., . . . Duraisingh, M. T. (2015). Malaria. A forward genetic screen identifies erythrocyte CD55 as essential for *Plasmodium falciparum* invasion. *Science, 348*(6235), 711-714. doi:10.1126/science.aaa3526

Egan, E. S., Weekes, M. P., Kanjee, U., Manzo, J., Srinivasan, A., Lomas-Francis, C., . . . Duraisingh, M. T. (2018). Erythrocytes lacking the Langereis blood group protein ABCB6 are resistant to the malaria parasite *Plasmodium falciparum*. *Commun Biol, 1*, 45. doi:10.1038/s42003-018-0046-2

EVIMalaR. (2013). Methods in malaria research, sixth edition In. Glasgow, UK: EVIMalaR

Fairlie, W. D., Spurck, T. P., McCoubrie, J. E., Gilson, P. R., Miller, S. K., McFadden, G. I., . . . Hodder, A. N. (2008). Inhibition of malaria parasite development by a cyclic peptide that targets the vital parasite protein SERA5. *Infect Immun, 76*(9), 4332-4344. doi:10.1128/IAI.00278-08

Farrow, R. E., Green, J., Katsimitsoulia, Z., Taylor, W. R., Holder, A. A., & Molloy, J. E. (2011). The mechanism of erythrocyte invasion by the malarial parasite, *Plasmodium falciparum*. *Semin Cell Dev Biol, 22*(9), 953-960. doi:10.1016/j.semcdb.2011.09.022

Filby, A., Begum, J., Jalal, M., & Day, W. (2015). Appraising the suitability of succinimidyl and lipophilic fluorescent dyes to track proliferation in non-quiescent cells by dye dilution. *Methods, 82*, 29-37. doi:10.1016/j.ymeth.2015.02.016

Foquet, L., Schafer, C., Minkah, N. K., Alanine, D. G. W., Flannery, E. L., Steel, R. W. J., . . . Kappe, S. H. I. (2018). *Plasmodium falciparum* Liver Stage Infection and Transition to Stable Blood Stage Infection in Liver-Humanized and Blood-Humanized FRGN KO Mice Enables Testing of Blood Stage Inhibitory Antibodies (Reticulocyte-Binding Protein Homolog 5) In Vivo. *Front Immunol, 9*, 524. doi:10.3389/fimmu.2018.00524

Galatas, B., Bassat, Q., & Mayor, A. (2016). Malaria Parasites in the Asymptomatic: Looking for the Hay in the Haystack. *Trends Parasitol*, *32*(4), 296-308. doi:10.1016/j.pt.2015.11.015

Garcia, Y., Puentes, A., Curtidor, H., Cifuentes, G., Reyes, C., Barreto, J., . . . Patarroyo, M. E. (2007). Identifying merozoite surface protein 4 and merozoite surface protein 7 *Plasmodium falciparum* protein family members specifically binding to human erythrocytes suggests a new malarial parasite-redundant survival mechanism. *J Med Chem*, *50*(23), 5665-5675. doi:10.1021/jm070773z

Gardner, M. J., Hall, N., Fung, E., White, O., Berriman, M., Hyman, R. W., . . . Barrell, B. (2002). Genome sequence of the human malaria parasite *Plasmodium falciparum*. *Nature*, *419*(6906), 498-511. doi:10.1038/nature01097

Gardner, M. J., Shallom, S. J., Carlton, J. M., Salzberg, S. L., Nene, V., Shoaibi, A., . . . Fraser, C. M. (2002). Sequence of *Plasmodium falciparum* chromosomes 2, 10, 11 and 14. *Nature*, *419*(6906), 531-534. doi:10.1038/nature01094

Gardner, M. J., Tettelin, H., Carucci, D. J., Cummings, L. M., Aravind, L., Koonin, E. V., . . . Hoffman, S. L. (1998). Chromosome 2 sequence of the human malaria parasite *Plasmodium falciparum*. *Science*, *282*(5391), 1126-1132. Retrieved from https://www.ncbi.nlm.nih.gov/pubmed/9804551

Gaur, D., & Chitnis, C. E. (2011). Molecular interactions and signaling mechanisms during erythrocyte invasion by malaria parasites. *Curr Opin Microbiol*, *14*(4), 422-428. doi:10.1016/j.mib.2011.07.018

Gaur, D., Mayer, D. C., & Miller, L. H. (2004). Parasite ligand-host receptor interactions during invasion of erythrocytes by *Plasmodium* merozoites. *Int J Parasitol, 34*(13-14), 1413-1429. doi:10.1016/j.ijpara.2004.10.010

Gaur, D., Storry, J. R., Reid, M. E., Barnwell, J. W., & Miller, L. H. (2003). *Plasmodium falciparum* is able to invade erythrocytes through a trypsin-resistant pathway independent of glycophorin B. *Infect Immun, 71*(12), 6742-6746. Retrieved from http://www.ncbi.nlm.nih.gov/pubmed/14638759

Gett, A. V., & Hodgkin, P. D. (2000). A cellular calculus for signal integration by T cells. *Nat Immunol, 1*(3), 239-244. doi:10.1038/79782

Gilberger, T. W., Thompson, J. K., Triglia, T., Good, R. T., Duraisingh, M. T., & Cowman, A. F. (2003). A novel erythrocyte binding antigen-175 paralogue from *Plasmodium falciparum* defines a new trypsin-resistant receptor on human erythrocytes. *J Biol Chem, 278*(16), 14480-14486. doi:10.1074/jbc.M211446200

Gilson, P. R., & Crabb, B. S. (2009). Do apicomplexan parasite-encoded proteins act as both ligands and receptors during host cell invasion? *F1000 Biol Rep, 1*, 64. doi:10.3410/B1-64

Gilson, P. R., Nebl, T., Vukcevic, D., Moritz, R. L., Sargeant, T., Speed, T. P., . . . Crabb, B. S. (2006). Identification and stoichiometry of glycosylphosphatidylinositol-anchored membrane proteins of the human malaria parasite *Plasmodium falciparum*. *Mol Cell Proteomics, 5*(7), 1286-1299. doi:10.1074/mcp.M600035-MCP200

Gomez-Escobar, N., Amambua-Ngwa, A., Walther, M., Okebe, J., Ebonyi, A., & Conway, D. J. (2010). Erythrocyte invasion and merozoite ligand gene expression in severe and mild *Plasmodium falciparum* malaria. *J Infect Dis, 201*(3), 444-452. doi:10.1086/649902

Goncalves, B. P., Fried, M., & Duffy, P. E. (2014). Parasite burden and severity of malaria in Tanzanian children. *N Engl J Med, 371*(5), 482. doi:10.1056/NEJMc1407114

Green, J. L., Hinds, L., Grainger, M., Knuepfer, E., & Holder, A. A. (2006). *Plasmodium* thrombospondin related apical merozoite protein (PTRAMP) is shed from the surface of merozoites by PfSUB2 upon invasion of erythrocytes. *Molecular and biochemical parasitology, 150*(1), 114-117. doi:10.1016/j.molbiopara.2006.06.010

Hadley, T. J., Klotz, F. W., Pasvol, G., Haynes, J. D., McGinniss, M. H., Okubo, Y., & Miller, L. H. (1987). *Falciparum* malaria parasites invade erythrocytes that lack glycophorin A and B (MkMk). Strain differences indicate receptor heterogeneity and two pathways for invasion. *J Clin Invest, 80*(4), 1190-1193. doi:10.1172/JCI113178

Hamid, M. M., Mohammed, S. B., & El Hassan, I. M. (2013). Genetic Diversity of *Plasmodium falciparum* Field Isolates in Central Sudan Inferred by PCR Genotyping of Merozoite Surface Protein 1 and 2. *N Am J Med Sci, 5*(2), 95-101. doi:10.4103/1947-2714.107524

Harris, P. K., Yeoh, S., Dluzewski, A. R., O'Donnell, R. A., Withers-Martinez, C., Hackett, F., . . . Blackman, M. J. (2005). Molecular identification of a malaria merozoite surface sheddase. *PLoS pathogens, 1*(3), 241-251. doi:10.1371/journal.ppat.0010029

Harvey, K. L., Gilson, P. R., & Crabb, B. S. (2012). A model for the progression of receptor-ligand interactions during erythrocyte invasion by *Plasmodium falciparum*. *Int J Parasitol, 42*(6), 567-573. doi:10.1016/j.ijpara.2012.02.011

Hayton, K., Gaur, D., Liu, A., Takahashi, J., Henschen, B., Singh, S., . . . Wellems, T. E. (2008). Erythrocyte binding protein PfRH5 polymorphisms determine species-specific pathways of *Plasmodium falciparum* invasion. *Cell Host Microbe, 4*(1), 40-51. doi:10.1016/j.chom.2008.06.001

Healer, J., McGuinness, D., Hopcroft, P., Haley, S., Carter, R., & Riley, E. (1997). Complement-mediated lysis of *Plasmodium falciparum* gametes by malaria-immune human sera is associated with antibodies to the gamete surface antigen Pfs230. *Infect Immun, 65*(8), 3017-3023. Retrieved from https://www.ncbi.nlm.nih.gov/pubmed/9234748

Healer, J., Wong, W., Thompson, J. K., He, W., Birkinshaw, R. W., Miura, K., . . . Cowman, A. F. (2019). Neutralising antibodies block the function of Rh5/Ripr/CyRPA complex during invasion of *Plasmodium falciparum* into human erythrocytes. *Cell Microbiol*, e13030. doi:10.1111/cmi.13030

Hill, A. V. (2011). Vaccines against malaria. *Philos Trans R Soc Lond B Biol Sci, 366*(1579), 2806-2814. doi:10.1098/rstb.2011.0091

Hill, D. L., Eriksson, E. M., Li Wai Suen, C. S., Chiu, C. Y., Ryg-Cornejo, V., Robinson, L. J., . . . Schofield, L. (2013). Opsonising antibodies to P. *falciparum* merozoites associated with immunity to clinical malaria. *PLoS One, 8*(9), e74627. doi:10.1371/journal.pone.0074627

Hirose, S., Takayama, N., Nakamura, S., Nagasawa, K., Ochi, K., Hirata, S., . . . Eto, K. (2013). Immortalization of erythroblasts by c-MYC and BCL-XL enables large-scale erythrocyte production from human pluripotent stem cells. *Stem Cell Reports, 1*(6), 499-508. doi:10.1016/j.stemcr.2013.10.010

Hodder, A. N., Drew, D. R., Epa, V. C., Delorenzi, M., Bourgon, R., Miller, S. K., . . . Crabb, B. S. (2003). Enzymic, phylogenetic, and structural characterization of the unusual papain-like protease domain of *Plasmodium falciparum* SERA5. *J Biol Chem, 278*(48), 48169-48177. doi:10.1074/jbc.M306755200

Hoffman, S. L., Vekemans, J., Richie, T. L., & Duffy, P. E. (2015a). The march toward malaria vaccines. *Vaccine, 33 Suppl 4*, D13-23. doi:10.1016/j.vaccine.2015.07.091

Hoffman, S. L., Vekemans, J., Richie, T. L., & Duffy, P. E. (2015b). The March Toward Malaria Vaccines. *Am J Prev Med, 49*(6 Suppl 4), S319-333. doi:10.1016/j.amepre.2015.09.011

Howard, R. F., Narum, D. L., Blackman, M., & Thurman, J. (1998). Analysis of the processing of *Plasmodium falciparum* rhoptry-associated protein 1 and localization of Pr86 to schizont rhoptries and p67 to free merozoites. *Mol Biochem Parasitol, 92*(1), 111-122. Retrieved from https://www.ncbi.nlm.nih.gov/pubmed/9574915

Huang, X., Shah, S., Wang, J., Ye, Z., Dowey, S. N., Tsang, K. M., . . . Cheng, L. (2014). Extensive ex vivo expansion of functional human erythroid precursors established from umbilical cord blood cells by defined factors. *Mol Ther, 22*(2), 451-463. doi:10.1038/mt.2013.201

Ito, D., Schureck, M. A., & Desai, S. A. (2017). An essential dual-function complex mediates erythrocyte invasion and channel-mediated nutrient uptake in malaria parasites. *Elife, 6*. doi:10.7554/eLife.23485

Janse, C. J., & Waters, A. P. (2007). The exoneme helps malaria parasites to break out of blood cells. *Cell, 131*(6), 1036-1038. doi:10.1016/j.cell.2007.11.026

Jennings, C. V., Ahouidi, A. D., Zilversmit, M., Bei, A. K., Rayner, J., Sarr, O., . . . Duraisingh, M. T. (2007). Molecular analysis of erythrocyte invasion in *Plasmodium falciparum* isolates from Senegal. *Infect Immun, 75*(7), 3531-3538. doi:10.1128/IAI.00122-07

Joanny, F., Held, J., & Mordmuller, B. (2012). In vitro activity of fluorescent dyes against asexual blood stages of *Plasmodium falciparum*. *Antimicrob Agents Chemother, 56*(11), 5982-5985. doi:10.1128/AAC.00709-12

Kadekoppala, M., & Holder, A. A. (2010). Merozoite surface proteins of the malaria parasite: the MSP1 complex and the MSP7 family. *Int J Parasitol, 40*(10), 1155-1161. doi:10.1016/j.ijpara.2010.04.008

Kaneko, O., Tsuboi, T., Ling, I. T., Howell, S., Shirano, M., Tachibana, M., . . . Torii, M. (2001). The high molecular mass rhoptry protein, RhopH1, is encoded by members of the clag multigene family in *Plasmodium falciparum* and *Plasmodium* yoelii. *Mol Biochem Parasitol, 118*(2), 223-231. Retrieved from https://www.ncbi.nlm.nih.gov/pubmed/11738712

Kanjee, U., Gruring, C., Chaand, M., Lin, K. M., Egan, E., Manzo, J., . . . Duraisingh, M. T. (2017). CRISPR/Cas9 knockouts reveal genetic interaction between strain-transcendent

erythrocyte determinants of *Plasmodium falciparum* invasion. *Proc Natl Acad Sci U S A, 114*(44), E9356-E9365. doi:10.1073/pnas.1711310114

Karnchanaphanurach, P., Mirchev, R., Ghiran, I., Asara, J. M., Papahadjopoulos-Sternberg, B., Nicholson-Weller, A., & Golan, D. E. (2009). C3b deposition on human erythrocytes induces the formation of a membrane skeleton-linked protein complex. *J Clin Invest, 119*(4), 788-801. doi:10.1172/JCI36088

Kasasa, S., Asoala, V., Gosoniu, L., Anto, F., Adjuik, M., Tindana, C., . . . Vounatsou, P. (2013). Spatio-temporal malaria transmission patterns in Navrongo demographic surveillance site, northern Ghana. *Malar J, 12*, 63. doi:10.1186/1475-2875-12-63

Kats, L. M., Black, C. G., Proellocks, N. I., & Coppel, R. L. (2006). *Plasmodium* rhoptries: how things went pear-shaped. *Trends Parasitol, 22*(6), 269-276. doi:10.1016/j.pt.2006.04.001

Kauth, C. W., Woehlbier, U., Kern, M., Mekonnen, Z., Lutz, R., Mucke, N., . . . Bujard, H. (2006). Interactions between merozoite surface proteins 1, 6, and 7 of the malaria parasite *Plasmodium falciparum*. *J Biol Chem, 281*(42), 31517-31527. doi:10.1074/jbc.M604641200

Kennedy, A. T., Schmidt, C. Q., Thompson, J. K., Weiss, G. E., Taechalertpaisarn, T., Gilson, P. R., . . . Tham, W. H. (2016). Recruitment of Factor H as a Novel Complement Evasion Strategy for Blood-Stage *Plasmodium falciparum* Infection. *J Immunol, 196*(3), 1239-1248. doi:10.4049/jimmunol.1501581

Khoory, J., Estanislau, J., Elkhal, A., Lazaar, A., Melhorn, M. I., Brodsky, A., . . . Ghiran, I. C. (2016). Ligation of Glycophorin A Generates Reactive Oxygen Species Leading to Decreased Red Blood Cell Function. *PLoS One, 11*(1), e0141206. doi:10.1371/journal.pone.0141206

Kisalu, N. K., Idris, A. H., Weidle, C., Flores-Garcia, Y., Flynn, B. J., Sack, B. K., . . . Seder, R. A. (2018). A human monoclonal antibody prevents malaria infection by targeting a new site of vulnerability on the parasite. *Nat Med, 24*(4), 408-416. doi:10.1038/nm.4512

Klinkenberg, E., McCall, P., Wilson, M. D., Amerasinghe, F. P., & Donnelly, M. J. (2008). Impact of urban agriculture on malaria vectors in Accra, Ghana. *Malar J, 7*, 151. doi:10.1186/1475-2875-7-151

Kobbe, R., Neuhoff, R., Marks, F., Adjei, S., Langefeld, I., von Reden, C., . . . May, J. (2006). Seasonal variation and high multiplicity of first *Plasmodium falciparum* infections in children from a holoendemic area in Ghana, West Africa. *Trop Med Int Health, 11*(5), 613-619. doi:10.1111/j.1365-3156.2006.01618.x

Koch, M., & Baum, J. (2016). The mechanics of malaria parasite invasion of the human erythrocyte - towards a reassessment of the host cell contribution. *Cell Microbiol, 18*(3), 319-329. doi:10.1111/cmi.12557

Koch, M., Wright, K. E., Otto, O., Herbig, M., Salinas, N. D., Tolia, N. H., . . . Baum, J. (2017). *Plasmodium falciparum* erythrocyte-binding antigen 175 triggers a biophysical change in the red blood cell that facilitates invasion. *Proc Natl Acad Sci U S A, 114*(16), 4225-4230. doi:10.1073/pnas.1620843114

Koussis, K., Withers-Martinez, C., Yeoh, S., Child, M., Hackett, F., Knuepfer, E., . . . Blackman, M. J. (2009a). A multifunctional serine protease primes the malaria parasite for red blood cell invasion. *EMBO J, 28*(6), 725-735. doi:10.1038/emboj.2009.22

Koussis, K., Withers-Martinez, C., Yeoh, S., Child, M., Hackett, F., Knuepfer, E., . . . Blackman, M. J. (2009b). A multifunctional serine protease primes the malaria parasite for red blood cell invasion. *The EMBO journal, 28*(6), 725-735. doi:10.1038/emboj.2009.22

Krupnick, A. S., Kreisel, D., Szeto, W. Y., Popma, S. H., Amin, K. M., Moore, J. S., & Rosengard, B. R. (2001). Multiparameter flow cytometric approach for simultaneous evaluation of T lymphocyte-endothelial cell interactions. *Cytometry, 46*(5), 271-280. Retrieved from https://www.ncbi.nlm.nih.gov/pubmed/11746102

Kumar, D., Dhiman, S., Rabha, B., Goswami, D., Deka, M., Singh, L., . . . Veer, V. (2014). Genetic polymorphism and amino acid sequence variation in *Plasmodium falciparum* GLURP R2 repeat region in Assam, India, at an interval of five years. *Malar J, 13*, 450. doi:10.1186/1475-2875-13-450

Kurita, R., Suda, N., Sudo, K., Miharada, K., Hiroyama, T., Miyoshi, H., . . . Nakamura, Y. (2013). Establishment of immortalized human erythroid progenitor cell lines able to produce enucleated red blood cells. *PLoS One, 8*(3), e59890. doi:10.1371/journal.pone.0059890

Kweku, M., Liu, D., Adjuik, M., Binka, F., Seidu, M., Greenwood, B., & Chandramohan, D. (2008). Seasonal intermittent preventive treatment for the prevention of anaemia and malaria in Ghanaian children: a randomized, placebo controlled trial. *PLoS One, 3*(12), e4000. doi:10.1371/journal.pone.0004000

Lal, K., Prieto, J. H., Bromley, E., Sanderson, S. J., Yates, J. R., 3rd, Wastling, J. M., . . . Sinden, R. E. (2009). Characterisation of *Plasmodium* invasive organelles; an ookinete microneme proteome. *Proteomics, 9*(5), 1142-1151. doi:10.1002/pmic.200800404

Lamarque, M., Besteiro, S., Papoin, J., Roques, M., Vulliez-Le Normand, B., Morlon-Guyot, J., . . . Lebrun, M. (2011). The RON2-AMA1 interaction is a critical step in moving junction-dependent invasion by apicomplexan parasites. *PLoS Pathog, 7*(2), e1001276. doi:10.1371/journal.ppat.1001276

Lantos, P. M., Ahouidi, A. D., Bei, A. K., Jennings, C. V., Sarr, O., Ndir, O., . . . Duraisingh, M. T. (2009). Erythrocyte invasion profiles are associated with a common invasion ligand polymorphism in Senegalese isolates of *Plasmodium falciparum*. *Parasitology, 136*(1), 1-9. doi:10.1017/S0031182008005167

Lassailly, F., Griessinger, E., & Bonnet, D. (2010). "Microenvironmental contaminations" induced by fluorescent lipophilic dyes used for noninvasive in vitro and in vivo cell tracking. *Blood, 115*(26), 5347-5354. doi:10.1182/blood-2009-05-224030

Lebrun, M., Michelin, A., El Hajj, H., Poncet, J., Bradley, P. J., Vial, H., & Dubremetz, J. F. (2005). The rhoptry neck protein RON4 re-localizes at the moving junction during Toxoplasma gondii invasion. *Cell Microbiol, 7*(12), 1823-1833. doi:10.1111/j.1462-5822.2005.00646.x

Leffler, E. M., Band, G., Busby, G. B. J., Kivinen, K., Le, Q. S., Clarke, G. M., . . . Malaria Genomic Epidemiology, N. (2017). Resistance to malaria through structural variation of red blood cell invasion receptors. *Science, 356*(6343). doi:10.1126/science.aam6393

Lelliott, P. M., McMorran, B. J., Foote, S. J., & Burgio, G. (2015). The influence of host genetics on erythrocytes and malaria infection: is there therapeutic potential? *Malar J, 14*, 289. doi:10.1186/s12936-015-0809-x

Li, J., Matsuoka, H., Mitamura, T., & Horii, T. (2002). Characterization of proteases involved in the processing of *Plasmodium falciparum* serine repeat antigen (SERA). *Mol Biochem Parasitol, 120*(2), 177-186. Retrieved from https://www.ncbi.nlm.nih.gov/pubmed/11897123

Li, J., Mitamura, T., Fox, B. A., Bzik, D. J., & Horii, T. (2002). Differential localization of processed fragments of *Plasmodium falciparum* serine repeat antigen and further processing of its N-terminal 47 kDa fragment. *Parasitol Int, 51*(4), 343-352. Retrieved from https://www.ncbi.nlm.nih.gov/pubmed/12421632

Lobo, C. A., de Frazao, K., Rodriguez, M., Reid, M., Zalis, M., & Lustigman, S. (2004). Invasion profiles of Brazilian field isolates of *Plasmodium falciparum*: phenotypic and genotypic analyses. *Infect Immun, 72*(10), 5886-5891. doi:10.1128/IAI.72.10.5886-5891.2004

Long, C. A., & Zavala, F. (2016). Malaria vaccines and human immune responses. *Curr Opin Microbiol, 32*, 96-102. doi:10.1016/j.mib.2016.04.006

Lopaticki, S., Maier, A. G., Thompson, J., Wilson, D. W., Tham, W. H., Triglia, T., . . . Cowman, A. F. (2011). Reticulocyte and erythrocyte binding-like proteins function cooperatively in invasion of human erythrocytes by malaria parasites. *Infect Immun, 79*(3), 1107-1117. doi:10.1128/IAI.01021-10

Lopez-Perez, M., Villasis, E., Machado, R. L., Povoa, M. M., Vinetz, J. M., Blair, S., . . . Lustigman, S. (2012). *Plasmodium falciparum* field isolates from South America use an atypical red blood cell invasion pathway associated with invasion ligand polymorphisms. *PLoS One, 7*(10), e47913. doi:10.1371/journal.pone.0047913

Lopez, R., Valbuena, J., Curtidor, H., Puentes, A., Rodriguez, L. E., Garcia, J., . . . Patarroyo, M. E. (2004). *Plasmodium falciparum*: red blood cell binding studies using peptides derived from rhoptry-associated protein 2 (RAP2). *Biochimie, 86*(1), 1-6. doi:10.1016/j.biochi.2003.11.013

Lyons, A. B., & Parish, C. R. (1994). Determination of lymphocyte division by flow cytometry. *J Immunol Methods, 171*(1), 131-137. Retrieved from https://www.ncbi.nlm.nih.gov/pubmed/8176234

Maier, A. G., Baum, J., Smith, B., Conway, D. J., & Cowman, A. F. (2009). Polymorphisms in erythrocyte binding antigens 140 and 181 affect function and binding but not receptor specificity in *Plasmodium falciparum*. *Infect Immun, 77*(4), 1689-1699. doi:10.1128/IAI.01331-08

Malpede, B. M., Lin, D. H., & Tolia, N. H. (2013). Molecular basis for sialic acid-dependent receptor recognition by the *Plasmodium falciparum* invasion protein erythrocyte-binding antigen-140/BAEBL. *J Biol Chem, 288*(17), 12406-12415. doi:10.1074/jbc.M113.450643

Mello, K., Daly, T. M., Morrisey, J., Vaidya, A. B., Long, C. A., & Bergman, L. W. (2002). A multigene family that interacts with the amino terminus of *Plasmodium* MSP-1 identified using the yeast two-hybrid system. *Eukaryot Cell, 1*(6), 915-925. Retrieved from http://www.ncbi.nlm.nih.gov/pubmed/12477792

Mensah-Brown, H. E., Amoako, N., Abugri, J., Stewart, L. B., Agongo, G., Dickson, E. K., . . . Awandare, G. A. (2015). Analysis of Erythrocyte Invasion Mechanisms of *Plasmodium falciparum* Clinical Isolates Across 3 Malaria-Endemic Areas in Ghana. *J Infect Dis, 212*(8), 1288-1297. doi:10.1093/infdis/jiv207

Mensah-Brown, H. E., Aspeling-Jones, H., Delimini, R. K., Asante, K. P., Amlabu, E., Bah, S. Y., . . . Awandare, G. A. (2019). Antibody Reactivity to Merozoite Antigens in Ghanaian Adults Correlates With Growth Inhibitory Activity Against *Plasmodium falciparum* in Culture. *Open Forum Infectious Diseases, 6*(7). doi:10.1093/ofid/ofz254

Mercier, C., Adjogble, K. D., Daubener, W., & Delauw, M. F. (2005). Dense granules: are they key organelles to help understand the parasitophorous vacuole of all apicomplexa parasites? *Int J Parasitol, 35*(8), 829-849. doi:10.1016/j.ijpara.2005.03.011

Miao, T., Symonds, A. L. J., Singh, R., Symonds, J. D., Ogbe, A., Omodho, B., . . . Wang, P. (2017). Egr2 and 3 control adaptive immune responses by temporally uncoupling expansion from T cell differentiation. *J Exp Med, 214*(6), 1787-1808. doi:10.1084/jem.20160553

Mohammed, H., Mindaye, T., Belayneh, M., Kassa, M., Assefa, A., Tadesse, M., . . . Kebede, A. (2015). Genetic diversity of *Plasmodium falciparum* isolates based on MSP-1 and MSP-2 genes from Kolla-Shele area, Arbaminch Zuria District, southwest Ethiopia. *Malar J, 14*, 73. doi:10.1186/s12936-015-0604-8

Molina-Cruz, A., Garver, L. S., Alabaster, A., Bangiolo, L., Haile, A., Winikor, J., . . . Barillas-Mury, C. (2013). The human malaria parasite Pfs47 gene mediates evasion of the mosquito immune system. *Science, 340*(6135), 984-987. doi:10.1126/science.1235264

Morahan, B. J., Sallmann, G. B., Huestis, R., Dubljevic, V., & Waller, K. L. (2009). *Plasmodium falciparum*: genetic and immunogenic characterisation of the rhoptry neck protein PfRON4. *Exp Parasitol, 122*(4), 280-288. doi:10.1016/j.exppara.2009.04.013

Mordmuller, B., Szywon, K., Greutelaers, B., Esen, M., Mewono, L., Treut, C., . . . Issifou, S. (2010). Safety and immunogenicity of the malaria vaccine candidate GMZ2 in malaria-exposed, adult individuals from Lambarene, Gabon. *Vaccine, 28*(41), 6698-6703. doi:10.1016/j.vaccine.2010.07.085

Murray, C. J., Rosenfeld, L. C., Lim, S. S., Andrews, K. G., Foreman, K. J., Haring, D., . . . Lopez, A. D. (2012). Global malaria mortality between 1980 and 2010: a systematic analysis. *Lancet, 379*(9814), 413-431. doi:10.1016/S0140-6736(12)60034-8

Mwingira, F., Nkwengulila, G., Schoepflin, S., Sumari, D., Beck, H. P., Snounou, G., . . . Mugittu, K. (2011). *Plasmodium falciparum* msp1, msp2 and glurp allele frequency and diversity in sub-Saharan Africa. *Malar J, 10*, 79. doi:10.1186/1475-2875-10-79

Narum, D. L., & Thomas, A. W. (1994). Differential localization of full-length and processed forms of PF83/AMA-1 an apical membrane antigen of *Plasmodium falciparum* merozoites. *Mol Biochem Parasitol, 67*(1), 59-68. Retrieved from http://www.ncbi.nlm.nih.gov/pubmed/7838184

Neafsey, D. E., Juraska, M., Bedford, T., Benkeser, D., Valim, C., Griggs, A., . . . Wirth, D. F. (2015). Genetic Diversity and Protective Efficacy of the RTS,S/AS01 Malaria Vaccine. *N Engl J Med, 373*(21), 2025-2037. doi:10.1056/NEJMoa1505819

Nery, S., Deans, A.-M., Mosobo, M., Marsh, K., Rowe, J. A., & Conway, D. J. (2006). Expression of *Plasmodium falciparum* genes involved in erythrocyte invasion varies among isolates cultured directly from patients. *Mol Biochem Parasitol, 149*(2), 208-215. doi:10.1016/j.molbiopara.2006.05.014

Niang, M., Bei, A. K., Madnani, K. G., Pelly, S., Dankwa, S., Kanjee, U., . . . Preiser, P. R. (2014). STEVOR is a *Plasmodium falciparum* erythrocyte binding protein that mediates merozoite invasion and rosetting. *Cell Host Microbe, 16*(1), 81-93. doi:10.1016/j.chom.2014.06.004

Okoyeh, J. N., Pillai, C. R., & Chitnis, C. E. (1999). *Plasmodium falciparum* field isolates commonly use erythrocyte invasion pathways that are independent of sialic acid residues of glycophorin A. *Infect Immun, 67*(11), 5784-5791. Retrieved from https://www.ncbi.nlm.nih.gov/pubmed/10531229

Olivieri, A., Collins, C. R., Hackett, F., Withers-Martinez, C., Marshall, J., Flynn, H. R., . . . Blackman, M. J. (2011). Juxtamembrane shedding of *Plasmodium falciparum* AMA1 is sequence independent and essential, and helps evade invasion-inhibitory antibodies. *PLoS pathogens, 7*(12), e1002448. doi:10.1371/journal.ppat.1002448

Osier, F. H., Fegan, G., Polley, S. D., Murungi, L., Verra, F., Tetteh, K. K., . . . Marsh, K. (2008). Breadth and magnitude of antibody responses to multiple *Plasmodium falciparum* merozoite antigens are associated with protection from clinical malaria. *Infect Immun, 76*(5), 2240-2248. doi:10.1128/IAI.01585-07

Osier, F. H., Feng, G., Boyle, M. J., Langer, C., Zhou, J., Richards, J. S., . . . Beeson, J. G. (2014). Opsonic phagocytosis of *Plasmodium falciparum* merozoites: mechanism in human immunity and a correlate of protection against malaria. *BMC Med, 12*, 108. doi:10.1186/1741-7015-12-108

Owusu-Agyei, S., Asante, K. P., Adjuik, M., Adjei, G., Awini, E., Adams, M., . . . Chandramohan, D. (2009). Epidemiology of malaria in the forest-savanna transitional zone of Ghana. *Malar J, 8*, 220. doi:10.1186/1475-2875-8-220

Pachebat, J. A., Kadekoppala, M., Grainger, M., Dluzewski, A. R., Gunaratne, R. S., Scott-Finnigan, T. J., . . . Holder, A. A. (2007). Extensive proteolytic processing of the malaria parasite merozoite surface protein 7 during biosynthesis and parasite release from erythrocytes. *Mol Biochem Parasitol, 151*(1), 59-69. doi:10.1016/j.molbiopara.2006.10.006

Pachebat, J. A., Ling, I. T., Grainger, M., Trucco, C., Howell, S., Fernandez-Reyes, D., . . . Holder, A. A. (2001). The 22 kDa component of the protein complex on the surface of *Plasmodium falciparum* merozoites is derived from a larger precursor, merozoite surface protein 7. *Mol Biochem Parasitol, 117*(1), 83-89. Retrieved from http://www.ncbi.nlm.nih.gov/pubmed/11551634

Partey, F. D., Castberg, F. C., Sarbah, E. W., Silk, S. E., Awandare, G. A., Draper, S. J., . . . Barfod, L. (2018). Correction: Kinetics of antibody responses to PfRH5-complex antigens in Ghanaian children with *Plasmodium falciparum* malaria. *PLoS One, 13*(9), e0204452. doi:10.1371/journal.pone.0204452

Patel, S. D., Ahouidi, A. D., Bei, A. K., Dieye, T. N., Mboup, S., Harrison, S. C., & Duraisingh, M. T. (2013). *Plasmodium falciparum* merozoite surface antigen, PfRH5, elicits detectable levels of invasion-inhibiting antibodies in humans. *J Infect Dis, 208*(10), 1679-1687. doi:10.1093/infdis/jit385

Pathak, V., Colah, R., & Ghosh, K. (2016). Correlation between 'H' blood group antigen and *Plasmodium falciparum* invasion. *Ann Hematol, 95*(7), 1067-1075. doi:10.1007/s00277-016-2663-5

Paul, G., Deshmukh, A., Chourasia, B. K., Kalamuddin, M., Panda, A., Singh, S. K., . . . Malhotra, P. (2018). Protein-protein interaction studies reveal the *Plasmodium falciparum* Merozoite surface protein-1 region involved in complex formation that binds to human erythrocytes. *Biochem J*. doi:10.1042/BCJ20180017

Perrin, A. J., Bartholdson, S. J., & Wright, G. J. (2015). P-selectin is a host receptor for *Plasmodium* MSP7 ligands. *Malar J, 14*, 238. doi:10.1186/s12936-015-0750-z

Persson, K. E., McCallum, F. J., Reiling, L., Lister, N. A., Stubbs, J., Cowman, A. F., . . . Beeson, J. G. (2008). Variation in use of erythrocyte invasion pathways by *Plasmodium falciparum* mediates evasion of human inhibitory antibodies. *J Clin Invest, 118*(1), 342-351. doi:10.1172/JCI32138

Peyerl-Hoffmann, G., Jelinek, T., Kilian, A., Kabagambe, G., Metzger, W. G., & von Sonnenburg, F. (2001). Genetic diversity of *Plasmodium falciparum* and its relationship to parasite density in an area with different malaria endemicities in West Uganda. *Trop Med Int Health, 6*(8), 607-613. Retrieved from https://www.ncbi.nlm.nih.gov/pubmed/11555426

Pinzon, C. G., Curtidor, H., Bermudez, A., Forero, M., Vanegas, M., Rodriguez, J., & Patarroyo, M. E. (2008). Studies of *Plasmodium falciparum* rhoptry-associated membrane antigen (RAMA) protein peptides specifically binding to human RBC. *Vaccine, 26*(6), 853-862. doi:10.1016/j.vaccine.2007.11.086

Prakash, P., Zeeshan, M., Saini, E., Muneer, A., Khurana, S., Kumar Chourasia, B., . . . Malhotra, P. (2017). Human Cyclophilin B forms part of a multi-protein complex during erythrocyte invasion by *Plasmodium falciparum*. *Nat Commun, 8*(1), 1548. doi:10.1038/s41467-017-01638-6

Prinz, B., Harvey, K. L., Wilcke, L., Ruch, U., Engelberg, K., Biller, L., . . . Gilberger, T. W. (2016). Hierarchical phosphorylation of apical membrane antigen 1 is required for efficient red blood cell invasion by malaria parasites. *Sci Rep, 6*, 34479. doi:10.1038/srep34479

Proellocks, N. I., Kats, L. M., Sheffield, D. A., Hanssen, E., Black, C. G., Waller, K. L., & Coppel, R. L. (2009). Characterisation of PfRON6, a *Plasmodium falciparum* rhoptry neck protein with a novel cysteine-rich domain. *Int J Parasitol, 39*(6), 683-692. doi:10.1016/j.ijpara.2008.11.002

Proellocks, N. I., Kovacevic, S., Ferguson, D. J., Kats, L. M., Morahan, B. J., Black, C. G., . . . Coppel, R. L. (2007). *Plasmodium falciparum* Pf34, a novel GPI-anchored rhoptry protein found in detergent-resistant microdomains. *Int J Parasitol, 37*(11), 1233-1241. doi:10.1016/j.ijpara.2007.03.013

Prudencio, M., Mota, M. M., & Mendes, A. M. (2011). A toolbox to study liver stage malaria. *Trends Parasitol, 27*(12), 565-574. doi:10.1016/j.pt.2011.09.004

Puentes, A., Ocampo, M., Rodriguez, L. E., Vera, R., Valbuena, J., Curtidor, H., . . . Patarroyo, M. E. (2005). Identifying *Plasmodium falciparum* merozoite surface protein-10 human erythrocyte specific binding regions. *Biochimie, 87*(5), 461-472. doi:10.1016/j.biochi.2005.01.001

Quah, B. J., & Parish, C. R. (2012). New and improved methods for measuring lymphocyte proliferation in vitro and in vivo using CFSE-like fluorescent dyes. *J Immunol Methods*, *379*(1-2), 1-14. doi:10.1016/j.jim.2012.02.012

Reddy, K. S., Amlabu, E., Pandey, A. K., Mitra, P., Chauhan, V. S., & Gaur, D. (2015). Multiprotein complex between the GPI-anchored CyRPA with PfRH5 and PfRipr is crucial for *Plasmodium falciparum* erythrocyte invasion. *Proc Natl Acad Sci U S A*, *112*(4), 1179-1184. doi:10.1073/pnas.1415466112

Reddy, K. S., Pandey, A. K., Singh, H., Sahar, T., Emmanuel, A., Chitnis, C. E., . . . Gaur, D. (2014). Bacterially expressed full-length recombinant *Plasmodium falciparum* RH5 protein binds erythrocytes and elicits potent strain-transcending parasite-neutralizing antibodies. *Infect Immun*, *82*(1), 152-164. doi:10.1128/IAI.00970-13

Reed, M. B., Caruana, S. R., Batchelor, A. H., Thompson, J. K., Crabb, B. S., & Cowman, A. F. (2000). Targeted disruption of an erythrocyte binding antigen in *Plasmodium falciparum* is associated with a switch toward a sialic acid-independent pathway of invasion. *Proc Natl Acad Sci U S A*, *97*(13), 7509-7514. Retrieved from https://www.ncbi.nlm.nih.gov/pubmed/10861015

Reiling, L., Richards, J. S., Fowkes, F. J., Wilson, D. W., Chokejindachai, W., Barry, A. E., . . . Beeson, J. G. (2012). The *Plasmodium falciparum* erythrocyte invasion ligand Pfrh4 as a target of functional and protective human antibodies against malaria. *PLoS One*, *7*(9), e45253. doi:10.1371/journal.pone.0045253

Reyes, C., Patarroyo, M. E., Vargas, L. E., Rodriguez, L. E., & Patarroyo, M. A. (2007). Functional, structural, and immunological compartmentalisation of malaria invasive proteins. *Biochem Biophys Res Commun, 354*(2), 363-371. doi:10.1016/j.bbrc.2006.12.220

Richard, D., Kats, L. M., Langer, C., Black, C. G., Mitri, K., Boddey, J. A., . . . Coppel, R. L. (2009). Identification of rhoptry trafficking determinants and evidence for a novel sorting mechanism in the malaria parasite *Plasmodium falciparum*. *PLoS Pathog, 5*(3), e1000328. doi:10.1371/journal.ppat.1000328

Richard, D., MacRaild, C. A., Riglar, D. T., Chan, J. A., Foley, M., Baum, J., . . . Cowman, A. F. (2010). Interaction between *Plasmodium falciparum* apical membrane antigen 1 and the rhoptry neck protein complex defines a key step in the erythrocyte invasion process of malaria parasites. *J Biol Chem, 285*(19), 14815-14822. doi:10.1074/jbc.M109.080770

Richards, J. S., Stanisic, D. I., Fowkes, F. J., Tavul, L., Dabod, E., Thompson, J. K., . . . Beeson, J. G. (2010). Association between naturally acquired antibodies to erythrocyte-binding antigens of *Plasmodium falciparum* and protection from malaria and high-density parasitemia. *Clin Infect Dis, 51*(8), e50-60. doi:10.1086/656413

Rodriguez, L. E., Curtidor, H., Urquiza, M., Cifuentes, G., Reyes, C., & Patarroyo, M. E. (2008). Intimate molecular interactions of P. *falciparum* merozoite proteins involved in invasion of red blood cells and their implications for vaccine design. *Chem Rev, 108*(9), 3656-3705. doi:10.1021/cr068407v

Rodriguez, M., Lustigman, S., Montero, E., Oksov, Y., & Lobo, C. A. (2008). PfRH5: a novel reticulocyte-binding family homolog of *Plasmodium falciparum* that binds to the erythrocyte, and an investigation of its receptor. *PLoS One, 3*(10), e3300. doi:10.1371/journal.pone.0003300

Rts, S. C. T. P. (2015). Efficacy and safety of RTS,S/AS01 malaria vaccine with or without a booster dose in infants and children in Africa: final results of a phase 3, individually randomised, controlled trial. *Lancet, 386*(9988), 31-45. doi:10.1016/S0140-6736(15)60721-8

Sam-Yellowe, T. Y., & Perkins, M. E. (1991). Interaction of the 140/130/110 kDa rhoptry protein complex of *Plasmodium falciparum* with the erythrocyte membrane and liposomes. *Exp Parasitol, 73*(2), 161-171. Retrieved from https://www.ncbi.nlm.nih.gov/pubmed/1889471

Sam-Yellowe, T. Y., Shio, H., & Perkins, M. E. (1988). Secretion of *Plasmodium falciparum* rhoptry protein into the plasma membrane of host erythrocytes. *J Cell Biol, 106*(5), 1507-1513. Retrieved from https://www.ncbi.nlm.nih.gov/pubmed/2453514

Schmidt-Christensen, A., Sturm, A., Horstmann, S., & Heussler, V. T. (2008). Expression and processing of *Plasmodium* berghei SERA3 during liver stages. *Cell Microbiol, 10*(8), 1723-1734. doi:10.1111/j.1462-5822.2008.01162.x

Scully, E. J., Kanjee, U., & Duraisingh, M. T. (2017). Molecular interactions governing host-specificity of blood stage malaria parasites. *Curr Opin Microbiol, 40*, 21-31. doi:10.1016/j.mib.2017.10.006

Sherling, E. S., Knuepfer, E., Brzostowski, J. A., Miller, L. H., Blackman, M. J., & van Ooij, C. (2017). The *Plasmodium falciparum* rhoptry protein RhopH3 plays essential roles in host cell invasion and nutrient uptake. *Elife, 6*. doi:10.7554/eLife.23239

Singh, S., Alam, M. M., Pal-Bhowmick, I., Brzostowski, J. A., & Chitnis, C. E. (2010). Distinct external signals trigger sequential release of apical organelles during erythrocyte invasion by malaria parasites. *PLoS Pathog, 6*(2), e1000746. doi:10.1371/journal.ppat.1000746

Singh, S., Plassmeyer, M., Gaur, D., & Miller, L. H. (2007a). Mononeme: a new secretory organelle in *Plasmodium falciparum* merozoites identified by localization of rhomboid-1 protease. *Proceedings of the National Academy of Sciences of the United States of America, 104*(50), 20043-20048. doi:10.1073/pnas.0709999104

Singh, S., Plassmeyer, M., Gaur, D., & Miller, L. H. (2007b). Mononeme: a new secretory organelle in *Plasmodium falciparum* merozoites identified by localization of rhomboid-1 protease. *Proc Natl Acad Sci U S A, 104*(50), 20043-20048. doi:10.1073/pnas.0709999104

Singh, S., Soe, S., Weisman, S., Barnwell, J. W., Perignon, J. L., & Druilhe, P. (2009). A conserved multi-gene family induces cross-reactive antibodies effective in defense against *Plasmodium falciparum*. *PLoS One, 4*(4), e5410. doi:10.1371/journal.pone.0005410

Sinka, M. E., Bangs, M. J., Manguin, S., Coetzee, M., Mbogo, C. M., Hemingway, J., . . . Hay, S. I. (2010). The dominant Anopheles vectors of human malaria in Africa, Europe and the Middle East: occurrence data, distribution maps and bionomic precis. *Parasit Vectors, 3*, 117. doi:10.1186/1756-3305-3-117

Sironi, M., Forni, D., Clerici, M., & Cagliani, R. (2018). Genetic conflicts with *Plasmodium* parasites and functional constraints shape the evolution of erythrocyte cytoskeletal proteins. *Sci Rep, 8*(1), 14682. doi:10.1038/s41598-018-33049-y

Snounou, G., Zhu, X., Siripoon, N., Jarra, W., Thaithong, S., Brown, K. N., & Viriyakosol, S. (1999). Biased distribution of msp1 and msp2 allelic variants in *Plasmodium falciparum* populations in Thailand. *Trans R Soc Trop Med Hyg, 93*(4), 369-374. Retrieved from https://www.ncbi.nlm.nih.gov/pubmed/10674079

Snow, R. W., Guerra, C. A., Noor, A. M., Myint, H. Y., & Hay, S. I. (2005). The global distribution of clinical episodes of *Plasmodium falciparum* malaria. *Nature, 434*(7030), 214-217. doi:10.1038/nature03342

Sondo, P., Derra, K., Lefevre, T., Diallo-Nakanabo, S., Tarnagda, Z., Zampa, O., . . . Tinto, H. (2019). Genetically diverse *Plasmodium falciparum* infections, within-host competition and symptomatic malaria in humans. *Sci Rep, 9*(1), 127. doi:10.1038/s41598-018-36493-y

Spadafora, C., Awandare, G. A., Kopydlowski, K. M., Czege, J., Moch, J. K., Finberg, R. W., . . . Stoute, J. A. (2010). Complement receptor 1 is a sialic acid-independent erythrocyte receptor of *Plasmodium falciparum*. *PLoS Pathog, 6*(6), e1000968. doi:10.1371/journal.ppat.1000968

Srinivasan, P., Baldeviano, G. C., Miura, K., Diouf, A., Ventocilla, J. A., Leiva, K. P., . . . Miller, L. H. (2017). A malaria vaccine protects Aotus monkeys against virulent *Plasmodium falciparum* infection. *NPJ Vaccines, 2*. doi:10.1038/s41541-017-0015-7

Srinivasan, P., Beatty, W. L., Diouf, A., Herrera, R., Ambroggio, X., Moch, J. K., . . . Miller, L. H. (2011). Binding of *Plasmodium* merozoite proteins RON2 and AMA1 triggers commitment to invasion. *Proc Natl Acad Sci U S A, 108*(32), 13275-13280. doi:10.1073/pnas.1110303108

Sterkers, Y., Scheidig, C., da Rocha, M., Lepolard, C., Gysin, J., & Scherf, A. (2007). Members of the low-molecular-mass rhoptry protein complex of *Plasmodium falciparum* bind to the surface of normal erythrocytes. *J Infect Dis, 196*(4), 617-621. doi:10.1086/519685

Straub, K. W., Cheng, S. J., Sohn, C. S., & Bradley, P. J. (2009). Novel components of the Apicomplexan moving junction reveal conserved and coccidia-restricted elements. *Cell Microbiol, 11*(4), 590-603. doi:10.1111/j.1462-5822.2008.01276.x

Stubbs, J., Simpson, K. M., Triglia, T., Plouffe, D., Tonkin, C. J., Duraisingh, M. T., . . . Cowman, A. F. (2005). Molecular mechanism for switching of P. *falciparum* invasion pathways into human erythrocytes. *Science, 309*(5739), 1384-1387. doi:10.1126/science.1115257

Tario, J. D., Jr., Conway, A. N., Muirhead, K. A., & Wallace, P. K. (2018). Monitoring Cell Proliferation by Dye Dilution: Considerations for Probe Selection. *Methods Mol Biol, 1678*, 249-299. doi:10.1007/978-1-4939-7346-0_12

Tham, W. H., Healer, J., & Cowman, A. F. (2012). Erythrocyte and reticulocyte binding-like proteins of *Plasmodium falciparum*. *Trends Parasitol, 28*(1), 23-30. doi:10.1016/j.pt.2011.10.002

Tham, W. H., Lim, N. T., Weiss, G. E., Lopaticki, S., Ansell, B. R., Bird, M., . . . Cowman, A. F. (2015). *Plasmodium falciparum* Adhesins Play an Essential Role in Signalling and Activation of Invasion into Human Erythrocytes. *PLoS Pathog, 11*(12), e1005343. doi:10.1371/journal.ppat.1005343

Tham, W. H., Wilson, D. W., Lopaticki, S., Schmidt, C. Q., Tetteh-Quarcoo, P. B., Barlow, P. N., . . . Cowman, A. F. (2010). Complement receptor 1 is the host erythrocyte receptor for

Plasmodium falciparum PfRh4 invasion ligand. *Proc Natl Acad Sci U S A, 107*(40), 17327-17332. doi:10.1073/pnas.1008151107

Tham, W. H., Wilson, D. W., Reiling, L., Chen, L., Beeson, J. G., & Cowman, A. F. (2009). Antibodies to reticulocyte binding protein-like homologue 4 inhibit invasion of *Plasmodium falciparum* into human erythrocytes. *Infect Immun, 77*(6), 2427-2435. doi:10.1128/IAI.00048-09

Theisen, M., Soe, S., Oeuvray, C., Thomas, A. W., Vuust, J., Danielsen, S., . . . Druilhe, P. (1998). The glutamate-rich protein (GLURP) of *Plasmodium falciparum* is a target for antibody-dependent monocyte-mediated inhibition of parasite growth in vitro. *Infect Immun, 66*(1), 11-17. Retrieved from http://www.ncbi.nlm.nih.gov/pubmed/9423833

Theron, M., Cross, N., Cawkill, P., Bustamante, L. Y., & Rayner, J. C. (2018). An in vitro erythrocyte preference assay reveals that *Plasmodium falciparum* parasites prefer Type O over Type A erythrocytes. *Sci Rep, 8*(1), 8133. doi:10.1038/s41598-018-26559-2

Theron, M., Hesketh, R. L., Subramanian, S., & Rayner, J. C. (2010). An adaptable two-color flow cytometric assay to quantitate the invasion of erythrocytes by *Plasmodium falciparum* parasites. *Cytometry A, 77*(11), 1067-1074. doi:10.1002/cyto.a.20972

Thompson, J. K., Triglia, T., Reed, M. B., & Cowman, A. F. (2001). A novel ligand from *Plasmodium falciparum* that binds to a sialic acid-containing receptor on the surface of human erythrocytes. *Mol Microbiol, 41*(1), 47-58. Retrieved from https://www.ncbi.nlm.nih.gov/pubmed/11454199

Topolska, A. E., Lidgett, A., Truman, D., Fujioka, H., & Coppel, R. L. (2004). Characterization of a membrane-associated rhoptry protein of *Plasmodium falciparum*. *J Biol Chem, 279*(6), 4648-4656. doi:10.1074/jbc.M307859200

Trager, W., Rozario, C., Shio, H., Williams, J., & Perkins, M. E. (1992). Transfer of a dense granule protein of *Plasmodium falciparum* to the membrane of ring stages and isolation of dense granules. *Infection and immunity, 60*(11), 4656-4661. Retrieved from http://www.ncbi.nlm.nih.gov/pubmed/1398979

Tran, T. M., Ongoiba, A., Coursen, J., Crosnier, C., Diouf, A., Huang, C. Y., . . . Crompton, P. D. (2014). Naturally acquired antibodies specific for *Plasmodium falciparum* reticulocyte-binding protein homologue 5 inhibit parasite growth and predict protection from malaria. *J Infect Dis, 209*(5), 789-798. doi:10.1093/infdis/jit553

Vimonpatranon, S., Chotivanich, K., Sukapirom, K., Lertjuthaporn, S., Khowawisetsut, L., & Pattanapanyasat, K. (2019). Enumeration of the Invasion Efficiency of *Plasmodium falciparum* In Vitro in Four Different Red Blood Cell Populations Using a Three-Color Flow Cytometry-Based Method. *Cytometry A*. doi:10.1002/cyto.a.23750

Wallace, P. K., Tario, J. D., Jr., Fisher, J. L., Wallace, S. S., Ernstoff, M. S., & Muirhead, K. A. (2008). Tracking antigen-driven responses by flow cytometry: monitoring proliferation by dye dilution. *Cytometry A, 73*(11), 1019-1034. doi:10.1002/cyto.a.20619

WAMIN. (2016). Malaria Vaccine Development: Focusing Field Erythrocyte Invasion Studies on Phenotypic Diversity: The West African Merozoite Invasion Network (WAMIN). *Trends Parasitol, 32*(4), 274-283. doi:10.1016/j.pt.2015.11.009

Wang, G., Drinkwater, N., Drew, D. R., MacRaild, C. A., Chalmers, D. K., Mohanty, B., . . . Scanlon, M. J. (2016). Structure-Activity Studies of beta-Hairpin Peptide Inhibitors of the *Plasmodium falciparum* AMA1-RON2 Interaction. *J Mol Biol*. doi:10.1016/j.jmb.2016.07.001

WHO. (2015). *World Malaria Report*. Retrieved from Geneva, Switzerland:

WHO. (2017). *World Malaria Report*. Retrieved from Geneva, Switzerland:

WHO. (2018a). *Update on the E-20 Initiative of 21 Malaria-Eliminating Countries*. Retrieved from Geneva, Switzerland: http://apps.who.int/iris/bitstream/handle/10665/272724/WHO-CDS-GMP-2018.10-eng.pdf?ua=1

WHO. (2018b). *World Malaria Report.* Retrieved from Geneva, Switzerland:

Wickramarachchi, T., Devi, Y. S., Mohmmed, A., & Chauhan, V. S. (2008). Identification and characterization of a novel *Plasmodium falciparum* merozoite apical protein involved in erythrocyte binding and invasion. *PLoS One*, *3*(3), e1732. doi:10.1371/journal.pone.0001732

Williams, T. N. (2006). Red blood cell defects and malaria. *Mol Biochem Parasitol*, *149*(2), 121-127. doi:10.1016/j.molbiopara.2006.05.007

Wright, G. J., & Rayner, J. C. (2014). *Plasmodium falciparum* erythrocyte invasion: combining function with immune evasion. *PLoS Pathog*, *10*(3), e1003943. doi:10.1371/journal.ppat.1003943

Wu, T., Black, C. G., Wang, L., Hibbs, A. R., & Coppel, R. L. (1999). Lack of sequence diversity in the gene encoding merozoite surface protein 5 of *Plasmodium falciparum*. *Mol*

Biochem Parasitol, 103(2), 243-250. Retrieved from http://www.ncbi.nlm.nih.gov/pubmed/10551366

Yang Y, H. L. T., Neu B. (2009). The impact of enzymatic treatment on red blood cell adhesion to the endothelium in plasma like suspensions. In I. Proceedings (Ed.), *13th International Conference on Biomedical Engineering* (Vol. 23): Springer, Berlin, Heidelberg.

Yap, X. Z., Lundie, R. J., Feng, G., Pooley, J., Beeson, J. G., & O'Keeffe, M. (2019). Different Life Cycle Stages of *Plasmodium falciparum* Induce Contrasting Responses in Dendritic Cells. *Front Immunol, 10*, 32. doi:10.3389/fimmu.2019.00032

Ye, L., Zhao, F., Yang, Q., Zhang, J., Li, Q., Wang, C., . . . Zhu, Z. (2018). OK/basigin expression on red blood cells varies between blood donors and correlates with binding of recombinant *Plasmodium falciparum* reticulocyte-binding protein homolog 5. *Transfusion, 58*(8), 2046-2053. doi:10.1111/trf.14635

Yeoh, S., O'Donnell, R. A., Koussis, K., Dluzewski, A. R., Ansell, K. H., Osborne, S. A., . . . Blackman, M. J. (2007). Subcellular discharge of a serine protease mediates release of invasive malaria parasites from host erythrocytes. *Cell, 131*(6), 1072-1083. doi:10.1016/j.cell.2007.10.049

Zhang, M. Y., Zhang, Y., Wu, X. D., Zhang, K., Lin, P., Bian, H. J., . . . Chen, Z. N. (2018). Disrupting CD147-RAP2 interaction abrogates erythrocyte invasion by *Plasmodium falciparum*. *Blood, 131*(10), 1111-1121. doi:10.1182/blood-2017-08-802918

Zhou, W., Kang, H. C., O'Grady, O., Chambers, K. M., Dubbels, B., Melquist, P., & Gee, K. R. (2016). CellTrace™ Far Red & CellTracker™ Deep Red—long term live cell tracking for

flow cytometry and fluorescence microscopy. *Journal of Biological Methods* | *e36, Vol. 3*(1), 7. doi:10.14440/jbm.2016.113

APPENDIXES

List of supplementary figures

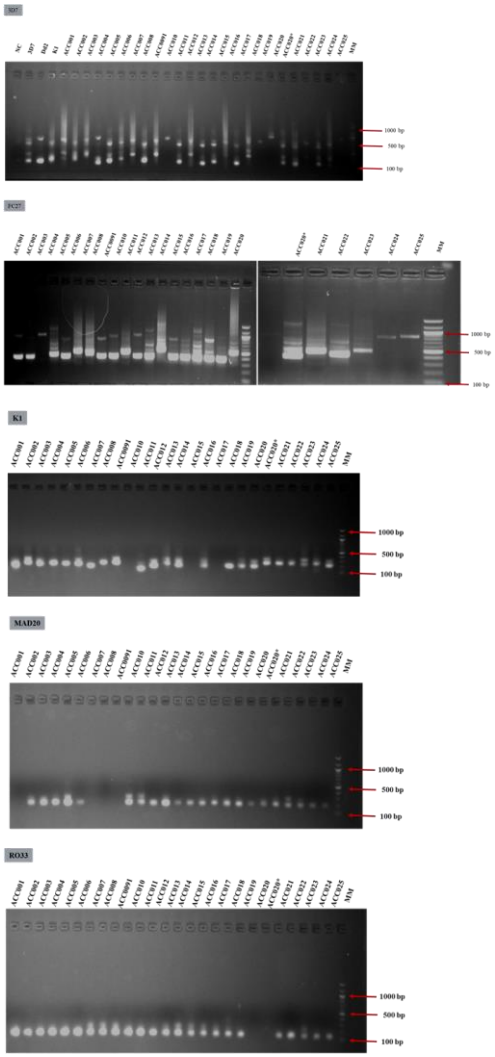

Figure 3.A1: Genotyping of freshly collected *P. falciparum* clinical (Day 0) used the assessment of the effect of freeze-thaw protocols in *P. falciparum* invasion phenotyping assays. Parasites were genotyped using the highly polymorphic genes *msp1* and *2. P. falciparum* laboratory strains (3D7, Dd2 and K1) were used as controls. PCR products were run on a 2% Ethidium bromide agarose gel and visualized by UV trans-illumination.

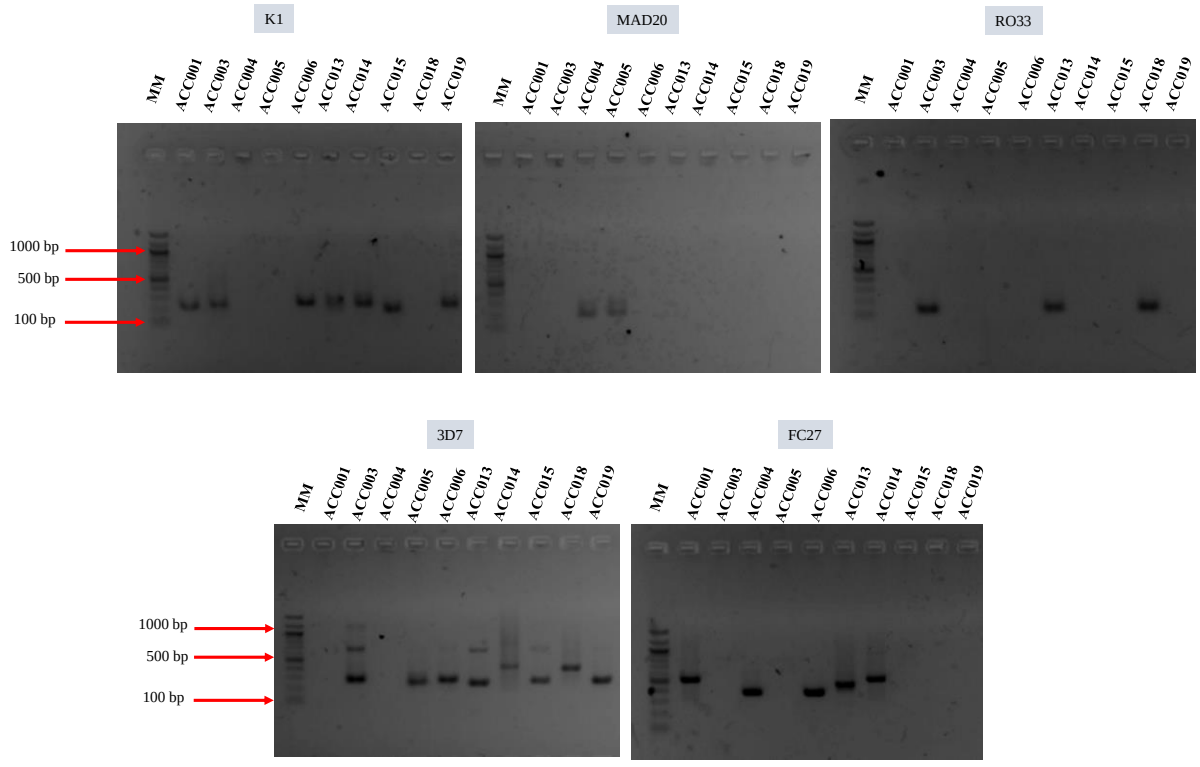

Figure 3.A2: Genotyping of short-term culture adapted collected *P. falciparum* clinical (Day 28) used the assessment of the effect of freeze-thaw protocols in *P. falciparum* invasion phenotyping assays. Parasites were genotyped using the highly polymorphic genes *msp1* and *2*.. PCR products were run on a 2% Ethidium bromide agarose gel and visualized by UV trans-illumination.

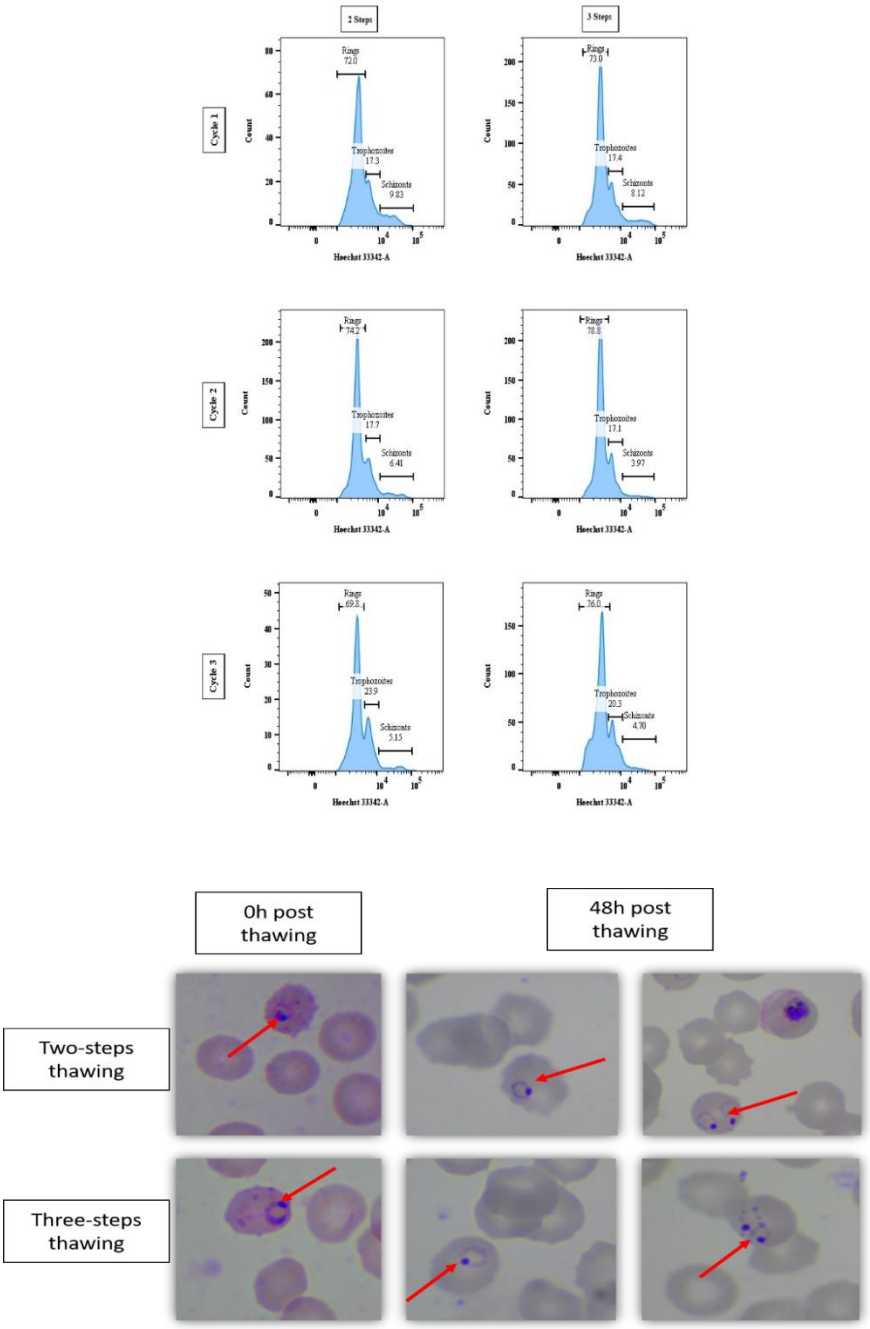

Figure 3.A3: *P. falciparum in vitro* multiplication following cryopreservation. Revived *P. falciparum* clinical isolates were allowed to grow in complete parasite media and monitored for growth during their three first *in vitro* cycles. Parasites' DNA content (top panel) and morphologies (bottom panel) were monitored by flow cytometry and microscopy, respectively.

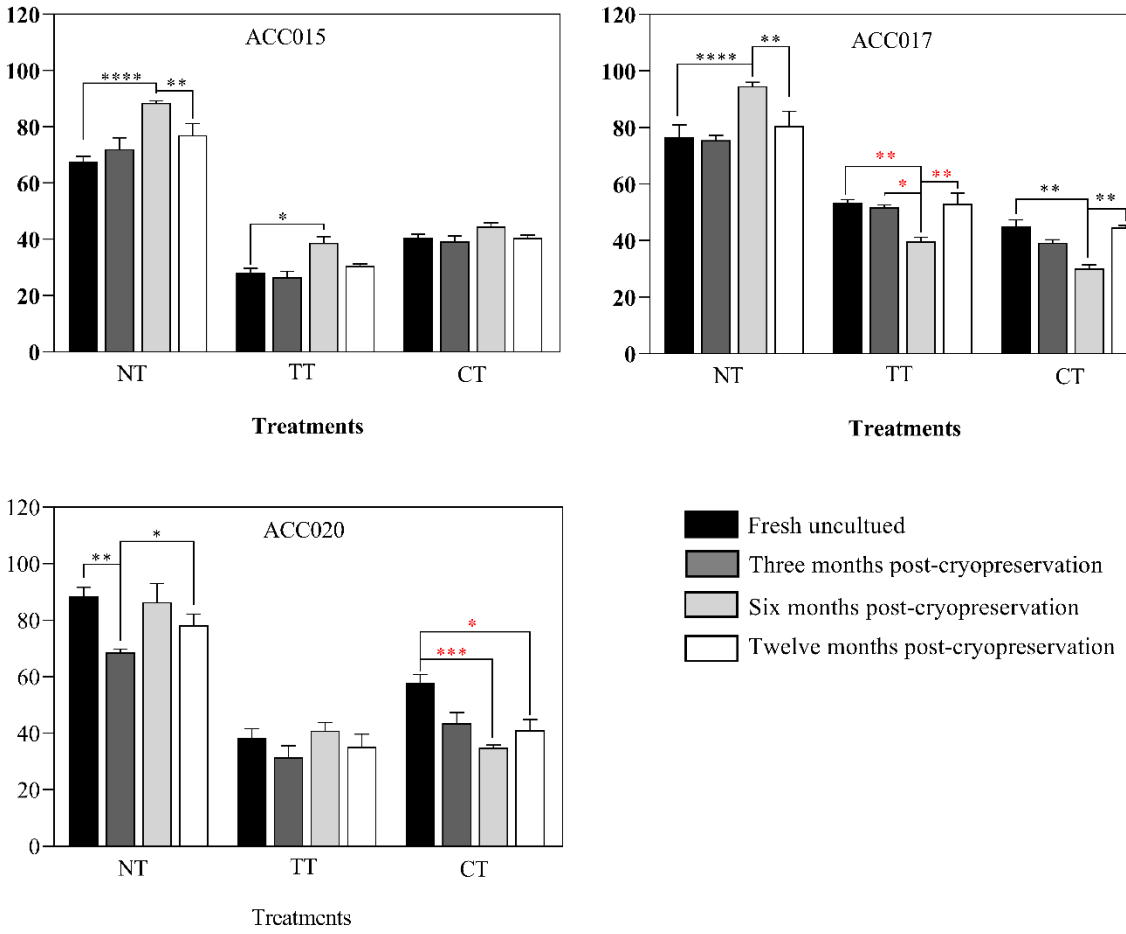

Figure 3.A4**:** Invasion phenotypes of *P. falciparum* clinical isolates before and after short-term cryopreservation. The assays were set up between 24- and 36-hours following sample processing and the parasites were incubated for another 18 to 24 hours prior to flow cytometry analysis. For each isolate, the invasion phenotype of freshly culture adapted parasites (black bars) was compared to that obtained after three months (dark grey bars), six months (light grey bars) and twelve months (white bars) post cryopreservation. Kruskal Wallis was conducted to test for statistical differences in invasion efficiency of fresh versus cryopreserved isolates. Red stars denote significant differences associated with changes in invasion profile of a given treatment and black stars depict significant differences with no changes in the invasion profile.

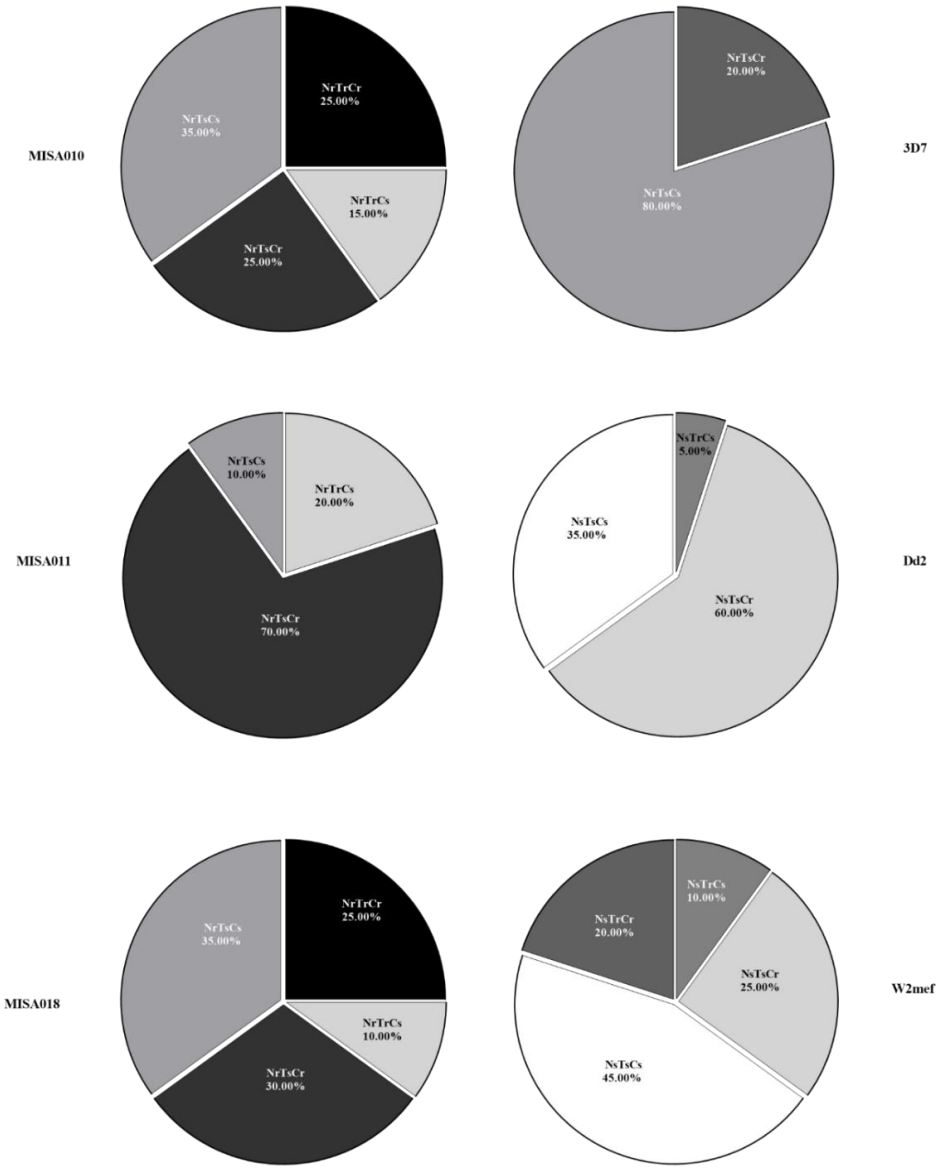

Figure 3.A5: *P. falciparum* invasion profile varies between donors. The graph shows the frequency of a given profile with regards to the different donors. For each donor erythrocyte, the parasites' invasion profile was determined as the combination of sensitivity to the three enzymes using a cut-off of 50% as a threshold to classify the observed profile as sensitive (≤50%) or resistance (>50%) for each given treatment.

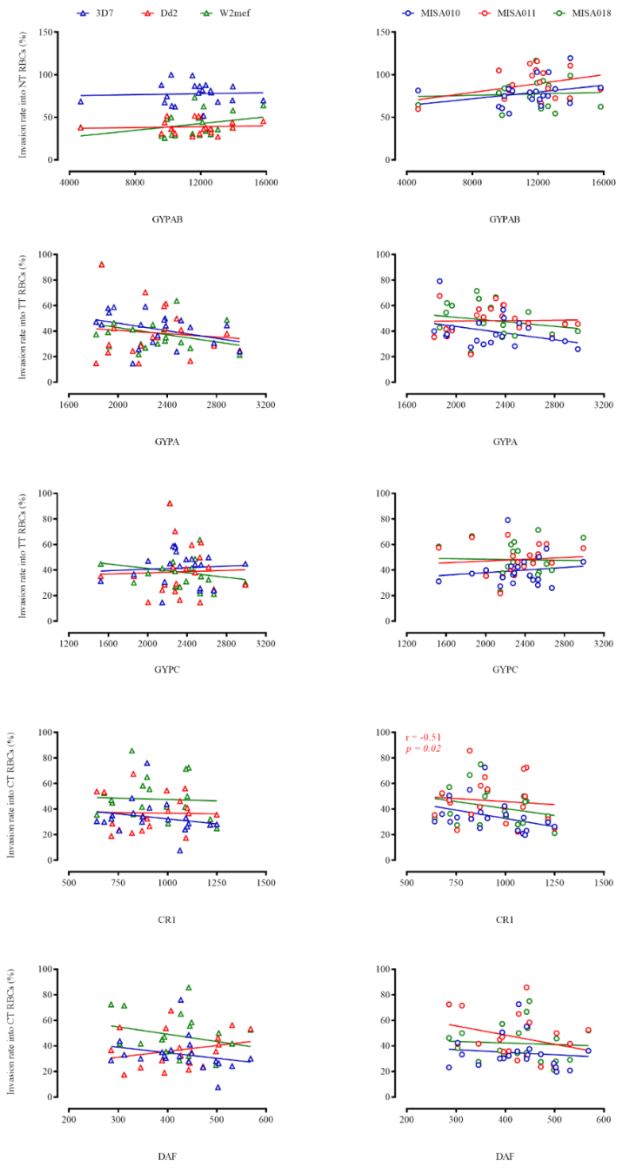

Figure 3.A6: Correlation of receptor density with invasion efficiency into enzyme-treated erythrocyte. The Spearman correlation test was used to assess the relationship between the density of individual erythrocyte surface receptors (X-axis) and the invasion efficiency following enzyme treatment of the same erythrocyte (Y-axis). The data were acquired as MFI for the receptor density and per cent parasitemia relative to untreated control erythrocyte for the invasion efficiency and the graphs were plotted using GraphPad Prism v.7.01.

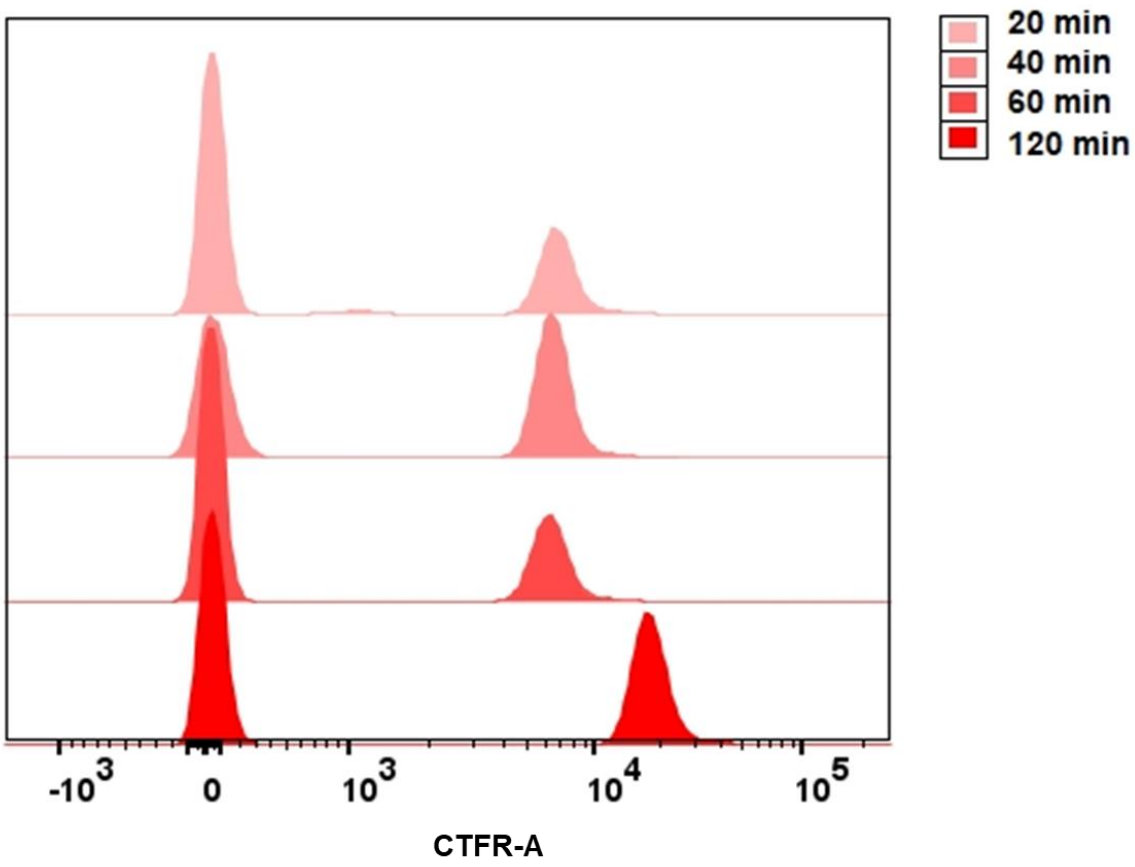

Figure 3.A7: Estimation of the minimal incubation time to stain target RBCs with CT Far Red. Freshly washed RBCs were separetely incubated with the same concentration of CT Far Red and collected at different time points ranging from 20 to 120 minutes. To monitor the level of fluorescent intensity, stained RBCs were co-incubated with mock-stained RBCs (incubated in DMSO-containing solution) and analyzed by flow cytometry.

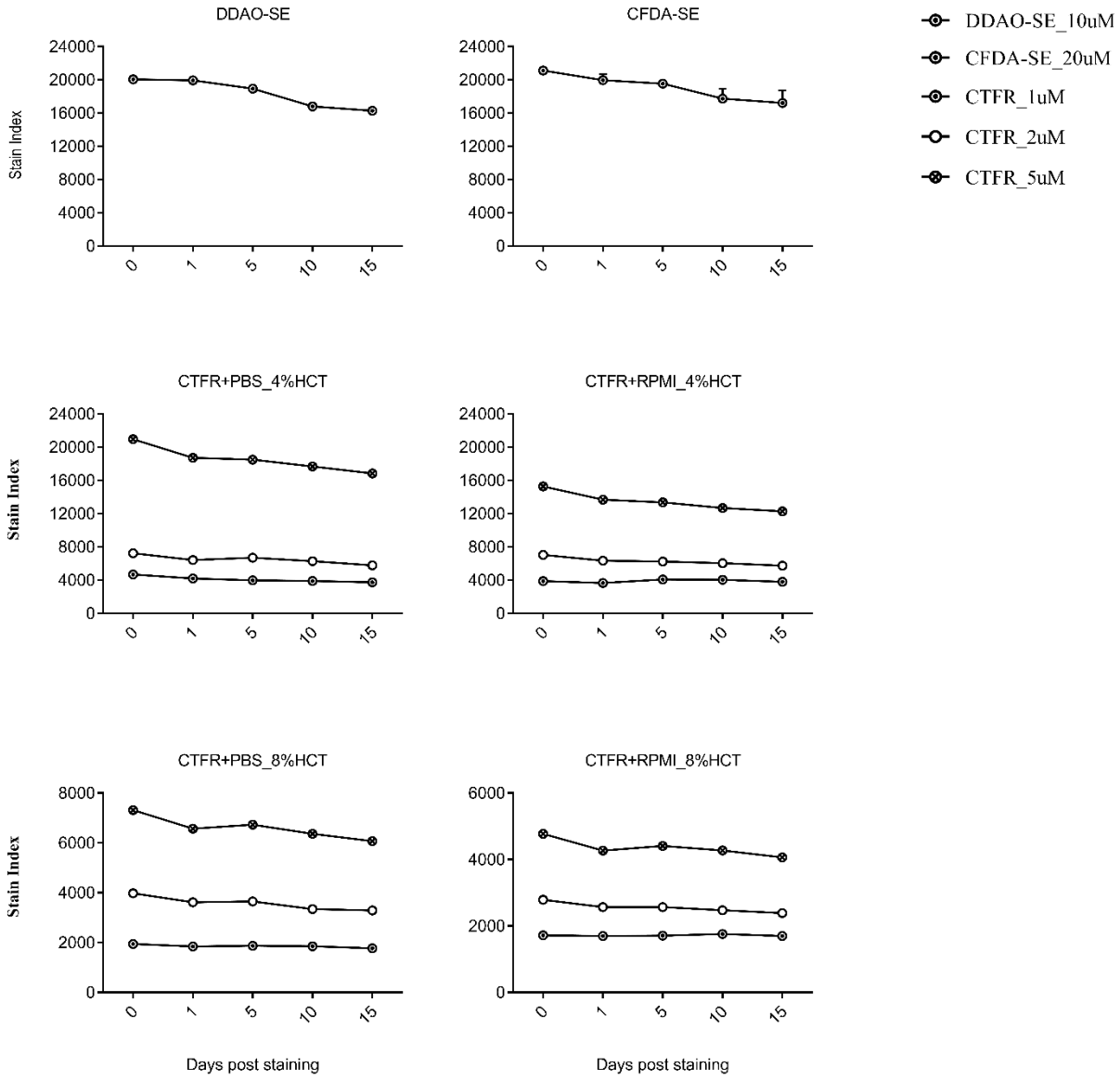

Figure 3.A8: Graphs showing the stability of CTFR stain index following RBC labelling.

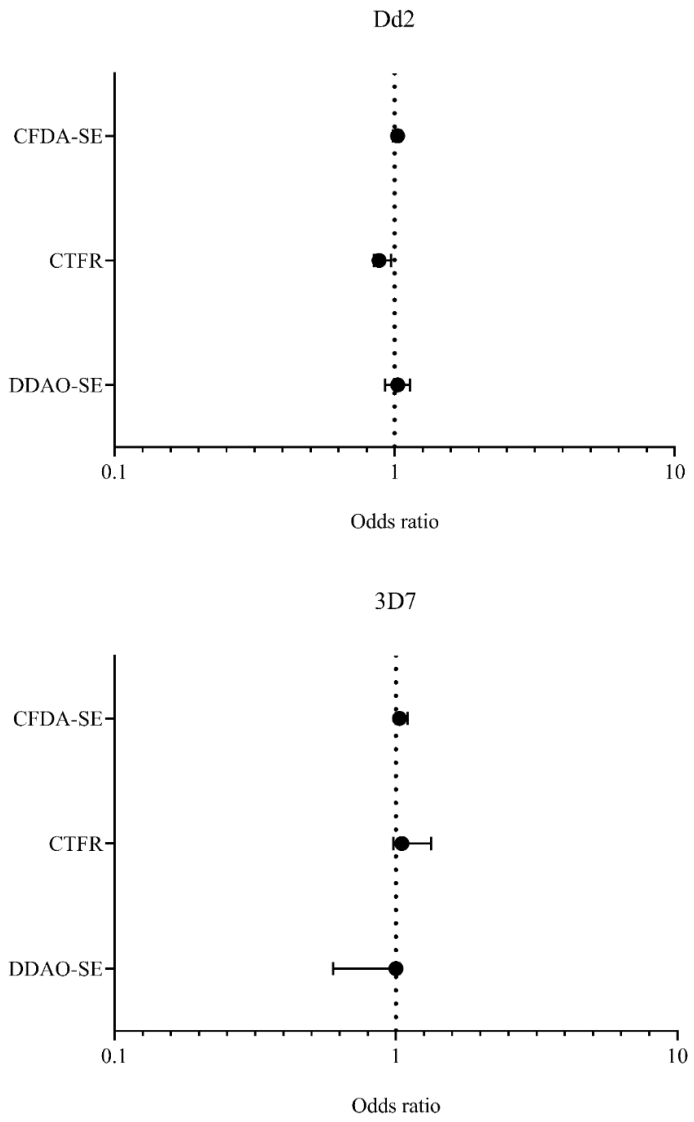

Figure 3.A9: Effect of erythrocyte labelling on *P. falciparum* invasion efficiency. Schizont-infected erythrocyte from (A) 3D7 and (B) Dd2 parasite cultures were incubated with unlabelled or CFDA-SE (20 µM), DDAO-SE (10 µM) or CTFR (2 µM) labelled erythrocytes, stained with Hoechst 33342 upon reinvasion and parasitemia quantified by flow cytometry. The ratio of labelled invaded/unlabelled invaded was calculated. A ratio greater than 1.0 represents an increased invasion rate into labelled erythrocytes, while a ratio smaller than 1.0 indicates a decreased invasion rate into labelled erythrocytes.

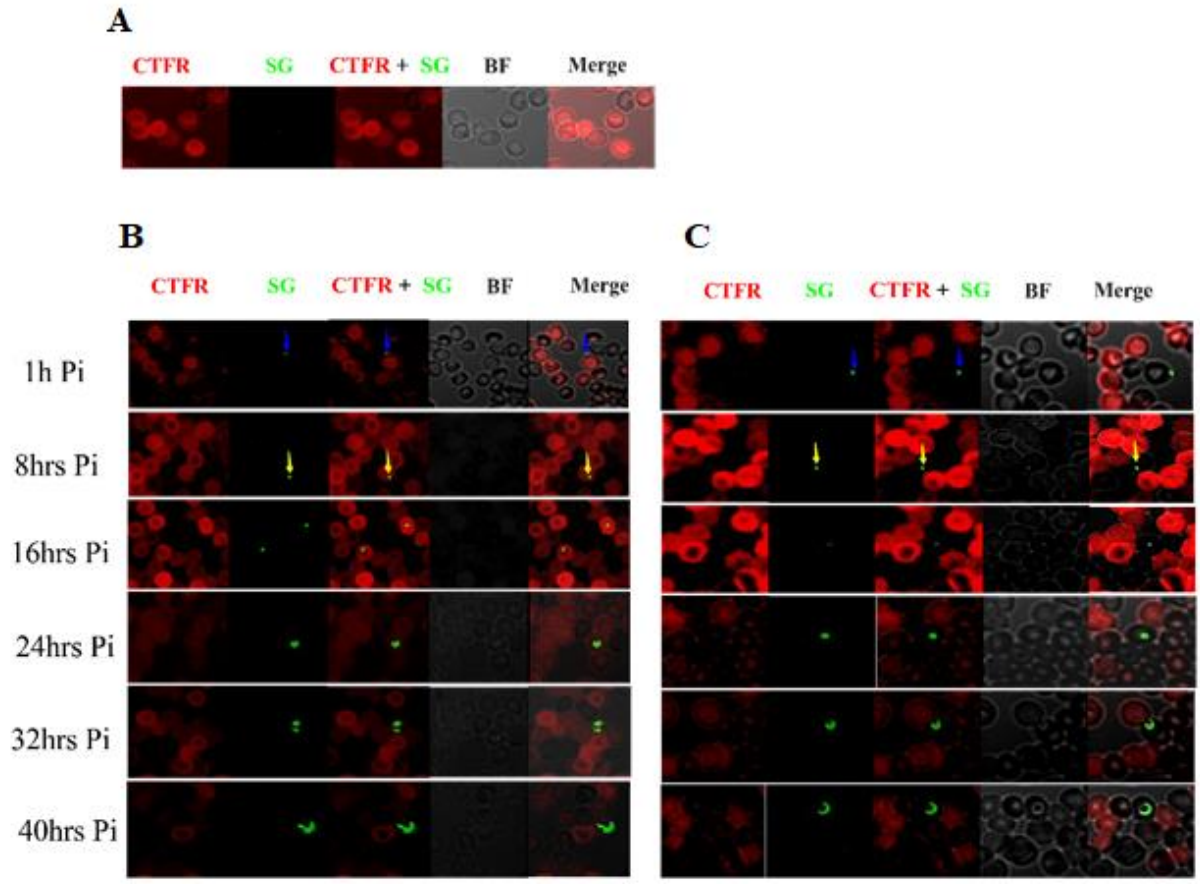

Figure 3.A10: CTFR does not impair *P. falciparum* intra-erythrocytic development. Culture aliquots, harvested at regular time intervals were fixed with 4% paraformaldehyde, stained with SYBR Green I and smeared on glass microscope slides. Images were taken with a laser scanning confocal microscope. Mixed erythrocyte populations (CTFR-labelled and unlabelled) used in this assay are shown (A). In addition, panels showing parasites developing at selected time-points within CTFR-labelled (B) and unlabelled (C) erythrocytes are shown. Blue arrows indicate invading merozoites onto erythrocytes and yellow arrows indicate parasites developing within erythrocytes. CTFR, Cell Trace Far-Red; SG, SYBR Green I; BF, Bright Field.

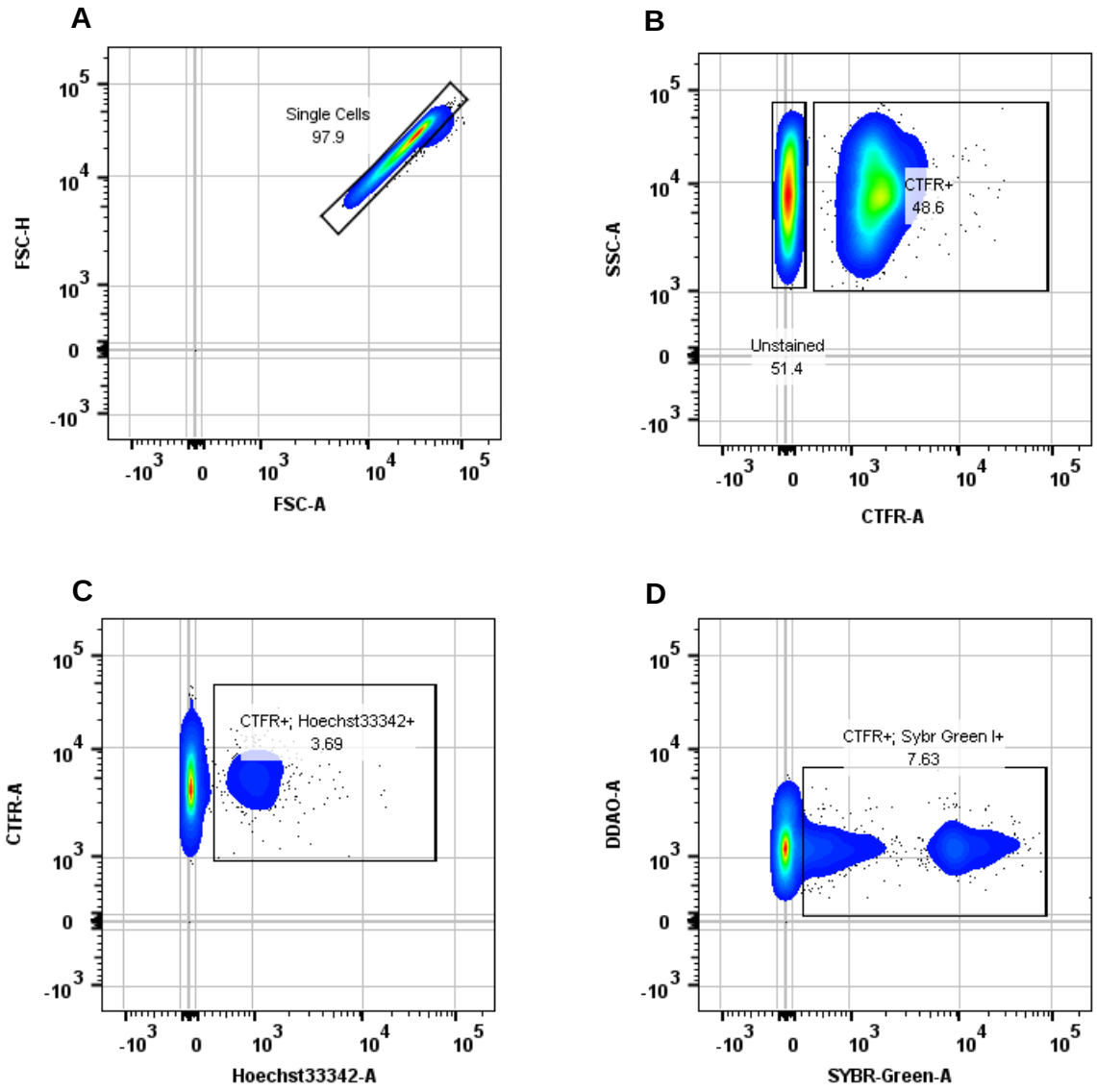

Figure 3.A11: Gating strategy of invasion phenotyping data generated by CTFR staining. (A): Pseudocolor showing single erythrocytes plot gated throughplot gated through the forward scatter hight (FSC-H) by the FSC-A. (B): Pseudocolor plot showing labelled and unlabelled eruthrocytes gated through the SSC-A by the Fluoresecnt intensity of CTFR. (C-D) Pseudocolor plots of CTFR-labelled infected erythrocytes detected by Hoechst 33342 and Sybr Green I staining, respectively.

List of supplementary tables

Table 3.A1: List of primers for *P. falciparum* genotyping

	Sequences
Gene-specific primers	
MSP1-F	5'-CTAGAAGCTTTAGAAGATGCAGTATTG-3'
MSP1-R	5'-CTTAAATAGTATTCTAATTCAAGTGGATCA-3
MSP2-F	5'-ATGAAGGTAATTAAAACATTGTCTATTATA-3'
MSP2-R	5'-CTTTGTTACCATCGGTACATTCTT-3
Allele-specific primers	
K1-F	5'-AAATGAAGAAGAAATTACTACAAAAGGTGC-3
K1-R	5'-GCTTGCATCAGCTGGAGGGCTTGCACCAGA-3'
Mad20-F	5'-AAATGAAGGAACAAGTGGAACAGCTGTTAC-3
Mad20-R	5'-ATCTGAAGGATTTGTACGTCTTGAATTACC-3
RO33-F	5'-TAAAGGATGGAGCAAATACTCAAGTTGTTG-3
RO33-F	5'-CAAGTAATTTTGAACTCTATGTTTTAAATCAGCGTA-3
FC27-F	5'-GCAAATGAAGGTTCTAATACTAATAG-3
FC27-R	5'-GCATTGCCAGAACTTGAA-3
3D7/IC-F	5'-GCAGAAAGTAAGCCTTCTACTGGTGCT-3
3D7/IC-R	5'- CTGAAGAGGTACTGGTAG-3

Table 3.A2: In vitro adaptation of *falciparum* clinical isolates

Sample Code	N/12	Median PMR ± SD	In vitro phenotyping*
ACC01	11	1.51±0.27	YES
ACC03	10	1.75 ± 0.76	YES
ACC04	9	1.83±0.19	YES
ACC05	11	1.8 ± 0.32	YES
ACC06	8	2.43 ± 0.11	YES
ACC07	10	1.92 ± 0.42	YES
ACC13	8	1.57 ± 0.73	YES
ACC14	12	1.5 ± 0.95	YES
ACC15	8	1.13 ± 0.3	YES
ACC19	8	1.95 ± 0.18	YES
ACC20	9	2.14 ± 0.3	YES
ACC25	12	1.63 ± 0.21	YES

* Refers to invasion assays set up prior to cryopreservation

The parasite multiplication rates (PMR) were assessed for a period of 24 days following culture adaptation during the first 96 hours in the laboratory (see Figure 1). Culture flasks were supplemented with fresh erythrocyte at each round of parasite multiplication (48h) and the parasitemia was assessed by flow cytometry. The PMR was considered as the fold change in parasitemia between two successive cycles and the median PMR was calculated with regards to the number of cycles.

Table 3.A3-7: Summary of invasion profiles of *P. falciparum* isolates into enzyme-treated erythrocyte from different donors.

Data represent mean values ± the standard deviation from two independent experiments conducted in triplicates. A cut-off of 50% was taken as a threshold to classify the observed profile as sensitive (≤50%) or resistance (>50%) for each given treatment.

Table 3.A3: MISA010

			% invasion relative to untreated control		
Donor Erythrocyte	**Gender**	**Invasion profile**	**Neuraminidase (250 mU/ml)**	**Trypsin (1mg/ml)**	**Chymotrypsin (1mg/ml)**
O+/AA	F	NrTsCr	103.1 ± 16.3	41.7 ± 4.1	60.4 ± 17.0
B+/AA	M	NrTsCr	75.0 ± 8.1	25.0 ± 7.0	61.3 ± 11.2
B+AS	M	NrTsCs	119.6 ± 22.4	28.6 ± 4.2	42.9 ± 8.6
O+AS	M	NrTsCs	62.5 ± 6.1	35.4 ± 15.6	35.4 ± 18.9
O+AA	M	NrTsCr	75.7 ± 23.3	23.6 ± 4.3	51.7 ± 19.5
A+/AA	F	NrTrCr	71.43 ± 18.31	85.71 ± 1,23	57.14 ± 17.73
O-/AA	M	NrTsCs	75.22 ± 9.87	44.95 ± 1.47	45.45 ± 12.55
A+/AA	M	NrTrCs	66.66 ± 17.36	55.55 ± 4.78	46.29 ± 4,78
O+/AA	M	NrTrCr	80.55 ± 13.58	58.33 ± 29.48	65.74 ± 14.3
A+/AS	M	NrTrCr	81.31 ± 5.62	52.52 ± 16.52	57.57 ± 16.26
O+/AA	M	NrTrCr	81.62 ± 5,87	72.46 ± 14.54	51.0 ± 5.85
O+/AA	M	NrTrCs	75.12 ± 2.17	71.52 ± 13.18	40.59 ± 7.25
B+/AA	M	NrTsCr	54.35 ± 4.24	47.06 ± 8.5	67.64 ± 7.15
B+/AS	F	NrTsCs	60.71 ± 0.92	25 ±13.04	41.67 ± 16.34
O+/AA	M	NrTsCs	71.23 ± 21.05	32 ± 15.31	36 ± 7.37
A+/AC	M	NrTsCr	83.33 ± 11.72	41.67 ± 13.44	50.42 ± 13.1
A+/AA	M	NrTrCr	83.33 ± 14.91	50.34 ± 19.72	52.5 ± 5.1
O+/AA	F	NrTrCs	85.36 ± 16.71	65.13 ± 12.19	45.65 ± 5.59
O+/AC	M	NrTsCs	79.48 ± 11.14	35.90 ± 14.56	21.88 ± 9.97
O+/AA	M	NrTsCs	63.49 ± 15.69	22.22 ± 0.65	34.75 ± 7.70

Table 3.A4: MISA018

		% invasion relative to untreated control			
Donor Erythrocyte	**Gender**	**Invasion profile**	**Neuraminidase (250 mU/ml)**	**Trypsin (1mg/ml)**	**Chymotrypsin (1mg/ml)**
O+/AA	F	NrTsCr	90.48 ± 7.84	38.28 ± 5.14	44.8 ± 5.13
B+/AA	M	NrTsCr	87.47 ± 11.81	27.58 ± 12.07	38.24 ± 12.42
B+AS	M	NrTsCs	99.08 ± 6.46	34.31 ± 14.28	43.72 ± 11.36
O+AS	M	NrTsCs	78.91 ± 4.89	33.15 ± 13.31	35.51 ± 6.58
O+AA	M	NrTsCr	92.89 ± 4.59	27.46 ± 6.22	35,45 ± 5.68
A+/AA	F	NrTrCr	75.59 ± 4.59	66.67 ± 7.07	65.38 ± 16.79
O-/AA	M	NrTsCs	63.09 ± 11.75	36.36 ± 8.76	45.80 ± 9.87
A+/AA	M	NrTrCr	71.21 ± 18.51	53.98 ± 16.55	55.21 ± 9.61
O+/AA	M	NrTrCr	116.98 ± 24.10	75.26 ± 30.78	66.67 ± 9,24
A+/AS	M	NrTrCr	81.34 ± 25.29	52.76 ± 26.97	58.5 ± 13.99
O+/AA	M	NrTsCs	64.61 ± 7.60	46.15 ± 2.65	43.25 ± 10.92
O+/AA	M	NrTrCr	84.31 ± 14.20	50.15 ± 15.49	60.74 ± 8.94
B+/AA	M	NrTrCs	85.71 ± 12.65	57.14 ± 4.92	42.86 ± 5,53
B+/AS	F	NrTsCr	52.57 ± 10.63	21.2 ± 2.99	54.55 ± 12.96
O+/AA	M	NrTsCr	68.36 ± 27.85	34.48 ± 8,51	62.07 ± 16.79
A+/AC	M	NrTsCs	54.54 ± 5,63	20.09 ± 4,30	36.36 ± 14.76
A+/AA	M	NrTsCr	85.71 ± 2.95	45.71 ± 6.76	71.42 ± 17.21
O+/AA	F	NrTrCs	62.50 ± 15.86	50.36 ± 16.45	40.93 ± 23.05
O+/AC	M	NrTsCs	73.85 ± 10.27	32.31 ± 11.19	23.08 ± 7.96
O+/AA	M	NrTsCs	60.29 ± 5.31	27.94 ± 9.33	37.65 ± 10.11

Table 3.A5: 3D7

			% invasion relative to untreated control		
Donor Erythrocyte	**Gender**	**Invasion profile**	**Neuraminidase (250 mU/ml)**	**Trypsin (1mg/ml)**	**Chymotrypsin (1mg/ml)**
O+/AA	F	NrTsCs	86.54 ± 9.82	43.76 ± 11.41	49.9 ± 7.22
B+/AA	M	NrTsCs	79.24 ± 16.54	30.05 ± 9.74	44.26 ± 4.43
B+AS	M	NrTsCs	86.36 ± 11.64	31.76 ± 8.91	48.37 ±7.05
O+AS	M	NrTsCs	88.02 ± 15.45	30.57 ± 2.00	47.19 ± 4.61
O+AA	M	NrTsCs	88.07 ± 14.44	23.25 ± 11.51	48.70 ± 7.05
A+/AA	F	NrTsCs	86.93 ± 8.26	48.52 ± 7.97	45 ± 8.21
O-/AA	M	NrTsCs	81.39 ± 8.92	35 ± 8.21	44.44 ± 6.34
A+/AA	M	NrTsCs	69.98 ± 6.48	40.98 ± 5.75	43.06 ± 3.06
O+/AA	M	NrTsCs	78.67 ± 6.69	34.17 ± 6.44	36.61 ± 7.87
A+/AS	M	NrTsCs	62.36 ± 9.78	30.00 ± 6.27	31.37 ± 5.95
O+/AA	M	NrTsCr	68.61 ± 8.55	28.72 ± 9.3	59.18 ± 7.89
O+/AA	M	NrTsCr	74.68 ± 9.55	33.03 ± 6.81	58.81 ± 6.34
B+/AA	M	NrTsCs	63.43 ± 43	32.37 ± 6.19	45.09 ± 8.43
B+/AS	F	NrTsCr	67.57 ± 10.84	28.14 ± 21.94	57.95 ± 18.05
O+/AA	M	NrTsCr	82.13 ± 11.59	27.8 ± 9.09	54.52 ± 13.83
A+/AC	M	NrTsCs	68.17 ± 3.87	24.18 ± 2.97	24.01 ± 2.04
A+/AA	M	NrTsCs	100 ± 6.70	26.31 ± 0.39	25.66 ± 4.72
O+/AA	F	NrTsCs	69.89 ± 10.98	76 ± 15.4	24.1 ± 1.04
O+/AC	M	NrTsCs	99.23 ± 3.79	36.71 ± 4.09	14.68 ± 7.78
O+/AA	M	NrTsCs	51.87 ± 14.31	7.67 ± 3.21	30.70 ±2.69

Table 3.A6: Dd2

			% invasion relative to untreated control		
Donor Erythrocyte	**Gender**	**Invasion profile**	**Neuraminidase (250 mU/ml)**	**Trypsin (1mg/ml)**	**Chymotrypsin (1mg/ml)**
O+/AA	F	NsTsCs	30.94 ± 4.34	32.25 ± 1.85	37.87 ± 4.47
B+/AA	M	NsTsCr	31.03 ± 3.08	37.93 ± 16.82	51.72 ± 2.05
B+AS	M	NsTsCr	36.71 ± 13.75	44.05 ± 5.69	51.39 ± 2.05
O+AS	M	NsTsCr	31.03 ± 3.08	37.93 ± 6.04	51.72 ± 2.05
O+AA	M	NsTsCr	36.71 ± 5.76	44.05 ± 5.69	51.4 ± 6.69
A+/AA	F	NsTsCs	23.08 ± 6.89	30.77 ± 6.95	38.46 ± 7.94
O-/AA	M	NsTsCr	27.27 ± 11,56	36.06 ± 8.21	54.26 ± 4.69
A+/AA	M	NsTsCr	23.07 ± 13.24	38.46 ± 7.94	53.85 ± 7.94
O+/AA	M	NsTsCs	23.80 ± 3.25	21.42 ± 5.61	28.57 ± 7.38
A+/AS	M	NsTsCr	26.67 ± 8.27	35.53 ± 6.49	53.33 ± 5.96
O+/AA	M	NsTsCs	36.65 ± 2.82	17.79 ± 10.54	18.43 ± 5.31
O+/AA	M	NsTsCr	35.57 ± 1.50	28.07 ± 3.51	56.14 ± 13.54
B+/AA	M	NsTsCr	41.03 ± 4.13	32.5 ± 3.09	67.5 ± 18.43
B+/AS	F	NsTsCr	46.15 ± 2.16	42.31 ± 15,75	61.54 ± 10.14
O+/AA	M	NsTsCr	41.03 ± 5.05	14.80 ± 6.39	59.59 ±10.87
A+/AC	M	NsTsCs	28.57 ± 2.83	38.09 ± 12.13	16.67 ± 2.56
A+/AA	M	NsTsCr	35.18 ± 11.04	35.12 ± 12.59	70.37 ± 13.18
O+/AA	F	NsTrCs	42.10 ± 4.24	92.10 ± 4.08	23.39 ± 3.51
O+/AC	M	NsTsCs	29.30 ± 4.96	49.82 ± 11.23	14.65 ± 4.34
O+/AA	M	NsTsCs	25.05 ± 11.88	24.46 ± 4.59	28.59 ± 8.27

Table 3.A7: W2mef

			% invasion relative to untreated control		
Donor Erythrocyte	**Gender**	**Invasion profile**	**Neuraminidase (250 mU/ml)**	**Trypsin (1mg/ml)**	**Chymotrypsin (1mg/ml)**
O+/AA	F	NsTsCr	29.14 ± 3.37	36.05 ± 11.15	58.02 ± 14.32
B+/AA	M	NsTsCr	28.36 ± 6.49	34.14 ± 9.6	73.41 ± 10.43
B+AS	M	NsTsCs	30.16 ± 5.17	37.67 ± 8.84	49.53 ± 12.87
O+AS	M	NsTsCs	28.89 ± 3.61	38.52 ± 0	48.15 ± 3.1
O+AA	M	NsTsCs	29.63 ± 3.13	25.92 ± 3.89	44.44 ± 2.88
A+/AA	F	NsTrCr	35.71 ± 8.21	50.32 ± 3,69	64.28 ± 13.29
O-/AA	M	NsTrCr	30.77 ± 9.54	62.82 ± 14.15	53.85 ± 4.42
A+/AA	M	NsTrCr	22.72 ± 4.06	54.54 ± 0.78	63.64 ± 17.84
O+/AA	M	NsTsCr	23.67 ± 6.49	45.45 ± 7,33	51.14 ± 10.58
A+/AS	M	NsTrCr	37.87 ± 3.91	60.61 ± 11.37	65.75 ± 22.12
O+/AA	M	NsTsCs	27.08 ± 13.13	22.32 ± 12.01	18.75 ± 17.40
O+/AA	M	NsTsCr	37.44 ± 10.42	27.78 ± 2.14	55.56 ± 17.46
B+/AA	M	NsTsCr	48.82 ± 7.63	44.44 ± 7.63	73.73 ± 18.10
B+/AS	F	NsTsCs	40.79 ± 14.31	32.46 ± 2.72	35.05 ± 16.70
O+/AA	M	NsTsCs	31.25 ± 17.39	37.5 ± 14.82	41.44 ± 15.00
A+/AC	M	NsTsCs	29.83 ± 11.68	48.72 ± 8.18	26.76 ± 4.03
A+/AA	M	NsTsCs	30.08 ± 9.89	44.84 ± 3.37	26.89 ± 3.55
O+/AA	F	NsTrCs	46.38 ± 3.56	92.44 ± 7.85	37.61 ± 4.31
O+/AC	M	NsTrCs	28.07 ± 4.01	63.64 ± 8.73	21.832 ± 5.38
O+/AA	M	NsTsCs	21.33 ± 0.49	41.33 ± 8.39	30.11 ± 4.87

Key: N: neuraminidase, T: trypsin, C: chymotrypsin, s: sensitive, r: resistant

Table 3.A8: Binding stability of the different fluorescent dyes used in this study

	MFI (Mean ± SD) *						SI (Mean ± SD) *		
	CFDA-SE		DDAO-SE		CTFR		CFDA-SE	DDAO-SE	CTFR
	+	-	+	-	+	-			
Day 0	6352 ± 29.0	32 ± 2.0	6063 ± 13.0	38 ± 0.0	6335 ± 8.0	25 ± 1.0	21110 ± 100.0	20046 ± 43.0	2092 ± 30.0
Day 15	5250 ± 45.9	25 ± 1.0	4929 ± 0.0	25 ± 0.0	5347 ± 24.0	27 ± 1.0	17531 ± 15.0	16267 ± 0.0	1769 ± 74.0

* The Wilcoxon matched-pairs signed-rank test shows no significant difference in both MFI and SI between day 0 and day 15 post-incubation.

Table 5.A9: Comparison of sample seroprevalence across study sites

PF3D7_0210600-1

	Accra		Hohoe		Navrongo		Kintampo	
	Z	P-value	Z	P-value	Z	P-value	Z	P-value
Hohoe	1.37	0.172						
Navrongo	4.16	<0.0001	2.67	0.007				
Kintampo	2.72	0.006	1.16	0.24	1.34	0.179		
Adults	0.43	0.67	0.61	0.543	3.37	<0.0008	1.92	0.055

PF3D7_0210600-3

	Accra		Hohoe		Navrongo		Kintampo	
	Z	P-value	Z	P-value	Z	P-value	Z	P-value
Hohoe	0.57	0.566						
Navrongo	7.34	<0.0001	6.75	<0.0001				
Kintampo	7.34	<0.0001	6.75	<0.0001	ND	ND		
Adults	2.12	0.033	1.33	0.182	5.35	<0.0001	5.35	<0.0001

PF3D7_1136200-3

	Accra		Hohoe		Navrongo		Kintampo	
	Z	P-value	Z	P-value	Z	P-value	Z	P-value
Hohoe	1.54	0.123						
Navrongo	6.01	<0.0001	4.89	<0.0001				
Kintampo	4.38	<0.0001	3.06	0.002	1.82	0.067		
Adults	ND	ND	1.35	0.178	5.55	<0.0001	4.00	<0.0001

Statistical differences were computed using the Chi-square test, Z scores and P-values are shown, significant differences are in bold.